Development of pan-cancer immunotherapies to target stressed cells within the tumour microenvironment.

Emma Louise Page

Wadham College

University of Oxford

A thesis submitted for the degree of Doctor of Philosophy to the

Department of Oncology, University of Oxford, Trinity Term 2024.

Supervisor: Professor Len Seymour

A statement addressing the impact of the COVID-19 global pandemic on this thesis

The COVID-19 pandemic was ongoing during the start of my DPhil in October 2020. All students have been advised to attach documentation of the effects that these restrictions had upon their research.

Whilst, unlike students in the previous 4 years, I did not experience a time when I was unable to enter the laboratory at all, there was restricted access until May 2021.

These restrictions allowed be to enter the laboratory a few times a week for up 4 hours at a time. Owing to how early this happened, it is difficult to detail the magnitude to which this disruption effected this thesis. Nevertheless, with minimal lab members allowed in at one time, there was a lack of day-to-day supervision and shadowing opportunities that prevented the initial period of my DPhil being as fruitful as it could be.

Declaration of Authentication

The work presented in this thesis is wholly my own; any contribution made my others have been acknowledged accordingly. The content submitted here does not form part of another thesis in this or any other university. This work was carried out under the supervision of Professor Leonard Seymour at the Department of Oncology, Medical Science Division, University of Oxford.

Emma Page

October 2024

Publication notes

Contributions to published work made over the course of this DPhil:

Baugh, R., Khalique, H., **Page, E**., Lei-Rossmann, J., Kok-Ting Wan, P., Johanssen, T., Ebner, D., Ansorge, O., & Seymour, L. W. (2024). Targeting NKG2D ligands in glioblastoma with a bispecific T-cell engager is augmented with conventional therapy and enhances oncolytic virotherapy of glioma stem-like cells. J Immunother Cancer, 12, 8460. https://doi.org/10.1136/jitc-2023-008460

Abstract

Targeted cancer immunotherapies have been described as a 'magic bullet' which allow for the specific targeting of cancerous cells whilst leaving healthy cells unharmed. By targeting proteins that a highly upregulated in tumours, we can specifically target cancer cells for destruction via the immune system. The selecting of target protein or antigen is critical, the pressure of the therapy can lead to the emergence of clonal populations that have downregulated the target protein, leading to therapy resistant recurrence. Furthermore, most immunotherapies target molecules that, while overexpressed in tumour cells, are also present at low levels in healthy cells, raising concerns about on-target, off-tumour side effects.

NKG2D ligands are upregulated in almost every tumour cell, serving as a warning flag to the immune system, in particular Natural Killer cells, of cellular stress such as malignant transformation. They are also minimally expressed in normal, healthy tissue. By targeting the immune system's own warning molecules, using an alternative T cell-based strategy, we hope to reduce on-tumour, off-target side effects.

In this thesis we have developed multiple NKG2D ligand targeting, bispecific T cell engagers. Bispecific T cell engagers are small antibody-like structures which can bind to two different targets. One side will bind to a T cell (via CD3) whilst the other binds to a tumour associated protein, such as an NKG2D ligand, on a tumour cell. This brings the two cells into proximity, resulting in the formation of a pseudo-immune synapse, activation the T cell, leading to killing of the tumour cell.

One of these molecules, the NKG2D TriTE, contains two copies of the NKG2D ectodomain, allowing it to bind to each of the eight NKG2D ligands, minimising the chance of loss of antigen mediated resistance, which is often seen when targeting a single protein. In this thesis, we have shown that the NKG2D TriTE can induce the activation of T cells and subsequent cytotoxicity against a broad spectrum of cancer cell lines from a wide variety of tissue types, while exhibiting minimal toxicity in

non-malignant cell lines. Additionally, we show evidence that the NKG2D TriTE mediated cytotoxicity is resistant to soluble NKG2D ligands, a major immune evasion mechanism utilised by tumours to evade detection as well as inhibiting NKG2D positive immune cells by releasing the proteins as 'decoys'.

Furthermore, we have investigated alternative strategies to the NKG2D TriTE, such as the use of the T cell-co-stimulatory molecule, CD2; testing the effect of increasing the affinity to the target cell utilising an ScFv molecules against a smaller subset of the NKG2D ligands; and inhibiting the shedding of the NKG2D ligands. Overall, the results from this thesis show that the NKG2D TriTE is the superior NKG2D ligand T cell engager format investigated and should be taken forward into further pre-clinical testing as a novel pan-cancer immunotherapy.

Acknowledgements

Firstly, I would like to thank CRUK for offering the financial support to allow future scientists the opportunity to learn and develop their skills. I came back to academia to have the opportunity to develop scientific ideas independently, and this would not have been possible without this funding.

Secondly, I would like to thank my supervisor, Len Seymour. Thank you for giving students to freedom to explore and learn through experience whilst always being available to offer a helping hand when needed. Going beyond your duties to ensure than your students are taken care of, whilst under his supervision and afterwards. A special thank you as well for putting up with me in the final weeks of writing this thesis.

To Dr Flurin Caviezel and Dr Richard Baugh, you both have made the Seymour lab an entertaining yet incredibly supportive place to work, and I consider myself incredibly fortunate to consider the both of you friends. Any lab that you work in is lucky to have you, as evidenced by Richard's new lab members drunkenly thanking me for letting them have him.

Flurin - what would the Seymour lab be without you and your many roles, DPhil Student, Post Doc, Lab Manager and therapist. It has been a pleasure working with you over the past 4 years, both within science as well as carrying out the most elaborate viva hats and leaving day treasure hunts.

To Hena - my lab Mum. You prove to the world that some Slytherins still have a heart of gold. Your voice has been a constant motivation in my head when things have got tough these last few weeks.

I would like the thank Seymour and Jiang lab members, both past and present. To my fellow DPhil students, Kate, Fernando, Peter, Mahnoor, Henry, Amy, Yuqian and Sichen. Thank you for being there for me whenever I have needed you and making the lab such an enjoyable place to work every day. And to the post-docs in the lab, Dr Kerry Fisher, Dr Ahmet Hazini, Dr Gulsah Albayrak and Dr Hena Khalique (yes you're last but I mentioned you twice), thank you for all of your guidance over the years and keeping the lab together in one people.

Thank you to Dr Weiheng Su, Dr Qian Liu and Corinne Branciaroli for all of your support and making me into the scientist I am today. Qian, you took me from an inexperienced graduate to an independent scientist. Thank you for your patience in the early days and for taking the time whenever I needed you. Su - Thank you for encouraging me to apply to this DPhil in the first place. Thank you for allowing me to ask you stupid questions, even if you make fun of me.

A special thank you to Lorna. You have been an incredible friend over the last few years, for helping me out when I was in a tough spot, and for always being around when I need to get out of my university bubble.

Thank you to my family for your unwavering support throughout my life but specifically in these last few years. I can't promise I will get better at answering you phone cells, but I will try. Not working late in a concrete building should definitely help a bit.

And finally, to Chris – who knew when we would procrastinate revising in the library for our undergrads that we would be able to get here. Still procrastinating and cramming right until the deadline. I am so proud of how far both of us have come. Thank you for always being there when I need someone's ear; for being my literal shoulder to cry on; and for any weekends away escaping to the "other place" for some normalcy. I cannot wait for the rest of our lives together.

Table of Contents

List of Figures

List of Tables

List of Abbreviations

5-FU	5-fluorouracil
ACT	Adoptive cell therapy
ADAM	A disintegrin and metalloprotease
APC	Antigen presenting cell
ATM	Ataxia telangiectasia mutated
ATR	ATM- and Rad3-related
BCMA	B-cell maturation antigen
BiTE	Bispecific T cell engager
BV	Brilliant violet
CAF	Cancer associated fibroblast
CAR	Chimeric antigen receptor
CD	Cluster of Differentiation
CHO	Chinese hamster ovary
CMV	Cytomegalovirus
CO_2	Carbon dioxide
CPE	Cytopathic effect
CTLA-4	Cytotoxic T lymphocyte-associated antigen
CtrlNB	Control nanobody
CXCL12	C-X-C motif ligand 12
DAP 12	DNAX-activating protein of 12 kDa
DAP10	DNAX-activating protein of 10 kDa
DDR	DNA damage response
DLBCL	Diffuse large B-cell lymphoma
DLL3	Delta-like ligand 3
DMEM	Dulbecco's Modified Eagle's Medium
DMSO	Dimethyl sulfoxide
dTTT	deoxythymidine triphosphate
ELISA	Enzyme-linked immunosorbent assay
EnAd	Enadenotucirev
EpCAM	Epithelial cell adhesion molecule
EV	Extracellular vesicle
FAP	Fibroblast activating protein
FBS	Fetal bovine serum
FDA	Food and Drug Administration
FR-β	Folate receptor β
GBM	Glioblastoma
GM-CSF	Granulocyte-macrophage colony stimulating factor
gMFI	Geometric mean fluorescent intensity
GPI	Glycophosphatidylinositol
Gy	Gray
HDAC	histone deacetylase
HDACi	HDAC inhibitor
HEK293	Human embryonic kidney 293

His	Histidine
HLA	Human leukocyte antigen
HPV	Human papillomavirus
HSV	Herpes simplex virus
HUVEC	Human Umbilical Vein Endothelial Cells
ICI	Immune checkpoint inhibitor
IFN	Interferon
IgG	Immunoglobulin G
IL	Interleukin
IMAC	Immobilized Metal Affinity Chromatography
ITAM	Immunoreceptor tyrosine-based activation motif
ITIM	Immunoreceptor tyrosine-based inhibitory motif
ITSM	immunoreceptor tyrosine-based switch motif
KO	Knock out
LFA	Lymphocyte function-associated antigen
MAGE-A3	Melanoma-associated antigen 3
MHC	Major histology complex
MICA	MHC-class-I-polypeptide-related sequence A
MICB	MHC-class-I-polypeptide-related sequence B
MLP	Major late promoter
MMP	Matrix metalloproteases
MOI	Multiplicity of infection
mRNA	Messenger RNA
MWCO	Molecular weight cut off
NaBut	Sodium Butyrate
NB	Nanobody
NFAT	Nuclear factor of activated T cells
NK cells	Natural Killer cells
NKG2D	Natural Killer Group 2 Member D
NKG2DL	NKG2D ligands
oHSV	Oncolytic HSV
PBMC	Peripheral blood mononuclear cells
PCR	Polymerase chain reaction
PD-1	Programmed cell death protein 1
PD-L1	Programmed death ligand 1
PD-L2	Programmed death ligand 2
PE	Phycoerythrin
PI3K	Phosphatidylinositol 3-kinase
RPMI	Roswell Park Memorial Institute
SA	Splice acceptor
scFV	Single chain variable fragment
SDS-PAGE	Sodium dodecyl sulphate-polyacrylamide gel electrophoresis
siRNA	Short interfering RNA
sMICA	soluble MICA
sMICB	soluble MICB
sNKG2DL	Soluble NKG2D ligands

SP	Signal peptide
TAA	Tumour associated antigens
TACE	Tumour necrosis factor-α converting enzyme
TCR	T cell receptor
TGF-β	Transforming growth factor β
TIL	Tumour infiltrating lymphocyte
TriTE	Trispecific T cell engager
T-VEC	Talimogene Laherparevac
ULBP	UL16-binding proteins
VPA	Valproic acid
WT	Wildtype
γδ T cells	Gamma delta T cells

Chapter 1: Introduction

1.1 Cancer

Despite the rapid development of new cancer therapies over recent decades, 167 000 people died from cancer in the UK from 2017-2019 (Cancer Research UK). Additionally, there are almost 400 000 new cases of cancer each year in the UK, with cancers of the breast, prostate, lung and bowel accounting for over half of these (Cancer Research UK, 2017-2019). Whilst half of cancer patients will survive for 10 years or more with treatment, there is still an enormous burden of mortality and morbidity, and innovative new treatments are urgently needed.

1.1.1 The Hallmarks of Cancer

The term 'cancer' is used to refer to a multitude of conditions involving the uncontrolled proliferation of cells, often leading to the invasion of alternative tissues and organs. This is caused via the accumulation of DNA mutations, which can be inherited, occur spontaneously or be induced by carcinogenic agents (Loeb et al., 1974, 2003; Miki et al., 1994; Proctor, 2012; Venitt, 1996; Wagner et al., 1960). Collectively, these mutations alter the finely tuned pathways and processes within the cell evolved to maintain homeostasis, leading to deregulated growth and the formation of a tumour.

Despite cancer cells showing high levels of heterogeneity, both within the tumour itself, but more broadly amongst different patients and tumour types, Hanahan and Weinberg identified key features of cancer cells which they state must be acquired through tumorigenesis, initially described in the first release of 'The Hallmarks of Cancer' released in 2000 (Hanahan & Weinberg, 2000). This described the six characteristics that commonly define a cancer cell: evading apoptosis, self-sufficiency of growth factors, resistance to anti-growth-factors, replicative immortalisation, induce angiogenesis and the ability to invade other tissue and metastasis. Since 2000, two more updated versions of their seminal paper have been released, identifying additional hallmarks as well as

enabling characteristics, summarising the ever-evolving landscape of cancer research (Hanahan, 2022; Hanahan & Weinberg, 2011). These include the evasion of the immune system as well as genome instability (Hanahan & Weinberg, 2011).

1.1.2 Cell stress induced by tumourigenesis

Tumourigenesis induces several stresses within the transforming cells. These can include genomic instability, metabolic stress and oxidative stress. During tumour development, cancer cells accumulate mutations, leading to DNA damage, abnormal cell processes and disruption of the cellular homeostasis. They also face metabolic and oxidative stress due changes such as the Warburg effect and increased reactive oxygen species (ROS), as well as hypoxia (Liberti & Locasale, 2016; Tafani et al., 2016). While such stresses typically induce apoptosis or cell cycle arrest in healthy cells, cancer cells often evade this, promoting survival and growth through the selection of advantageous mutations. For example, the tumour suppressor gene, p53, is mutated in around 50% of all cancer, allowing the cell to escape apoptosis pathways (Chen et al., 2022).

1.1.3 Current therapies

Surgical resection, radiotherapy and chemotherapy are the most common treatments for cancer used in the UK, with 68% of call patients receiving at least one of these treatments (PHE Official Stats, 2020). Where feasible, tumour masses are surgically resected, with the tumour being entirely, or partially removed in a process called debulking (Silberman, 1982). Whilst this seems the most intuitive approach, it is often not 100% effective due to the incomplete removal of the tumour cells, and inaccessibility to many tumours meaning it is not always a viable option.

Radiotherapy has been used in the treatment of regionally localised cancers for over 100 years and is currently used in around half of all cancer patient treatment regiments, either as a monotherapy or as part of a combined treatment plan (Atun et al., 2015; Barton et al., 2014). Modern radiotherapy utilises ionising radiation to direct high-energy particles directly at the tumour to cause both single

and double strand breaks, as well as the release of free radicals which can cause further DNA damage, with the goal to induce apoptosis. The main limitation of radiotherapy is the toxicity to normal cells which are within the path of the radiation beam (Barnett et al., 2009). Many strategies have been employed to reduce this effect, in particular intensity-modulated radiation therapy which uses multiple beams of radiation at various angles which intersect at the tumour site (Zelefsky et al., 2000).

The final, major treatment option for cancer patients is chemotherapy, which refers to the administration of a chemical compound to kill cancer cells and is typically delivered via *intravenous* injection. Traditionally chemotherapeutic agents refers to a variety of different drugs which in general aim to either kill cancer cells or prevent them from diving with the main categories being, alkylating agents, anti-metabolites, topoisomerase inhibitors and mitotic inhibitors (Anand et al., 2023). In recent years there have been important advances in drugs exploiting tumour-acquired mutations, most notably kinase inhibitors such as the tyrosine kinase inhibitor, Gleevec (Imatinib), which targets Philadelphia chromosome positive cancers(Cohen MH et al., 2002; Deininger et al., 1997) . However, the majority of chemotherapy agents lead to severe side effects which can significantly impact the patient's quality of life (Anand et al., 2023).

The main limitations of these less targeted approaches are that due to the lack of specificity to the tumour cells, there is often off target effects, leading to damage of healthy cells. The major concern is that by damaging these cells, specifically by methods which induce DNA damage, further pro-tumour mutations may be acquired. Additionally, resistance mechanisms are often developed from both chemotherapy and radiotherapy treatments.

1.2 Immunotherapy

The role of the immune system in the development of cancer has been studied for decades, with the initial observations in the 1890s by Dr William Coley who found that patients that developed an infection after surgery saw an increased regression in their tumours for a short period of time (Coley, 1909; Jessy, 2011; McCarthy, 2006). However, it wasn't until more recently, that the role of the immune system in the eradication of tumour cells was more widely accepted, with immune evasion being included as one of the second generation of 'Hallmarks of Cancer' by Hanahan and Weinburg in 2011 (Hanahan & Weinberg, 2011).

The cancer immunity cycle (Figure 1.1) was proposed in 2013, by Chen and Mellman, to describe the role of the immune system in controlling tumour growth via immunosurveillance (D. S. Chen & Mellman, 2013). Whilst tumours can be detected and eliminated by the innate immune system, for example by natural killer (NK) cells detecting NKG2D ligands presented on the cell surface of stressed cells, they can also activate the adaptive immune system through the detection of tumour associated antigens (TAAs) (Guerra et al., 2008; Ljunggren, 2008). TAAs refers to antigens from proteins that originate almost exclusively from tumours, such as neoantigens generated from mutated proteins, and could induce an immune, and anti-tumour response. The detection TAAs by antigen presenting cells (APC), such as dendritic cells, promotes them to migrate to the lymph nodes where they present the antigen to naïve T cells via major histocompatibility complex (MHC) molecules. Here, upon successful cross-presentation, activated T cells proliferate and are trafficked to the tumour. Once within the tumour, the activated T cells can kill their target cells via the recognition of TAA peptides via the T cell receptor (TCR). Subsequently, the targeted tumour cells will release more TAAs whilst being killed, reinitiating the cycle with a wider breadth of TAAs.

The cancer immunity cycle is thought to be a major part of a process called cancer immunoediting, which can be divided into three stages, elimination, equilibrium and escape (Dunn et al., 2002).

Immunoediting describes the process in which a tumour evades immunosurveillance, inhibiting the cancer immunity cycle.

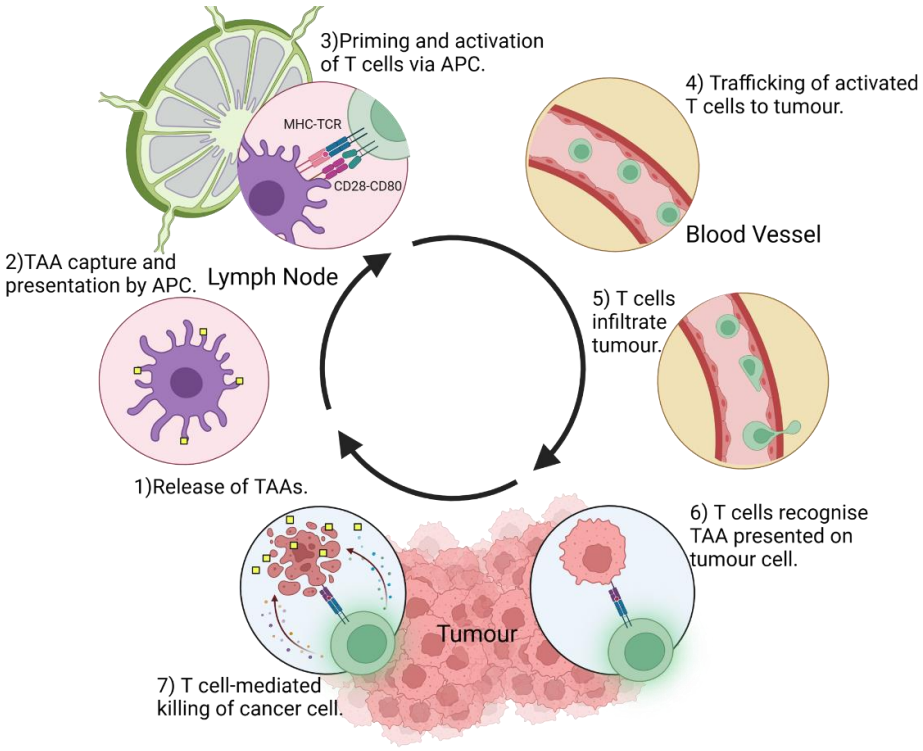

Figure 1.1: The cancer immunity cycle.

Created in BioRender, inspired by D. S. Chen & Mellman, 2013.

Mutations are continuously being induced or spontaneously occurring within our cells, producing neoantigens or inducing the presentation of self-proteins, such an NKG2D ligands, that induce elimination by the immune system, similarly to the detection of a bacterial or viral infection (Rathe et al., 2019; Y. Zhang et al., 2021). Immune surveillance detects these changes and eliminates both cancer cells and pre-cancerous cells, often before detection of the tumour clinically.

The equilibrium stage of immunoediting is the least understood stage and is thought to arise from a balance between tumour cells acquiring mutations allowing them to avoid detection and clearance by the immune system, and the immune system suppressing their proliferation. It is thought that tumour cells can remain in the equilibrium state for years, including those in patients currently in remission, without progressing to the evasion phase if additional mutations are not acquired. The

suppression by the immune system will however apply a selection pressure that would be favourable to tumour clones with mutations that allow for the avoidance of the immune system, such as the recruitment of as the downregulation of MHC molecules, preventing the presentation of TAAs (McGranahan et al., 2017). Interestingly, evidence for this step can be found by looking at cases of organ donor transmitted cancer, in which donated organs, unknowingly containing dormant cancer cells, are implanted into the recipient who is taking immunosuppressive drugs to prevent rejection (Desai & Neuberger, 2014). Without the donor immune system to dampen the growth, the tumour rapidly develops.

For a tumour to fully develop and potentially metastasise, it must be able to effectively evade the immune system (Dunn et al., 2002). This stage is known as escape, and involves the rapid growth of the tumour, typically to a size that can be clinically detected. To achieve immune escape, the tumour must evolve mechanisms to more effectively evade suppression by the immune system. Mechanisms which have been identified include loss of antigen presentation (e.g. downregulation of MHC molecules) (Hazini et al., 2021; McGranahan et al., 2017), expression of immune checkpoint proteins (e.g. programmed death ligand-1 (PD-L1)) (Huang & Zappasodi, 2022; Juneja et al., 2017) and recruitment of non-cancerous immunosuppressive cells such as Tregs and myeloid derived suppressor cells (MDSCs) which, along with tumour cells, secrete a variety of immunosuppressive factors (e.g. TGF-β and IL-10) as well as express inhibitory proteins on their surface for contact mediated immunosuppression (e.g. cytotoxic T-lymphocyte antigen 4 (CTLA-4)) (Cinier et al., 2021; Groth et al., 2019; B. H. Li et al., 2020; Yokokawa et al., 2008).

The model of immunoediting has facilitated the development of a multitude of different immunotherapy agents, many aiming to target specific immune evasion mechanisms.

1.2.1 Immune checkpoint inhibitors

Immune checkpoints were discovered in the 1990s and 2000s, identifying CTLA-4 and PD-1, and have revolutionised the treatment of cancer; leading to Honjo and Allison being awarded the Nobel Prize

in 2018 (Iwai et al., 2002; Leach et al., 1996). Immune checkpoints are a key immune regulatory mechanism to 'turn off' activated T cells, preventing harm to healthy tissue which could lead to auto-immune disorders. Tumour cells, however, have taken advantage of these proteins and utilise them to escape T cell mediated targeting.

PD-L1, as well as PD-L2, are ligands for the PD-1 immune checkpoint protein, and upon binding inhibit T cell activation through the immunoreceptor tyrosine-based inhibitory motif (ITIM) and immunoreceptor tyrosine-based switch motif (ITSM) that are present in the cytoplasmic region of PD-1 (Keir et al., 2008). PD-L1 has been reported to be upregulated in a wide variety of cancers, on tumour cells as well as fibroblasts and macrophage (Cha et al., 2019; L. Wang et al., 2024). CTLA-4 is expressed on T cells and acts as a competitive inhibitor for CD28 by binding to CD80 and CD86 on APCs with a higher affinity than CD28, thereby preventing the co-stimulatory function of CD28 binding (Rudd et al., 2009). Lack of effective CD28 co-stimulation has been shown to decrease T cell activation along with proliferation and cytokine release, as well as potentially inhibiting the formation of memory T cells (Ville et al., 2015). Tregs, which are often recruited into the TME to supress immune responses, express high levels of CTLA-4 (Tekguc et al., 2021).

In 2011 the first immune checkpoint inhibitor (ICI), ipilimumab - a monoclonal antibody against CTLA-4, was approved by the FDA for advanced melanoma, followed by the approval of Nivolumab, in 2014 for the targeting PD-1 (Deeks, 2014; Stephen Hodi et al., 2010). Since then, more ICIs have been approved with the majority against PD-1 and PD-L1, with other checkpoint inhibitor targets, such as TIGIT, LAG-3 and TIM-3 currently under clinical trials (Lee et al., 2022; Sun et al., 2023).

1.2.2 Cancer vaccines

Cancer vaccines are designed to stimulate the immune system to attack tumour cells. They are typically categorised as either prophylactic or therapeutic. Prophylactic vaccines aim to prevent the cancer occurring at all, such as the human papillomavirus (HPV) vaccine which immunises patients against 4 HPV serotypes that are linked to cervical cancer (Asif et al., 2006). 90 % of cervical cancer

are linked to HSV serotype infections and since the initiation of the immunisation program in the UK in 2008, cervical cancer rates in these women have dropped by 34-90% (Falcaro et al., 2024).

Therapeutic cancer vaccines, however, are designed to stimulate the immune system of cancer patients to better recognise and attack the tumour. The main limitation of therapeutic cancer vaccines is that most TAAs are likely to be self-antigens and high affinity TCRs against them will have been depleted during thymic selection, as shown in the disappointing anti-tumour efficacy data from clinical trials (Grimmett et al., 2022). Despite this, a dendritic cell-based therapeutic vaccine, Sipuleucel, was approved for the use in castration-resistant prostate cancer, after showing an increased median survival of 4.1 months in comparison to the placebo group (Cheever & Higano, 2011).

1.2.3 Adoptive cell therapy (ACT)

Adoptive cell therapy refers to the process of activating/engineering a patient's own cells *ex vivo*, prior to re-infusion back into the patient. Initially, this involved the isolation of tumour infiltrating lymphocytes from a patients surgically resected tumour, followed by expansion and infusion of large number of tumour-specific lymphocytes. In clinical trials carried out in the 1980s on melanoma patients, there was an objective overall response rate of 16% when combined with high dose IL-2, with complete response seen in a third of these patients (Atkins et al., 1999). However, whilst seemingly effective in melanoma, TIL (tumour infiltrating lymphocyte)-based ACT has shown minimal success in other cancer types (Hinrichs & Rosenberg, 2014).

Alternative forms of ACT involve the engineering of T cells to express either an alternative TCR or a chimeric antigen receptor (CAR), typically formed of a single chain fragment variable (scFv) against a target antigen. Alternative TCR engineered T cells (TCR-T cells) allow for the recognition of intracellular proteins, a limitation of CAR-T cells which is restricted to membrane targets, by genetically altering T cells to express a TCR for specific TAA antigens/peptides as a targeted therapy. In August 2024, the FDA approved a MAGE-A4 directed TCR-T therapy, afamitresgene autoleucel

(Tecelta), for the treatment of metastatic synovial sarcoma, following Phase II trial in which an overall response rate of 39% was seen (D'Angelo et al., 2024). Whilst an appealing approach, the field is hindered by our understanding of TCR-peptide specificity and that each TCR can recognise many presented peptide sequences (Sewell, 2012). This is exemplified by clinical trials targeting peptides from the melanoma-associated antigen 3 (MAGE-A3), whereby in two separate clinical trials fatal side effects occurred due to cross reactivity, with the first clinical trial reacting to peptides derived from MAGE-A12 which is expressed in the brain; and the second to TITIN, a protein expressed in cardiomyocytes (Cameron et al., 2013; Linette et al., 2013; Morgan et al., 2013). More recently, work is being carried out to better predict the peptide specificity of engineered TCRs to be able to safely target TAAs in cancer patients.

1.2.4 Chimeric antigen receptor (CAR) – T cells

CAR-T cells consist of a single chain variable fragment (scFv) fused to the CD3 ζ intracellular domain, to elude the requirement of TCR engagement with an MHC-peptide complex. Instead, the T cell specificity is controlled by the target antigen of the scFv. Initial generations of CAR-Ts, containing solely the CD3 ζ intracellular domain, found this signalling to be insufficient (Brocker & Karjalainen, 1995). Therefore, second generations were developed which contain additional co-stimulatory domains, such as from CD28 and 4-1BB (Imai et al., 2004; Maher et al., 2002). Additional generations have since been developed with various alterations to the intracellular region, including the addition of an NFAT (nuclear factor for activated T cells) responsive element to induce the expression of IL-12 and IFN-γ, as well as elements to increase stimulation through the JAK/STAT pathway (Chmielewski & Abken, 2015; Kagoya et al., 2018; Kueberuwa et al., 2017).

Presently, most success in CAR-T therapies have been seen for haematological malignancies, in particular B cell cancers with CAR-Ts targeting CD19 and BCMA (B-cell maturation antigen), with Kymriah being approved for B cell malignancies in 2017 and Abecma for multiple myeloma in 2021 (Kochenderfer & Rosenberg, 2013; Maude et al., 2018; Neelapu et al., 2017; Schuster et al., 2017,

2019; J. Yang et al., 2023), whilst there has been limited success in solid tumours (Brudno & Kochenderfer, 2016).

1.2.5 Limitations of immunotherapy

Despite the huge potential in immunotherapy and significant impact it has had on patients, response rates hugely vary. Overall, the response rate has been reported as between 10-30% across a variety of different cancers, with efficacy being reported as better in certain tumour types such as melanoma where an overall response rate up to 50% has been reported (He & Xu, 2020; Valero et al., 2021).

Many immunotherapy strategies, such as ICIs, rely on the ability of tumour cells to express reactive neoantigens via MHC molecules. As the majority of tumour associated proteins are self-proteins, the immune system is likely unable to effectively detect them with high affinity due to self-tolerance, unless the proteins are mutated sufficiently to be detected by as neoantigens (Mariuzza et al., 2023). Additionally, tumour cells often downregulate the expression of MHC molecules, or associated proteins, such as β2M (beta-2-microglobulin), to prevent detection via these peptides (Hazini et al., 2021; Y. Zhao et al., 2021).

Whilst targeted therapies offer the advantage of fewer off target effects due to their specificity, the treatments also apply a selection pressure on the tumour to select for target antigen negative tumour cells, as seen in ICIs and CAR-T therapies (Majzner & Mackall, 2018; McGranahan et al., 2016; Rizvi et al., 2015; Van Rooij et al., 2013). In a Phase I trial of CD19-4-1BB-ζ CAR T-cell therapy for paediatric B-cell acute lymphoblastic leukaemia (B-ALL), which showed an initial response rate of 93%, antigen loss accounted for 24% of relapses loss (Maude et al., 2016). This shows that the selection of the target antigen is critical for successful immunotherapy. Dual targeting immunotherapies are now being targeting as a strategy to prevent loss of antigen resistance (Spiegel et al., 2021).

An additional reason for lack of efficacy in solid tumours specifically is the lack of therapeutic permeability typically associated with the high intratumoural pressure, lack of effective vasculature as well as cancer-associated fibroblasts (CAFs) that help to form their distinct architecture (Ma et al., 2019). CAFs in particular pose a significant, and literal, barrier to the treatment of solid tumours, by both physically excluding immune cells, as well as the secretion of immunosuppressive cytokines and chemokines such as IL-10, TGF-β and CXCL12, to both inhibit the entry of T cells as well as 'turn off' any T cells that succeed (Cinier et al., 2021; Groth et al., 2019; Maia et al., 2023; Mariathasan et al., 2018; Rhim et al., 2014; Yokokawa et al., 2008).

1.3 T cell engagers

1.3.1 T cell activation

T cell activation is generally described by the 3-signal model. where the initial signal alone, the TCR binding to a peptide presented on the MHC molecule, is typically insufficient to lead to full T cell activation. To achieve complete activation, additional signals from co-stimulatory molecules as well as the presence of pro-inflammatory cytokines such as IFN-γ are required (Curtsinger & Mescher, 2010; Jenkins,' et al., 1991; Leitner et al., 2010; Mescher et al., 2006).

When a TCR binds a complementary peptide-MHC complex it triggers the rapid phosphorylation of tyrosine residues present in the ten immunoreceptor tyrosine-based activation motifs (ITAMs) of the TCR-CD3 complex, by the kinases Lck and Fyn (Smith-Garvin et al., 2009). The detection of the MHC:peptide complex by a TCR is known as signal one. Signal two comes from a co-stimulatory protein, such as CD28, which binds to B7 molecules on antigen presenting cells (APCs) (June et al., 1990). The absence of CD28 significantly impairs T cell proliferation and cytokine proliferation (Shahinian et al., 1993).

In addition to CD28, other co-stimulatory proteins and accessory proteins (e.g. CD2) have been identified which are thought to help to provide a broader context to the interaction to prevent inappropriate activation (L. Chen & Flies, 2013). The CD2-CD58 interaction in spoken about in more detail in Chapter 5.

1.3.2 Bispecific T Cell Engagers (BiTEs)

Bispecific T cell engagers can be produced in a variety of different formats but in essence consist of a molecule with two targeting moieties, with one binding to T cell, typically to CD3 ε, and the other binding to a tumour associated antigen (Figure 1.2). Typically, BiTEs are formed of two scFvs joined with a flexible linker domain, with one scFv binding to CD3ε on a T cell. ScFvs are small antibody-like molecules that are formed of the variable regions of the heavy and light chain of an antibody and are typically linked together by a flexible linker.

Simultaneous binding of BiTEs between a T cell and a target cell leads to CD3 clustering, T cell activation and T cell mediated cytotoxicity towards the target cell, through the release of cytotoxic granules containing perforin and granzyme, as well as the release of IFN-γ (Freedman et al., 2017; Khalique et al., 2021; Wolf et al., 2005). T cells have been shown to elicit cytotoxicity against APCs presenting as few as 10 MHC:peptide molecules, whilst CAR-T cells and BiTEs have been shown to have less sensitivity (Purbhoo et al., 2006; Stone et al., 2012).

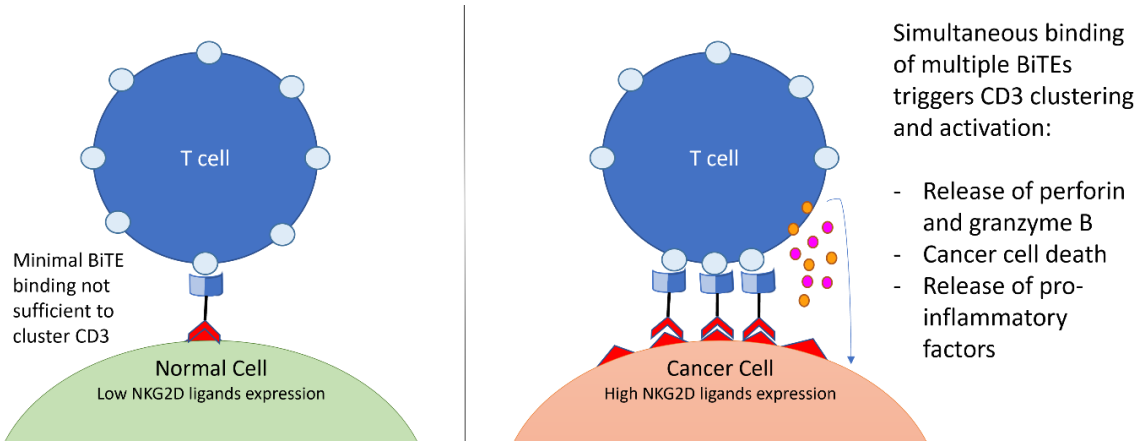

Figure 1.2: Schematic of NKG2D BiTE-induced T cell activation.

BiTE-mediated T cell activation is independent of the specificity of the T cell's TCR, HLA status of the target cell, or co-stimulation of CD28, however co-stimulation been found to enhance some BiTEs (Correnti et al., 2018; Dreier et al., 2002; Offner et al., 2006). Additionally, BiTEs can induce T cell activation of CD4+ and CD8+ T cells, with both cell types being shown to mediated BiTE-directed target cell killing (Mack et al., 1995). Furthermore, their small size (~ 60 kDa) should allow them easier penetration into the tumour where they can re-purpose *in situ* T cells.

Whilst being originally developed in the 1960, BiTEs have only quite recently have been shown to be effective against a multitude of target with the most well-known being CD19, which was the target of the first FDA approved BiTE, blinatumomab, which in the phase II TOWER trial demonstrated increased overall survival in comparison to standard chemotherapy (7.7 months vs 4.0 months (Goebeler et al., 2016; Kantarjian et al., 2017; Klinger et al., 2012; Nisonoff & Rivers, 1961). Other BiTEs currently undergoing clinical trials include those targeting CD20, BCMA, and recently DDL3, for the treatment of extensive stage small cell lung cancer (ES-SCLC) - the first FDA approved BiTE against a solid tumour (Harrison et al., 2020; Paz-Ares et al., 2023). In the Phase II clinical trial for Tarlatamab-dlle, a BiTE targeting DLL3, there was as 40% objective response rate, with a median survival of 9.7 month (Paz-Ares et al., 2023; NCT05060016). The main limitation of BiTEs is their significantly shorter half-life when compared to IgG delivery intravenously, requiring blinatumomab to be administered via continuous infusion for the typical 4-week cycle (Klinger et al., 2012; Stork et al., 2009).

1.4 Utilising innate immune ligands as immunotherapy targets

In this thesis we have chosen to focus our attention on NKG2D ligands (NKG2DLs), a group of eight ligands upregulated in response to stress, that are detected by the NKG2D receptor, most notable expressed on natural killer (NK) cells. The NKG2D-NKG2DL axis has been widely reported to be key in

immune surveillance and the simultaneous targeting of eight separate ligands by one therapeutic should also minimise the chance of loss of antigen resistance mechanisms as tumour cells.

1.4.1 NKG2D receptor

NKG2D (encoded by KLRK1) is the most characterised activating receptor on NK cells. It can recognise a group of 8 ligands, known as NKG2D ligands, which are upregulated in response to stress to allow detection via a process called induced-self recognition (Wensveen et al., 2018). Whilst it is predominantly expressed on NK cells, it is also present on NKT cells, CD8+ T cells and subsets of γδ T cells (Raulet, 2003). NKG2D has been shown to play a key role in immune surveillance, with NKG2D KO mice showing increased rate of arising spontaneous tumours than WT mice (Guerra et al., 2008; López-Soto et al., 2015).

NKG2D is a C-type, lectin-like, type II transmembrane glycoprotein that forms a homodimer with each monomer associated with a dimer of the adapter molecule DAP10 though attraction via opposing charges (DNAX-activating protein of 10 kDa) (Raulet, 2003). In mice, a second isoform of NKG2D is expressed which is formed from alternative splicing and is 13 residues shorter. This shorter form of NKG2D, NKG2D-S, is capable to bind to both DAP10 and DAP 12 (DNAX-activating protein of 12 kDa).

DAP10 contains a YINM motif that facilitates association of the p85 subunit of PI3 kinase, as well as Vav1 through Grb2 (Raulet, 2003). This complex is responsible for the continuation of the downstream signal via the PI3K-Akt pathway (Upshaw et al., 2006). DAP12 however, contains ITAM sequences which are phosphorylated upon NKG2D binding, which facilitates signalling through Syk and Zap70 (Raulet, 2003). The role for NKG2D in T cell co-stimulation may be critical in mice than in humans, as shown by the conditional expression of NKG2D on mice CD8+ T cells upon activation and the additional signalling capability though DAP12 facilitated by the expression of the alternative NKG2D-S isoform (Wensveen et al., 2018).

1.4.2 NKG2D ligands

Human NKG2D ligands (NKG2DLs) fall into two families, MIC proteins and the ULBP proteins (Figure 1.3A). MHC class I chain-related proteins A and B (MICA and MICB) are so named due to their similarities to MHC molecules, in particular MHC class I. (Bauer et al., 1999; Cerwenka et al., 2000; Diefenbach et al., 2000). As in MHC-I, MICA and B contain 3 domains, termed α1-3, however, does not associate with β-2 microglobulin (β2M) which is required for MHC-I stability and function (Bauer et al., 1999). A second family of ligands, referred to as the RAET-1 proteins or ULBP (UL16-binding proteins) 1 to 6, so named due to their ability to bind to the UL16 protein of human cytomegalovirus to prevent detection by the host immune system (Cosman et al., 2001). These proteins also have homology with MHC molecules, including the α1 and α2 domain which interact with the NKG2D receptor; however, they lack the α3 domain. The affinity of each human NKG2DL and the NKG2D receptor has not been determined yet, however in mice there is a large variation, with ligands binding in the μM range in humans (Table 1-1) (Raulet et al., 2013).

A

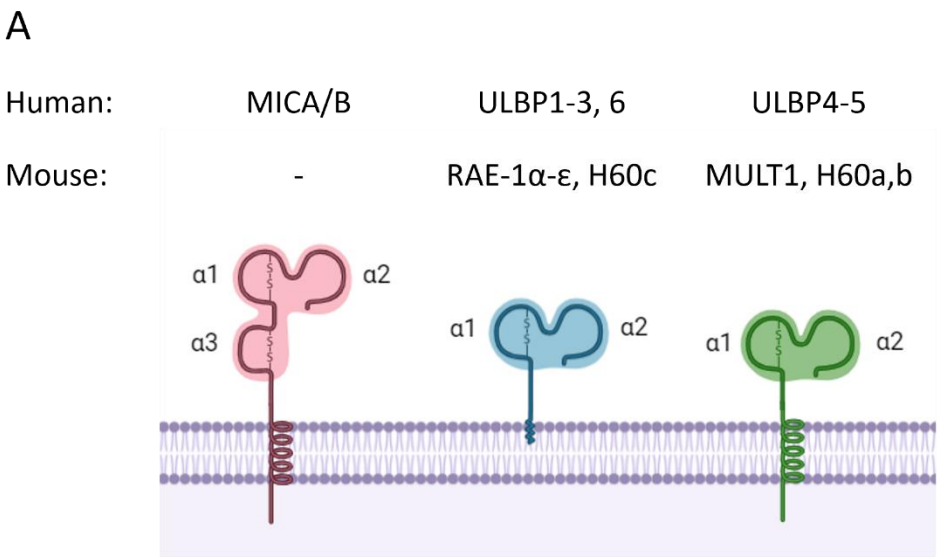

B

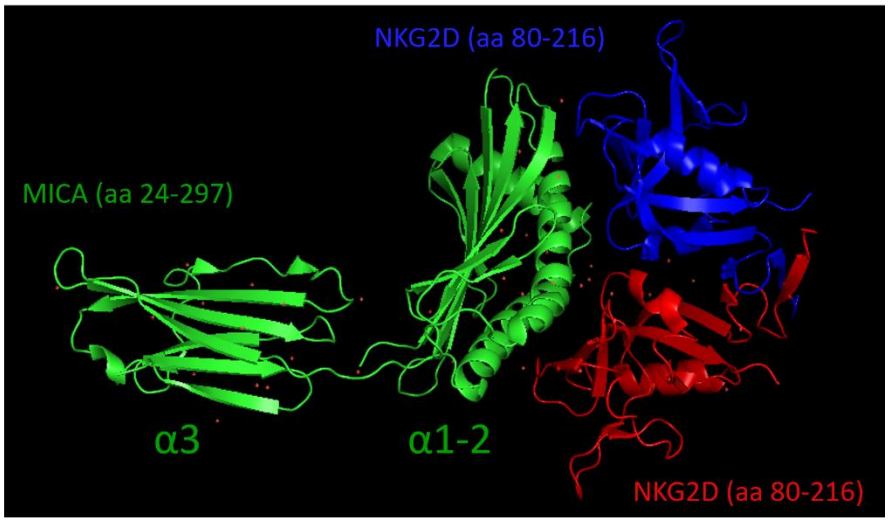

Figure 1.3: NKG2D ligands expressed in human and mouse, and binding to the NKG2D homodimer. (A) Schematic of the human and mouse NKG2D ligands and their general structure. (B) C Crystal structure (1HYR) of the extracellular regions of MICA (green) and extracellular regions of the NKG2D homodimer (red and blue). Visualised using PyMol. Crystal structure source: (P. Li et al., 2001).

In mice, the RAE-1 family of proteins in mice are homologous to the ULBP family in humans, whilst there have not been homologues of MICA/B identified as of yet (Diefenbach et al., 2000). These proteins are categorised into three groups, RAE1 proteins (retinoic acid early inducile-1, RAE1α-ε), which associate to the membrane through GPI-anchors, MULT1 (murine UL16-binding protein-like transcript 1) and H60 proteins which both contain a transmembrane domain. It is thought that the redundancy is NKG2D ligands is an evolved mechanism to both better react to various cell stresses as well as prevents immune escape by evasion strategies to downregulate immunostimulatory proteins, such as those evoked by viruses. This will be discussed further in 1.4.6.

Human	Anchoring	Affinity, K_D
MICA	Transmembrane	1 μM
MICB	Transmembrane	0.8 μM
ULBP1	GPI	1.1 μM
ULBP2	GPI*	-
ULBP3	GPI	-
ULBP4	Transmembrane	-
ULBP5	Transmembrane	-
ULBP6	Transmembrane	-

Mouse	Anchoring	Affinity, K_D
RAE-1α	GPI	70 μM
RAE-1β	GPI	0.19 μM
RAE-1	GPI	60 μM
RAE-1	GPI	70 μM
RAE -1ε	GPI	0.3 nM
MULT1	Transmembrane	6 nM
H60a	Transmembrane	0.3 nM
H60b	Transmembrane	0.3 μM
H60c	GPI	9 μM

Table 1-1: Human and mouse NKG2D ligands

Summary of tethering type and reporter affinity for human and mouse NKG2D ligands to NKG2D (Raulet et al., 2013). *Also reported to be expressed as a transmembrane protein (Fernández-Messina et al., 2011).

1.4.3 Regulation of NKG2D ligand expression

The regulation of the NKG2D ligands is highly complex and seems to be controlled at multiple levels, presumably to allow for rapid presentation upon response to stress. There are reports of control being orchestrated at multiple points from transcription and mRNA stability to presentation at the cell membrane, with the majority of control in healthy cells being at the transcription and mRNA stability stages (M. Fuertes, et al., 2008; Ghadially et al., 2017). Expression of NKG2DLs on the cell surface is also known to be upregulated by various cellular pathways, including the DNA damage response (DDR) which is activated in response to tumorigenesis and infection (Gasser et al., 2005; Nikitin & Luftig, 2012; Ward et al., 2009; Weitzman et al., 2004).

1.4.4 NKG2D ligands and the DNA damage response

The link between DNA damage and immunity, through the induction of NKG2DLs, was first described in 2005 upon investigating the causes of NKG2DL upregulation in response to malignant transformation (Gasser et al., 2005). Whilst Gasser et al. originally thought that uncontrolled proliferation was the trigger for NKG2DL expression, they found that it was the DNA damage induced by genotoxic and replication stress, including ionising radiation and chemotherapeutic agents. This increase in surface expression could be inhibited by preventing the activation of the DDR through ATR/ATM inhibitors as well as ATR targeted siRNA and knock out experiments (Gasser et al., 2005). Whilst the link between the DDR and NKG2DL expression is well documented, the exact mechanism as to how this occurs remains unclear. Additionally, there is evidence of other cellular pathways being involved in the regulation of NKG2DL expression, as discussed in 1.4.5, and the full picture is yet to be elucidated.

1.4.5 Regulation of NKG2DL at various levels

Transcriptional regulation of NKG2DLs has been associated to a number of pathways due to binding sites identified within the promoter regions of the genes encoding NKG2D ligands. In humans, MICA and MICB promoters contain heat shock elements which when mutated result in a reduced level of protein detected in response to viral infection (Venkataraman et al., 2007). Additionally, there are HSE related sequences in the promoter of some ULBP genes (Eagle et al., 2006). NKG2DL transcription has also been linked to proliferation through E2F transcription factors although this was not seen to be consistent in humans, however inhibition of proliferation in the human colorectal cancer cell line, HCT116, via chemical agents or serum starvation did result in an increase in some NKG2DLs (Jung et al., 2012a). Furthermore, whilst the ULBP1-2 promoter regions have been shown to contain p53 response elements, as well as ULBP1-2 protein levels being increased upon p53 induction, p53 deficient H1299 cells were able to express NKG2DL on their surface and be specifically targeted for NK cell lysis, albeit to a lesser extent than the p53 WT cells (Gasser et al., 2005; Textor et al., 2011). This highlights that whilst some pathways do not have a key role in the expression of NKG2DL expression, they may help to amplify the signal.

Gasser and Raulet report that whilst levels of ULBP proteins increase in response to activation of the DDR, there is no increase in the rate of transcription of genes, however the degradation of the mRNA transcripts is inhibited (Raulet et al., 2013). Therefore suggesting that the DDR response mainly controls NKG2DL expression at the stage of mRNA stability. Additionally, miRNAs have been identified which regulate the expression of NKG2DLs, such as miR-175p, miR-20a and miR-93, which target MICA and MIB transcripts (Stern-Ginossar et al., 2008). Stern-Ginossar et al. have suggested that expression of these micro RNAs, as well as others, is a mechanism to suppress the basal expression of NKG2DLs transcripts (Stern-Ginossar et al., 2008).

Finally, there is also some evidence of NKGDL regulation at the protein level, however much of this data relates to murine NKG2DL, with minimal data available for human NKG2DL. Fuertes et al, have

reported that the majority of MICA protein levels are retained intracellularly via an unknown mechanism and thus prevents targeting via NK cells (M. B. Fuertes et al., 2008). This is additionally supported by Ghadially et al., who found that in patient samples, MICA/B protein is found in much greater quantities within the cell than on the surface, in both normal and tumour samples (Ghadially et al., 2017).

1.4.6 Immune evasion of NKG2D ligands by tumours

As discussed earlier, in order for a tumour to progress and eventually metastasise, it must evade the immune system, including the detection via NKG2DLs. This includes both repressing the expression of the NKG2DL, as well as removing them from the cell surface. The most characterised strategy for NKG2DL detection is through the removal of the ligands from the cell surface, also known as shedding (Xing & Ferrari de Andrade, 2020a; Zingoni et al., 2020). This has been reported to occur via two main mechanisms, proteolytic cleavage or packaging into extracellular vesicles (EVs). Furthermore, the soluble, shed NKG2DLs has also shown to have a role in general immunosuppression by binding to NKG2D, leading to internalisation of the receptor (Groh et al., 2002; Serritella et al., 2024; Vyas et al., 2017; Y. Zhang et al., 2023). The shedding of NKG2DLs and it's role in BiTE-mediated cytotoxicity is investigated in Chapter 6.

Moreover, TGF-β has been implicated in both reducing the transcription of MICA in glioma cells as well as reducing the expression of the NKG2D receptor on NK cells and CD8+ T cells (Friese et al., 2004). Additionally, the overexpression of miRNAs targeting MICA and MICB have also been suggested to be an NKG2DL-mediated immune evasion strategy, supported by the silencing of these miRNAs leading to an increase in NK-cell mediated cytotoxicity in breast cancer (J. Shen et al., 2017; Stern-Ginossar et al., 2008).

1.4.7 Selection of NKG2DLs as an immunotherapy target.

NKG2D ligands are upregulated in response to malignant transformation to indicate to the immune system that the cell is under stress and to induce clearance of the affected cell. The importance of this role is exemplified in the upregulation of multiple proteases to cleave the proteins from the surface of the tumour cell to evade recognition by in particular NK cells (Groh et al., 2002; Zocchi et al., 2012). Finally, the broad expression of NKG2D ligands on tumour cell types whilst being minimally expressed on normal, healthy cells should result in a highly selective pan-cancer treatment option, with minimal off-tumour effects (Ghadially et al., 2017).

1.5 Oncolytic Viruses

Oncolytic viruses (OVs) are able to infect and selectively replicate in tumour cells, whilst leaving normal cells unharmed (Figure 1.4). Once a tumour cell is infected, the virus is able to replicate and lyse to release progeny virions that can go on to initial subsequent rounds of viral infection and lysis. Upon cell lysis, there is also a release of damage associated molecular patterns (DAMPs), pathogen-associated molecular patterns (PAMPs) and TAAs which help to initiate an anti-viral as well as an anti-tumour response, aiding in the cancer immunity cycle.

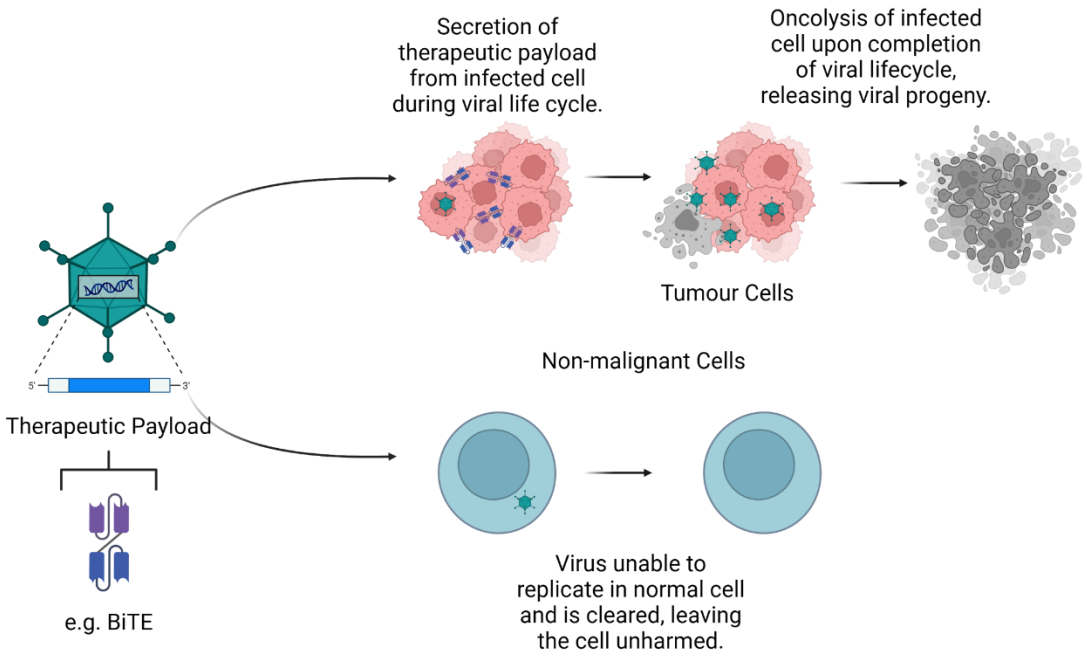

Figure 1.4: Viral oncolysis mechanism of action.

Viruses show a natural tropism for cancer cells with many of the described 'Hallmarks of Cancer' overlapping with ideally conditions for viral replication, (Seymour & Fisher, 2016). The innate anti-tumour effects of viruses have been investigated for decades, with observations that some cancer patients would see an improvement, sometimes going into partial remission, upon contracting an infectious disease, be that viral or bacterial (Pelner et al., 1958). The use of viruses in cancer therapy was not initially used for its oncolytic ability but instead as a strategy to stimulate the immune system, typically using attenuated viruses that are unable to replicate (Minton, 1973). However, a clinical trial with non-attenuated mumps virus in the 1970s showed minimal toxicity with 41% of patients showing complete regression of shrinking of tumours to less than half the original size in a variety of advanced tumour types (Asada, 1974). Therapeutic effects were often seen within days, prior to neutralisation of the virus by the host immune system. Unfortunately, follow up trials were not as successful and concerns about the regulation of using a wild-type viral pathogen as a therapeutic lead to a decline in the field.

The development of genetic engineering led to a revival of the field. Genetic manipulation allowed for the better understanding of viral biology, permitting the deletion of key viral genes to produce more tumour specific viruses, and increasing their safety profile (Tian et al., 2022). This is generally achieved by the deletion of genes whose function can be provided in *trans* via the tumour cell phenotype, such as the deletion of ICP 34.5 from herpes simplex virus (HSV) which is responsible for inhibiting the production of type I interferons which block viral replication (B. L. Liu et al., 2003). Interferon signalling is typically non-functional in tumours and so viral replication will be unaffected in tumour cells, whilst being susceptible antiviral interferon signalling in normal cells. Alternative ways to achieve cancer selectivity include the use of tumour-specific inducible promoters for key viral proteins, directed evolution to select for cancer specific clones; and altering the viral entry receptor to target those upregulated in cancer (Hashimoto et al., 2012; Kuhn et al., 2008; Russell & Peng, 2007; M. Yang et al., 2017).

Two OVs are currently approved for clinical use: H101 an engineered adenovirus (serotype 5) for the treatment of head and neck cancer in 2005; and more recently Talimogene Laherparevac (T-VEC), an oncolytic (Andtbacka et al., 2015; Liang, 2018) HSV virus approved for use in metastatic melanoma. In the phase III trial of T-VEC, overall response rate of 31.5% was achieved with T-VEC in combination with GM-CSF), compared to 6.4% with GM-CSF alone. Additionally, 16.9% of patients in the T-VEC + GM-CSF arm achieved complete remission with a median overall survival of around 2 years (Andtbacka et al., 2015, 2019). Additional trials using T-VEC in the treatment of other cancers as well as in combination with other agents, such as ICIs are ongoing and have shown promising results (T. Zhang et al., 2023).

1.6 Enadenotucirev (EnAd)

Enadenotucirev (EnAd), previously known as ColoAd1, is a Ad11p/Ad3 chimeric Group B adenovirus with selective oncolytic abilities. It contains a complete deletion of the adenovirus E3 region, responsible for host immune evasion, a partial deletion of the E4 region and a chimeric Ad3/Ad11p E2B region (Kuhn et al., 2008). EnAd was selected through a process called 'Directed Evolution' whereby a library of recombined adenoviral genomes was screened for candidates that were simultaneously highly potent in cancer cells and yet replicated poorly in normal cells (Kuhn et al., 2008). The initial library was produced by the co-infection of HT29 colorectal cells at high MOI to encourage recombination. This pool of virions was then used to infect fresh HT-29 cells and were serially passaged 18 times at the first sign of cytopathic effect (CPE) to select for the most potent candidates. Clones were isolated from the final pool and assessed for tumour selective potency, with EnAd being selected as the top candidate.

In a clinical trial for primary colon cancer, it was shown that EnAd could reach the tumour after intravenous delivery, with viral proteins detected in the nucleus of resected tumour cells indicating both successful infection as well as viral replication (Garcia-Carbonero et al., 2017a). This confirmed pre-clinical data showing the stability of EnAd in whole human blood, owing to the low prevalence of anti-Ad11p neutralising antibodies in the general population (Di et al., 2014; Marino et al., 2017). Further pre-clinical work is currently ongoing, aiming to 'arm' EnAd with immune stimulating components such as BiTEs targeting EpCAM, FAP, CD206 and folate receptor – β (FR-β) (Freedman et al., 2017, 2018; Scott et al., 2019).

1.7 Thesis Hypothesis and aims

1.7.1 Thesis hypothesis

We hypothesise that NKG2D ligands are ubiquitously expressed by cancer cell lines whilst being minimally expressed by normal, non-malignant cells, positioning them as an ideal candidate for an immunotherapy target, such as the NKG2D BiTE and TriTE alongside convention cancer therapies.

1.7.2 Thesis aims

1. Assess effect of conventional cancer therapies such as chemotherapy and radiotherapy on NKG2D ligand expression on the plasma membrane of both malignant and non-malignant cell lines to NKG2D ligand targeted treatments of malignant cells without sensitising non-malignant cells. (Chapter 3 and 4)
2. Assess the potency of NKG2D ligand targeting T cell engagers against a range of cancer types both in cell lines and in clinically relevant *ex vivo* samples. (Chapter 4)
3. Determine the feasibility of utilising an oncolytic virus to deliver the NKG2D ligand T cell engager to tumours to achieve both BiTE-mediated cytotoxicity as well as oncolysis. (Chapter 4)
4. Assess strategies to enhance the targeting of NKG2D ligands using co-stimulatory molecules, inhibiting the shedding of NKG2D ligands, and increasing the affinity of the ligand binding domain. (Chapter 5 and 6)

Chapter 2: Materials and Methods

2.1 Cell culture

2.1.1 Cell lines and general maintenance

Cell lines utilised within this thesis along with their culture conditions are summarised below in Table 2-1. Cell lines were cultured in static incubators at 37°C, 5% CO_2. Cell lines were routinely passaged every 3-4 days. For suspension cells, confluency was visually observed by the acidification of the media (using the colour change of the phenol red containing media as a visual determination). For adherent cells, confluency and visual confirmation of cell health and lack of contamination was determined via inspection with an inverted microscope. Adherent cells were sub-cultured as follows: removal of the cell culture media followed by a PBS wash to remove any remaining serum. Trypsin was used to dissociated cells and the cells were incubated at 37°C until the cells dissociated. Once dissociated, to neutralise the trypsin, complete media was added, and cells were split typically at a 1 in 10 ratio for 3-4 days. For functional assays, cells were seeded at 6.25 x $10^4/cm^2$, unless otherwise stated. Cell lines were routinely tested for mycoplasma contamination using the MycoAlert Detection Kit (LT07-318, Lonza).

Table 2-1: Details about cell lines used.

Cell line	Description	Media	Source
HEK293A	Human embryonic kidney cells (immortalised with Ad5-E1 region)	DMEM + 10% FBS	Gifted by Oxford Genetics, UK.
HEK293T	HEK293A subclone containing the SV40 large T antigen		

DLD-1	Human colorectal adenocarcinoma		ATCC
A549	Human lung adenocarcinoma		ATCC
U87 MG WT	Human glioblastoma		Dushek Lab
U87 MG CD58KO			
U2OS	Human osteosarcoma		Higgins Lab
MDA-MB-231	Human breast adenocarcinoma (triple negative)		ATCC
Panc-1	Human pancreatic carcinoma		ATCC
HT-1080	Human fibrosarcoma		Itoh Lab
SKOV-3	Human ovarian adenocarcinoma		ATCC
RPE-19	Retinal pigment epithelia		Higgins Lab
NHDF	Normal human dermal fibroblast		Lonza
JJN-3	Human multiple myeloma	RPMI + 10% FBS	Hammond La
MM1S	Human multiple myeloma		
U266	Human multiple myeloma		ATCC
CHO	Chinese hamster ovary		ATCC
Molt-4	Human acute lymphoblastic leukaemia		ATCC
CT26	Murine colorectal carcinoma		ATCC

PSN-1	Human pancreatic adenocarcinoma		ATCC
Raji	Burkitt lymphoma		ATCC
THP1	Human acute monocytic leukaemia		ATCC
Jurkat	Human T cell leukaemia	RPMI + 10% FBS + 1% NaPyr + 1% GlutaMAX	ATCC
K562	Human chronic myelogenous leukaemia		ATCC
HIEC-6	Human intestinal epithelial	OptiMEM + 4% FBS + 20 mM HEPES + 10 ng/mL EGF	ATCC
HUVEC	Human umbilical vein endothelial cells	Large Vessel Medium (M200500) + Low Serum Growth Supplement (S00310)	ThermoFisher Scientific
ARPE-19	Arising retinal pigment epithelial	DMEM:F12 + 10% FBS	Higgin's lab

2.1.2 Cryopreservation

Cell lines were cryopreserved at a concentration of 3 x 10^6 cells/mL in 1mL aliquots in 90% FBS, 10% DMSO. Vials were gradually cooled to -80^{o}C using a CoolCell (Corning) to control freezing at 1^{o}C/minute.

2.2 Molecular Cloning

2.2.1 Polymerase Chain Reaction (PCR)

To amplify specific DNA sequences, PCRs were carried out using either Q5 (M0492, NEB) or Phusion (F531L, ThermoFisher) polymerase master mixes in a final volume of 50 µL, following manufacturer's instructions. 1 ng of DNA was used as template and 0.5 µM of the forward and reverse primers. Primers were custom synthesised by Integrated DNA Technologies (IDT). Thermocycler program is detailed below in Table 2-2, using the ProFlex PCR system (ThermoFisher). When applicable, methylated template DNA was digested using 2 µL DpnI enzyme (R0176, NEB) following the PCR reaction, samples were incubated for 20 minutes at 37°C.

Table 2-2: General thermocycler settings for thermocycler.

1	Initial Denature	98°C, 30 seconds
2	Denature	98°C, 5 seconds
3	Annealing	Primer specific temp, 10 seconds
4	Extension	72°C, 20 seconds/kb product
	Repeat steps 2-4 for 30 cycles	
5	Final Extension	72°C, 2 minutes

2.2.2 Restriction digests

Restriction digests were carried out on plasmid DNA to linearise plasmids to enable cloning and viral recovery or for diagnostic purposes. Digests were carried out according to manufacturer's instructions (NEB) using the recommended digestion buffers. For restriction digests, plasmid DNA (200-500 ng) was digested with specified enzymes and corresponding buffers, in a final

volume of 10 µL, to generate a unique pattern of bands to allow for verification of the correct insertion of fragments. Samples were incubated at the optimal temperature for the enzymes (typically 37°C) for 1-2 hours before bands were visualised by gel electrophoresis. For digest of plasmid backbones for cloning or viral recovery, plasmids were digested at least for 2-3 hours if not overnight to ensure efficient cutting. When applicable, digested plasmids were treated with calf intestinal phosphatase (CIP, M0525, NEB) to remove the terminal phosphates to prevent re-ligation of the plasmid.

2.2.3 Agarose gel electrophoresis

DNA fragments from PCR reactions or restriction digests were visualised using gel electrophoresis. Size of the fragments was determined by comparison to a standard 1kb DNA ladder (NO468, NEB) of known DNA sizes. Briefly, samples were resolved using a 1% (w/v) agarose (A4718) gel containing 1X GelRed nucleic acid gel stain (BT41003, Biotium) in Tris-acetate-EDTA (TAE) buffer (recipes in appendix A). Samples were mixed with 6X loading dye and loaded into the gel submerged in 1X TAE buffer. The gel was run at 100V for 40-60 minutes or until the loading dye had reached the far end of the gel. DNA was visualised using the BioRad imager (Bio-Rad Laboratories).

2.2.4 Isolation of DNA fragments for plasmid assembly

DNA fragments, either from PCR amplifications or restriction digested were purified for plasmid assembly either using a gel extraction kit (T1020, NEB) if isolating from an agarose gel, or using a PCR clean-up kit (T1130, NEB) if isolating directly from a PCR reaction or restriction digest, following manufacturer's instructions. Bands isolated from an agarose gel were cut once the correct size had been determined.

2.2.5 HiFi Assembly

For assembly of new constructs, HiFi assembly was utilised by adding overlapping sequences when amplifying DNA sequences or by including them in newly synthesised DNA. Newly synthesised DNA was provided in the form of a 'g block' via IDT, USA. A 10 uL reaction using the 2X HiFi master mix (E2621, NEB) was prepared following manufacturer's instructions. Briefly, 50 ng of digested backbone was mixed at a 1:2 ratio with the linearised fragment and the master mix. This was then incubated at 50°C for 1 hour.

2.2.6 Bacterial transformation

Once thawed, 48uL of 10-B E.coli are mixed with 2 µL of the assembly reaction product and incubated on ice for 10 minutes. Cells were subjected to heat-shocked at 42°C for 45 seconds and then returned to the ice for 2 minutes. 500 µL of SOC recovery media (15544-034, ThermoFisher) was added to each reaction and then incubated at 37°C on a bacterial shaker for 30 (ampicillin resistant) or 60 minutes (kanamycin resistant). Cultures were spread onto agar plates containing the appropriate antibiotic and incubated at 37°C overnight. Agar plates were prepared using LB broth with ager (L2897, Merck) with either 50 µg/mL of kanamycin sulphate (K1377, Merck) or ampicillin sodium salt (A9518, Merck).

2.2.7 Plasmid preparation and purification

To select a correctly assembled plasmid, individual bacterial colonies were picked from the agar plate and grown overnight in 5 mL of LB broth (L3022, Merck) overnight at 37°C, 200 RPM. Plasmid DNA was then purified using the Monarch® Plasmid Miniprep Kit (T1010, NEB) following manufacturer's instructions. Correct plasmid sequence was confirmed using diagnostic restriction digest and/or Sanger sequencing.

For larger DNA preparation, midi preps or maxi preps were carried out. As with the mini prep set up, bacterial preparations were set up overnight, 50mL for midi prep, 200 mL for maxi prep and purified

using the QIAGEN Plasmid Plus Midi Kit (12943, QIAGEN) or Maxi Kit (12963, QIAGEN), following manufacturer's instructions.

2.2.8 DNA quantification

DNA was quantified using the Nanodrop 2000 spectrophotometer (Thermo Fisher Scientific). The machine was blanked using the elution buffer of the DNA prior to sample measurement.

2.2.9 Sanger sequencing

To confirm the sequence of newly cloned plasmids and detect potential point mutations, samples were sent for Sanger sequencing by Genewiz (UK) using custom primers following the service providers instructions. Reads were aligned to the predicted sequence using SnapGene software.

2.3 Protein production and purification

2.3.1 General transfection

HEK293A/T cells were seeded for transfection in an appropriate culture vessel, one day prior to transfection, at a density of 6.26 x $10^4/cm^2$. Plasmids were transfected using either Lipofectamine 2000 (11668019, ThermoFisher) or PEI MAX (40 kDa, 24765, Polysciences). Typically, 0.4 µg DNA/cm^2 was utilised with a 1 to 3 ratio to the transfection reagent. Plasmid DNA and the transfection reagent were diluted separately into OptiMEM (31985062, ThermoFisher) and incubated at RT for 5 minutes. These were then combined and incubated for a further 20 minutes at RT to allow the formation of transfection reagents. Complexes were added to cells gently to avid distortion of the cell monolayer.

2.3.2 Production of BiTEs and TriTEs

To increase protein yield, additional serum free media (10% of total volume added to flask) was added to the transfections 24 hours post transfection. 72 hours post transfection, supernatant was collected and clarified via centrifugation, 500 x g for 5 minutes. Supernatants were then

concentrated around 50-fold using 10 kDa MWKO Amicon Ultra-15 filter (UFC9010, Merck) prior to aliquoting and storing at -80°C or further purified using nickel beads (detailed in 2.3.3).

2.3.3 Purification of His-tagged proteins via immobilised metal affinity chromatography.

Clarified supernatants were incubated with Ni-NTA beads (30230, QIAGEN) overnight with agitation. The following day the supernatant-beads mixture was passed through a chromatography column (7372512, Bio-Rad), washed with 20 mM imidazole in HBS and eluted with 200 mM imidazole in HBS. Elute was injected into a 10 kDa molecular weight cut off dialysis cassette (Slide-A-Lyzer™ Dialysis Cassettes, 66810, ThermoFisher) to remove imidazole with 3-rounds of dialysis, using 500 mL of PBS each time. Dialysed protein was concentrated in a 10 kDa amicon filter prior to aliquoting and storage at -80°C.

2.3.4 SDS-PAGE

Samples were mixed with Laemmli buffer (J61337, Alfa Aesar) and boiled at 95°C for 10 minutes to denature the proteins. Samples were then loaded onto a premade SDS-PAGE gel (Mini-PROTEAN TGX precast gels, Bio-Rad), along with a protein ladder (26619, PageRuler Plus, ThermoFisher) and ran at 120 V for 60 minutes, in 1X SDS running buffer (see appendix A), or until the loading dye had fully run through. Gels were either transferred to a nitrocellulose membrane for western blotting (2.3.6) or treated with Instant Blue to visualise total protein (2.3.7).

2.3.5 Native PAGE

Samples were mixed with sample buffer (BN2003, Life Technologies) then loaded onto a premade SDS-PAGE gel (Mini-PROTEAN TGX precast gels, Bio-Rad), along with a protein ladder (LC0725, Native Mark unstained protein standard, Life Technologies) and ran at 120 V for 120 minutes, in 1X native running buffer (see appendix A). Gels were either transferred to a nitrocellulose membrane for western blotting (2.3.6) or treated with Instant Blue to visualise total protein (2.3.7).

2.3.6 Western Blotting

Resolved proteins were transferred from the SDS-PAGE membrane to a 0.2 µm nitrocellulose, membrane using the TransBlot turbo transfer system (1704158, BioRad) and transfer packs (1704158, BioRad), following the manufacturer's instructions. Effective transfer efficiency was determined mainly by the successful transfer of the pre-stained protein ladder but additionally through Ponceau staining (22001, Biotium) prior to blocking.

Membranes were blocked using the EveryBlot Blocking Buffer (12010020, BioRad) for 5 minutes at RT, following manufacturer's instructions. Membranes were then incubated with a primary antibody (see Table 2-3 for details), diluted in blocking buffer, overnight at 4^{o}C. Membranes were washed thrice with PBS-T and further incubated with an appropriate secondary antibody conjugated to horseradish peroxidase (HRP) for 1 hour at RT. Membranes were again washed thrice with PBS-T (PBS + 0.05% Tween 20 (P1379, Merck)) before the addition of substrate (West Dura Extended Duration Substrate, 34075, ThermoFisher). Membranes were incubated with the substrate for up to 2 minutes before imaging or chemiluminescence using the BioRad imager.

Table 2-3: Antibodies utilised for western blot.

Target	Clone	Species	Dilution Factor	Supplier	Catalogue Number
Chk1	2G1D5	Mouse	1,000	Cell Signalling Tech.	2360
Chk1-P (Ser345)	133D3	Rabbit	1,000	Cell Signalling Tech.	2348
His tag	3D5	Mouse	5,000	Invitrogen	930-25
Mouse IgG	-	Horse	10,000	Cell Signalling Tech.	7076
Rabbit IgG	-	Goat	10,000	Cell Signalling Tech.	7074

2.3.7 Coomassie Protein staining

Resolved proteins were visualised using the Coomassie InstantBlue protein stain (ab119211, abcam). SDS-PAGE gels of resolved proteins were incubated in the InstantBlue solution of 15 minutes with gentle rocking. Gels were imaged using the BioRad imager.

2.3.8 His tag ELISA

The concentration of BiTEs and TriTEs produced was determined using a commercially available His-Tag competitive ELISA kit (L00436, GenScript) following the manufacturer's instructions. Briefly, diluted samples or provided standards were added to a His-tag protein coated plate along with a monoclonal anti-His antibodies. The level of antibody binding was negatively correlated to the amount of His-tagged protein present in the sample or standard. The concentration of the BiTEs and TriTEs was determined using the standard curve and GraphPad Prism Software.

2.3.9 MICA binding ELISA

To determine the ability of molecules to bind to NKG2D ligands prior to using cell lines, constructs were tested via ELISA for their ability to bind to recombinant MICA. ELISA plates were coated with recombinant MICA protein (50 ng/well, 1300-MA-050, Bio-Techne) overnight at 4^{o}C. Plates were then washed thrice with PBS-T to remove unbound antigen prior to blocking with 1% BSA in PBS (1 hour, RT). After washing thrice, diluted samples were added and incubated at RT for 2 hours with gentle agitation. Plates were washed five times prior to addition of an HRP-conjugated anti-his antibody (Direct-Blot™ HRP anti-His Tag, 362614, Biolegend, 1 in 15,000). Plates were again washed five times prior to the addition of TMB substrate (N301, ThermoFisher) for 10-15 minutes. The reaction was stopped using 0.18 M sulphuric acid (339741, Merck) and absorbance measured at 450 nm.

2.3.10sMICA and sMICB ELISA

Soluble MICA and MICB were detected using the Human MICA DuoSet ELISA kit (DY1300, Bio-Techne) and Human MICB DuoSet ELISA kit (DY1599, Bio-Techne), following Manufacturer's instructions.

2.4 Viral protocols

2.4.1 General note of insertion of transgene in viral plasmid and viral plasmid preparation

Transgene expression cassettes encoding the BiTEs or TriTEs were inserted into a AsiSI (R0630, NEB) and SbfI (R3642, NEB) linearised parental EnAd plasmid (EnAd2.4) using HiFi assembly (previously described in 2.2.5). Primers were designed to amplify expression cassettes to include the CMV promoter from the pSF expression plasmid or to introduce a splice acceptor sequence (SA) to allow expression to be controlled via the major late promoter within the viral (controls that the expression of the transgene will only occur in the second stage of the viral lifecycle). Correct insertion was confirmed via diagnostic restriction digest and Sanger sequencing. Prior to virus rescue, 5 µg of each plasmid was linearised using the restriction enzyme AscI (R0558, NEB) to linearise the viral genome and expose the ITRs (inverted terminal repeats). Samples were incubated at 37°C overnight to ensure efficient digestion and heat treated at 80°C for 20 minutes to inactivate the enzyme and sterilise the sample prior to transfection.

2.4.2 Transfection of linearised viral plasmid for viral rescue

HEK293A cells were seeded in T25 (1.5 x 10^6 cells/flask) the day prior to transfection using Lipofectamine 2000 (11668019, ThermoFisher Scientific). Briefly, 5 µg of the linearised EnAd plasmid DNA were diluted to 50 µL in OptiMEM (Gibco). Alongside this, 20 µL of Lipofectamine was added to 30 µL OptiMEM (1:4 ratio of DNA to Lipofectamine). These samples were incubated for 5 minutes at RT before being combined and then incubated for a further 20 minutes at RT. During these incubations, the HEK293A cells were washed with PBS and 4 mL of OptiMEM added to the flask. After the incubation, the transfect complexes were added to the flask for 4-6 hours. The OptiMEM and remaining complexes are then replaced with DMEM containing 2% FBS. Flasks were observed every other day to check upon the development of viral plaques known as cytopathic effect (CPE).

Upon extensive CPE, supernatant and cells were harvested, subjected to three freeze thaw cycles and then centrifuged (500 x g, 5 minutes) to remove cell debris. Clarified viral supernatant was aliquoted and stored at -80^{o}C until required.

2.4.3 Clonal isolation and large-scale preparations.

To obtain a stock originating from a single viral particle, to reduce variation within the viral prep, the initial clarified viral supernatant was serially diluted and used to infect A549 cells. The process of diluting the virus and infecting A549 cells is carried out in the same way as for the TCID50 assay which is explained in more detail below (2.4.4). Wells were identified that clearly contained one single plaque. One well was selected and serially diluted again to ensure a clonal viral stock was identified. This stock was then expanded by serially infecting fresh A549s in larger scale vessels. The freeze thaw cycles, and clarification was repeated as for the initial viral supernatant. The viral supernatant was then aliquoted into smaller aliquots, for use in functional assays, and stored at -80^{o}C.

2.4.4 Titre determination via TCID50

To determine infectious titres of adenoviral stocks a Tissue Culture Infectious Dose (TCID50) assay was carried out. A549 cells were seeded in a 96 well plate (1.5 x 10^4 cells/well) one day prior to infection. In a total volume of 1.2 mL of DMEM supplemented with 2% FBS, 8 serial dilutions (1 in 10) of adenovirus stock were generated. 100 uL of each dilution was added to the A549 cells with 10 replicates per dilution. Virus free DMEM supplemented with 2% FBS was added to the extra wells as a negative control for viral infection. 5 days post infection, each well was assessed via an inverted light microscope for signs of CPE. The highest dilutions showing CPE were counted and infectious particles (TCID50/mL) was calculated using the Karber formula.

$$\text{Titre (TCID50/mL)} = 10^{1 + D(S - 0.5)}$$

D = log(dilution factor)

S = sum of the ratios of wells with infection to infection-free wells

2.5 Flow Cytometry

2.5.1 Adherent cell preparation

To prevent the removal of the extracellular domain of membrane protein caused by trypsin cleavage, Cells were dissociated with enzyme-free dissociation buffer (13151014, Gibco) following PBS washing. Cells were counted and aliquoted into 96 well V-bottomed plates for staining.

2.5.2 Surface protein staining

Staining was performed in 96 well V-bottom plates with 100 000-200 000 cells/well. All centrifugation steps were carried out at 400 x g for 5 minutes. Briefly, cells were washed twice with PBS prior to blocking for 10 minutes at room temperature with either MACS buffer or, for immune cells, FcR block (130-059-901, Miltenyi Biotec) diluted 1 in 100 in MACS buffer. Cells were incubated for the 30 minutes at 4°C with the primary antibodies, diluted in MACS, in a volume of 50 uL per well. Details of antibodies are listed below in Table 2-4. Where a secondary antibody stain was required, cells were washed twice with PBS before the secondary stain (50uL/well, 30 minutes at 4oC). Once stained, cells were washed twice with PBS prior to fixing with 10% neutral buffered formalin for 10 minutes at room temperature. Cells were stored in MACS buffer and protected from light at 4oC until analysis. Cells were analysed on the Attune™ NxT Flow Cytometer (ThermoFisher Scientific).

2.5.3 Intracellular staining

Where intracellular staining was carried out post extracellular staining, cells were instead fixed with 4% PFA. Cells were then washed twice with Perm/Wash to permeabilise the cells. Cells were then incubated with primary antibodies for 30 minutes at 4°C and then washed twice with PBS before being resuspended in MACS buffer for analysis as described above.

2.5.4 Biotinylation of NKG2D-Fc and IgG1-Fc for NKG2D ligands staining

To determine the overall expression level of all eight NKG2D ligands, a recombinant human NKG2D-Fc chimera (rhNKG2D-Fc, Phe78 - Val216, 1299-NK-050, R&D Biosystems) was utilised which contains an IgG1 Fc region, allowing for a homodimer to be formed. To enable detection, the protein, along with a human IgG1 control (rhIgG1-Fc, 1299-HG,100, R&D Biosystems), were biotinylated using the Biotin Conjugation Kit, following manufacturer's instructions (ab201795, Abcam). Biotinylated proteins were stored at 4°C until use. Cells were stained as detailed in 2.5.3, with the biotinylated NKG2D or IgG1 as a primary stain, followed by streptavidin-PE for detection via flow cytometry (Figure 2.1).

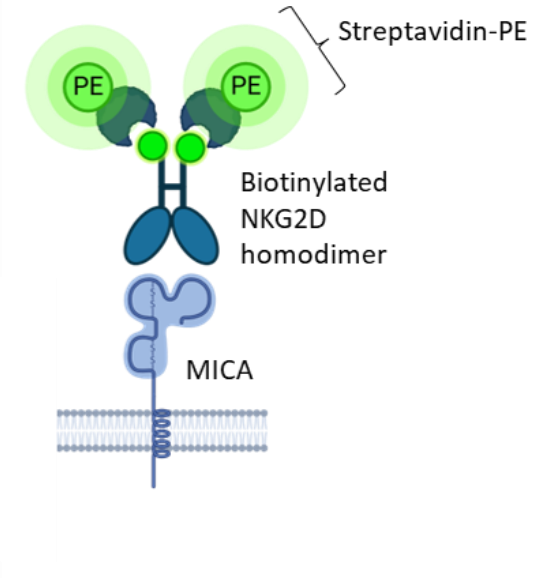

Figure 2.1: Schematic of NKG2D ligand staining utilising the NKG2D ectodomain.

2.5.5 Antibodies

Table 2-4: List of antibodies used for flow cytometry.

Target	Clone	Dilution	Isotype	Fluorophore	Supplier	Cat. #
Histidine Tag	J095G46	1 in 100	IgG2a, mouse	PE	Biolegend	362603
CD4	OKT4	1 in 200	IgG2b, mouse	APC, FITC, PE	Biolegend	317416, 317410, 317410
CD8a	HIT8a	1 in 200	IgG1, mouse	APC	Biolegend	300912
CD25	BC96	1 in 200	IgG1, mouse	PE, PE-Cy7	Biolegend	302606, 302612
CD69	FN50	1 in 200	IgG1, mouse	FITC, BV605	Biolegend	310904, 310938
4-1BB	4B4-1	1 in 100	IgG1, mouse	BV421	Biolegend	309822
CD107a	H4A3	1 in 100	IgG1, mouse	PE-Cy7	Biolegend	394110
Granzyme B	GB11	1 in 100	IgG1, mouse	Pacific Blue	Biolegend	515408
Perforin	BD48	1 in 100	IgG1, mouse	PE	Biolegend	353304
IFN-γ	4S.B3	1 in 100	IgG1, mouse	FITC	Biolegend	502506

CD45	HI20	1 in 100	IgG1, mouse	FITC	Biolegend	304006
EpCAM	9C4	1 in 100	IgG2b	BV421	Biolegend	324219
, FAP	427819	1 in 100	IgG1, mouse	PE	R&D Systems	MAB3715
MICAB	6D4	1 in 100	IgG2a, mouse	APC	Biolegend	320908
rhNKG2D-Biotin	-	1 in 100	IgG1-Biotin	-	R&D Biosystems	1299-NK-050
Streptavidin-PE	-	1 in 100	-	PE	ThermoFisher	SA10041

Table 2-5: List of isotypes used for flow cytometry.

Target	Clone	Fluorophore	Supplier	Cat. #
Mouse	IgG1	APC, PE-Cy7, FITC, BV605, BV421, Pacific Blue, PE.	Biolegend	400119, 400108, 400112, 400151, 400126, 400162, 400158
Mouse	IgG2a	PE, APC.	Biolegend	400212, 400220
Mouse	IgG2b	APC, FITC, PE, BV421.	Biolegend	402206, 402208, 402204, 400342
	IgG1-Biotin	-	R&D Biosystems	10-HG

2.5.6 Flow cytometry data analysis

Flow cytometry data was analysed using FlowJo software (BD Biosciences). An example of a typical gating strategy is detailed in Figure 2.2. Live Dead gating was determined by live dead controls generated by boiling half of a sample for 5 minutes to achieve a sample with both live and dead cells.

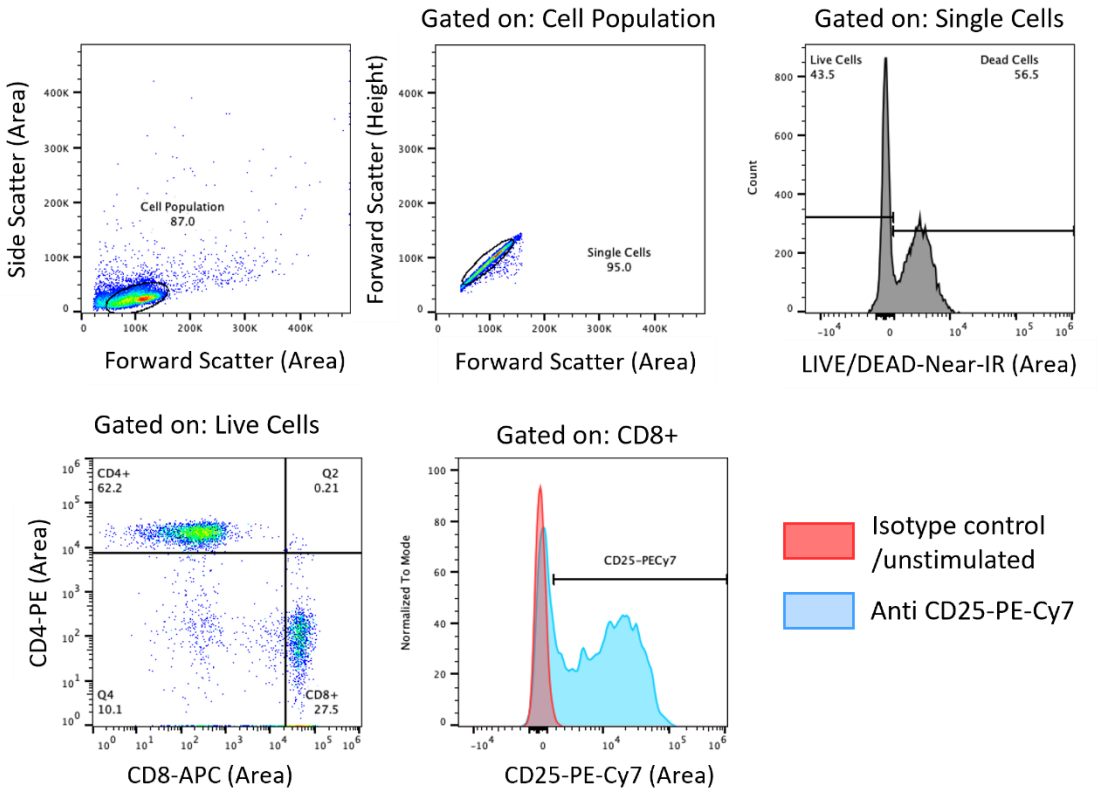

Figure 2.2: Exemplary gating strategy for flow cytometry.

2.6 Immune cell isolation and assays

2.6.1 General statement

Leukocyte cones utilised were acquired from the NHS Blood and Transplant Services (Oxford, UK). Informed consent was obtained at the time of donation by the NHSBT. Ethical approval for the study was obtained from the Health Research Authority (REC reference 19/LO/1848; IRAS ID 253836).

2.6.2 Isolation of lymphocytes and monocytes from leukocyte cones

Lymphocytes and monocytes were isolated from PBMCs sources from leukocyte cones using double-density gradient centrifugation. Briefly, blood from the leukocyte cone was diluted in PBS and overlayed on top of 15mL Ficoll Paque Plus (GE17-1440-02, GE Healthcare) in a SepMate™-50 tube (85450, Stemcell Technologies) and then centrifuged at 950 x g for 30 minutes. The PBMCs accumulate at the interface between the plasma and Ficoll. The PBMC layer was collected and washed three times with PBS (1st spin, 950 x g for 10 minutes, 2nd spin – 450 x g for 10 minutes, 3rd spin – 200 x g for 10 minutes).

To separate the PBMCs into lymphocytes and monocytes, they were subjected to an additional density gradient using Percoll PLUS. Washed PBMCs were resuspended in RPMI media supplemented with 10% FBS. Resuspended PBMCs were overlayed with Percoll PLUS (46%, 285 mOsm, GE Healthcare) and centrifuged at 950 x g for 30 minutes with no braking. The lymphocyte (at RPMI and Percoll interface) and monocyte (pellet) were separately collected and washed three times with PBS (same spin conditions as for PBMC washing). Monocytes were seeded in low adherence flasks in X-VIVO-10 media supplemented with 2% human serum at a density of 3-4 x 106 cells/mL. Lymphocytes were cryopreserved at a density of 3 x 10^7 cells/mL in freezing media.

2.6.3 T cell isolation

T cells were isolated from thawed lymphocytes utilising a negative selection method. Frozen lymphocytes were thawed in RPMI supplemented with 10% FBS at least 16 hours prior to use. T cells were isolated using the Pan T cell isolation kit (130-096-535, Miltenyi Biotec), following manufacturer's instructions. Briefly, cells are incubated with a biotinylated antibody cocktail targeting a variety of immune cell markers except for T cells markers. Streptavidin linked magnetic beads are then incubated with the cells. The suspension is then passed through a magnetic LS column (130-042-401, Miltenyi Biotec) to allow the removal of cell types other than T cells.

2.6.4 BiTE/virus efficacy assay

To determine the efficacy of BiTEs, co-culture experiments were set up using PMBC-derived T cells and cancer cell lines at an effector to target ratio of 5 to 1. Adherent target cells were seeded and allowed to settle overnight. The following day, freshly isolated T cells were resuspended in RPMI + 2% FBS and combined with target cells alongside the relevant treatments or viral particles. CD3/CD28 DynaBeads (1uL/well, 11131D, ThermoFisher Scientific) were used as a positive control for T cell activation. Cells were incubated at 37°C, 5% CO2 until harvested for analysis.

2.6.5 Characterisation of T cell activation by flow cytometry

T cell activation was determined at a minimum by surface expression of CD25 and CD69 via flow cytometry. T cells were gated for using CD4 and CD8a, and live cells were gated for using sample in which 50% of the cells were killed via boiling. To assess production of granzyme B, perforin and interferon γ, 4-6 hours prior to staining, cells were treated with GolgiStop (Monensin, 554724, BD Biosciences) and GolgiPlug (Brefeldin, 555029, BD Biosciences) to prevent the secretion into the supernatant. T cell mediated cytotoxicity of the target cells was determined using either XTT assay (described in 2.6.6), or via flow cytometry determining the percentage of live target cells (CD4-CD8-).

2.6.6 Viability assay via XTT assay

Viability was determined with the XTT assay (11465015001, Roche) following Manufacturer's instructions. Briefly, XTT solution was prepared by adding 100 µL to 5 mL of Solution B and 10 mL PBS. Target cells were washed once with PBS prior to addition of XTT solution (150 µL/well). Cells are then incubated at 37°C for 1-2 hours. 450 nm absorbance was then determined using the VarioScan plate reader (ThermoFisher). Results were normalised to the untreated control to determine viability.

2.6.7 Cytotoxicity – xCELLigence

The xCELLigence machine (Agilent) is used to analyse cytotoxicity in real time by measuring impedance over time. For all experiments, target cells were seeded the day prior to allow the cell to adhere to the plate. Subsequently, the impedance was measured for up to 6 days.

2.7 Ex vivo tumour models

2.7.1 General statement

Ascites samples and colorectal liver metastases utilised were acquired with informed consent from routine procedures carried out at Churchill Hospital, Oxford. Ethical approval for these studies was obtained from the Health Research Authority (Ascites samples - REC: 19/SC/0173 ORB 20/A013; Colorectal liver metastases - REC: 21/YH/0206 – 17/LS/PJ). For the ascites samples, the cancer type of the patient as well as other details such as their treatment history are unknown.

2.7.2 Processing ascites samples

Processing of ascitic samples to isolate the cellular fraction from the ascitic fluid was carried out by Dr Gulsah Albayrak. Briefly, ascites samples were transferred into vessels for centrifugation to pellet the cellular fraction (400 x g, 10 minutes). Acellular supernatant (ascitic fluid) was retained and stored in aliquots at -20^{o}C. Ascitic cells were washed once with PBS prior to treatment with red blood cell lysis buffer (10 minutes, 4^{o}C, 158904, Qiagen). Cells were washed twice with PBS again, prior to cryopreservation in FBS + 10% DMSO (20 x 10^6 cells/mL, 1mL/vial).

2.7.3 Slicing colorectal liver metastases with vibratome

Colorectal liver metastases were collected from the theatre just after surgeries at the Churchill Hospital in Oxford under ethics number: EC: 21/YH/0206– 17/LS/PJ, Start: 11/11/2021, End: 11/11/2026. Consenting was done by Katy Gordon-Quayle and Martin Pirkl. Samples were subsequently brought to Pathology in the John Radcliff Hospital, Oxford, for assessment by

pathologists. Tumours were cut into evenly sized blocks (around 1 cm^3) and mounted onto a flat piece of thin plastic. Tumour blocks were then embedded in 4% low melting point agarose (16520050, ThermoFisher) and left to set at RT. Following this, the embedded tumour blocks were fixed to the vibratome stage. Tumour blocks were sliced at 250 µm thick and transferred to a plate initially containing 500 µL of slice media overnight. The following day, media is changed to slice media containing the 1 nM free BiTE. Samples of media was taken at day 2, 4 and 6 for IFN-γ ELISA.

2.7.4 IFN-γ ELISA

Concentrations of IFN-γ released in tissue slice experiments was measured using the ELISA MAX kit (430104, Biolegend), following Manufacturer's instruction. Briefly, plates were coated with the IFN- γ capture antibody overnight. The following day, plates were washed, blocked with 1% BSA in PBS, followed by incubation with diluted samples for 2 hours with 2 hours of agitation at RT. Once plates are washed again, samples are detected using the biotinylated detection antibody followed by streptavidin-HRP. To detect bound antibody, TMB substrate (Thermo Fisher Scientific, USA, #N301) was added and incubated for 10-15 minutes before being stopped using 0.18 M sulphuric acid (Sigma Aldrich, USA, #339741). 450nm absorption was then measured in a plate reader and concentrations were interpolated from the standard curve.

2.8 Pre-treatment assays

2.8.1 Radiation

Cell lines were seeded into culture vessels at a density of 6.26 x $10^4/cm^2$ the day before treatment. Vessels were then exposed to the relevant dose of ionising radiation using a caesium 137 irradiator or left untreated as a mock. Cells were then incubated for the required period prior to analysis.

2.8.2 Chemical treatment

Cell lines were seeded into culture vessels at a density of 6.26 x $10^4/cm^2$ the day before treatment. Suspension cell lines were seeded at 90% of the typical volume to allow for the drug to be added at a

later point. Cells were then treated with the relevant concentration of drug as well as the appropriate vehicle control.

Chapter 3: Determine methodologies to adjust the expression of NKG2DLs in human tumours.

3.1 Introduction

NKG2D ligands (NKG2DLs) refers to a family of eight proteins, divided further into MICA/B and the ULBP proteins 1-6. It is generally thought that NKG2DLs are expressed on all cancer cells due to the 'stressed' tumour microenvironment (TME), whilst being minimally expressed on normal, healthy cells. This chapter will focus on establishing the breadth of cancer cell types that NKG2DLs are expressed on and assess the effect conventional treatments have on their cell surface expression.

Whilst it was initially thought that NKG2DL expression was linked to proliferation, Gasser et al. discovered almost 20 years ago that hyperproliferation was insufficient to induce expression in normal cells (Gasser et al., 2005). They then identified that activation of the DNA damage response pathway was a critical regulator, showing the upregulation of NKG2DLs through various chemotherapeutic compounds as well as radiation. Inhibition of ATM, ATR or Chk1, through genetic or pharmacological methods, prevented this, demonstrating the role of DNA damage in the induction of NKG2DL expression on the plasma membrane.

As briefly discussed earlier, ionising radiation and chemotherapy are the most commonly used treatments for cancer patients. Both therapies have been shown to activate the DNA damage response pathway due to either direct DNA breaks caused by the treatment itself, as is the case for ionising radiation, or through the production of replication stress caused by the inhibition of essential enzymes or the cross-linking of DNA through chemotherapy (O'Connor, 2015; Woods & Turchi, 2013; Y. Zhang, Fu, et al., 2022). One of the most prominent examples of this is 5-fluorouracil (5-FU), which inhibits thymidylate synthase when converted into fluorodeoxyuridine monophosphate (FdUMP). This in turn inhibits the production of deoxythymidine triphosphate (dTTT), one of the four

nucleotides required for DNA synthesis, inducing replicative stress (Grem, 2000). dTTT is not required for RNA synthesis, therefore non-replicating cells are spared. Additionally, FdUMP which can be directly incorporated into DNA during synthesis, causing DNA breaks (Huehls et al., 2016).

An additional group of therapeutic chemicals linked to DNA damage are histone deacetylase inhibitors (HDACi), which inhibit enzymes responsible for condensing areas of the genome to epigenetically repress transcription (Bolden et al., 2006; Bose et al., 2014). Therefore, much of the genome is more accessible, leading to changes in gene expression (Bolden et al., 2006). Additionally, the more open chromatin structure allows for greater sensing of DNA damage, thereby increasing the activation of key DDR proteins (Robert & Rassool, 2012). Panobinostat, also known as Farydak, is a HDACi that is used in conjunction with other drugs in the treatment of multiple myeloma ("Panobinostat Approved for Multiple Myeloma," 2015).

Whilst the development of these treatments in cancer was intended to trigger apoptosis or senescence in cancer, resistance is often seen. Therefore, their use in combination treatment strategies is being extensively evaluated. In Chapter 4 of this thesis, we combine ionising radiation and chemotherapy, to increase cell surface NKG2DL expression via activation of the DNA damage response pathway, and a Bi-/Trispecific T cell engager targeting NKG2DLs(Kim et al., 2006; Sauer et al., 2017a; M. J. Shen et al., 2017; Weiss et al., 2018). Kim et al. found that in a number of different cell lines, ionising radiation induced NKG2DL expression, both at the mRNA and protein level at the cell surface, making them more susceptible to NK cell-mediated cytotoxicity (Kim et al., 2006).

This chapter will focus on the establishment of NKG2DLs being a pan-cancer target and whether the ligand levels can be manipulated through commonly used therapeutic treatments. In addition, we will investigate the effect of these treatments on normal cells, using non-malignant cell lines.

3.2 Chapter Hypothesis and Aims

3.2.1 Chapter Hypothesis

We hypothesis that all cancer cell lines will express high cell surface levels of NKG2DLs, which can be further increased using conventional cancer therapies.

3.2.2 Chapter Aims

1. Screen a range of both cancer and non-malignant cell lines for NKG2DL expression.

2. Identify conventional cancer therapies to combine with NKG2DL targeting Bi/Trispecific T cell engager mediated killing for potential synergies.

3.3 Results

3.3.1 NKG2DLs are expressed on a variety of different human cancer cell lines.

In order to determine how widely NKG2DLs are expressed amongst human cancers, a range of cell lines derived from a range of different cancer types including leukaemia, lymphoma, sarcomas and epithelial cells, were screened for surface expression of NKG2DLs. Whilst there are several antibodies available for some of the individual ligands, especially for MICA and MICB, some of the ligands are not able to be distinguish from each other using antibody-based techniques, due to their highly similar structure. To detect the total levels of NKG2DLs on the cell surface, we utilised a commercially available recombinant NKG2D receptor, which was biotinylated and then detected using streptavidin conjugated to PE, to allow detection via flow cytometry. A biotinylated IgG1 was used in replacement of an isotype control. A better control would have been a mutated form of NKG2D which was unable to bind to the ligands, however this was not commercially available.

As shown in Figure 3.1 and Table 3-1, expression of NKG2DLs were detected in all human cell lines, with minimal but varying non-specific binding of the IgG-biotin or streptavidin-PE alone, with the exception of all three multiple myeloma cell lines and Raji cells. Representative flow cytometry plots are shown for each cell line tested (Figure 3.1A).

Epithelial, leukemic, sarcoma and some lymphoma derived cell lines in general expressed high levels of NKG2DLs with the highest expressing cell lines being K562, a chronic myelogenous leukaemia (CML) cell line, and Jurkat, a leukemic T cell line. To show the specificity of the recombinant NKG2D protein, non-human cancer cell lines, CHO and CT26, were used as the NKG2DLs are reported to have significantly different structures (Raulet et al., 2013). As expected, both cell lines showed minimal (Figure 3.1).

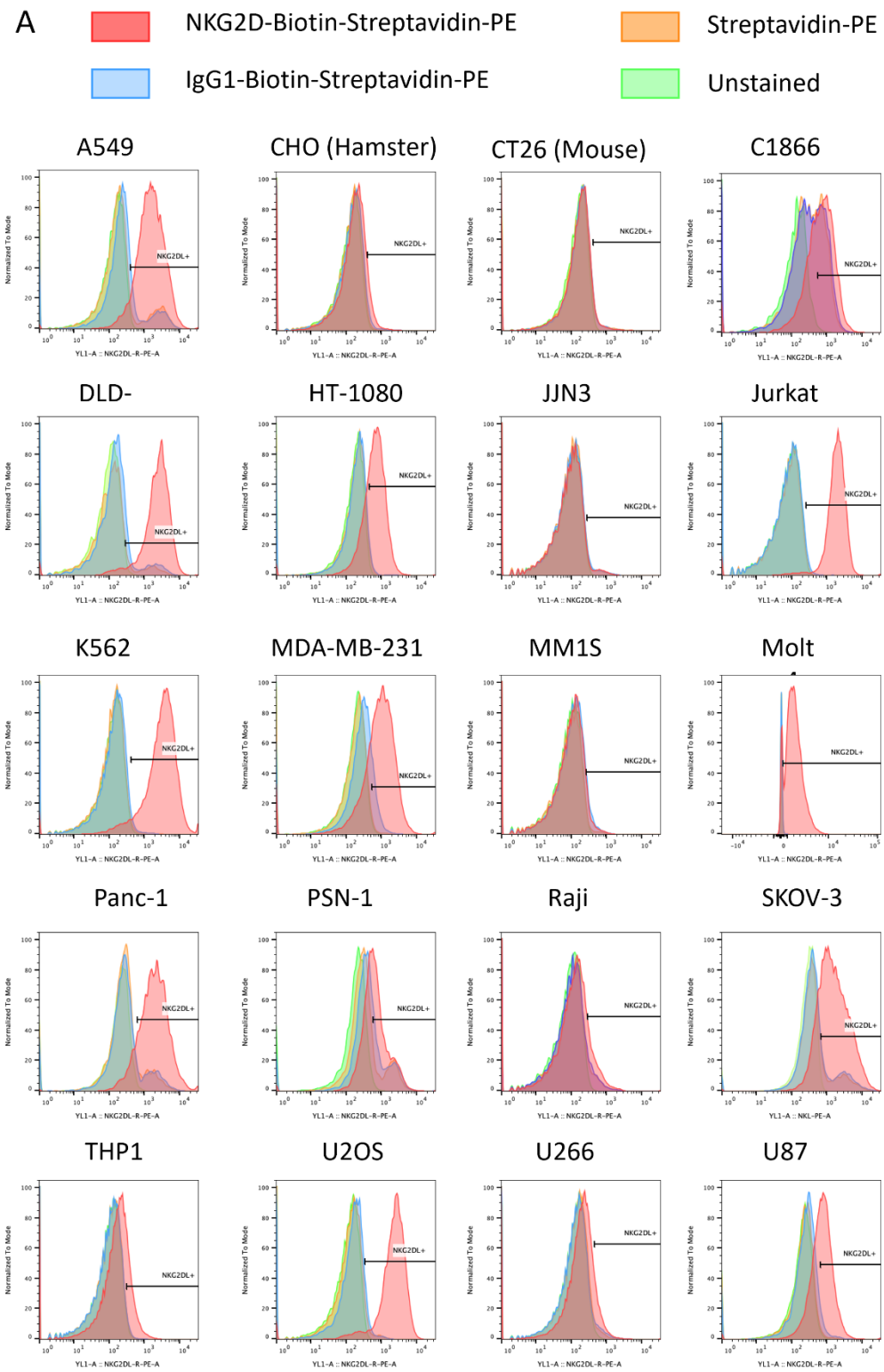
A
NKG2D-Biotin-Streptavidin-PE
Streptavidin-PE
IgG1-Biotin-Streptavidin-PE
Unstained
A549
CHO (Hamster)
CT26 (Mouse)
C1866
DLD-
HT-1080
JJN3
Jurkat
K562
MDA-MB-231
MM1S
Molt
Panc-1
PSN-1
Raji
SKOV-3
THP1
U2OS
U266
U87
NKG2DL+
Normalized To Mode

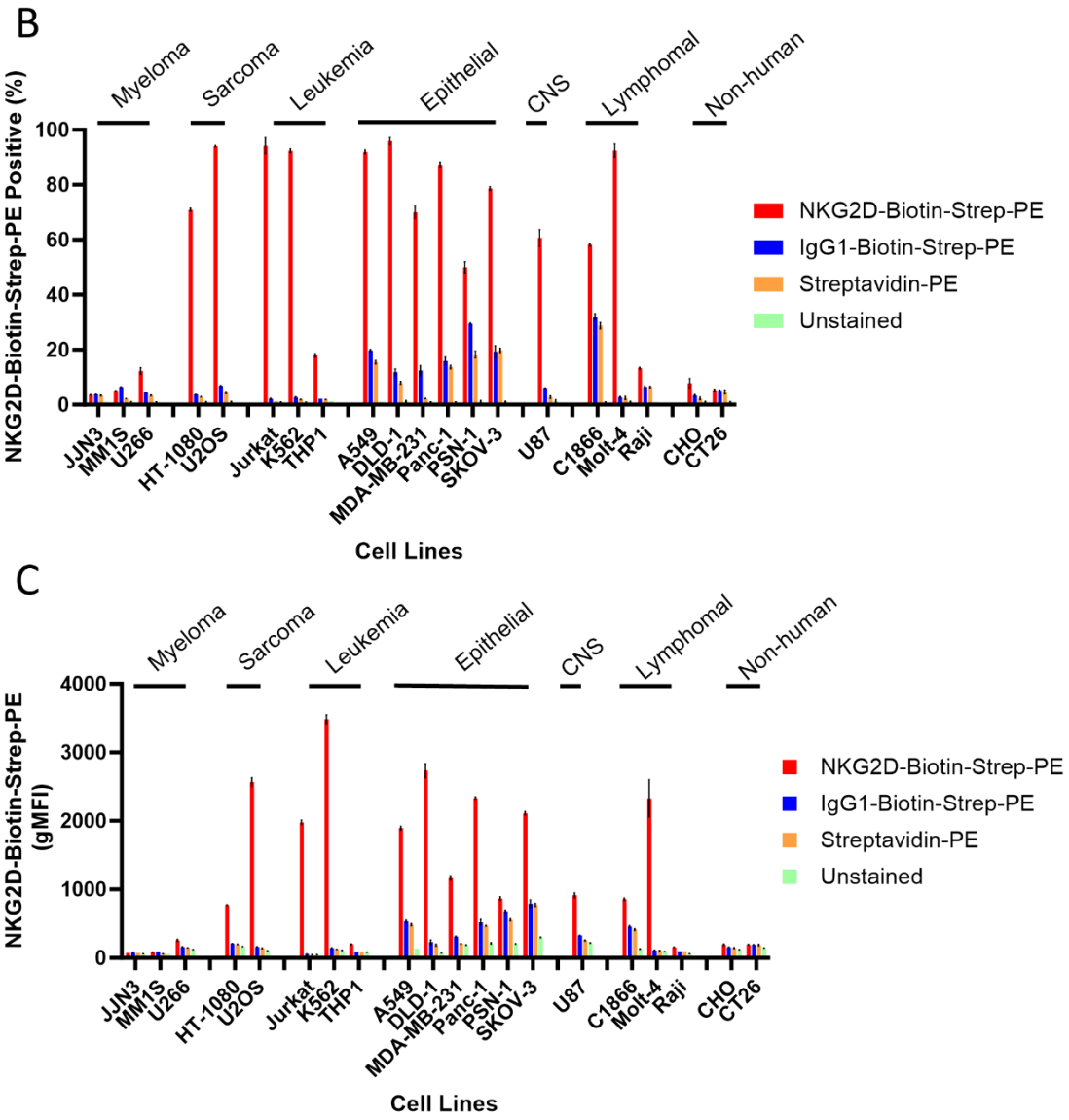

Figure 3.1: NKG2DLs are highly expressed in multiple human cancer cell lines.

Indicated human, hamster and mouse cancer cell lines were stained for NKG2DLs using a biotinylated NKG2D or biotinylated IgG in replace of an isotype control followed by streptavidin-PE to detect binding via flow cytometry. (A) Individual flow cytometry plots for cancer cell lines showing PE expression for unstained, streptavidin-PE only, IgG1-Biotin-Streptavidin-PE or NKG2D-Biotin-Streptavidin-PE. Average percentage positive (B), using unstained control to gate at 1% for each cell line, and gMFI (C) are presented. Data represented as mean +/- SD. N=3. Statistical significance assessed by one-way ANOVA with Dunnett's multiple comparisons test to unstained, $p<0.001$ ***, $p<0.0001$ ****, detailed in Table 3-1.

Table 3-1: Summary of NKG2DL expression within panel of cancer cell lines detailed in Figure 3.1.

	Average % positive	Average gMFI	Relative gMFI	gMFI significance	
				Summary	p-value
Myeloma					
JJN3	3.6	75.1	1.0	ns	>0.9999
MM1S	5.2	84.3	0.9	ns	>0.9999
U266	12.3	257.3	1.6	ns	0.3343
Sarcoma					
HT-1080	71.0	771.0	3.7	****	<0.0001
U2OS	94.1	2566.3	15.8	****	<0.0001
Leukaemia					
Jurkat	94.2	1978.3	36.6	****	<0.0001
K562	92.5	3482.7	24.3	****	<0.0001
THP1	18.0	200.3	2.3	ns	0.1646
Epithelial					
A549	92.0	1895.7	3.6	****	<0.0001
DLD-1	95.9	2733.3	11.9	****	<0.0001
MDA-MB-231	70.0	1167.3	3.8	****	<0.0001
Panc-1	87.3	2334.3	4.5	****	<0.0001
PSN-1	50.0	866.7	1.3	***	0.0006
SKOV-3	78.7	2112	2.7	****	<0.0001

CNS					
U87	60.7	913.7	2.8	****	<0.0001
Lymphoma					
C1866	58.2	857.7	1.9	****	<0.0001
Molt-4	92.5	2329.0	21.3	****	<0.0001
Raji	13.3	156.7	1.6	ns	0.9712
Non-human					
CHO	7.9	194.0	1.2	ns	0.9998
CT26	5.4	196.3	1.0	ns	>0.9999

Due to the varied non-specific binding from the IgG-biotin control, the 'relative gMFI' was calculated by normalising the NKG2D-biotin signal to the IgG-biotin (listed in Table 3-1). From this normalisation, a smaller subset of cell lines was identified as being high, medium or low expressers and selected for use in further experiments. These identified cell lines are detailed in Table 3-2.

Table 3-2: Summary of selected panel of cancer cell lines along with their expression level of NKG2DLs.

Expression Level	Cell line	Relative gMFI
High	Jurkat	36.6
	Molt-4	21.3
	K562	24.3
Medium	DLD-1	11.9
	A549	3.6
	U2OS	15.8
Low/None	Raji	1.6
	JJN3	1.0

3.3.2 NKG2DLs are minimally expressed on non-malignant human cell lines or PBMC-derived cells.

We then sought to investigate the expression of NKG2DLs on so-called 'normal', non-malignant cells, which should not express the ligands on the cell surface. The cell lines tested included a retinal pigment epithelial cell line (ARPE), human intestinal epithelial cells (HIEC-6), human umbilical vein endothelial cells (HUVEC) and normal human dermal fibroblasts (NHDF). Whilst these cell lines are considered to be 'normal', 3/4 showed expression of NKG2DLs to some extent (Figure 3.2). For example, 80% of HUVEC cells were positive for NKG2DLs however the level of expression (gMFI) was much lower than that of the colorectal cell line, DLD-1. The minimal expression seen may also not be indicative of typical *in vivo* expression levels due to the conditions in which these cells are cultured where they are supplied with excessive amounts of nutrients and in some instances, growth factors.

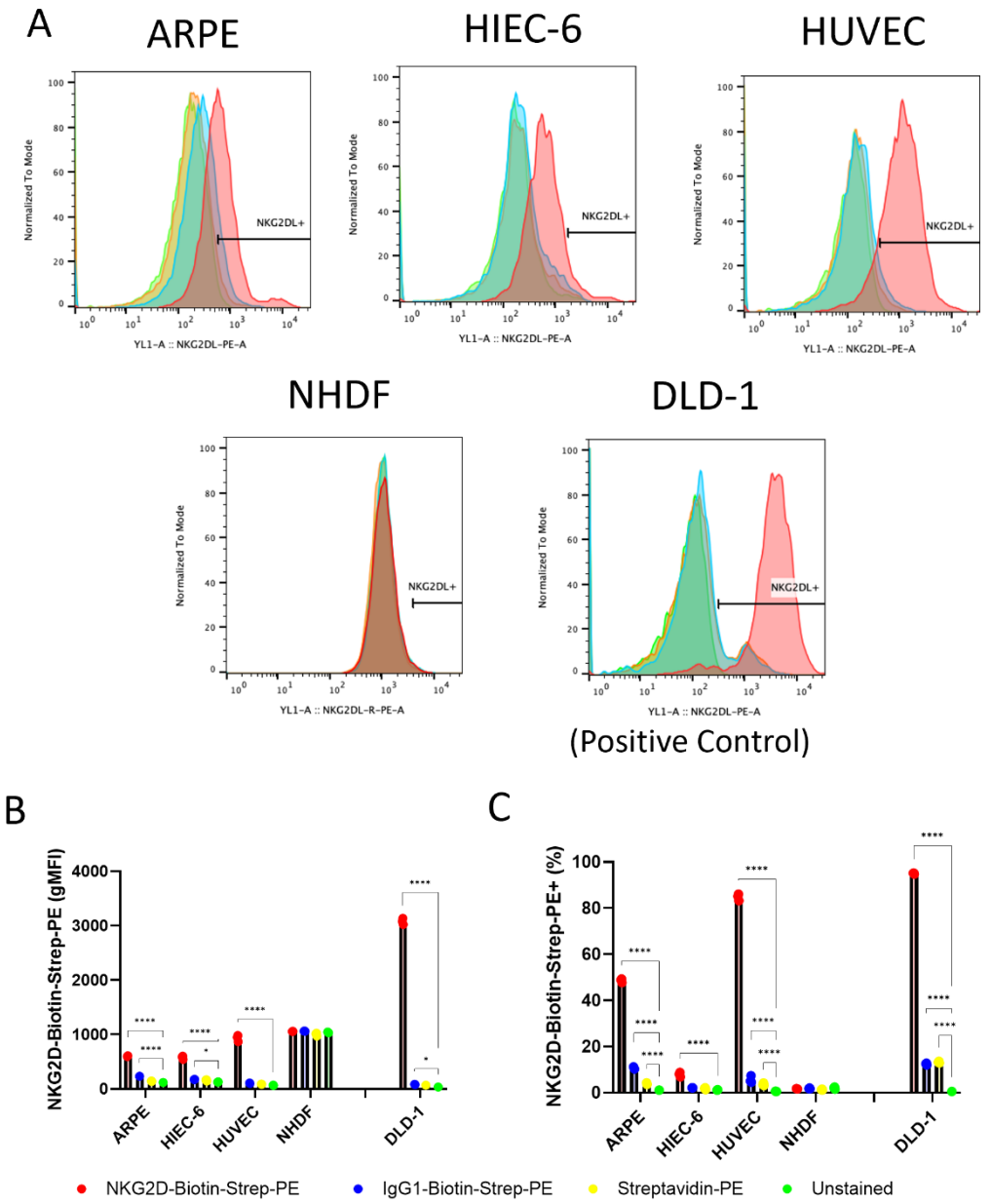

Figure 3.2: NKG2DLs are minimally expressed in multiple non-malignant human cell lines.

Non-malignant human cell lines were stained for NKG2DLs using a biotinylated NKG2D or biotinylated IgG in replace of an isotype control followed by streptavidin-PE to detect binding via flow cytometry. The colorectal cell line, DLD-1, was used as a positive control for staining. (A) Individual flow cytometry plots for cell lines showing PE expression for unstained, streptavidin-PE only, IgG1-Biotin-Streptavidin-PE or NKG2D-Biotin-Streptavidin-PE. Average percentage positive (C), using unstained control to gate at 1% for each cell line, and gMFI (B) are presented. Represented as mean +/- SD, n = 3. Statistical significance assessed by one-way ANOVA with Dunnett's multiple comparisons test to unstained, $p<0.05$ *, $p<0.0001$ ****.

Many forms of immunotherapy, such as bispecific T cell engagers, require the re-targeting of host immune cells against a tumour associated antigen. We have previously shown that the activation of T cells can cause the upregulation of immunotherapy target proteins such as PD-L1 on the T cells themselves (Khalique et al., 2021). We therefore thought it was important to look at the expression levels of NKG2DLs on both PBMCs and isolated T cells, both unstimulated and activated, to determine the likelihood of on-target, off-tumour effects, which is of considerable concern for PBMC derived cells if a therapeutic was to be delivered *intra venously*. If the target antigen is also expressed on CD3+ immune cell, T cells could be re-directed against each other, resulting in fratricide,

Whole PBMCs were negative for NKG2DL expression when stained for total NKG2DLs (Figure 3.3A+B). We then looked at isolated PBMC-derived T cells which had been activated for 48 hours using CD3/CD28 DynaBeads. We observed a minimal increase in the expression of NKG2DLs when comparing unstimulated to stimulated (Figure 3.3C-E, activation confirmed by high levels of CD25 and CD69). Additionally, activated cells seemed to be more 'sticky' than the resting T cells as shown by the increase non-specific binding of the streptavidin-PE.

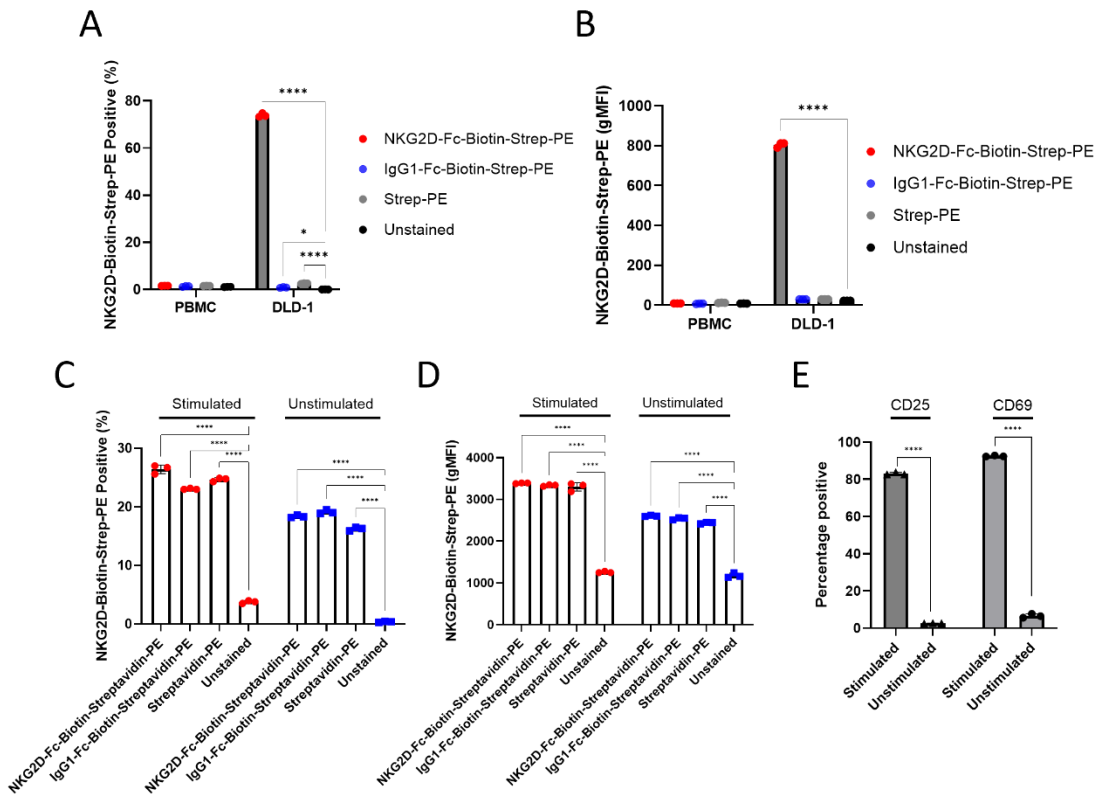

Figure 3.3: NKG2DLs are minimally expressed on healthy PBMC-derived immune cells.

(A-B) Human PBMCs were stained for NKG2DLs using a biotinylated NKG2D or biotinylated IgG in replace of an isotype control followed by streptavidin-PE to detect binding via flow cytometry. The colorectal cell line, DLD-1, was used as a positive control for staining. Average percentage positive (A), using unstained control to gate at 1% for each cell line, and gMFI (B) are presented. (C-E) PBMC-derived T cells were activated using CD3/CD28 Dynabeads or left unstimulated for hours. Cells were then stained for NKG2DLs as above as well as for CD25 and CD69 to confirm activation. Average percentage positive (C), using unstained control to gate at 1% for each cell line, and gMFI (D) are presented. (E) Average percentage positive of T cell activation markers, CD25 and CD69, in stimulated and unstimulated T cells. Data represented as mean +/- SD, N = 3. Statistical significance assessed by two-way ANOVA with Dunnett's multiple comparisons test to unstained, $p<0.05$ *, $p<0.0001$ ****.

3.3.3 Mimicking tumour like conditions increases the expression of NKG2DLs on some tumour cell lines.

Whilst cancer cell lines are a useful tool in research, the conditions under which they are studied *in vitro* do not generally reflect the tumour microenvironment, especially the concentrations of nutrients and oxygen. *In vitro* cell cultures are typically maintained at a controlled temperature and CO_2 concentration to somewhat mimic the general temperature and pH of the body, but they are also batch fed with high levels of nutrients at concentrations in far excess of those available in healthy tissue and quite different from those predicted in the tumour microenvironment.

To better reflect the tumour microenvironment, cell lines were therefore cultured in medium supplemented with different amounts of patient malignant peritoneal ascites. Peritoneal fluid is normally produced at low volumes in the peritoneal cavity to act as a lubricant however, in some late-stage cancers, the fluid can accumulate, either due to blockage of lymph ducts or due to an excess of fluid being produced. At this point it is referred to as ascites or ascitic fluid. Ascitic fluid is a grave prognostic factor as well as typically leading to a worsening in the patient's quality of life due to the increased pressure within the abdomen causing immense discomfort. The average survival time from the time of being diagnosed with ascitic fluid is in the range of weeks or months, depending on the primary tumour origin (Ayantunde & Parsons, 2007). The ascitic fluid from patients is typically drained as part of palliative treatment and comprises of both a cellular fraction as well as soluble factors including pro-inflammatory cytokines and chemokines, fragments of the extracellular matrix and various lipids (Han & Borazanci, 2023; Matte et al., 2012). Both the cellular fraction and the acellular ascitic fluid can be a useful tool in modelling the tumour microenvironment.

Cancer cell lines were cultured in varying amounts of patient acellular ascitic fluid for 72 hours prior to staining for NKG2DLs. In 3/3 ascites fluid samples tested, NKG2DLs increased in both percentage and expression levels in a dose dependent manner on the surfaces of both DLD-1 (Figure 3.4A-C) and A549 (Figure 3.4D-F) cell lines. Although both cell lines express relatively high amounts of NKG2DLs in

normal culture conditions, we can see a striking ascites concentration-dependent increase in gMFI (Figure 3.4B+E). This increase in the number of NKG2DLs present on the cell surface may lead to an increase in therapeutic effect seen when utilising immunotherapies against these targets however this will need to be balanced with the immunosuppressive effects typically observed when utilising ascitic fluid. We additionally saw a dose dependent increase in cell viability with all three ascitic fluid samples (Figure 3.4C+F). The lack of complete media does not seem to have a negative effect in terms of cell viability with 3/3 fluids leading to an increase in cell viability with most doses showing an ascites dose-dependent increase in viability.

Unlike the A549 and DLD-1 cells which already express NKG2DLs, Rajis and JJN3 cells did not significantly upregulate NKG2DLs (Figure 3.5A-D). Surprisingly, when treated with the same patient ascites fluid, Raji cells showed a slight decrease in the number of NKG2DL positive cells and the overall expression (Figure 3.5A+B). We additionally saw no significant increase in NKG2DLs in the non-malignant NHDF cells when treated with the same ascitic fluids (Figure 3.6). Due to the high autofluorescence of NHDFs than that of the positive control (as shown in Figure 3.6D), gMFI is reported as relative to the unstained.

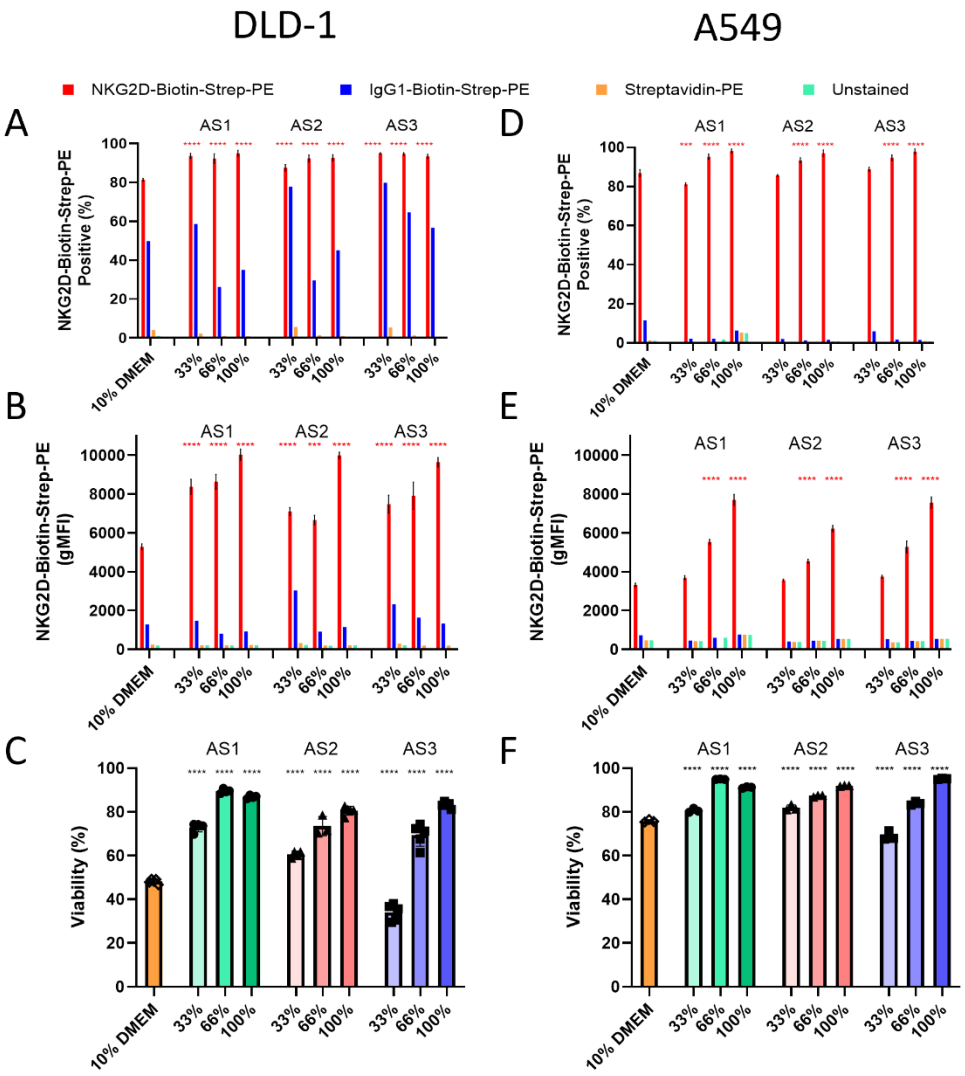

Figure 3.4: NKG2DLs are upregulated further on cancer cell lines in presence of acellular patient derived ascitic fluid.

Human colorectal, DLD-1, cells (A-C) and human lung adenocarcinoma, A549, cells (D-F) were cultured in various concentrations of one of three ascitic fluids (AS1-3) and DMEM supplemented with 10% FBS for 72 hours. Cell lines were then stained for NKG2DLs using a biotinylated NKG2D or biotinylated IgG in replace of an isotype control followed by streptavidin-PE to detect binding via flow cytometry. Viability was determined alongside using viability dye. Average percentage positive (A + D), using unstained control to gate at 1% for each cell line, and gMFI (B + E) are presented, along with cell viability (C + F). Data represented as mean +/- SD, N=3. Statistical significance assessed by one-way ANOVA with Dunnett's multiple comparisons test to 10% DMEM, $p<0.001$ ***, $p<0.0001$ ****.

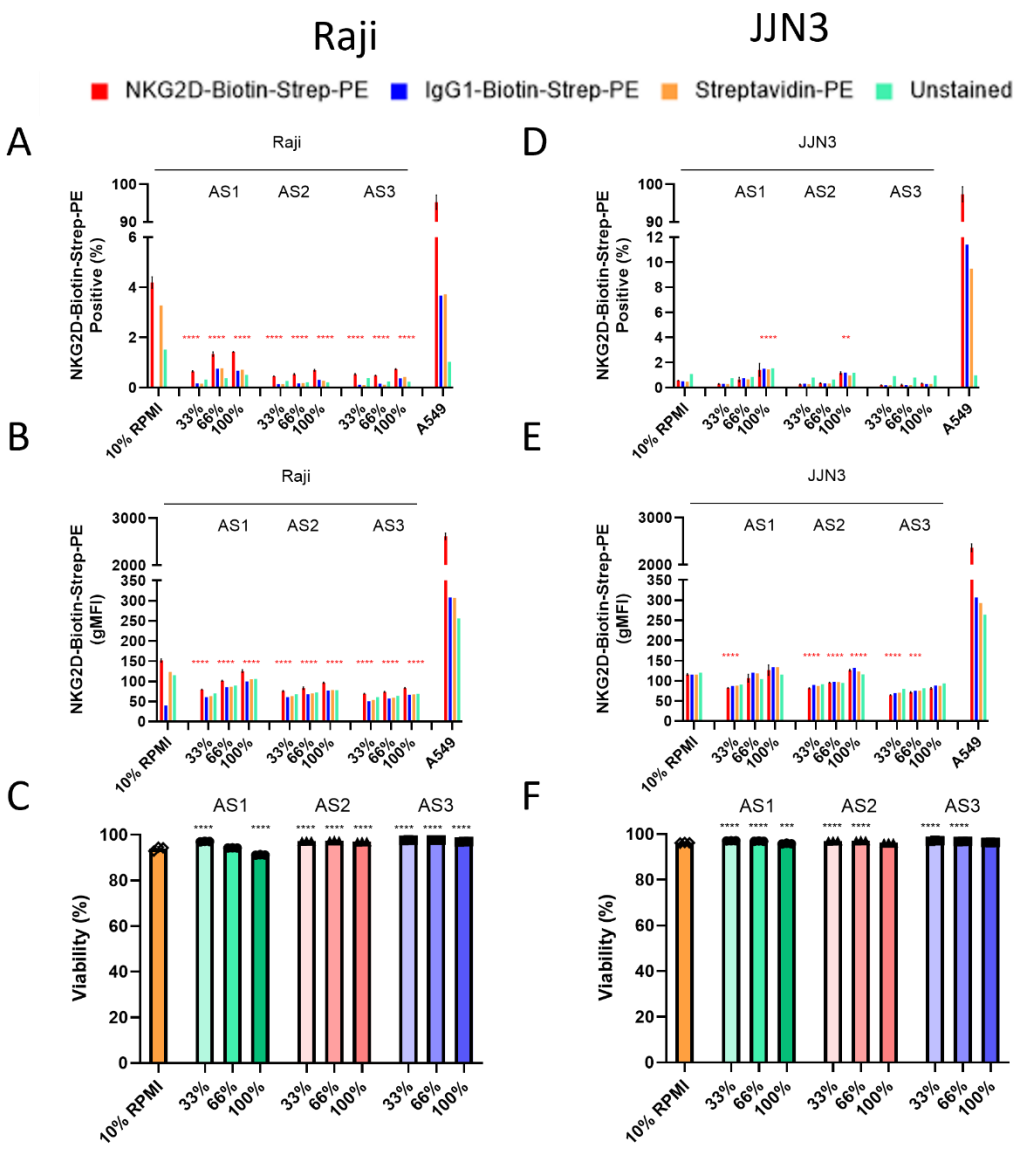

Figure 3.5: NKG2DLs on cancer cell lines are not upregulated on NKG2DL negative cell lines in the presence of acellular ascitic fluid.

Human B cell lymphoma, Raji, cells (A-C) and human multiple myeloma, JJN3, cells (D-F) were cultured in various concentrations of one of three ascitic fluids (AS1-3) and RPMI supplemented with 10% FBS for 72 hours. Cell lines were then stained for NKG2DLs using a biotinylated NKG2D or biotinylated IgG in replace of an isotype control followed by streptavidin-PE to detect binding via flow cytometry. Viability was determined alongside using viability dye. Average percentage positive (A + D), using unstained control to gate at 1% for each cell line, and gMFI (B + E) are presented, along with cell viability (C + F). Data represented as mean +/- SD, N = 3. Statistical significance assessed by one-way ANOVA with Dunnett's multiple comparisons test to 10% RMPI, $p<0.01$ **, $p<0.001$ ***, $p<0.0001$ ****.

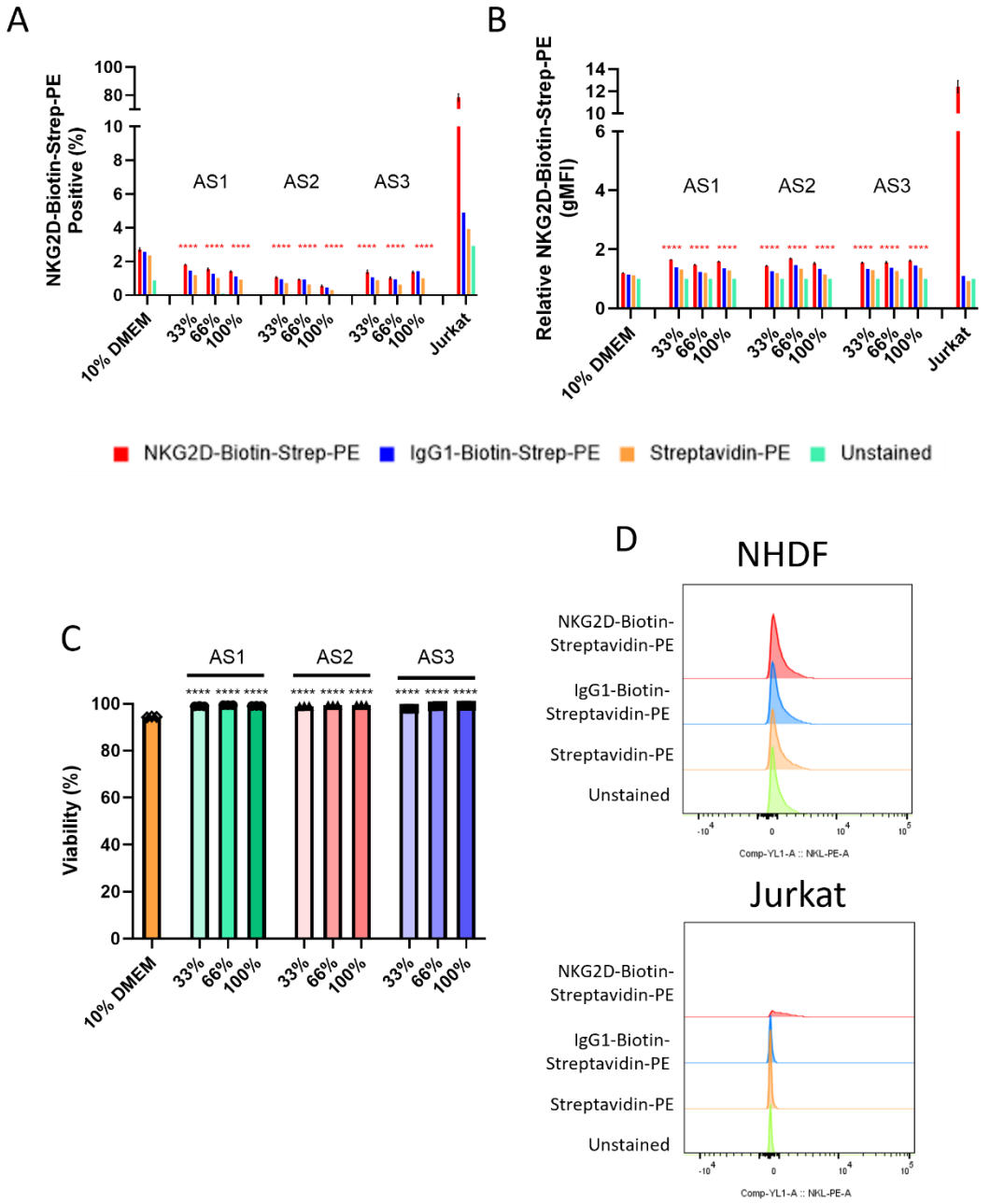

Figure 3.6: NKG2DLs are not upregulated on non-malignant cell lines when treated with acellular ascitic fluid.

NHDF cells were cultured in various concentrations of one of three ascitic fluids (AS1-3) and RPMI supplemented with 10% FBS for 72 hours. Cell lines, including Jurkat cells as a positive control, were then stained for NKG2DLs using a biotinylated NKG2D or biotinylated IgG in replace of an isotype control followed by streptavidin-PE to detect binding via flow cytometry. Viability was determined alongside using viability dye. Average percentage positive (A), using unstained control to gate at 1% for each cell line, and gMFI (B) are presented, along with cell viability (C). Data represented as mean +/- SD, N = 3. Statistical significance assessed by one-way ANOVA with Dunnett's multiple comparisons test to unstained, $p<0.0001$ ****. (D) Example flow cytometry plots for NHDF and Jurkat in the YL-1 channel.

3.3.4 MICA and B are detected on patient derived ascitic cells.

We also analysed the level of NKG2DLs expressed in the cellular fractions of ascitic fluid samples, which would better reflect the heterogeneity of the tumour cells in primary samples as well as the long-term exposure to the conditions within the tumour microenvironment. Three patient samples of ascitic cells were analysed for expression of NKG2DLs, however, due to difficulties in the staining with the recombinant NKG2D protein, we have shown data for staining using an antibody against MICA and MICB.

Figure 3.7A shows the basic composition of the ascitic cells, with two of the samples analysed containing a large amount of tumour cells (EpCAM+), whilst the third was highly enriched in immune cells (indicated by CD45 positivity). Minimal fibroblasts were detected in the samples, with the highest amount being detected in sample 2 with 4.6% of cells being identified as fibroblasts.

2/3 samples analysed were MICAB positive for CD45+ cells, however there was minimal difference in the gMFI for these samples (Figure 3.7B-C). In CD45 negative cells, which includes tumour cells and fibroblasts, we detected surface expression of MICAB in 2/3 samples, both in the percentage positive as well as gMFI (Figure 3.7B-C). Looking more in depth at these cells, both of these samples had MICAB detected on tumour cells as well as on fibroblasts (Figure 3.7D-G). The third sample also contained a small proportion of fibroblasts positive for MICAB.

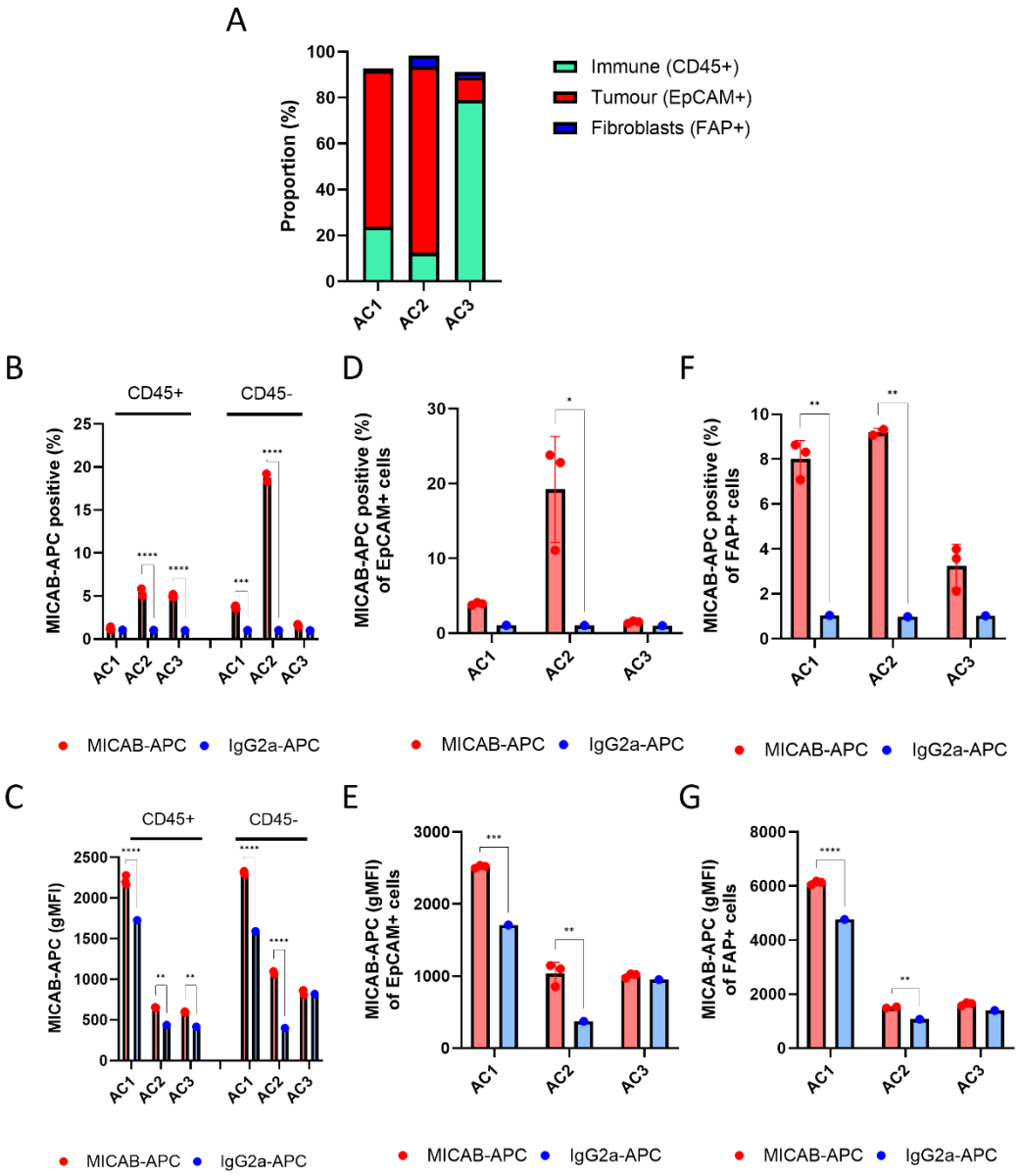

Figure 3.7: MICAB is expressed on tumour cells and cancer associated fibroblasts in primary cells isolated from ascitic fluid.

Ascitic cells were stained with various cell markers as well as aMICAB-APC or isotype control for flow cytometry analysis. (A) Simplistic overview of cellular composition of each sample. (B+C) MICAB expression of CD45- and CD45+ expressing subgroups. (D+E) MICA/B expression on tumour cells as determined by CD45-EpCAM+. (F+G) MICA/B expression on cancer associated fibroblasts as determined by CD45-FAP+. (B, D, F) Data shown as mean +/- SD, with isotype for each sample set to 1% positive. (C, F, G) Data shown as gMFI, represented as mean +/- SD, N = 3. Statistical significance assessed by two-way ANOVA with Dunnett's multiple comparisons test to untreated, $p<0.05$ *, $p<0.01$ **, $p<0.001$ ***, $p<0.0001$ ****.

3.3.5 Chemotherapy and radiotherapy treatment can further increase NKG2DL expression on cancer cell lines.

Chemotherapy and radiotherapy are two of the most widely used cancer treatment. Both radiation and certain chemotherapeutic drugs can activate the DNA damage response in cells, which has been shown to induce the expression of NKG2DLs and so we sought to investigate their effect on the surface expression of NKG2DLs (Gasser et al., 2005).

A549 and DLD-1 cells were treated with varying doses of the chemotherapeutic 5-flurouracil (5-FU) or ionising radiation and stained for NKG2DLs 48 or 72 hours later, respectively. As shown in Figure 3.8, A549 treated cells showed a dose-dependent increase in NKG2DL surface expression with both chemotherapy and radiotherapy treatment (Figure 3.8: NKG2DL are upregulated on A549 cells in response to radiation and chemotherapy, unlike DLD-1 cells.A-B). As A549 cells are almost 100% positive, the more prominent difference can be seen in gMFI. Additionally, there was only a slight reduction in the cell viability allowing for a therapeutic effect to be seen when in combination with NKG2DL targeted therapies.

Surprisingly, the opposite effect was seen for the colorectal cell line, DLD-1. Whilst for both 5-FU and radiation treatments, there were minimal changes in expression at the lower doses, the higher doses of both treatments lead to a significant decrease in NKG2DL expression. To confirm that the DDR pathway was functional in DLD-1 cells, we assessed the levels of activated Chk1 protein via western blot, indicated by phosphorylation of Serine 345, and confirmed that there was a dose dependent increase in phosphorylated Chk1 protein in DLD-1 cells (Figure 3.8E).

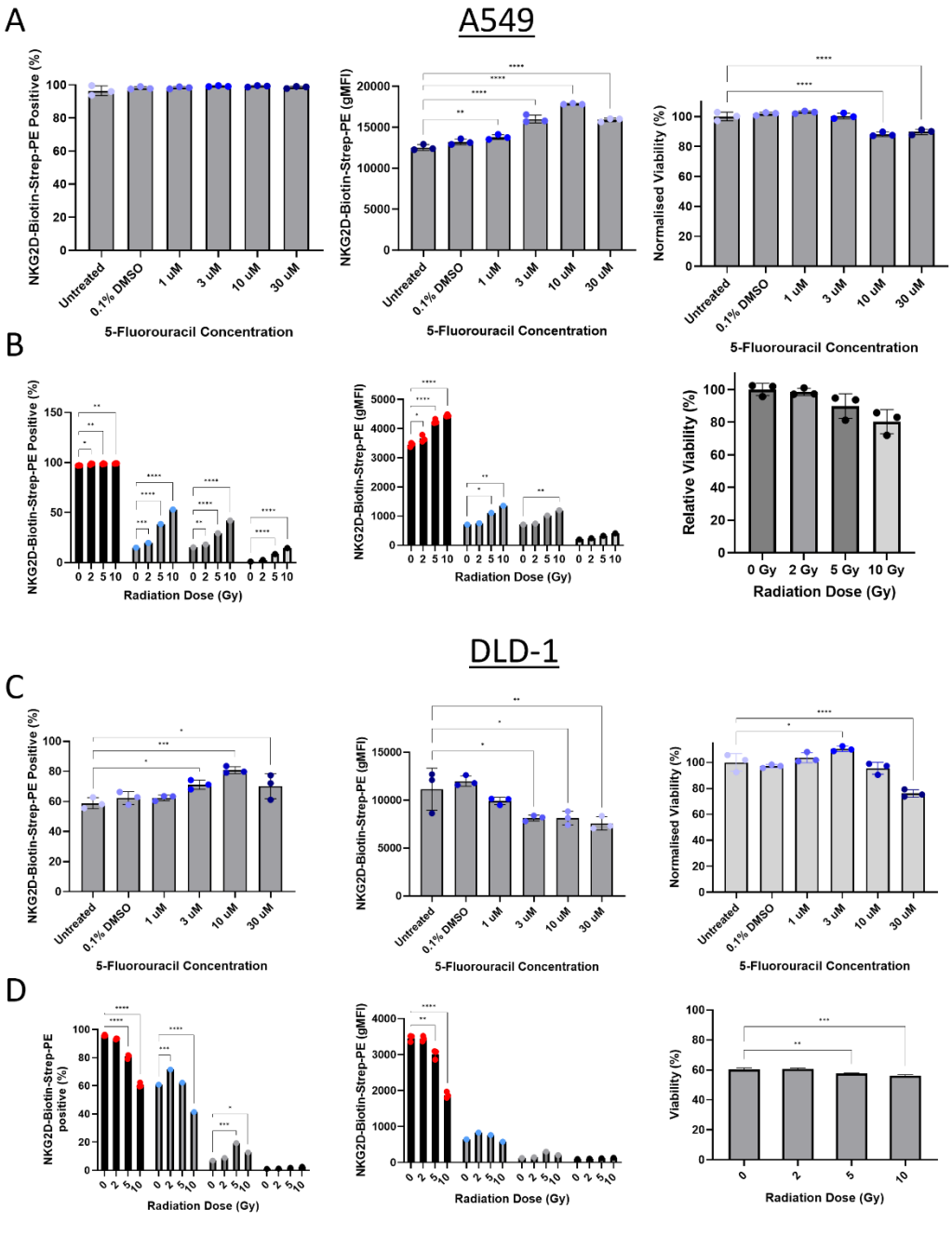

E

DLD-1

Radiation Dose (Gy):

0 2 5 10

pChk1(Ser345)

Chk1

B-actin

Figure 3.8: NKG2DL are upregulated on A549 cells in response to radiation and chemotherapy, unlike DLD-1 cells.

Human lung adenocarcinoma, A549, cells (A+B), and human colorectal, DLD-1, (C+D) were treated with a range doses of 5-FU for 48 hours (A+C) or of ionising radiation and left for 72 hours (B+D). (A-D) Cell lines were then stained for NKG2DLs using a biotinylated NKG2D or biotinylated IgG in replace of an isotype control followed by streptavidin-PE to detect binding via flow cytometry. Viability was determined alongside using viability dye. Average percentage positive using determined unstained control to gate at 1% for each cell line, and gMFI are presented, along with cell viability. Data represented as mean +/- SD, N = 3. Statistical significance assessed by two-way ANOVA with Dunnett's multiple comparisons test to untreated, $p<0.05$ *, $p<0.01$ **, $p<0.001$ ***, $p<0.0001$ ****. (E) A proportion of DLD-1 cells were analysed via western blot to show activation of the DNA damage response, as indicated by phosphorylation of Chk1 protein at Ser354, N = 1.

3.3.6 Chemotherapy and radiotherapy treatment can induce NKG2DL expression on NKG2DL-negative cancer cell lines.

Once we had determined that we could increase the expression on cancer cell lines that already expressed NKG2DLs, we turned our attention to investigate if conventional cancer treatments, such as chemotherapy and radiation, could induce expression of NKG2DLs on negative cancer cell lines, thereby making them susceptible to NKG2DL mediated killing.

Raji and JJN3 cells were subjected to chemotherapy and radiotherapy at a range of doses, as above and stained for NKG2DLs. In Raji cells, NKG2DL expression was increased in a dose dependent manner by both treatments (Figure 3.9A+B). JJN3 cells also saw an increase in ligand expression at higher concentration of 5-FU treatment with a slight decrease in cell viability seen at the highest concentration (Figure 3.9C). Whilst we saw a dose dependent increase in in gMFI and percentage positive JJN3 cells when treating with ionising radiation, a similar increase was also seen for the IgG1 control (Figure 3.9D).

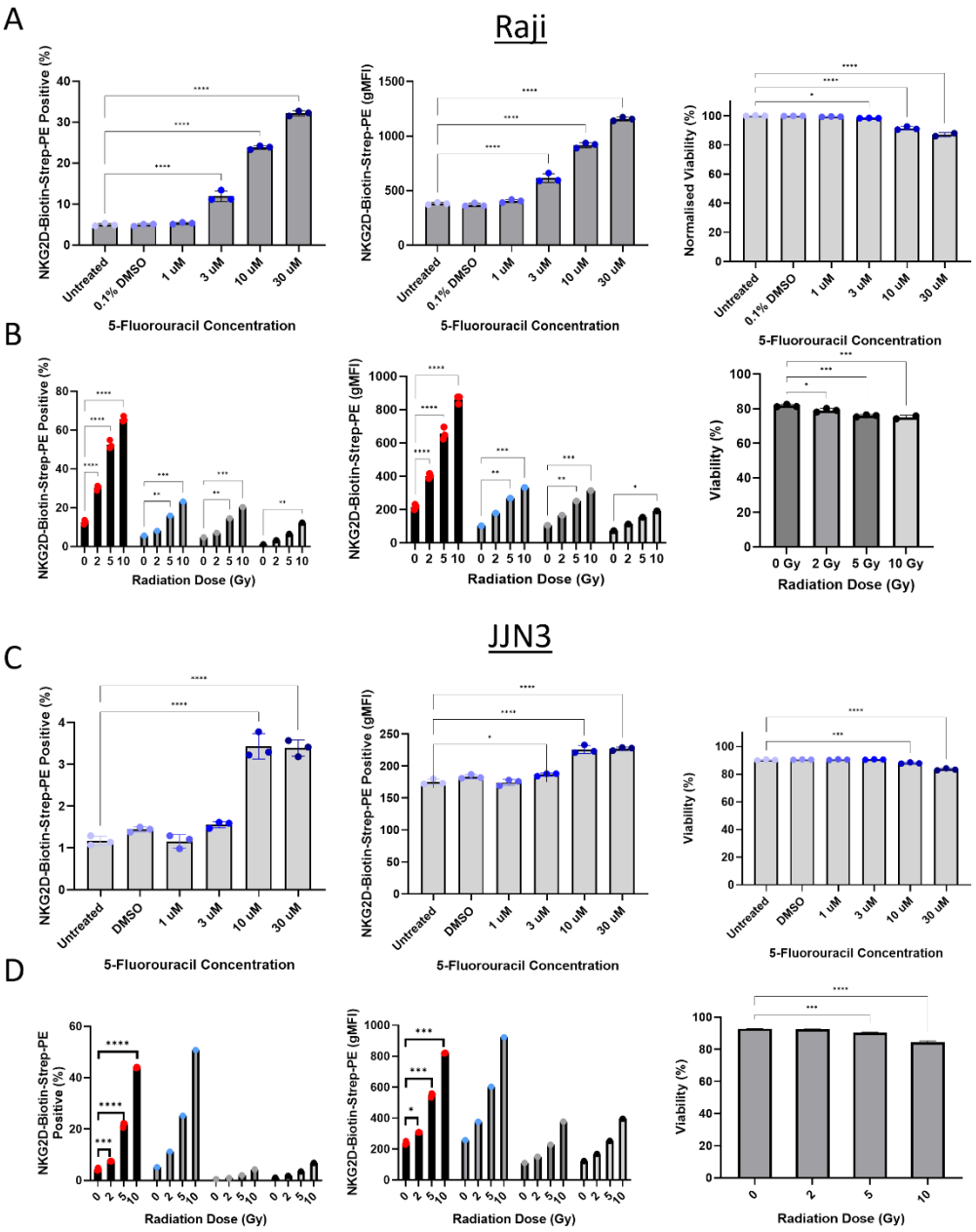

Figure 3.9: NKG2DL are upregulated on the NKG2DL negative cell line, Raji cells, in response to radiation and chemotherapy.

Raji (A+B) and JJN3 (C+D) cells were treated with a range doses of 5-FU for 48 hours (A+C) or of ionising radiation and left for 72 hours (B+D). (A-D) Cell lines were then stained for NKG2DLs using a biotinylated NKG2D or biotinylated IgG in replace of an isotype control followed by streptavidin-PE to detect binding via flow cytometry. Viability was determined alongside using viability dye. Average percentage positive using determined unstained control to gate at 1% for each cell line, and gMFI are presented, along with cell viability. Data represented as mean +/- SD, N = 3. Statistical significance assessed by two-way ANOVA with Dunnett's multiple comparisons test to untreated, $p<0.05$ *, $p<0.01$ **, $p<0.001$ ***, $p<0.0001$ ****.

Another form of chemotherapy frequently used in cancer treatment are HDACi, in particular as part of the treatment regimen for multiple myeloma. HDAC proteins are often upregulated in cancers due to their role in epigenetic regulation, by removing acetyl groups from histones, leading to chromatin condensation and transcriptional repression which can help to reduce the expression of tumour suppressor genes (Ropero & Esteller, 2007). Two potent HDACi, valproic acid (VPA) and sodium butyrate (NaBut) have been shown to increase the levels of MICA and B in HeLa and HepG2 cells which increased their susceptibility to NK cell lysis (C. Zhang et al., 2009). We therefore sought to investigate if this was also applicable in cell lines used within this thesis.

A549, DLD-1, Raji and JJN3 cells were treated with increasing concentrations of VPA or NaBut for 48 hours prior to staining for NKG2DLs. As shown in Figure 3.10, we can see a dose dependent increase in total surface expression of NKG2DLs in all four cell lines, with the most dramatic increase being in the multiple myeloma cell line, JJN3, when treated with VPA whereby the gMFI roughly triples. (Figure 3.10J+K). We additionally see a high increase in NKG2DL expression on JJN3 cells treated with NaBut, as well as a decrease in cell viability with the highest doses of both drugs, however more so with NaBut. Raji cells showed a dose dependent increase in the percentage of NKG2DL positive cells in response to both VPA and NaBut, as well as a slight increase in gMFI, however the overall level remained low, with the IgG1-biotin control background being similar to that of the NKG2D-Biotin signal (Figure 3.10G+H). Similarly to the radiation and 5-FU treatment, A549 cells showed a dose dependent increase in NKG2DL expression levels by gMFI (Figure 3.10B). DLD-1 cells also showed a similar response, in contrast to the radiation and 5-FU treatments previously tested (Figure 3.10E).

To determine the effect of these treatments on non-malignant cells, NHDFs were treated with the previously described treatments and stained for NKG2DLs at the same timepoints (Figure 3.11). Radiation, 5-FU and HDACi treatments lead to minimal increase in the NKG2DLs expressed. Small increases in both percentage positive and relative gMFI were observed, seemingly in a dose

dependent manner, however this was far below the levels seen for the cancer cell line, Jurkat (Figure 3.11A,B,D,E,G,H).

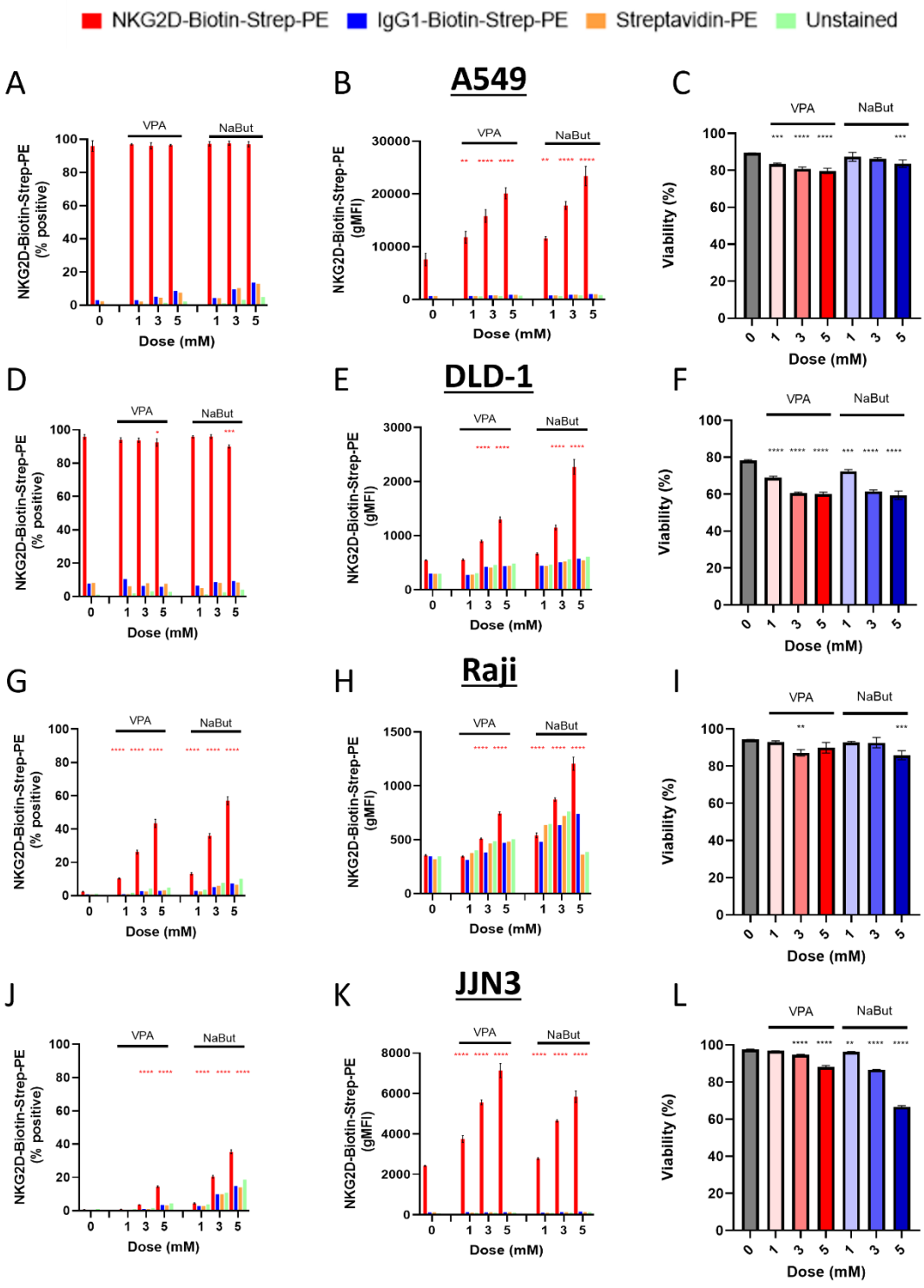

Figure 3.10: HDAC inhibitors upregulate NKG2D ligands in multiple cancer cell lines.

Human cancer cell lines (A549 – A-C, DLD-1 – D-F, Raji – G-I, JJN3 – J-L) were treated with various concentrations of valproic acid (VPA) or sodium butyrate (NaBut) for 48 hours prior to staining for NKG2D ligands and viability before analysis via flow cytometry. Cells were stained using a biotinylated NKG2D or biotinylated IgG in replace of an isotype control followed by streptavidin-PE to detect binding via flow cytometry. A live/dead dye was utilised to determine cell viability. Average percentage positive using unstained untreated control to gate at 1% (A, D, G, J). Average gMFI (B, E, H, K). Average cell viability (C, F, I, L).

Data represented as mean +/- SD, N = 2. Statistical significance assessed by one-way ANOVA with Dunnett's multiple comparisons test to untreated, $p<0.01$ **, $p<0.001$ ***, $p<0.0001$ ****.

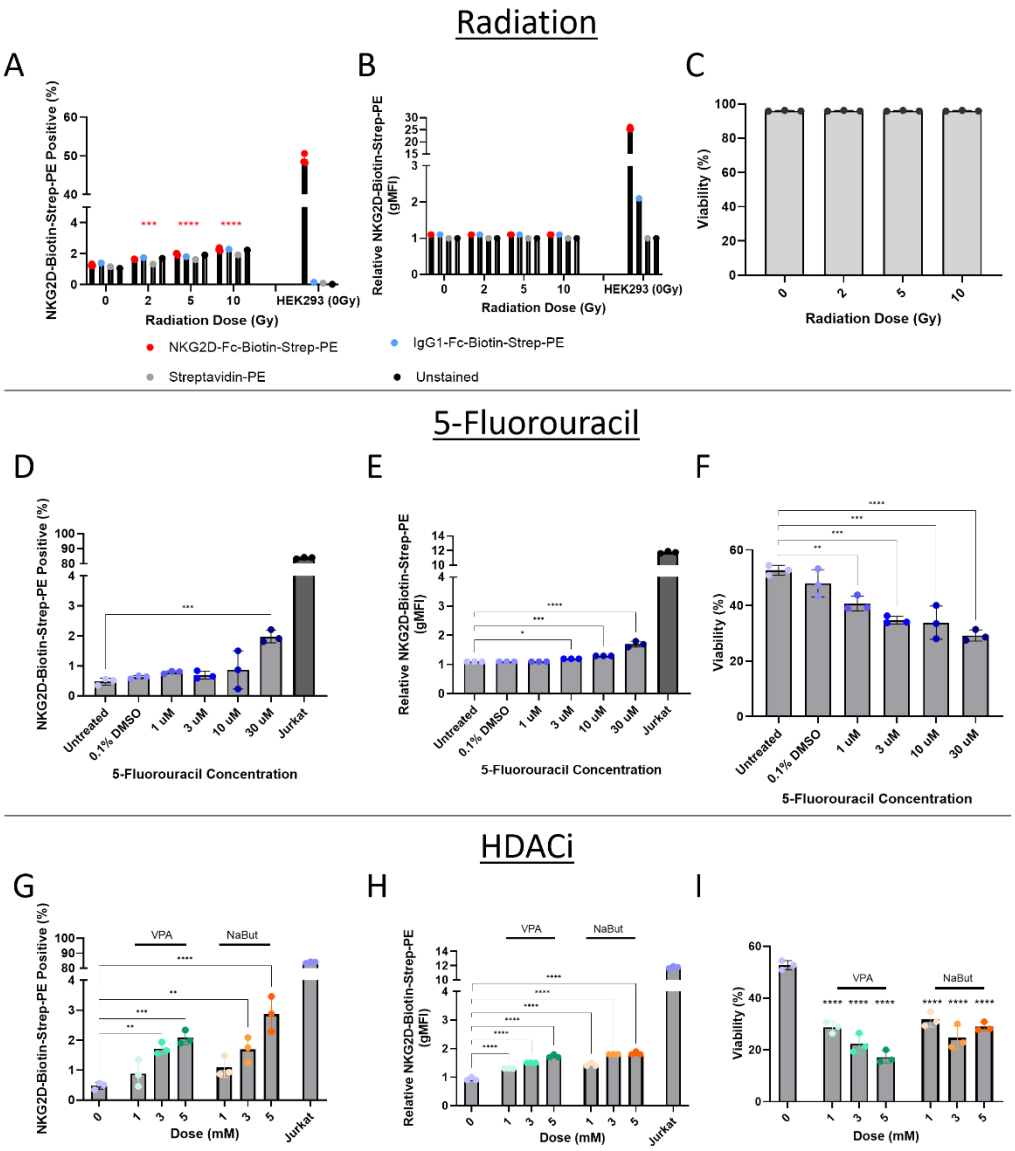

Figure 3.11: Radiation and chemotherapy minimally upregulate NKG2D ligands in a non-malignant cell line.

Normal human dermal fibroblasts (NHDFs) were treated with either ionising radiation for 72 hours (A-C), 5-FU for 48 hours (D-F) or HDACis (G-I) for 48 hours prior to staining for NKG2D ligands and viability before analysis via flow cytometry. Cells were stained using a biotinylated NKG2D or biotinylated IgG in replace of an isotype control followed by streptavidin-PE to detect binding via flow cytometry. Jurkat cells were stained alongside as a positive control. A live/dead dye was utilised to determine cell viability. Average percentage positive using unstained untreated control to gate at 1% (A, D, G). Relative gMFI (B, E, H). Average cell viability (C, F, I). Data represented as mean +/- SD, N = 3. Statistical significance assessed by two-way ANOVA with Dunnett's multiple comparisons test to untreated, $p<0.05$ *, $p<0.01$ **, $p<0.001$ ***, $p<0.0001$ ****.

3.4 Discussion

To assess the range of cancer types that might be targetable via NKG2D ligands we initially analysed a wide range of cancer cell lines to assess the levels of NKG2DLs expressed, as well as 'normal', non-malignant cell lines. Using a biotinylated ectodomain of the NKG2D receptor itself, followed by streptavidin-PE, we detected all eight NKG2D ligands simultaneously by flow cytometry. We found high expression in virtually all types of cancer analysed, including sarcoma, leukaemia and epithelial cancers, with the exception of cell lines originating from B cell cancers such as multiple myeloma (Figure 3.1). This contrasts with Barber et al., who were able to detect NKG2DLs on the surface of a variety of multiple myeloma cell lines, including U266 and MM1S, as well as successfully target them using an NKG2D receptor CAR-T cell approach (Barber et al., 2008). Notable differences between the two studies are the media in which the cells are cultured in, with the U266 and MM1S cells using in Barber et al.'s work supplemented with additional nutrients such a non-essential amino acids and sodium pyruvate as well as the reducing agent β-mercaptoethanol. JJN3 cells have also previously been reported to express NKG2DLs, whilst there are mixed reports for Raji cells (El-Sherbiny et al., 2007; Kellner et al., 2012; Pende et al., 2002).

We additionally looked at non-malignant cell lines and confirmed that whilst some, in particular ARPE-19 and HUVECs, were positive for NKG2DL on their surface, they expressed them at very low levels based on gMFI (Figure 3.2). Furthermore, we assessed the expression of NKG2DL on PBMC cells, both to assess non-malignant primary cells as well as to determine the likeliness of toxicity within the blood. We were unable to detect NKG2DL on whole PBMCs (Figure 3.3A+B). This means that *intra venous* infusion of an NKG2DL targeting immunotherapy could be possible.

To more accurately model the TME, we utilised both the cellular and acellular fraction of patient derived malignant ascites, to determine both if cells isolated from patients express NKG2DLs as well as the effect the immunosuppressive acellular fluid would have on both cancer cell lines expressing

differing levels of NKG2DLs, as well as if NKG2DL surface expression could be induced on non-malignant cells.

We saw a dose dependent increase in NKG2DL expression in both cancer cell lines that express NKG2DL in typical cell culture conditions however saw minimal change or a decrease in NKG2DL in Raji and JJN3 cells (Figure 3.4+Figure 3.5). Additionally, in A549 and DLD-1 cells, all three ascitic fluids tested resulted in an increase in target cell viability (Figure 3.4C+F). Furthermore, in Figure 3.6 we show that treatment of non-malignant cells with ascitic fluid caused a minor increase in NKG2DL gMFI signal, however the overall levels of ligands was still low.

We are unsure as to the exact component of ascitic fluid that would cause an increase in NKG2DL expression in DLD and A549 cells whilst having minimal effects on Raji and JJN3 cells. Typically, we see that the ligands upregulated in response to ascitic fluid are a result of the immunosuppressive soluble factors such as IL-6, IL-10 and TGF-β, as shown previously. (Khalique et al., 2021; Scott et al., 2019). IL-10 has been shown to induce the expression of MICA/B and ULBP1-3 in macrophages, however it has also been shown to decrease the expression of MICA on the surface of melanoma (Schulz et al., 2010; Serrano et al., 2011). Additionally, TGF-β has been widely reported to inhibit the NKG2D-NKG2DL axis in a variety of cancers (Friese et al., 2004; Serrano et al., 2011; Shin Lee et al., 2021).

The increasing dose of ascites fluid simultaneously results in an equal reduction in complete media which provides additional nutrients such as amino acids, lipids and glucose to the cells. Therefore, another factor that could be involved is nutrient deprivation. Serum starved HCT116 (colorectal) showed decreased levels of MICA/B and ULBP2, however ULBP1 transcription has been linked to the ATF4 transcription factor, whose own expression is induced during nutrient deprivation (Gowen et al., 2015; Jung et al., 2012b). In future work, we would like to analyse the composition of the ascitic fluids to ascertain the key factor/s. However, it is still intriguing how the same ascitic fluids can have differing effects on cancer cell lines.

Whilst we did not see an increase in NKG2DLs on the ascites fluid treated NHDFs, we did detect a small amount of NKG2DLs on the CAFs within the cellular fraction of the ascites fluid, in 2/3 of the samples tested, however the number of CAFs in this analysis was low. That being said, if true, this suggests we could target both tumour cells as well as CAFs by targeting NKG2DL in tumours. Ben-Shmuel et al. have previously found that the NKG2D-NKG2DL interaction was critical for NK-cell mediated targeting of CAFs (Ben-Shmuel et al., 2023).

As the majority of cancer patients will undergo some form of chemotherapy or radiotherapy as part of their treatment regiment, we additionally looked at the effect of these standard of care treatments, which are known to induce the DNA damage response, on the NKG2DL expression levels in both malignant and non-malignant cells. When using ionising radiation, the path of the beam also hits healthy cells causing toxicity. We therefore sought to determine if there was a pre-treatment condition in which we could increase the therapeutic window for NKG2DL targeting therapies by increasing the NKG2DL expression on malignant cells whilst preventing the sensitisation of the non-malignant cells.

In A549 cells, we saw a dose dependent increase in NKG2DLs expressed (gMFI), in response to both radiation and treatment with 5-FU (Figure 3.8A+B). Surprisingly, the opposite effect was seen for DLD-1 cells, in which we saw a dose dependent decrease in NKG2DL in response to both radiation and 5-FU treatment, despite the dose dependent increase in P-Chk1 protein (Figure 3.8C+D+E). Furthermore, we saw no significant difference in NKG2DL surface expression in the NHDF treated cells at any radiation dose, with only small increases seen upon treatment with 5-FU and HDACis.

We additionally identified treatments to induce NKG2DL expression in Raji and JJN3 cells, which typically express low levels. Both radiation and 5-FU treatment led to significantly different NKG2DL expression in Raji cells, in a dose dependent manner (Figure 3.9A+B). This effect however was not as dramatic when looking at JJN3 cells, which when treated with HDACis, particularly VPA, showed a dramatic increase in NKG2DL surface expression (Figure 3.9C+D, Figure 3.10J-L). This indicates that

NKG2DL negative cancer cell lines may evolve different mechanisms to downregulate NKG2DL. HDACi inhibitors were also effective at upregulating NKG2DL on A549 and DLD-1 cells, and to a lesser extent, Raji cells (Figure 3.10A-I).

Whilst the concentrations of the chemotherapy drugs using is this thesis are typical of that used in *in vitro* assays, they may not be clinically relevant (C. Zhang et al., 2009; L. Zhao et al., 2014). VPA is used in the treatment of bipolar disorder at doses in which the serum concentration is likely to be between 50-74 µg/mL (Gugler & von Unruh, 1980). With the concentrations used within this thesis, we would be within the range of 144 – 721 µg/mL, much higher than the predicted levels. The plasma level of 5-FU in patients undergoing treatment was measured at between 3 – 5 µM. In the data presented in this thesis, we saw a significant increase in NKG2D ligand expression with 3 µM of 5-FU in A549, JJN3 and Raji cell lines.

Taking this together, the differences seen across multiple cancer cell types in response to various therapeutic treatment conditions, as well as a cellular ascitic fluid, indicates that the various evasion mechanisms that tumours employ to prevent NKG2DL mediated targeting may also make them sensitive to certain therapeutics. For example, the dramatic increase in NKG2DLs seen in JJN3 cells upon treatment with VPA, as well as the minimal induction in the non-malignant cell lines, indicates that these cells have evolved a mechanism to epigenetically silence NKG2DLs.

Many viruses are known to encode proteins to retain the NKG2DL proteins at the ER to prevent their presentation on the cell surface, evading detection by the immune system, however this has also been noted in uninfected cells which contain high levels of intracellular NKG2D ligands (Baugh et al., 2020; M. Fuertes et al., 2008; Ghadially et al., 2017). The exact mechanism that regulates the translocation of NKG2DLs in response to stress is unknown, however upregulation of proteins to retain NKG2DLs within the cell would be advantageous to a tumour. The regulation may also not be at the point of protein translocation, H157 cells showed decreased mRNA levels for multiple NKG2DL, including MICA/B and ULBP1-3, in response to increasing doses of radiation (M. J. Shen et al., 2017).

It therefore would be useful to investigate the total NKG2DL protein levels, including retained, intracellular protein, to get a better understanding in DLD-1 cells.

In conclusion, we have shown that a wide variety of cancer types express NKG2DL, whilst non-malignant cells express minimal to none. Additionally, we have shown that using standard of care therapies, we can increase the levels of NKG2DLs expressed on cancer cells that already express them on their surface, as well as induce NKG2DL expression on cancer cell lines that were initially negative, whilst minimal expression is retained on a non-malignant cell line. Furthermore, many of these treatments, did not lead to a dramatic decrease in cell viability alone, therefore these treatments allow the opportunity for synergistic effects with NKG2DL targeting therapeutics.

Chapter 4: Engineering of NKG2D ligand (NKG2DL) targeting Bispecific T cell engagers (BiTEs) for arming oncolytic adenoviruses.

4.1 Introduction

After showing in the previous chapter that NKG2DLs are highly expressed on a variety of cancer cell lines, whilst being minimally expressed in normal cell lines. We set out to explore the targeting of these ligands therapeutically, with the goal to arm the oncolytic adenovirus, EnAd, with a bispecific T cell engager (BiTE) to enable *in situ* production of the therapeutic, as well as providing oncolytic cell death of infected cells. Previously, EnAd has been armed with a variety of BiTEs, including those targeting EpCAM, fibroblast activating protein (FAP), CD206 and folate receptor β (FRβ), with the ability to successfully target antigen positive cells within a variety of clinically relevant samples (Freedman et al., 2017, 2018; Scott et al., 2019).

NKG2DLs have previously been explored as targets for immunotherapy, using monoclonal antibodies to target one or two of the ligands or using the NKG2D receptor to target all eight ligands (Ferrari De Andrade et al., 2018; Godbersen et al., 2017; Goulding et al., 2023; Hagelstein et al., 2021; Märklin et al., 2019; Sallman et al., 2023a; D. Yang et al., 2019; T. Zhang et al., 2006). CAR-T cell therapies engineered to express the NKG2D receptor have been underdeveloped for several years with Celyad Oncology being the most prominent in the field with multiple clinical trials ongoing (Curio et al., 2021; Sallman et al., 2023b; D. Yang et al., 2019; T. Zhang et al., 2006). Their primary candidate includes the full length NKG2D receptor engineered to also express the CD3 ζ intracellular signalling region, as with 1st generation CAR-Ts, which in currently undergoing clinical trials for the treatment of

metastatic colorectal cancer in combination with chemotherapy (Sallman et al., 2023b, NCT04991948).

Two bispecific T cell engager (BiTE) consisting of an αCD3 ScFv fused to a single copy of the NKG2D ectodomain have been published previously showing promising results against a number of tumour types, as the production of a bispecific NK cell engager using an αCD16 ScFv to allow engagement of NKG2D negative NK cells (Godbersen et al., 2017; Hagelstein et al., 2021; Märklin et al., 2019). Hagelstein et al. found that there was increased overall potency with the NKG2D-αCD3 bispecific, compared to the NKG2D-αCD16, showing upregulation of degranulation marker CD107a and increased production of IFN-γ and perforin.

We hypothesise that we can improve on these technologies by delivering the therapeutic via an oncolytic virus to allow for the continued production of the bispecific within the tumour. Additionally, we hypothesise that the addition of a second NKG2D ectodomain will improve the potency of the therapeutic. Further to this, BiTEs can repurpose T cells that are already residing within the tumour, as opposed to CAR-T cell which need to overcome the obstacle of gaining entry into the tumour from the bloodstream. In addition to this, the presence of replicating (oncolytic) virus within the tumour should elicit a pro-inflammatory immune response, leading to the influx of new T cells into the tumour which have not been exposed to the immunosuppressive environment for extended periods of time.

As previously discussed, the NKG2D receptor is formed of a homodimer, linked by disulphide bonds. The previously mentioned therapeutics containing the NKG2D ectodomain are all constructed using a single copy of the protein, as in the NKG2D BiTE presented in this thesis. We predict that, by having two copies of the NKG2D ectodomain within the same construct (referred to as a tri-specific T cell engager (TriTE)), the avidity to the target cell can be increased by the binding to two separate ligands, or the two protein domains will assemble into the extracellular homodimer complex allowing for a

more physiological interaction with the ligands to occur, most likely with higher affinity (schematics of predicted binding presented in Figure 4.1B).

Previously in our lab, a NKG2D-αCD3 construct (NKG2D BiTE) and a NKG2D-αCD3-NKG2D construct (NKG2D TriTE) have been developed. The preliminary work for these constructs was carried out by Dr Janet Lei and a more thorough evaluation of the NKG2D-CD3-NKG2D construct by Dr Richard Baugh was also undertaken in the context of GBM. Within this work, the NKG2D TriTE was encoded within an oncolytic herpes virus (oHSV), allowing the targeting of glioma stem-like cells (Baugh et al., 2024). Whilst this showed promising results, oHSV delivery is limited to *intra tumoral* injection due to high prevalence, and a large proportion of the population having pre-existing immunity (F. Xu et al., 2006). The oncolytic virus used in this chapter, EnAd, is a chimeric adenovirus that is mainly derived from serotype 11p which has a much lower plasma antibody prevalence (Vogels et al., 2003). This was shown *in vitro* by Di et al, assessing the ability of human plasma to neutralise different adenovirus serotypes, and was supported by a mechanism of action phase I trial in which the virus was delivered by intravenous injection to patients who subsequently had their primary colorectal tumours resected, showing significant uptake of virus into the tumour (Di et al., 2014; Garcia-Carbonero et al., 2017b).

This chapter will focus on the evaluation of the NKG2D BiTE and TriTE in a wider range of cancer types as well as in non-malignant cells. Additionally we will focus on evaluating the efficacy of these therapeutic agents in combination with conventional cancer treatments, as well as assess its potency when expressed from an oncolytic virus.

4.2 Chapter aims and hypothesis

4.2.1 Chapter hypothesis

We hypothesis that NKG2DLs expressed on a variety of cancer cell line can be targeted with an NKG2DL T cell engager formed of either one or two copies of the ectodomain of the NKG2D receptor fused to an αCD3 ScFv. Furthermore, we hypothesise that we can increase this potency using the combination of standard of care treatments identified in Chapter 3, which we have shown can significantly upregulate NKG2DLs on target cells, sensitising NKG2DL negative cell lines.

4.2.2 Chapter aims

1 - Engineer a NKG2D TriTE that can successfully be produced from the oncolytic virus, EnAd.

2 - Determine the breadth of cancer cell line in which the NKG2D BiTE and TriTE can induce cytotoxicity.

3 - Investigate the effect of combining NKG2D BiTE and TriTE treatments which conventional cancer therapies which were shown to increase surface levels of NKG2DLs.

4 - Assess the ability of the NKG2D BiTE/TriTE armed virus to induce T cell activation and kill NKG2DL+ cells.

4.3 Results

4.3.1 Design of NKG2D BiTE and TriTE utilised in this thesis.

As stated above, previous work carried out by Dr Janet Lei to design the original NKG2D BiTE and TriTE constructs, along with some preliminary evaluations of the constructs as pan cancer therapeutic molecules. The original NKG2D TriTE contained two identical copies of the NKG2D ectodomain (residues 78-216 of full length NKG2D as detailed in Figure 4.1A), which led to recombination upon construction of the viral plasmid. Therefore, to decrease the propensity for recombination and NKG2D ectodomain elimination from the TriTE during virus production, the NKG2D ectodomain sequence was codon optimised using the GenScript tool. This nucleotide sequence was then compared to the original sequence used and codons were altered to reduce the overall homology between the two sequences with as few adjacent corresponding bases as possible. The codon usage was kept as close to the codon optimised version to increase protein production. This NKG2D TriTE with reduced homology between the NKG2D domains was incorporated into an oHSV virus as part of Richard Baugh's DPhil thesis and subsequent publication (Baugh et al., 2024).

Originally a mutant version of the NKG2D, which had 5 mutations within the B6 loop of the NKG2D domain abolishing its binding ability, was to be used as the control construct however the protein production from this construct was insufficient for use in functional assays. Therefore, within this thesis I have utilised a nanobody against the rabies virus S protein (CtrlNB) as an irrelevant protein to use in the control construct (Scott et al., 2019). The CtrlNB-αCD3-CtrlNB construct was made similarly to the NKG2D-αCD3-NKG2D construct in that the second CtrlNB domain was codon optimised and then altered to reduce homology between the two sequences.

Whilst other groups have demonstrated the efficacy of similar, NKG2D BiTE constructs which contain only one extracellular domain of NKG2D, to our knowledge, the NKG2D TriTE is the first NKG2D ligand targeting T cell engager which utilises two copies of the NKG2D ectodomain. Whilst in other TriTEs

typically bind to three separate entities, we are unsure of the binding orientation in which the NKG2D TriTE will form (as detailed in Figure 4.1B). One possibility is that the extracellular region of the NKG2D receptor is able to assemble in this orientation, allowing for more binding of the NKG2D ligand similarly to that of the full length NKG2D homodimer. Another alternative is that the NKG2D ectodomains are unable to form a complex due to removal of the intracellular and transmembrane regions of the full-length protein. The homodimer interface is stabilised by non-covalent, hydrogen bonds, which may not be sufficient for dimerisation without the transmembrane region (Garrity et al., 2005; P. Li et al., 2001). The transmembrane region of NKG2D contains cysteine residues which form interchain disulphide bonds with DAP10 molecules, stabilising the NKG2D dimer (Garrity et al., 2005). In this instance, the NKG2D TriTE may be binding to multiple NKG2D ligands on the target cell.

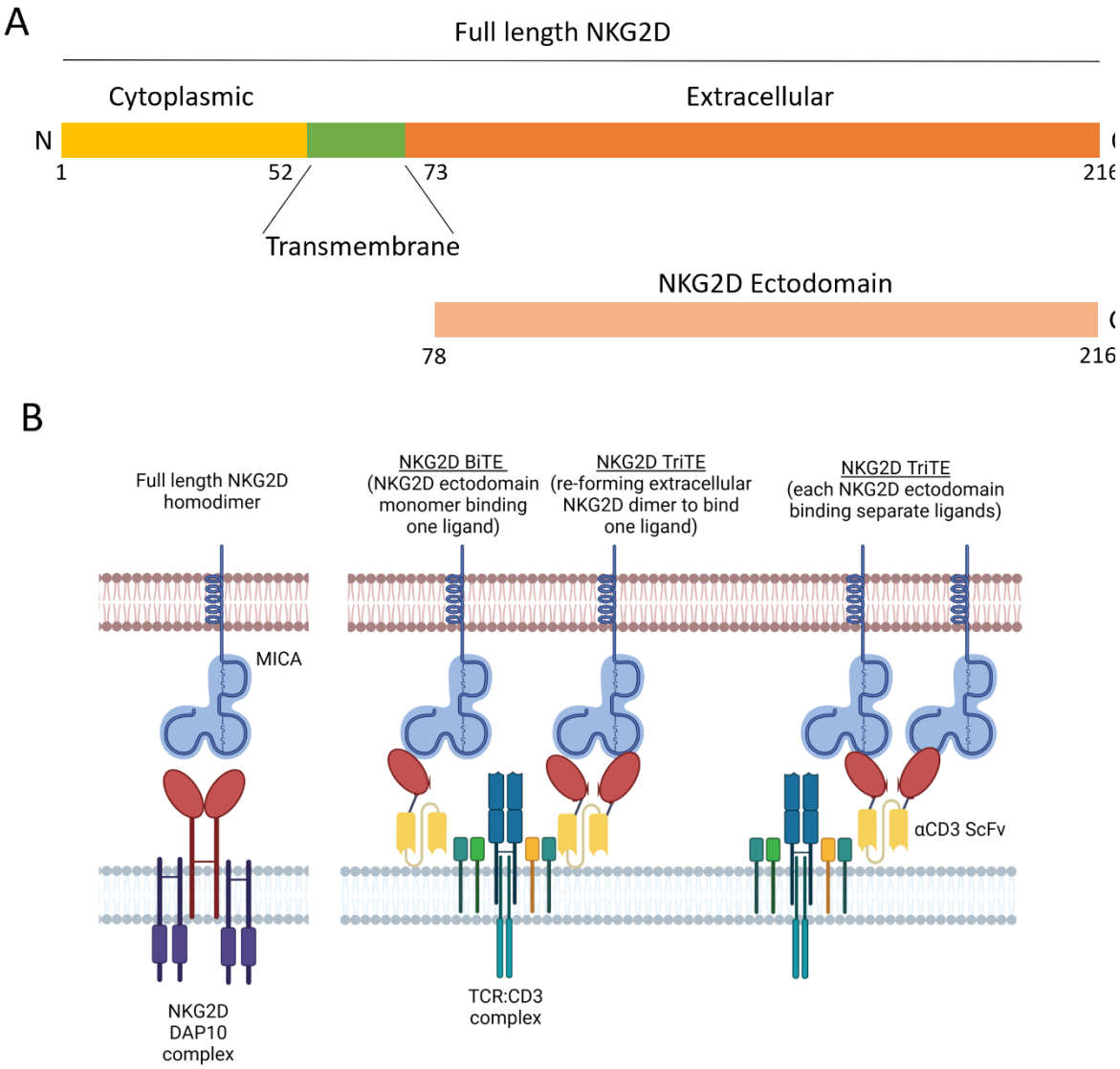

Figure 4.1: Design and predicted mode of action of NKG2D BiTE and TriTE.

(A) Domains of the full length NKG2D protein (P26718), along with the residues utilised in the NKG2D BiTE and TriTE for binding to all NKG2D ligands. (B) Predicted binding of the NKG2D BiTE and TriTE to bridge between a cell expressing NKG2D ligands, such as MICA, and CD3 within the TCR-CD3 complex. Created using BioRender.

4.3.2 Engineering and production of NKG2D bispecific constructs.

The minimal homology sequence of the NKG2D ectodomain was cloned into the pSF plasmid backbone, to be expressed under the CMV promoter, using standard cloning techniques to replace the second NKG2D ectodomain in the original construct to reduce the likelihood of recombination

(Figure 4.2A+B). An equivalent control construct was also that contained a nanobody sequence against the S protein of rabies (Scott et al., 2019). All constructs were cloned to contain an N-terminal secretion signal and a C terminal decahistidine tag for detection, purification and quantification. The four constructs utilised in this chapter are illustrated in Figure 4.2C.

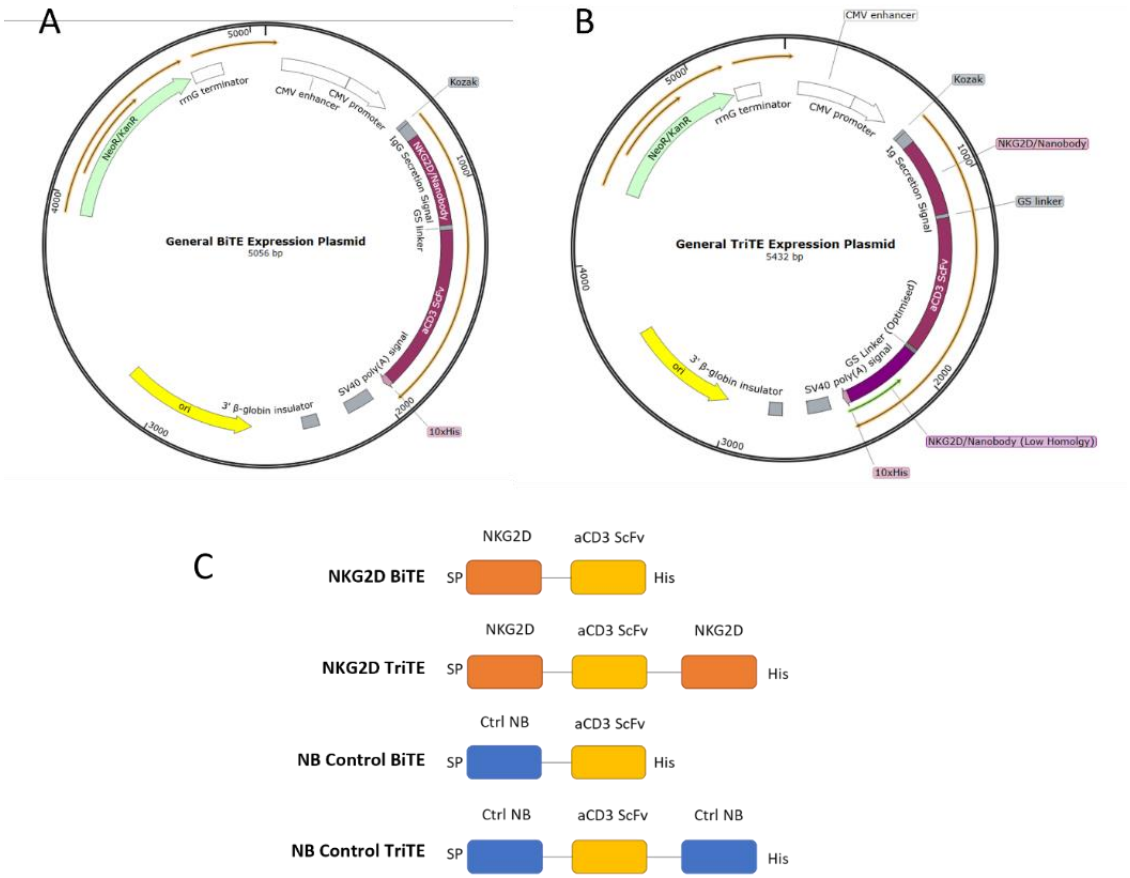

Figure 4.2: Generation of NKG2D BiTE and TriTE with matched control constructs.

(A+B) Schematic of expression plasmids for mammalian expression of BiTEs and TriTEs under the CV promoter. KanR – Kanamycin resistance. CMV – Cytomegalovirus, SV40 – simian vacuolating 40, GS linker – glycine serine linker. (C) Schematic representation of the structure of the NKG2D BiTE, TriTE and nanobody (NB) control BiTE and TriTE. The NKG2D domain (orange) composes of the ectodomain of the NKG2D receptor. Domains are linked via a GS linker (GSSGGGG) for flexibility. Each construct encodes an N-terminal immunoglobulin signal peptide (SP) and a C-terminal decahistidine tag (His).

HEK293-T cells were utilised for protein production as they are easy to transfect at high efficiency and yield large amounts of recombinant protein. 72 hours post transfection, supernatant and lysate

were harvested separately and the supernatant concentrated 50-fold, via centrifugal ultrafiltration, using a 10 kDa amicon filter. Protein expression and size was confirmed using SDS-PAGE and western blotting for qualitative purposes (Figure 4.3A). For all constructs, the protein was detected in the supernatant with a small amount of the CtrlNB BiTE also being detected in the lysate, showing that the proteins were being efficiently secreted from the producer cells. As commonly seen with BiTE constructs produced in our lab, the bands were running slightly higher on the gel than predicted (10kDa higher). We hypothesis that the increase in size is likely to be from post translation modifications that occur to the protein, such as glycosylation. We have previously sent BiTEs for mass spectrometry, which confirms the correct protein sequence. Quantification of BiTE and TriTE was then determined using a His tag ELISA. Both the CtrlNB BiTE and CtrlNB TriTE were produced at much higher levels than the NKG2D containing constructs (Figure 4.3A). Larger TriTE proteins showed a lower protein yield and the inclusion of the NKG2D ectodomain in general lead to a decreased yield.

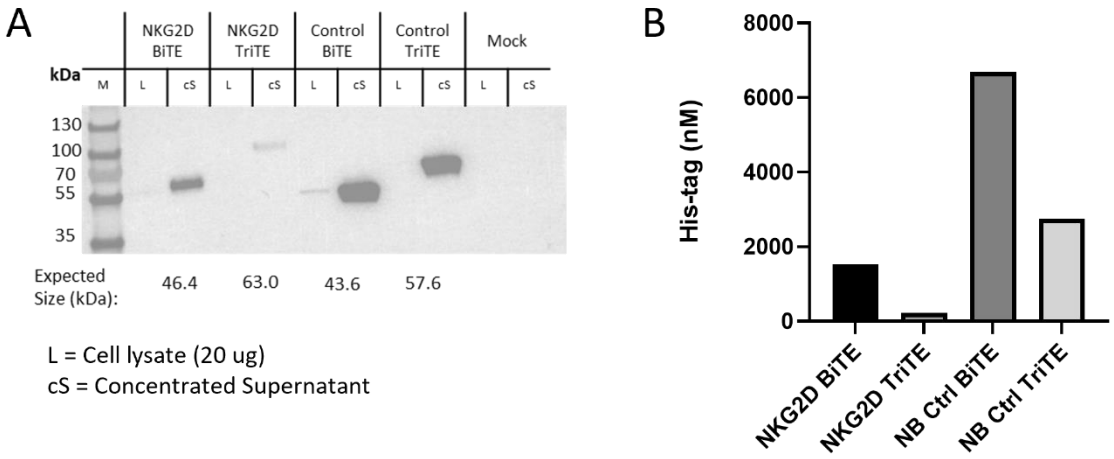

Figure 4.3: NKG2D BiTE and TriTE are successfully expressed and secreted from HEK293-T cells, along with matched controls.

HEK293-T cells were transfected with plasmids encoding the NKG2D BiTE, TriTE or control constructs. 72 hours post transfection, cell lysates and supernatants were harvested. Supernatant was concentrated around 50-fold using a 10 kDa MWKO amicon filter. Protein expression was confirmed using an anti-His tag immunoblot (A) and competitive His tag ELISA, N=1 (B).

4.3.3 The NKG2D BiTE and TriTE mediate antigen dependent cytotoxicity and induce several markers of T cell activation.

To initially assess the ability of the NKG2D BiTE and TriTE to induce T-cell mediated cytotoxicity against a NKG2DL positive cell line we used the xCELLigence system to detect target cell death. Briefly, the xCELLigence system passes an electric current through the bottom of the cell culture plate every 15 minutes. This signal is impeded by the presence of cells bound to the bottom of the plate in a dose dependent manner. Once a target cell is killed via a T cell, the cell will no longer be able to adhere to the plate and so the impedance will be reduced. This metric is displayed as a cell index whereby a higher value indicates a higher number of cells attached to the plate. In accordance with this, a lower cell index indicates an increase in cytotoxicity. Using this technology we can achieve real-time cytotoxicity analysis.

For this assay, the colorectal cell line, DLD-1, were seeded as target cells and allowed to adhere for 24 hours. The next day PBMC-derived T cells were added at an effector to target ratio of 5:1. An initial concentration of 1 nM for each construct was used based on the dose of other BiTE constructs utilised in our lab. As shown in Figure 4.4, both the NKG2D BiTE and TriTE reduce the amount of adherent target cell line with the NKG2D TriTE outperforming the NKG2D BiTE. Furthermore, the CtrlNB constructs and the T cells alone treated DLD-1s are unaffected and continue to proliferate, similarly to the DLD-1 alone condition.

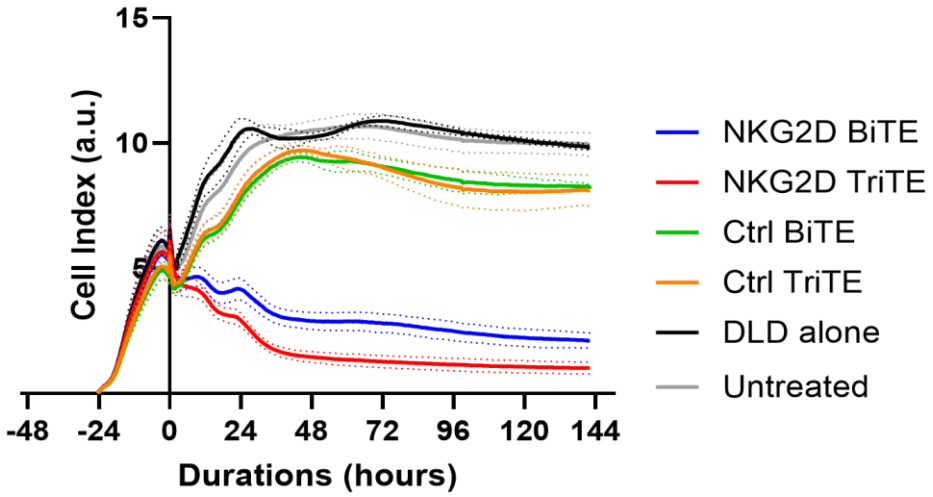

Figure 4.4: NKG2D BiTE and NKG2D TriTE are cytotoxic against the colorectal cell line, DLD-1.

DLD-1 cells were seeded and subsequently treated with PBMC-derived T cells (effector: target ratio – 5:1) and 1 nM of the indicated construct. Cell index recorded using the xCELLigence system, by measuring impedance of signal at 15-minute intervals. N = 2, represented as mean +/- SD.

Having determined that both the NKG2D BiTE and TriTE can mediate cytotoxicity, we next sought to investigate the optimal timepoint. As previously stated, DLD-1 cells were seeded 24 hours prior to the addition of PBMC-derived T cells and BiTE/TriTE. To determine whether the BiTE-mediated T cell activation was due to the presence of the NKG2DLs on the surface of the target cells, the assay was conducted both as a co-culture with DLD-1 cells as well with the T cells in a monoculture.

As shown in Figure 4.5A, we can see a decrease in DLD-1 viability when treated with either the NKG2D BiTE or TriTE from the 48-hour timepoint. This decrease in viability is T cell dependent as we see minimal changes in viability without the presence of T cells (Figure 4.5B). It is noted that this decrease in viability is not as dramatic as that seen in the initial assay (Figure 4.4) and this is likely an issue due to the variation between different PBMC batches.

T cell activation was assessed using the T cell activation markers CD25, CD69 and 4-1BB. There is an increase in the expression of all three markers, in both CD4+ and CD8+ T cells, in the co-culture conditions, when treated with either the NKG2D BiTE or TriTE whilst not for the control constructs

(Figure 4.5C-H). Additionally, we can see that in the monoculture conditions, there is no increase in any of the activation markers except for CD137 (4-1BB) at the later timepoints. Again, the NKG2D TriTE either outperformed or was equal to the NKG2D BiTE when looking at CD25 and CD69 expression. Looking at 4-1BB expression, the NKG2D BiTE treatments results in a higher expression in CD4+ T cells and similar levels of expression overall in CD8+ T cells. We also see a decrease in CD69 levels from 72 hours post treatments, consistent with CD69 being an early marker for T cell activation. For future experiments, the timepoint of 72 hours will be used for PBMC-derived T cell-based BiTE assays as this is when we see the maximal response for all markers.

From this data, we can conclude that both the NKG2D BiTE and TriTE are able to activate T cells in a target cell dependent manner. Additionally, the cytotoxicity observed is T cell dependent. Overall, we can see that the NKG2D TriTE is out competing the NKG2D BiTE showing that the increase in avidity between the target and T cell is a limiting factor for the NKG2D BiTE.

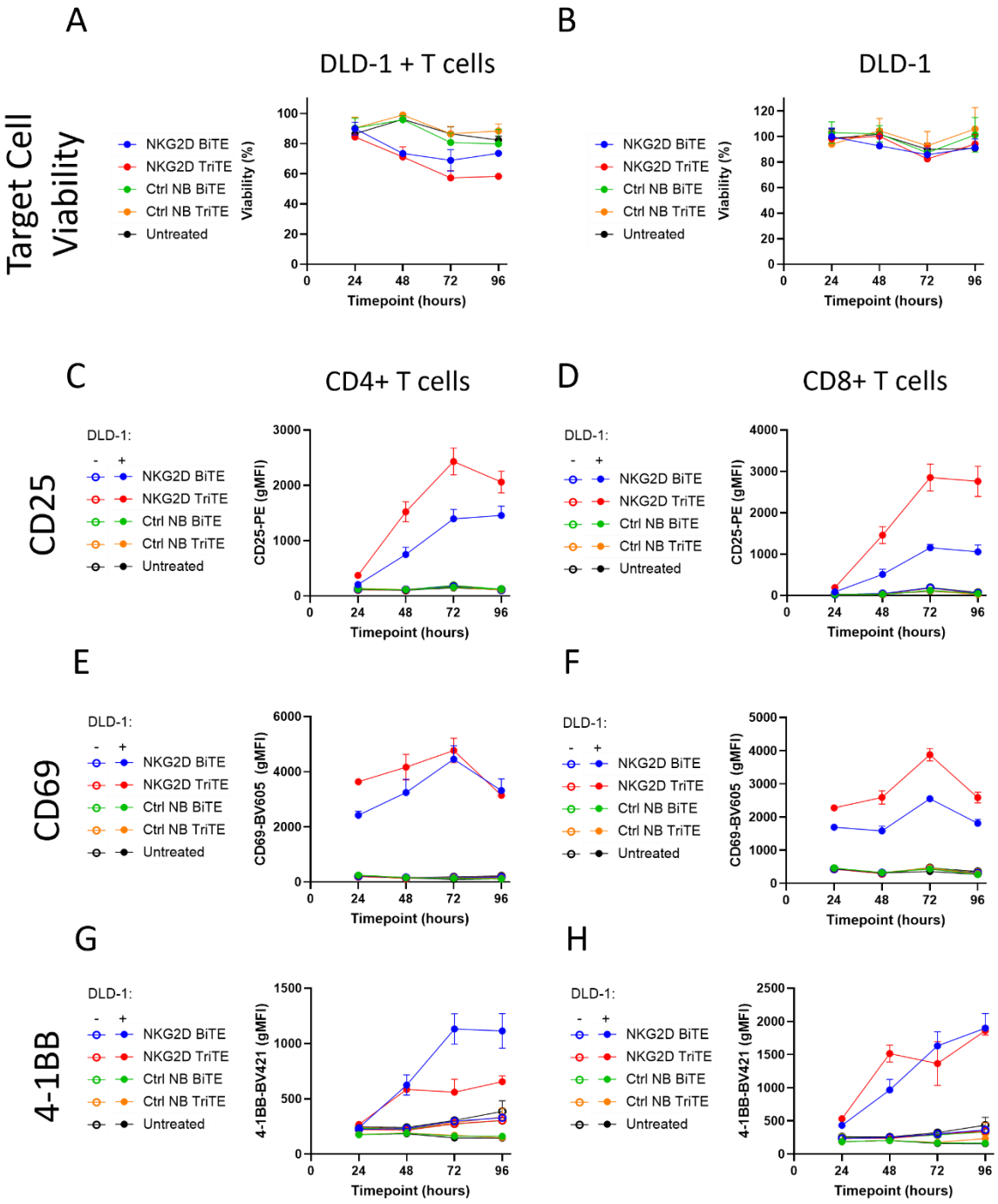

Figure 4.5: Peak potency of the NKG2D BiTE and TriTE occurs by 72 hours.

DLD-1 cells were seeded and subsequently treated with 1 nM of the indicated construct, in the (A, C, E + G) presence or (B, D, F + H) absence of PBMC-derived T cells (effector: target ratio – 5:1). (A+B) Viability was assessed via XTT assay at the indicated timepoints. (C-H) T cell activation was assessed via flow cytometry for T cell activation markers, CD25 (C+D), CD69 (E+F) and 4-1BB (G+H) at the indicated timepoints. (C, E, G) Data shown as average mean fluorescence. (D, F, H) Percentage positive, using unstimulated control to gate at 1%. N = 3, represented as mean +/- SD.

To confirm that we our using an optimal dose for these functions we carried out a brief dose response experiment using T cell activation markers as the main readout (Figure 4.6). For both the NKG2D BiTE and NKG2D TriTE, both the percentage positive and gMFI for CD25 and CD69 increase in a dose dependent manner, with the NKG2D TriTE reaching a plateau at around 0.1-1 nM. The NKG2D BiTE does not reach a plateau however higher doses were not able to be tested due to limitations in the yields of the NKG2D TriTE protein. The dose of 1 nM was selected for future assays as this gave the maximum response for the NKG2D TriTE whilst also giving a reasonable response for the NKG2D BiTE. Additionally, it would allow for a lower amount of starting material to be used which, due to the low yields of NKG2D TriTEs we were able to produce, was a limiting factor. Furthermore, both control constructs shown minimal to no activation when using these doses.

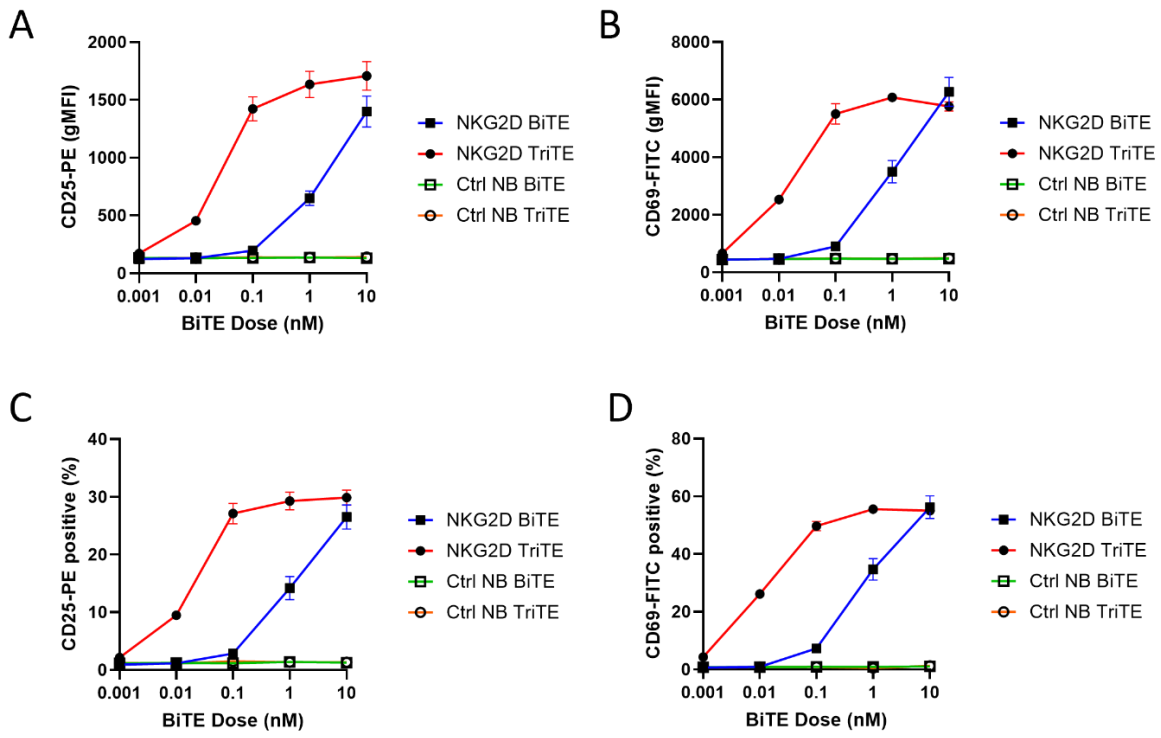

Figure 4.6: Dose response of NKG2D BiTE and TriTE.

Colorectal cancer cells, DLD-1, were co-incubated with PBMC-derived T cells for 72 hours with a range of concentrations of the indicated treatments. After incubation, T cells were stained for T cell activation markers, CD25 (A + C) and CD69 (B + D), and analysed via flow cytometry. N = 3, represented as mean +/- SD.

The previous data utilised concentrated supernatant from transfected HEK293 cells. Whilst we saw no cytotoxicity from the control constructs, and all the constructs were produced in the same manner, we sought to confirm that the cytotoxicity observed was due to the potency of the NKG2D BiTE and TriTE and not due to an unknown artefact within the supernatant. Therefore, the constructs were purified via IMAC via the decahistidine tags present on each protein construct.

Clarified and filtered supernatant from transfected HEK293 cells was incubated with nickel beads overnight, washed and then eluted using a higher concentration of imidazole. A PBS buffer exchange was carried out on the elute to remove the imidazole and the dialysed eluate was then concentrated using a 10 kDa MWKO amicon filter, aliquoted and stored at -80^{o}C. Samples were analysed via SDS-PAGE followed by instant blue to visualise the purity of the proteins and western blot to confirm presence of target protein (Figure 4.7). For all constructs, the concentrated elute showed one protein product of the correct size (Figure 4.7A+B). Bands of the same size were also detected via anti-his tag immunoblot (Figure 4.7C+D).

Aggregation or higher order oligomers could cause an issue in functionality by allowing non-specific activation of T cells, i.e. if a dimer where to form containing two αCD3 ScFvs, a pseudosynapse could be formed between T cells. To determine if the constructs were remaining as monomers, samples were analysed under native conditions to preserve the structure of the proteins. Proteins migrated as expected according to their net charge at pH 8.3 (detailed in Figure 4.7G), with the NKG2D BiTE and TriTE migrating further through the gel than the control constructs. Whilst the NKG2D TriTE has a more negative net charge that the NKG2D, they seem to migrate at a similar pace, most likely due to the difference in protein size.

1- Clarified Supernatant; 2 – Elute; 3 – Concentrated Elute.

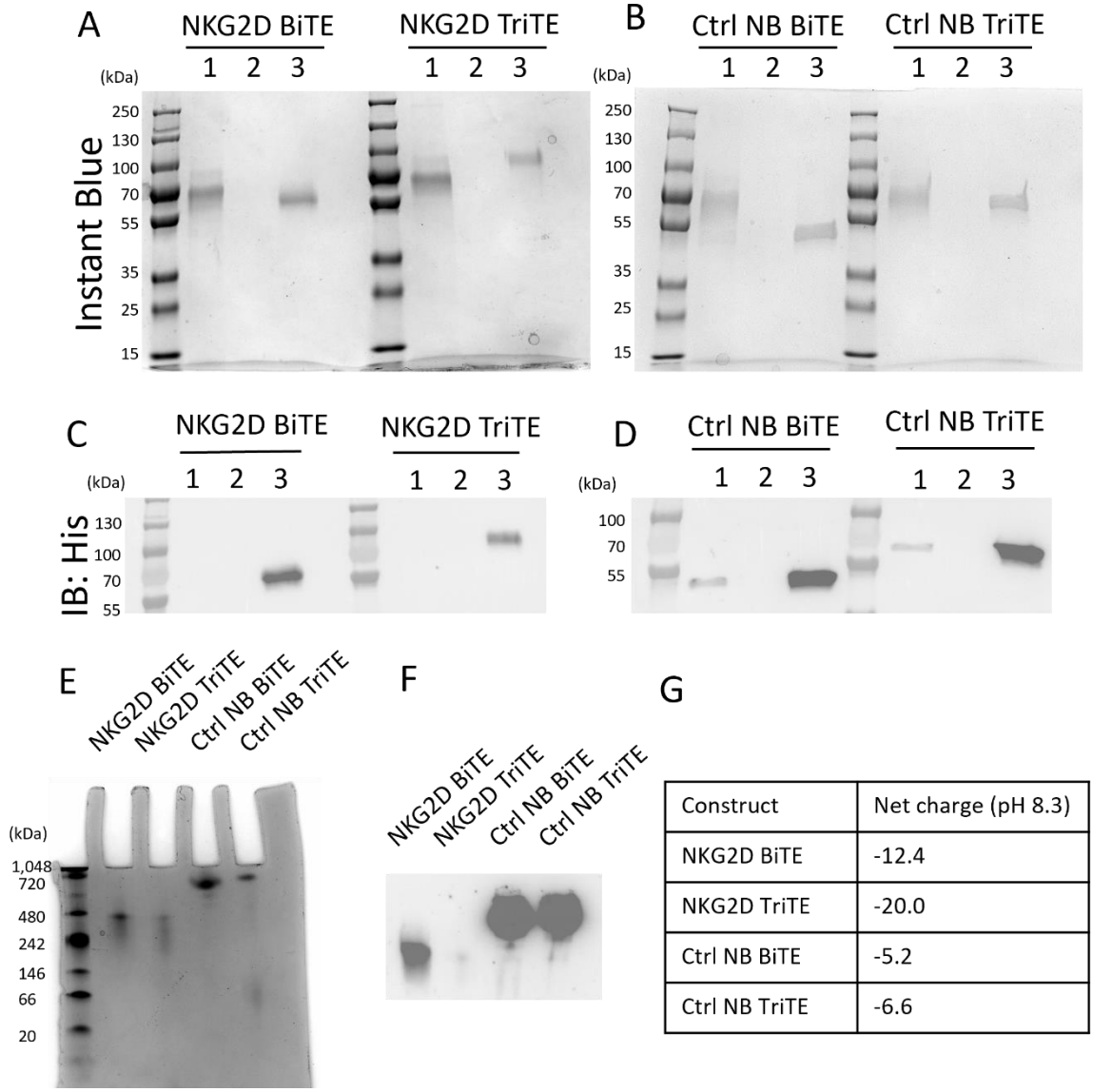

Construct	Net charge (pH 8.3)
NKG2D BiTE	-12.4
NKG2D TriTE	-20.0
Ctrl NB BiTE	-5.2
Ctrl NB TriTE	-6.6

Figure 4.7: Purification of NKG2D and control BiTEs and TriTEs via IMAC.

HEK293-T cells were transfected with plasmids encoding the NKG2D BiTE, TriTE or control constructs. 72 hours post transfection, supernatants were harvested and clarified. His tag protein was purified using an IMAC system and eluted with 200 mM imidazole. (A-D) Samples were analysed via SDS-PAGE gel under reducing conditions. 1 – Clarified supernatant, 2 – Dialysed elute, 3 – concentrated elute. (A + B) Total protein was detected using InstantBlue to assess purity. (C+D) Western blot analysis of His tag proteins to confirm size and identity of protein. (E+F) Concentrated elute was analysed via Native PAGE to assess the oligomerisation state of the protein. (E) Total protein was detected using InstantBlue to assess purity. (F) Western blot analysis of His tag proteins to confirm size and identity of protein. (G) Predicted charge of each protein at the pH of the Native PAGE conditions (pH 8.3). Calculated using https://www.protpi.ch/Calculator/ProteinTool

When tested functionally, in co-culture experiments, the purified constructs produced similar T-cell dependent, cytotoxic effects to the concentrated supernatant samples seen previously (Figure 4.8A). The NKG2D BiTE and TriTE treated co-cultures saw a significant decrease in target cell viability in comparison to the untreated condition, whereas there was no significant change for the control constructs.

Overall, we saw significant increase in all T cell activation markers assessed for the NKG2D BiTE and TriTE, with activation seen in both CD4+ and CD8+ T cells (Figure 4.8B). As seen previously, there was a significant increase in CD25, CD69 and CD137 (4-1BB), in both percentage positive as well as in median fluorescence. Additionally, the NKG2D TriTE again outperformed the NKG2D BiTE. Controls constructs showed no significant change in expression of T cell effector proteins apart from perforin expression, and there was no significant difference in expression of any markers in monocultures.

We looked more in depth at later T cell activation markers, particularly those with functions related to the release of cytotoxic molecules towards the target cell. The presence of CD107a (also known as LAMP-1) on the cell membrane is a marker for degranulation of CD8 T cells as well as NK cells. For both CD4 and CD8 T cells, we can see a significant increase in surface CD107a positive cells upon treatment with the TriTE only when in a co-culture with target cells and not when treated as a monoculture. Control constructs and untreated samples both showed minimal expression above the baseline both in the co-culture and monoculture. Surprisingly, there was a decrease in CD107a surface expression in the control and untreated conditions when in a co-culture with DLD-1 cells versus the monoculture, especially for the CD4+ T cells. Despite this, both the NKG2D BiTE and TriTE induce a significant difference in CD107a expression, in a target cell dependent manner, in comparison to the untreated condition.

To detect cytokines being produced by the T cells, protein secretion was inhibited for 6 hours prior to staining allowing the accumulation of protein within the cell. Post extracellular staining, T cells were fixed and permeabilised to allow for intracellular staining of interferon-γ, perforin and granzyme B.

Similarly to the other T cell markers assessed, a significant increase in the expression of all three of these molecules was detected in the NKG2D TriTE treated co-culture. As CD8+ T cells are characterised as having more of cytotoxic function, it is unsurprising to see higher levels of both granzyme B and perforin in these cells in comparison to the CD4+ T cells. Consistent with this is the basal level of granzyme B and perforin protein seen in CD8+ T cells but not in CD4+. Additionally, there was a significant increase in interferon-γ production in both CD4+ and CD8+ T cells from NKG2D TriTE treated co-cultures. IFNy production is important to establish a pro-inflammatory environment and aid in full T cell activation being achieved. The NKG2D BiTE does not show the same pattern with these later markers of T cell activation as the earlier ones with there being a slight increase in perforin expression in CD4+ T cells but not in other markers.

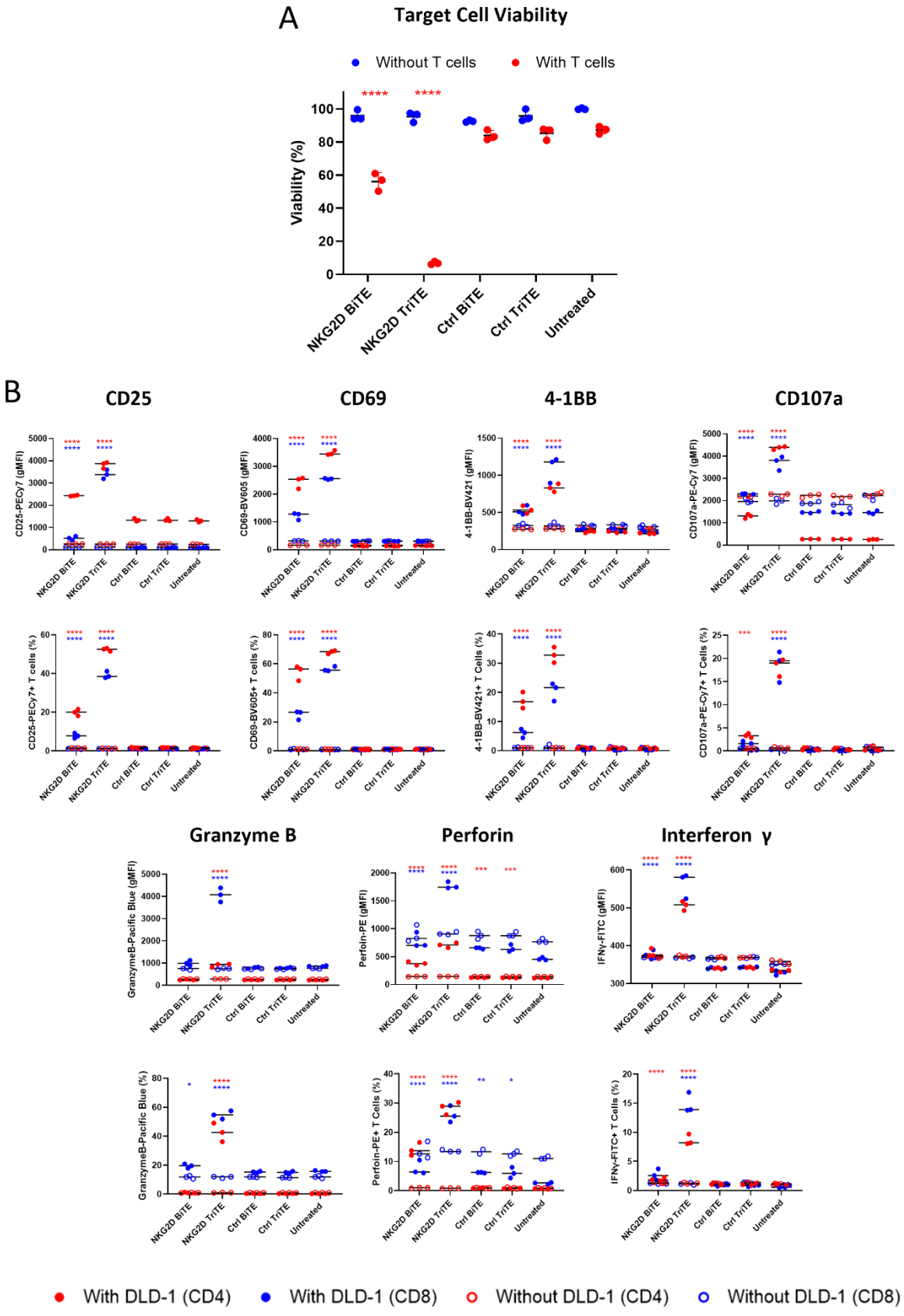

Figure 4.8: NKG2D BiTE and TriTE are the active components in the conditioned supernatant and induce T cell activation as shown by variety of different markers.

Colorectal cancer cells, DLD-1, were co-incubated with 1 nM of the indicated constructs in the presence (filled) or absence (unfilled) of PBMC-derived T cells for 72 hours. (A) Cell viability determine by XTT assay. (B) After incubation, T cells were treated with GolgiStop and GolgiPlug for 6 hours to prevent the secretion of cytokines. T cels were then stained for CD4 (red), CD8 (blue) and extracellular T cell activation markers, CD25, CD69, 4-1BB and CD107a, followed by fixation and permeabilization to stain for intracellular markers granzyme B, perforin and IFN- γ. Samples were then analysed via flow cytometry. Percentage positive, using unstimulated control to gate at 1% for each cell line. Data shown as average mean fluorescence. N = 3, represented as mean +/- SD. Statistical significance assessed by two-way ANOVA with Dunnett's multiple comparisons test to untreated, $p<0.05$ *, $p<0.01$ **, $p<0.001$ ***, $p<0.0001$ ****. Samples in the absence of T cells (monoculture) were not significantly different from the untreated. Asterisks refer to the co-culture samples.

4.3.4 Investigating the correlation between antigen abundance and T cell-mediated cytotoxicity.

We were intrigued about the sensitivity of the NKG2D BiTE/TriTE and hypothesised that the level of expression of the ligands was correlated with the level of T cell activation. As shown in Chapter 3, cancer cell lines isolated from a variety of different tissues express NKG2DLs and exhibit a large range of expression levels. A smaller panel of these human cancer cell lines were selected based on their relative expression levels, as described in Table 4-1. These eight cell lines were identified and being high, medium or low expressing based on their relative expression in comparison to the IgG1 control.

Table 4-1: Panel of cancer cell lines.

NKG2D ligand expression level	Cell line
High	Jurkat
	Molt-4
	K562
Medium	DLD-1
	A549
	U2OS
Low/None	Raji
	JJN3

T cell co-culture experiments with each of these cell lines were set-up in parallel to test the efficacy of the NKG2D BiTE and TriTE. Adherent cell lines were seeded 24 hours prior to allow them to settle and adhere to the plate. Suspension cells were added to the co-culture at the same time as the T cells and treatment. Co-cultures were incubated for 72 hours prior to harvest and staining for flow cytometry analysis to determine target cell viability and T cell activation.

Surprisingly we saw that the highest cytotoxicity and T cell activation was seen in the 'medium' expressing cell lines, and even within this group, the NKG2DL abundance did not correlate with the potency of the therapeutics (Figure 4.9F+G). In Figure 4.9A, both the NKG2D BiTE and TriTE caused a decrease in Jurkat cell viability, however this does not seem to be dependent on PBMC-derived T cell activation. The only 'high' expressing cell line that gave a significant increase in T cell activation was K562s, however this was to a much lower level that that seen in the 'medium' expressers and no significant difference in K562 viability was seen. We also observed some T-cell mediated cytotoxicity with the JJN3 cells which express low levels of NKG2DLs when treated with the NKG2D TriTE, however in another NKG2D negative cancer cell line, Raji, we saw a slight increase in viability upon treatment with either the NKG2D BiTE or TriTE (Figure 4.9A).

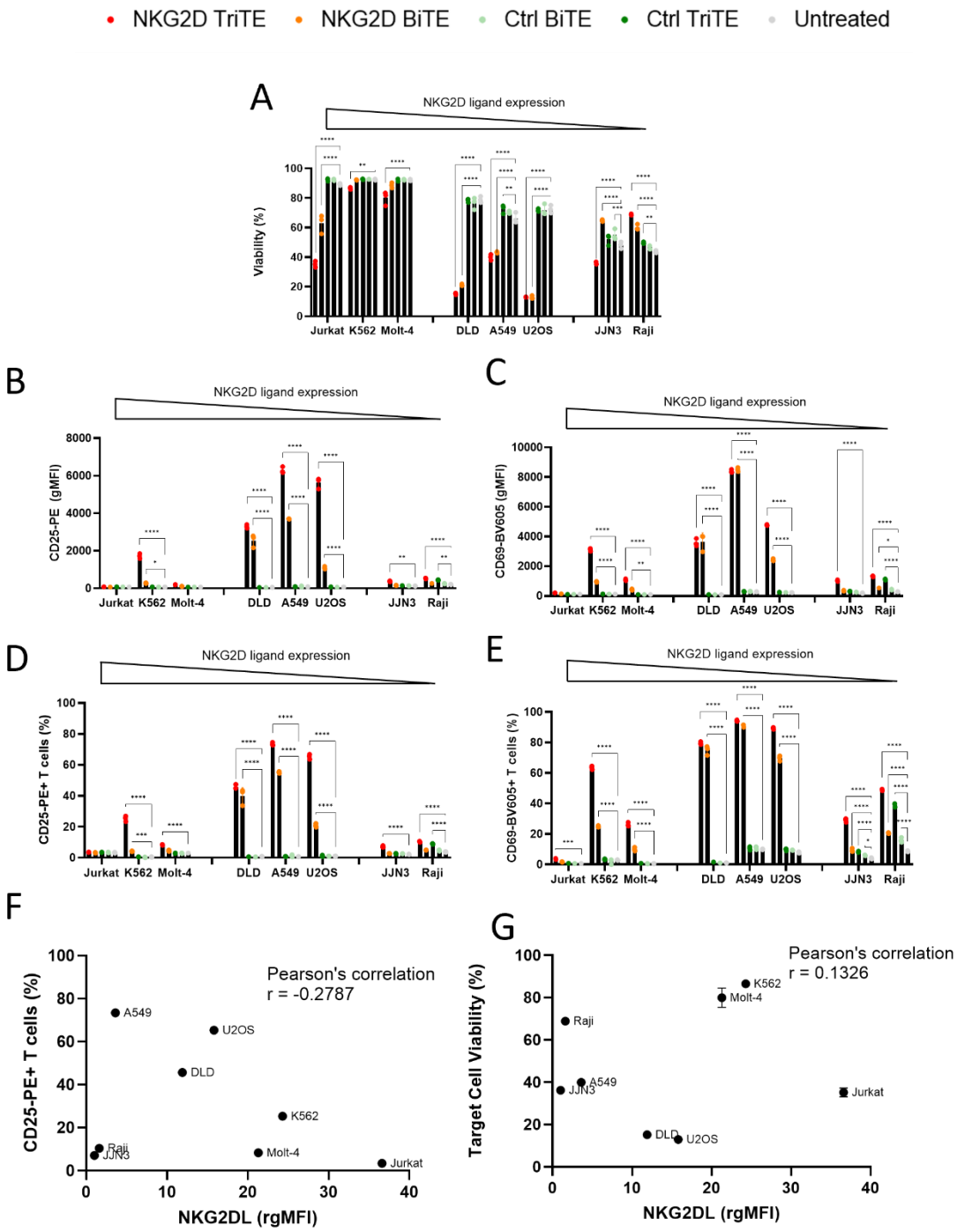

Figure 4.9: Expression of ligands on cancer cell lines does not correlate with cytotoxicity and T cell activation.

Target cell lines were incubated with PBMC-derived T cells and 1 nM of the indicated construct (effector: target ratio – 5:1). After treatment, cells were harvested and stained for T cell activation markers and target cell viability (A). (B-E) T cell activation markers were assessed via staining for CD25 (B+D) and CD69 (C+E). Statistical significance assessed by two-way ANOVA with Dunnett's multiple comparisons test to untreated, $p<0.05$ *, $p<0.01$ **, $p<0.001$ ***, $p<0.0001$ ****. (B-C) Data shown as average mean fluorescence. (D-E) Average percentage positive, using unstimulated

control to gate at 1% positive. N = 3, represented as mean +/- SD. (F+G) Comparison of NKG2DL relative gMFI (as detailed in Table 3-1) to target cell viability (F) and percentage CD25 positive (G) upon treatment with NKG2D TriTE.

As we previously saw in Chapter 3, non-malignant cell lines show minimal to no expression of NKG2DLs. We would then hypothesise that these cells would be spared from NKG2DL mediated cytotoxicity. However, as we saw a small amount of cytotoxicity with some of the cancer cell lines that express low levels of NKG2DLs, we sought to investigate the off-tumour effect of the NKG2D BiTE/TriTE on non-malignant cell lines. Cell lines were treated with the NKG2D BiTE/TriTE or control constructs in co-cultures as previously described.

In Figure 4.10A, we can see that there was no significant change in target cell viability in any of the three non-malignant cell lines tested, whilst in NKG2D positive breast cancer cell line, MDA-MB-231, there was a highly significant decrease in target cell viability. Surprisingly, we did see a significant increase in CD69 expression on T cells (Figure 4.10D-E), as well a small but significant increase in CD25 overall expression (Figure 4.10C), however this was to a much lower level than that seen for positive control cell line, MDA-MB-231 (Figure 4.10B-E).

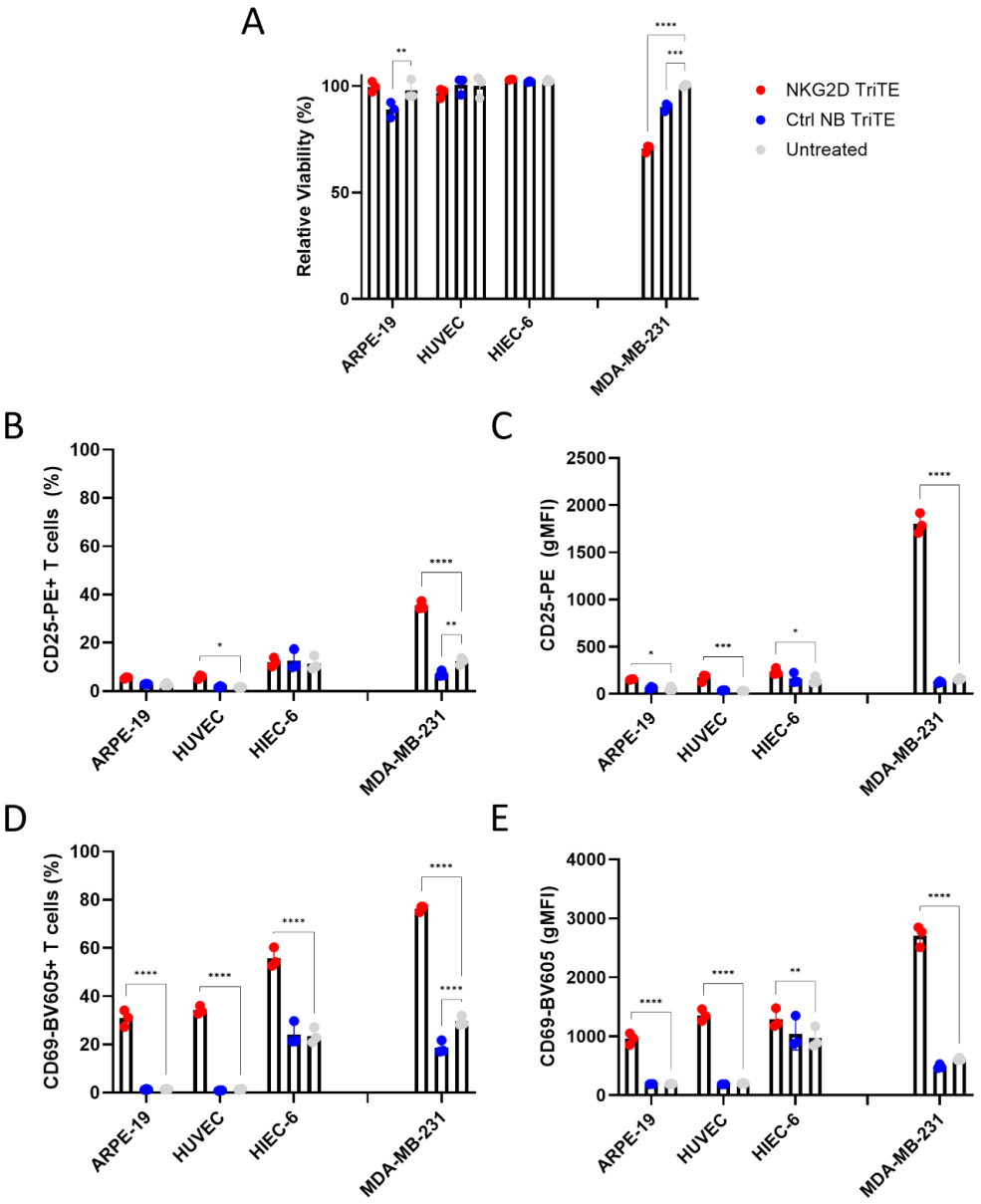

Figure 4.10 - NKG2D TriTE does not have significant potency against non-malignant cells.

Target cell lines were incubated with PBMC-derived T cells and 1 nM of the indicated construct for 72 hours (effector: target ratio – 5:1). After incubation, cells were stained for target cell viability (A) and T cell activation markers, CD25 (B+C) and CD69 (D+E), and analysed via flow cytometry. (B+D) Data shown as average mean fluorescence. (C+E) Average percentage positive, using unstimulated control to gate at 1% positive. N = 3, represented as mean +/- SD. Statistical significance assessed by two-way ANOVA with Dunnett's multiple comparisons test to untreated, $p<0.05$ *, $p<0.01$ **, $p<0.001$ ***, $p<0.0001$ ****.

4.3.5 NKG2D TriTE specifically activated in situ T cells in colorectal liver metastasis.

To test the NKG2D TriTE in a more physiologically relevant setting, we utilised a human tumour sample freshly resected from a patient with colorectal liver metastasis. Utilising primary tumours is far more clinically relevant than *in vitro* assays utilising cancer cell lines, retaining the spatial architecture of the tumour and allows for the testing of the therapeutics on *in situ* T cells, within the tissue. For this experiment, multiple sections of the same tumour were taken to assess how different areas of the tumour would respond to the therapeutic. Tumour sections were sliced at 250 µm thick and incubated in slice media overnight and then treated with the NKG2D TriTE, control TriTE or left untreated. Samples were taken every 2 days to assess the levels of IFNγ as a readout for T cell activation. As shown in Figure 4.11, the NKG2D TriTE was able to significantly increase IFN-γ production in both slices assessed, detectable 48 hours post treatment. There was no production of IFN- γ detected in the control TriTE or untreated slice cultures.

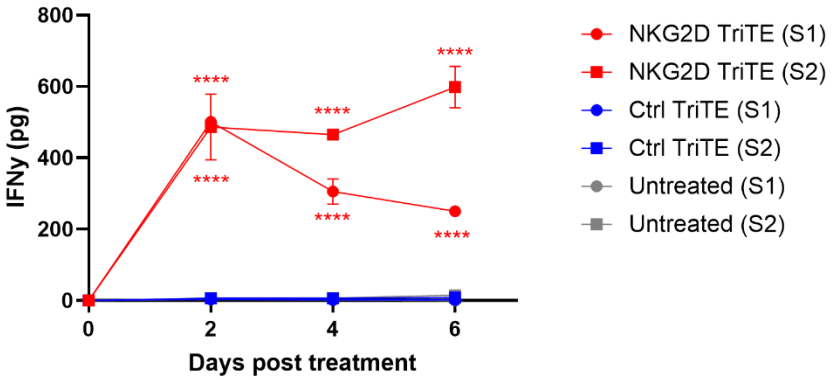

Figure 4.11: NKG2D TriTE treatment of colorectal liver metastasis induces a significant increase in IFN- γ production.

Slices of colorectal liver metastases were incubated with 1nM of the indicated constructs for 6 days. Conditioned supernatant was collected at the indicated timepoints. IFN-γ was detected in the conditioned supernatant for sandwich ELISA. N=2 slices from 1 patient. Statistical significance assessed by two-way ANOVA with Dunnett's multiple comparisons test to untreated (S1), $p<0.0001$ ****. S1 – slice 1; S2 – slice 2.

4.3.6 Conventional cancer treatments enhance NKG2D BiTE and TriTE mediated cytotoxicity.

As shown in Chapter 3, many treatments lead to an increase in NKG2DL surface expression, even in cancer cell lines that are negative when untreated. We next sought to determine if this increase in ligand expression leads to an increase in T cell activation as well as cytotoxicity. A549 cells were seeded in 96 well plates 24 hours prior to treatment. Plates were subjected to the indicated dose of radiation with T cells and treatments being added shortly after. 72 hours post treatment, T cells were harvested for staining and target cells were assessed for viability using an XTT assay. As shown in Figure 4.12D, there was a dose dependent increase in CD25 expression with NKG2D TriTE treatment up until the plateau of 5 Gy. There was a small increase in activation seen for the NKG2D BiTE, with a significant increase in CD69 expression and percentage positive CD25 cells at the highest dose of 10 Gy. No T cell activation was detected in either control construct or the untreated conditions. Interestingly these results did not correlate with the viability data which showed the largest decrease

in the 2 Gy dose for all conditions (Figure 4.12A). We hypothesise that the target cell upregulates DNA repair enzymes and anti-apoptosis proteins in response to the high dose of radiation, allowing for increased resistance to cell death in the higher radiation treatment, at least in the short term. However, at longer time points, we predict the 10 Gy would succumb to a similar fate.

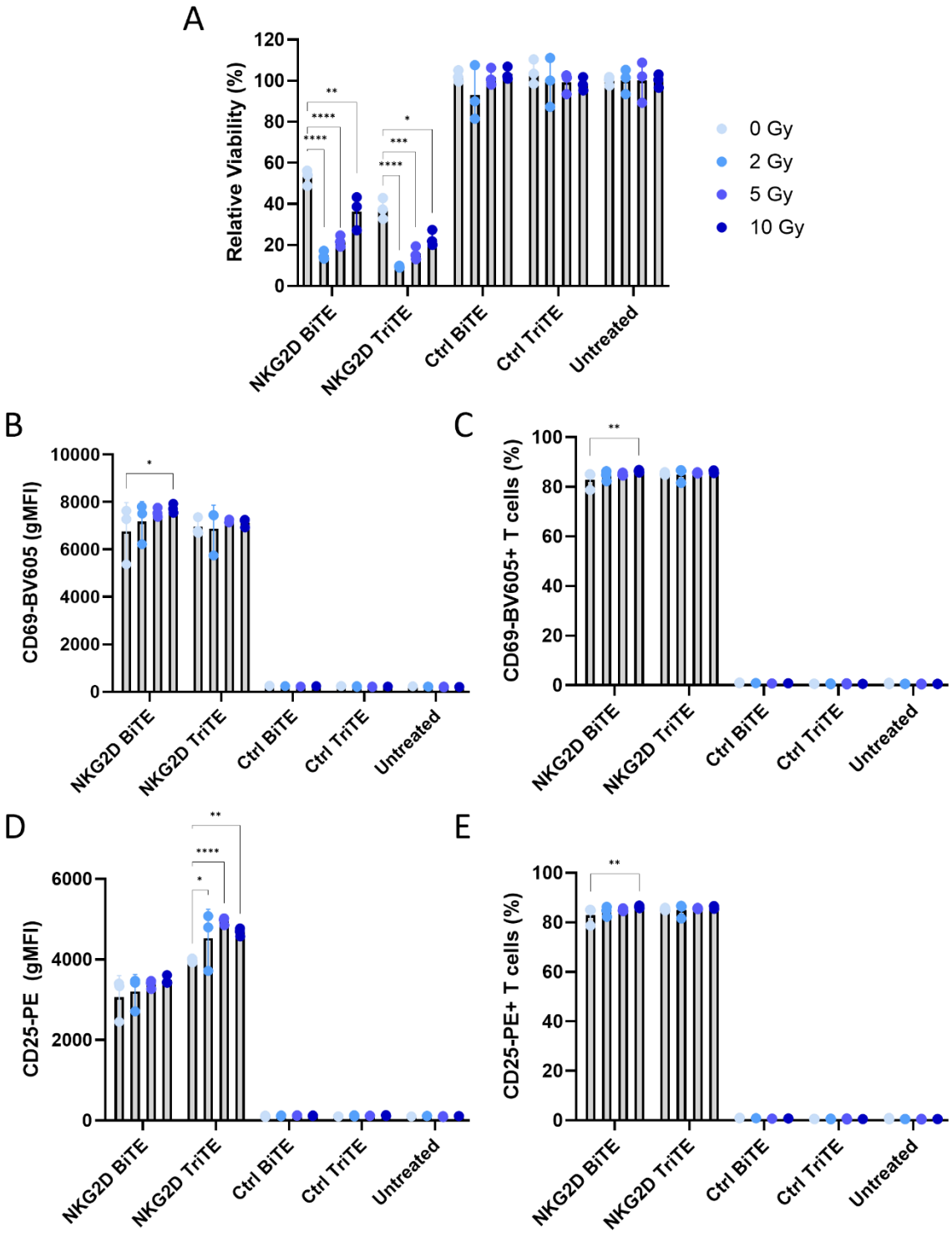

Figure 4.12: Radiation in combination with NKG2D BiTE and TriTE treatment leads to improved cytotoxicity.

A549 cells were seeded 24 hours prior to radiation to allow adherence. The following day, cells were exposed to the indicated dose of gamma irradiation before addition of PBMC-derived T cells and 1 nM of the indicated construct for 72 hours (effector: target ratio – 5:1). (A) Viability was assessed via XTT assay. (B-E) T cell activation was assessed via flow cytometry for T cell activation markers, CD69 (B+C) and CD25 (D+E). Statistical significance assessed by two-way ANOVA with Dunnett's multiple comparisons test to untreated, $p<0.05$ *, $p<0.01$ **, $p<0.001$ ***, $p<0.0001$

****. (B+D) Data shown as average mean fluorescence. (C+E) Percentage positive, using unstimulated control to gate at 1%. N = 3, represented as mean +/- SD.

We next turned our attention to tumour cell lines that typically do not express NKG2DLs, however their surface expression can be induced. In Chapter 3, we showed that HDAC inhibitors, such as valproic acid and sodium butyrate, are effective at significantly increasing surface expression of NKG2DLs in Raji and JJN3 cells. Following on from this, we sought to determine if this increase in ligands was sufficient to sensitise the cells to NKG2D BiTE/TriTE mediated killing.

JJN3 cells were incubated in a co-culture with PBMC-derived T cells and treated with NKG2D BiTE/TriTE or controls, as well as 5 mM valproic acid (VPA), 5 mM sodium butyrate (NaBut) or media. As seen in Figure 4.13A, NaBut treatment resulted in a large decrease in JJN3 viability overall, with the combined NKG2D TriTE resulting in only ~5% of JJN3 cell being viable. Similarly, we saw a significant increase in the overall expression of 2/3 T cell activation markers assessed (Figure 4.13B, D, F), in all NaBut treated co-cultures, alluding to the cytotoxicity of the target cell inducing non-specific T cell activation.

VPA treatment had a less dramatic effect on JJN3 viability as a monotherapy, however in combination with the NKG2D TriTE we see a highly significant decrease in viability, to around 40% (Figure 4.13A). Highly significant increases in T cell activation were observed in co-cultures treated with NKG2D TriTE, as well as to a lesser extent with the NKG2D BiTE (Figure 4.13B-G). No increase in expression of activation markers was observed with the control constructs or in the untreated condition.

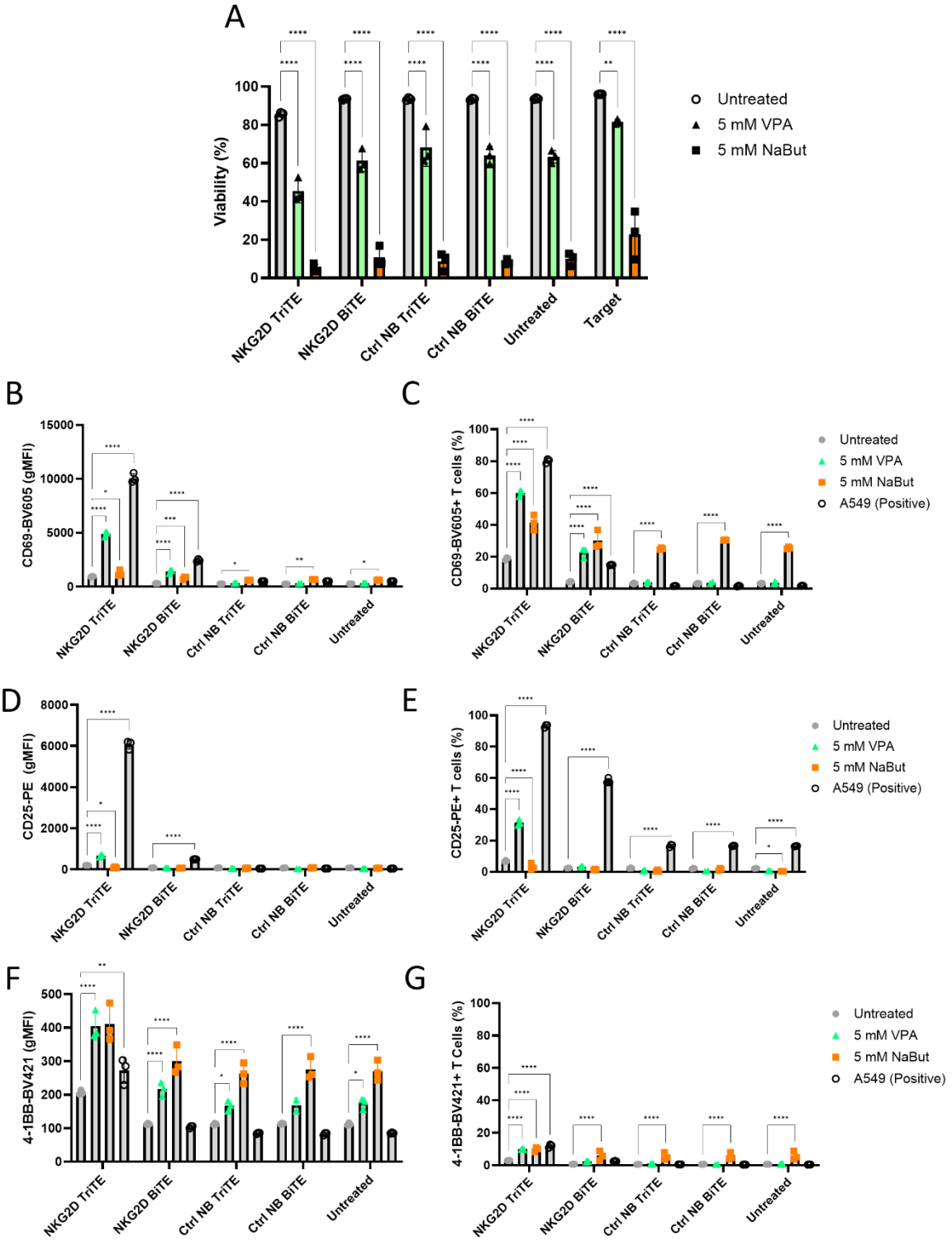

Figure 4.13: HDACi sensitise JJN3 cells to NKG2D TriTE mediated cytotoxicity.

JJN3 cells were treated with 5 mM of valproic acid (VPA) or sodium butyrate (NaBut) as well as PBMC-derived T cells and 1 nM of the indicated construct for 72 hours (effector: target ratio – 5:1). After treatment, cells were harvested and stained for T cell activation markers and target cell viability (A). (B-E) T cell activation was assessed via flow cytometry for T cell activation markers, CD69 (B+C), CD25 (D+E) and 4-1BB (F+G). N = 3, represented as mean +/- SD. Statistical

significance assessed by two-way ANOVA with Dunnett's multiple comparisons test to untreated, p<0.05 *, p<0.01 **, p<0.001 ***, p<0.0001 ****. (B, D, F) Data shown as average mean fluorescence. (C, E, G) Percentage positive, using unstimulated control to gate at 1%.

4.3.7 Arming an oncolytic adenovirus with NKG2DL targeting T cell engagers.

Via transient transfection, the NKG2D TriTE was produced at a far lower yield than the NKG2D BiTE; however, much of the work in this chapter displays the superior potency of the NKG2D TriTE when compared at equal molarity. This control of NKG2D BiTE and TriTE would not be attainable when utilising the virus to express the therapeutics. In Figure 4.6, we estimated that the NKG2D BiTE was 100-fold less potent than the NKG2D TriTE via a dose response experiment. Therefore, if the NKG2D BiTE was produced at far higher concentrations than the NKG2D TriTE it may be the more potent candidate. For this reason, we chose to engineer viruses encoding the NKG2D TriTE as well as the BiTE.

Therefore, the four constructs discussed above were cloned into the EnAd backbone using PCR to amplify the DNA sequence and adding overhangs to facilitate insertion. The EnAd backbone was digested using restriction enzymes sites, AsiSI and SbfI, that are located between the E4 and fibre regions to linearise the backbone and the fragments were inserted using HiFi assembly. Primers were designed to amplify the sequences to either contain the CMV promoter from the expression vector or to insert a splice acceptor site (SA) to allow for the expression of the constructs to be under the major late promoter (MLP) which would link the expression of the proteins to the late stage of the viral lifecycle (see Figure 4.14A for schematic).

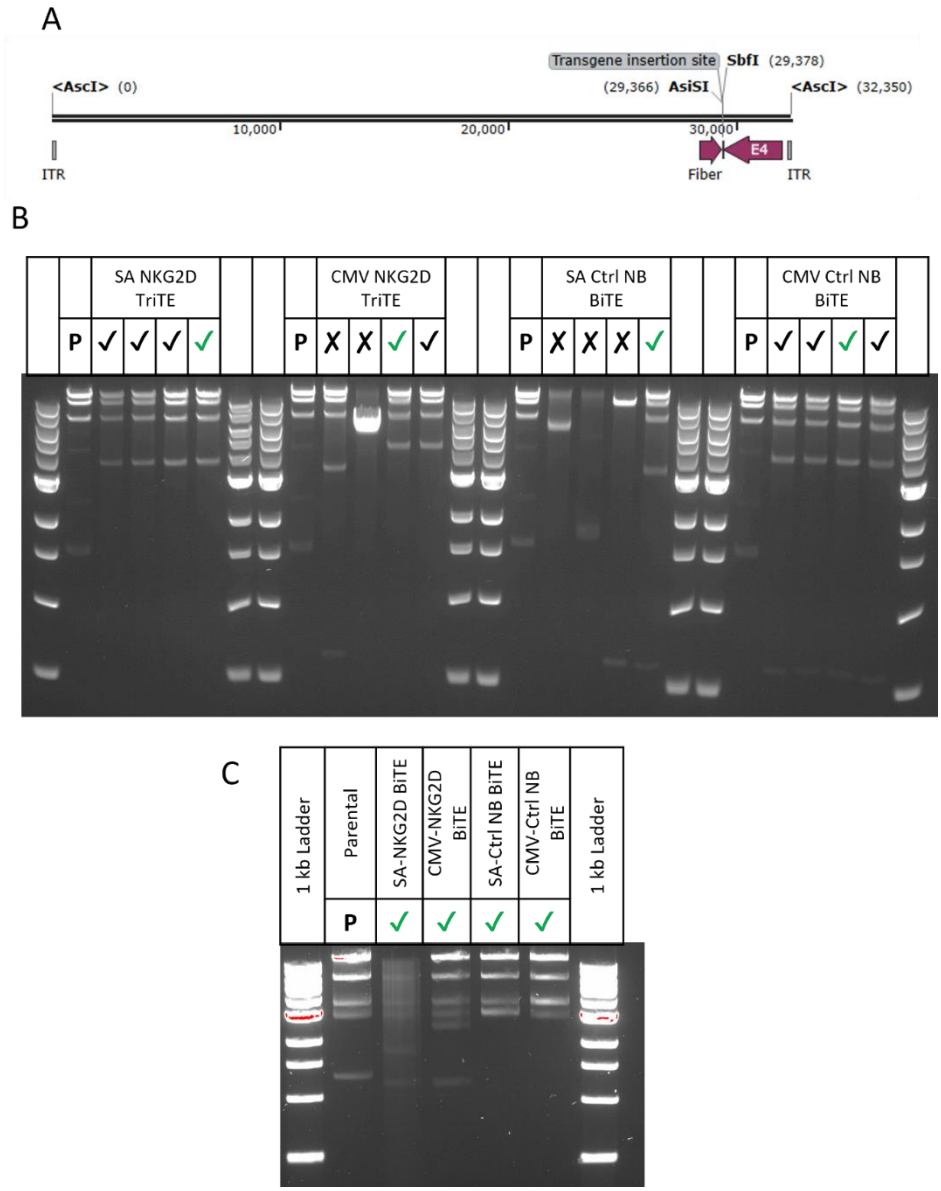

Figure 4.14: Schematic of transgene insertion into EnAd and verification of insertion.

(A) Schematic representation of the EnAd backbone depicting the insertion site used for encoding transgenes. (B+C) Test digests of NKG2D and control TriTEs (B) and BiTEs (C) to confirm correct insertion for the transgenes into the EnAd backbone. Correct clones indicated by a tick, selected clones with sequence confirmed by Sanger sequencing indicated by a green tick.

To initially validate the insertion, plasmids were subjected to a diagnostic test digest. Diagnostic test digests make us the of the unique pattern, or ‘molecular fingerprint’, that occurs when cutting a plasmid with restriction enzymes. These patterns can be used to determine if an insert has successfully been inserted. EnAd backbone plasmid or engineered constructs were digested with

ApaI and SbfI and samples were ran on an agarose gel to resolve the various bands produced. The bands produced, as seen in Figure 4.14B, were compared to the predicted sizes (using SnapGene software) to verify the insertion of the transgene, with correct insertion indicated as ticks above each lane. Correct insertion and integrity of the inserted sequence was further verified by Sanger sequencing, indicated by a green tick.

To produce virus from these plasmids, the backbones were linearised with AscI, exposing the ITRs of the viral genome. Linearised DNA was transfected in HEK293 cells to allow rescue of the viruses, being frequently checked for signs of cytopathic effect (CPE), indicating that the virus has been successfully recovered and is replicating. Upon 100% CPE, viral supernatants, plus any remaining attached cells, were subjected to three rounds of freeze thaw cycles to lyse cells, releasing any remaining viral particles. Individual clones were then isolated from the clarified viral supernatant via serial dilution. Wells with individual plaques were selected for further expansion and analysis. Titration of the expanded clarified supernatants was determined by $TCID_{50}$ in A549 cells (detailed in Figure 4.15A).

The compare the oncolytic properties of the engineered EnAd constructs to the parental virus a dose-response was carried out in DLD-1 cells. Target cell viability was determined three days post infection using an XTT assay. All viruses showed similar activity to the parental virus, with the engineered viruses being slightly more potent (Figure 4.15C). We additionally verified the production of the transgenes from the viruses. DLD-1 cells were infected at an MOI of 5 for three days. Supernatant was collected and concentrated using 100 kDa MWKO filters and analysed via His tag ELISA. All constructs could be detected with the BiTEs in general produced at higher levels that the TriTEs, with the EnAd-CMV-NKG2D BiTE produced at ~4-fold higher level than the TriTE counterpart. The control constructs were produced at much higher levels than the NKG2D ectodomain constructs, consistent with transient transfections (Figure 4.15B).

A

Viral Construct	Titre (TCID50/mL)
EnAd-SA-NKG2D BiTE	6.31E+09
EnAd-CMV-NKG2D BiTE	2.51E+09
EnAd-SA-Ctrl NB BiTE	3.98E+09
EnAd-CMV-Ctrl NB BiTE	2.51E+09
EnAd-SA-NKG2D TriTE	3.16E+09
EnAd-CMV-NKG2D TriTE	6.31E+08
EnAd-SA-Ctrl NB TriTE	7.94E+08
EnAd-CMV-Ctrl NB TriTE	1.26E+09
EnAd (parental)	1.26E+10

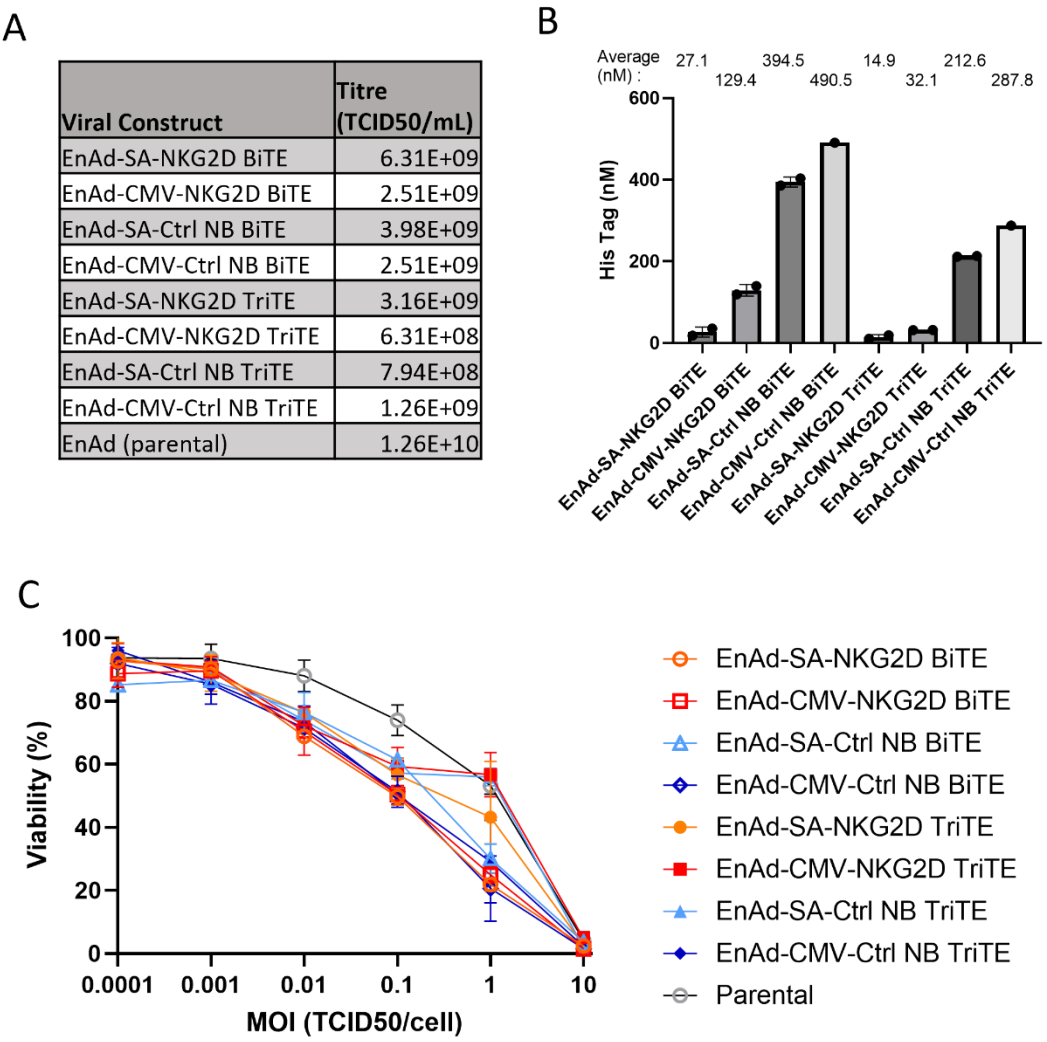

Figure 4.15: Validation and characterisation of engineered EnAd viruses encoding NKG2D BiTE and TriTE.

(A)Titres as calculated by $TCID_{50}$ in A549 cells. (B) Construct quantification via His tag ELISA. Mean concentration displayed above. N=1. (C) Cytotoxicity of viruses at a range of viral MOIs was assessed in DLD-1 cells. XTT assay measured after 3 days. Measured in triplicate, represented as mean +/- SD.

To determine the potency of the expressed NKG2D BiTE and TriTE in a co-culture of tumour cells and T cells, we decided to use an MOI of 0.1, to allow the therapeutic to be expressed from a smaller number of virally infected cells, without the effects of oncolysis masking the effect of BiTE-mediated cytotoxicity. DLD-1 cells were infected at an MOI of 0.1 in the presence of absence of PBMC-derived T cells, and assessed for cytotoxicity in real time using the xCELLigence system (Figure 4.16A+B). The

viruses encoding the NKG2D TriTE, either under the CMV promoter or MLP via a SA, showed a decrease in the cell index starting from around 72 hours when in a co-culture with T cells, however, little to no cytotoxicity was seen for the monoculture or in other conditions. Both viruses showed similar killing profiles with the EnAd-SA-NKG2D TriTE virus killing marginally quicker than then EnAd-CMV-NKG2D TriTE virus, and both resulting in complete cytotoxicity of the target cell at around 120 hours post infection (Figure 4.16B). This killing was associated with a significant difference in multiple T cell activation markers in both CD4+ and CD8+ T cells, including CD69, CD25 and 4-1BB, which was not seen in the monoculture, the NKG2D BiTE expressing viruses or with the control viruses (Figure 4.16C-E).

A

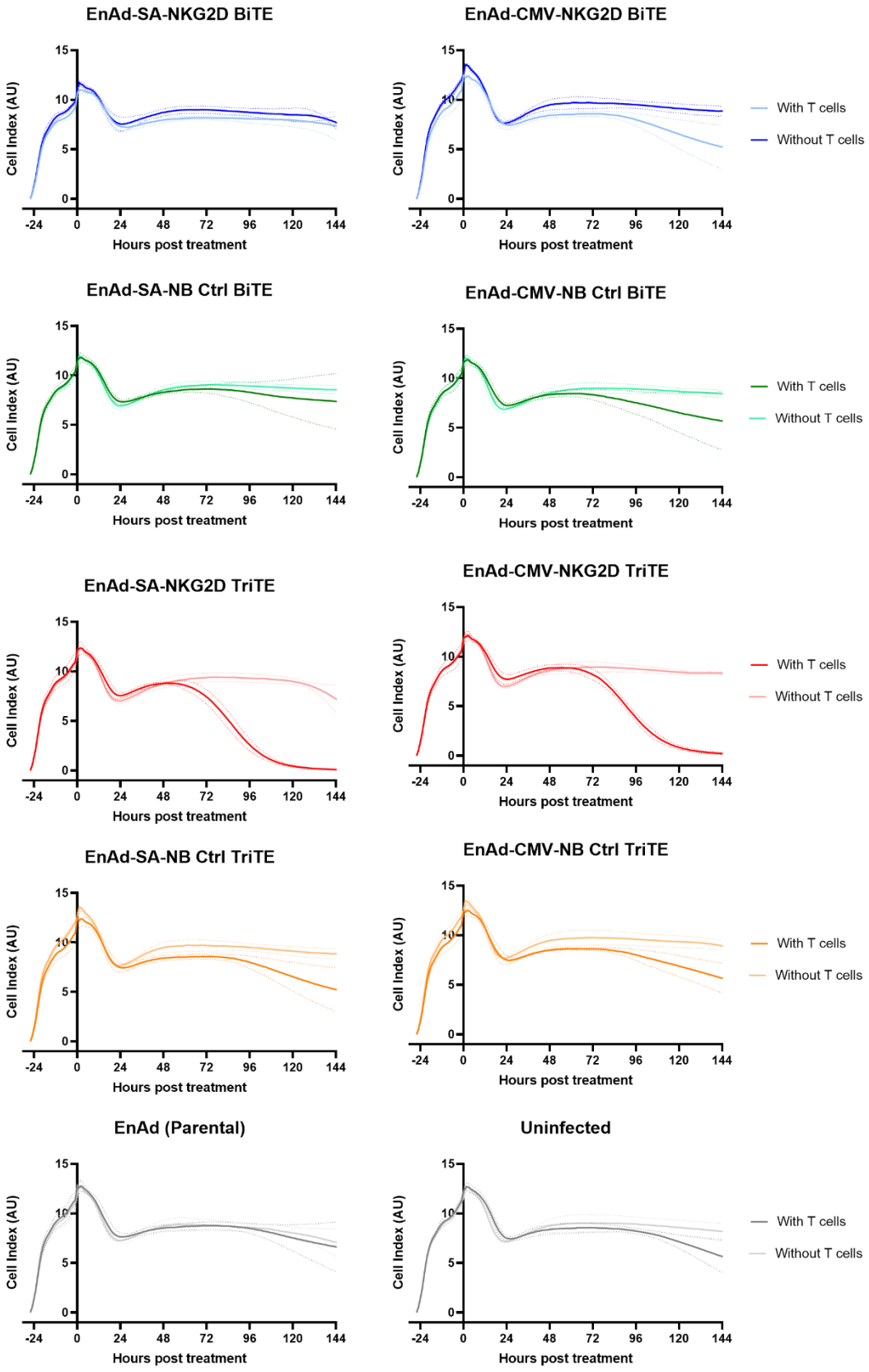
EnAd-SA-NKG2D BiTE
EnAd-CMV-NKG2D BiTE
EnAd-SA-NB Ctrl BiTE
EnAd-CMV-NB Ctrl BiTE
EnAd-SA-NKG2D TriTE
EnAd-CMV-NKG2D TriTE
EnAd-SA-NB Ctrl TriTE
EnAd-CMV-NB Ctrl TriTE
EnAd (Parental)
Uninfected
Cell Index (AU)
Hours post treatment
With T cells
Without T cells

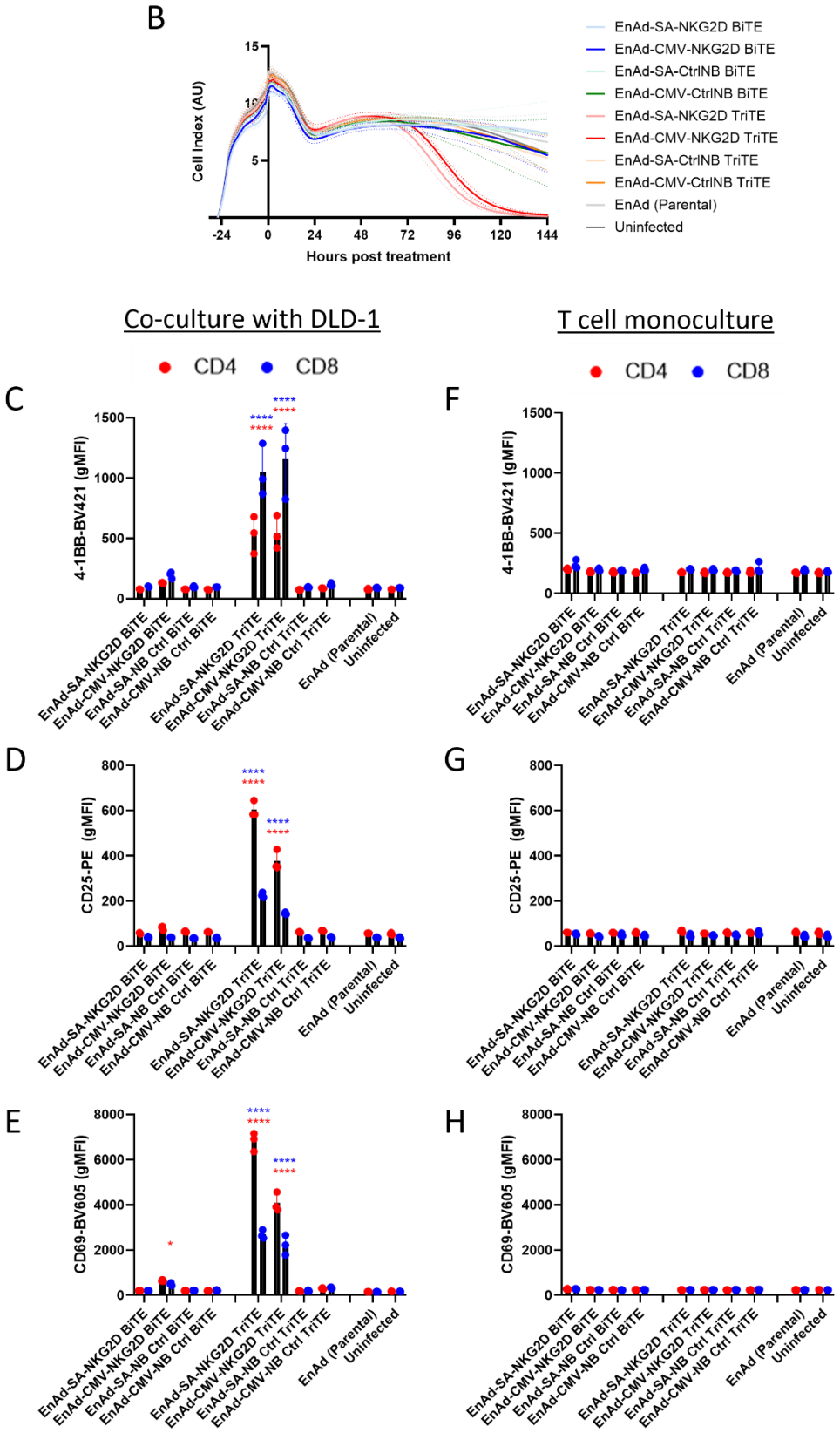

Figure 4.16: Oncolytic adenovirus encoding the NKG2D TriTE mediated target cell cytotoxicity in a T cell dependent manner at low MOI.

DLD-1 cells were seeded one day prior to infection via the indicated engineered virus (MOI-0.1) in the presence or absence of PBMC-derived T cells (effector: target ratio – 5:1). Replicate plates were seeded to allow for the analysis of T cell activation without stopping the real time cytotoxicity analysis of the xCELLigence plate. (A+B) Cell index recorded using the xCELLigence system, by measuring impedance of signal at 15-minute intervals. N = , represented as mean +/- SD. (A) Data plotted for each engineered virus, or untreated control, in the presence or absence of PBMC-derived T cells. (B) Data plotted for each engineered virus in the presence of PBMC-derived T cells. (C) 120 hours post infection, T cell activation was assessed via flow cytometry for T cell activation markers, CD25 (D+G), CD69 (E+H) and 4-1BB (C+F), in both co-culture conditions (C-E) as well as in a monoculture without a target cell line (F-H). Statistical significance assessed by two-way ANOVA with Dunnett's multiple comparisons test to untreated, $p<0.05$ *, $p<0.0001$ ****. (C-H) Data shown as average mean fluorescence. N = 2, represented as mean +/- SD.

4.4 Discussion

In this study, we investigated the versatility of the NKG2D BiTE and TriTE in targeting a variety of cancer cell types as well as non-malignant cell lines to determine which types of cancer they may be most suitable for. We additionally investigated the potency of these constructs in combination with standard of care treatments such as radiation and chemotherapy as well as encoding the constructs within an oncolytic virus in order to increase selectively the concentration of agent expressed within the tumour microenvironment.

Following the alterations to the NKG2D TriTE and Control NB TriTE plasmids to reduce homology between the repeated domain, we expressed the proteins and confirmed their production via western blot and ELISA, as shown in Figure 4.3. We noted that proteins containing the NKG2D ectodomain were produced at much lower yields that their control nanobody counterparts, as well as the smaller BiTEs resulting in higher protein yields than TriTEs.

We next sought to evaluate the functionality of these constructs using the colorectal cell line, DLD-1. Both the NKG2D BiTE and TriTE showed T cell-dependent cytotoxicity, with the NKG2D TriTE surpassing the potency of the NKG2D BiTE, whilst no significant different in target cell viability was observed for the control BiTE and TriTE, or in monocultures (Figure 4.8A). Looking at the overall T cell

activation profile induced by these agents we can see a significant difference in the expression of multiple T cell activation markers, cytotoxic proteins such as granzyme B and perforin and IFN-γ, in a target cell-dependent manner (Figure 4.8B). We observed activation of both CD4+ and CD8+ T cells, with granzyme B and perforin seen at higher levels in CD8+ T cells, consistent with their cytotoxic role. We did also see a slight increase of these proteins in CD4+ cells, indicating that they are also capable of mediating cytotoxicity, as well as also providing 'helper' functions for CD8+ T cells. Whilst there are few studies looking at this role for CD4 T cells, cytotoxic CD4 T cells are thought to be important in antiviral immunity (Knudson et al., 2021). Additionally, CD4+ CAR-T cells have been shown in vitro to induce target cell lysis independent of CD8 T cells, albeit at high target to effector ratios, and to a less extent than CD8 T cells (Bove et al., 2023). Consistent with the cytotoxicity data, the NKG2D TriTE induced higher levels of T cell activation than the NKG2D BiTE (Figure 4.8). No significant difference was observed in control BiTE or TriTE treated co-culture conditions, with the exception of perforin expression. In summary, both the NKG2D BiTE and TriTE induce T cell-mediated killing, activating both CD4+ and CD8+ T cells, but the NKG2D TriTE is the superior therapeutic candidate.

As discussed in earlier in this chapter, we are unsure about the structure of the NKG2D TriTE in comparison to the endogenous NKG2D homodimer as part of the NKG2D-DAP10 hexametric complex. The homodimer interface is supported via hydrogen bonds between the β1 and β strand-like elements (aa 148-150), with no interchain disulphide bonds (P. Li et al., 2001). Therefore there is a possibility that the two domains are able to form a functional NKG2D receptor region in solution, independent of the transmembrane region. However, ee could also expect that the NKG2D BiTE would also be able to do this, however we have seen much lower potency from this therapeutic in comparison to the NKG2D TriTE. This may be due to the NKG2D TriTE containing two NKG2D ectodomains within the same polypeptide chain providing more favourable kinetics. Higher concentrations of the NKG2D BiTE may be needed to promote the dimerisation between NK2D ectodomains on two separate chains.

To determine if the potency of the NKG2D TriTE is dependent on the homodimer formation, residues within the homodimer interface should be mutated to abolish binding between the two ectodomains. Furthermore, if it is the case that the two copies of the NKG2D ectodomain are able to correctly form the NKG2D receptor extracellular domain effectively, future work should be carried out to optimise the orientation of the domains to ensure that the most potent configuration is found, as well as to ideally increase the yield of the NKG2D TriTE.

Further to these *in vitro* experiments, we were able to obtain an *ex vivo* sample from a colorectal liver metastasis to test the NKG2D TriTE on clinically relevant material. In Figure 4.11, we saw that the NKG2D TriTE treatment was capable of activating *in situ* tumour infiltrating lymphocytes, as seen by an increase in IFN-γ production, over 6 days in comparison to the control TriTE and untreated slices. Whilst this is a promising start, future work needs to carried out to obtain more samples to repeat this work.

After confirming the functionality of the NKG2D BiTE and TriTE, we expanded our investigation to explore the range of tumour types they could potentially target. As discussed in Chapter 3, we detected a wide range of NKG2DL expression levels within the panel of cancer cell lines tested. We therefore selected cell lines to reflect this breadth as detailed in Table 4-1. Upon assessing the T cell-mediated cytotoxic potency of the NKG2D BiTE and TriTE against these cells lines we were surprised to observe that both treatments were most potent against the cell lines with 'medium' expression of NKG2DLs Figure 4.9A. Additionally, whilst there was a significant decrease in Jurkat cell viability with both the NKG2D BiTE and TriTE treatments, this was not associated with an increase in T cell activation markers (Figure 4.9B-E).

Upon further investigation, we realised that 'medium' NKG2DL expressing cell lines were all adherent, whereas the other cell lines used in the assay are suspension cells. Having the target cell line in a more fixed position, i.e. adhered to the plate, may be more favourable for T cell activation than having both the target and effector cells able to freely move around the well as can happen

with suspension cell lines. Treatment of two other 'high' expressing cell line, K562 and Molt-4, showed an increase in expression of CD69 and to a lesser extent CD25, with a slight decrease in target cell viability for the NKG2D TriTE (Figure 4.9). It may be that, for these cell lines, a longer timepoint was required to see the cytotoxic effects.

NKG2DLs are minimally expressed on normal, healthy cells, a point which we confirmed previously Chapter 3. We sought to determine if this low level of NKG2DL expression was sufficient to for NKG2D TriTE mediated cytotoxicity, which might lead to off-tumour cytotoxicity. We saw no significant difference in target cell viability for any of the NKG2D TriTE treated non-malignant cell lines (Figure 4.10A). Whilst there was no observed cytotoxicity, we did detect increases in expression of T cell activation markers, CD25 and CD69, with a highly significant difference in CD69 positive cells (Figure 4.10D). These levels were however lower than those for the positive control cell line, especially when looking at CD25 expression which is a later T cell activation marker.

In Chapter 3, we saw that radiation resulted in an increase in the expression of NKG2DLs on A549 cells in a dose dependent manner, despite their already high level of expression. This led us to wonder if this would translate into an increased potency of the NKG2D BiTE and TriTE. Surprisingly, we observed the largest reduction in viability with the lowest dose of radiation, 2 Gy (Figure 4.12A). There was also a dose dependent increase in target cell viability, excluding the mock irradiated samples. When looking at the corresponding T cell activation marker expression we can see a radiation dose dependent increase in overall CD25 expression when treated with the NKG2D TriTE (Figure 4.12D). From this we concluded that whilst the increase in NKG2DL translated to an increase in T cell activation, ionising radiation is having a radiation dose-dependent protective effect to target cells, sparing them from T cell mediated cytotoxicity. Potentially higher doses of radiation lead to the increase in pro-survival proteins, delaying the radiation induced cytotoxicity, and providing a resistance strategy for immune mediated targeting. The treatment of HeLa cells with x-ray radiation

led to a dose dependent increase in a variety of different DNA repair enzymes, including Rad51 (H. Zhao et al., 2019).

We found greater success when assessing the combination of NKG2DL negative cell lines with their standard of care treatments, whereby we were able to sensitise JJN3 cells to NKG2D BiTE and TriTE mediated killing through the use of HDAC inhibitors. Notably, in Figure 4.13A we saw a dramatic decrease in JJN3 viability in all NaBut treated samples. However, due to the highly toxic effect of NaBut treatment it was difficult to fully deduce the contributing effect of the NKG2D BiTE and TriTE. Valproic acid treatments were less potent as a monotherapy, however we saw large increases in multiple T cell markers (CD69, CD25 and 4-1BB) when JJN3 cells were treated with VPA in conjunction with the NKG2D TriTE (Figure 4.13B-G). We additionally saw an increase in CD69 expression in JJN3 cells treated with NKG2D BiTE and VPA. This work is consistent with other studies in the field in which treatment with HDACi enhances NKG2D ligand mediated killing, although to our knowledge this is the first documented case of sensitising a NKG2DL negative cancer cell line to a NKG2DL targeted immunotherapy using a standard of care treatment (Cho et al., 2021; Jensen et al., 2013; Sauer et al., 2017b). However, as discussed in Chapter 3, these concentrations may not be clinically relevant in patients. In future work we would like to use panobinostat which is more is a non-selective HDAC inhibitor currently in use to treat multiple myeloma (“Panobinostat Approved for Multiple Myeloma,” 2015).

Lastly in this chapter, we focused on the ability to arm an oncolytic adenovirus with the NKG2D BiTE and TriTE. Whilst we were able to detect His tagged protein from all viruses, the NKG2D BiTE and TriTE were produced at much lower yields than their control counterparts (Figure 4.15B). We have previously stated that due to the expression of the NKG2D TriTE in transient transfections, we were concerned about production of the proteins from the viruses *in situ*. Whilst the yields of the NKG2D BiTE and TriTE proteins from the viruses was much lower than that of the controls, the difference

between the NKG2D BiTE and TriTE was not dramatically different (2-4-fold). Additionally, the insertion of the transgenes within virus did not affect its oncolytic ability of the virus (Figure 4.15C).

Similarly to the free protein experiments, the viruses encoding the NKG2D TriTE showed T-cell mediated cytotoxicity, with the SA-NKG2D TriTE virus killing marginally quicker than the CMV-NKG2D TriTE (Figure 4.16A+B). This was supported by the significant difference in the expression of multiple T cell activation markers (Figure 4.16C-E). In comparison to the free BiTE experiment, complete eradication of the target cells took much longer, around 5 days in comparison to around 2-3 days for the free BiTE (Figure 4.4). We have attributed this to the amount of time required for the virus to produce the NKG2D TriTE after infection. This cytotoxic effect was not seen for either of the NKG2D BiTE encoding viruses, or for the control viruses. With the exception of a small significant difference in the expression of CD69 with the EnAd-CMV-NKG2D BITE, we did see not the induction of a T cell response, despite the production of the NKG2D being much higher than that used in free BITE experiments.

In conclusion, the NKG2D TriTE, and to a lesser extent the NKG2D BiTE, are potent against a number of different cancer cell lines in a T cell-dependent manner, whilst showing no cytotoxic effect against non-malignant cell lines. Furthermore, the NKG2D TriTE was able to activate *in situ* T cells in an ex vivo samples. We have additionally shown that we can sensitise a NKG2DL negative multiple myeloma cell line to NKG2D BiTE and TriTE mediated cytotoxicity via treatment with HDACi, in a T cell dependent manner. Furthermore, we showed promising data with the efficacy of arming EnAd with the NKG2D TriTE, under either the CMV promoter or the SA for more controlled expression. The delivery and expression of the NKG2D TriTE via EnAd provides an appealing opportunity for *in situ* production within the tumour itself, most likely allowing for higher local concentrations to be achieved than that possible from *intra venous* delivery.

Future experiments should be conducted to determine if there is a potential synergy with these viruses and other therapeutic treatments such as radiotherapy. Previous work within our lab has

shown a synergy between transgene expression from EnAd and radiation, putting forward the exciting possibility of an increased production of the NKG2D TriTE from EnAd-NKG2D TriTE infected cells, whilst additionally increasing number of NKG2DLs on the target cell (Pokrovska et al., 2020). Finally, we have previously observed a synergy with the herpes virus (oHSV) -NKG2D TriTE in GBM cells with a combined treatment of radiation and temozolomide, further emphasising the possible synergy of oncolytic virus delivery with targeted immunotherapy (Baugh et al., 2024).

Chapter 5: Improving NKG2D BiTE by incorporation of CD2 into the immune synapse.

5.1 Introduction

CD2 (also known as LFA-2) is an accessory protein expressed on the cell surface of some immune cells, including T cells and NK cells, and is highly expressed on memory T cells (Krensky et al., 1983; Lo et al., 2011). In humans its primary binding partner is the ubiquitously expressed CD58 (also known as LFA-3), although they have been shown to interact with a low affinity of between 9-22 µM (van der Merwe et al., 1994). In mice CD2 only binds to CD48, which is also present in humans but supposedly has a much lower affinity than CD58 (Mcardel et al., 2016). Knock out models of CD2 in mice show no obvious phenotype of T cell development or function, however CD2 may not be as critical in T cell development and function as in humans, owing to the lack of a homologue for CD58. CD2 has been associated with several different auto-immune disorders such as psoriasis and graft-versus-host disease, with Siplzumab, a humanised anti-CD2 monoclonal antibody, having undergone multiple clinical trials for various autoimmune disorders, including psoriasis and graft-versus-host and is currently being investigated for its use in diabetes (Podestà et al., 2020).

The major role of CD2 is thought to be to promote adhesion between the T cell and antigen presenting cell, stabilising the contact between the two cells to allow sufficient time for the TCR to screen peptides presented on MHC molecules (Burton et al., 2023). ICAM-1 has been described as having a similar adhesion role with LFA-1, however the CD2-CD58 interaction leads to a closer immune synapse being formed, creating a complex that is ~15 nm in length in comparison to ~ 40 nm, and so may help to increase the sensitivity of antigen detection and T cell activation (Shi & Shao, 2023; Wang et al., 1999). Consistent with this is the decrease in T cell activation seen when increasing the length of CD48 in a mouse cell line model (Milstein et al., 2008). The abolition of CD2-

CD58 and ICAM-1-LFA-1 interactions individually lead to a reduction in antigen sensitivity, with the blockade of both interactions having an additive effect (Bachmann et al., 1999; Burton et al., 2023). In a bilayer system, the interaction between CD2 and CD58 was sufficient to induce T cell activation, independent of a presented peptide (Kaizuka et al., 2009).

Mutations or loss of CD58 have been reported as a potential immune evasion strategy in cancer and blockade of the CD2-CD58 interaction has been shown to reduce tumour cell lysis, as well as be associated with a worse prognosis (Abdul Razak et al., 2016; Ho et al., 2023; Romain et al., 2022; Y. Shen et al., 2022; X. Xu et al., 2024). Ho et al. found in a cohort of melanoma patients undergoing immunotherapy treatment, non-responders had significantly less CD58 expression than their responding counterparts, indicating a potential immune evasion mechanism (Ho et al., 2023). Additionally, CD58 knock out experiments in *ex vivo* melanoma cells reduced tumour cell lysis and interferon-γ production, which could be rescued by overexpression of CD58. In a CRISPR screen aiming to identify genes that could generate resistance or sensitivity of a tumour cell to T cell engager mediated cytotoxicity, CD58 was identified as providing a resistance mechanism genetically knocked out, as well as sensitising the tumour cell when overexpressed (Y. Shen et al., 2022). The CD2-CD58 axis has gained attention in recent years in the CAR-T field after it was found that the CD2-CD58 axis is not being effectively utilised (Burton et al., 2023; Patel et al., 2024; Y. Shen et al., 2022). Burton et al., found that typical CAR-T cell therapy products which express a scFv from the cell surface are unable to effectively utilise the CD2-CD58 interaction, resulting in a reduction in antigen sensitivity in comparison to the native TCR or CAR-T modalities that more closely mimic the native TCR structure such as STARs (Burton et al., 2023).

In addition to its role in adhesion, CD2 has also been shown to promote T cell activation and proliferation, as well as being shown to be crucial in the organisation of the immune synapse (Demetriou et al., 2020; Gollob et al., 1996). Whilst the intracellular region of CD2 does not contain ITAMs, it does contain a highly conserved proline rich region which have been shown to interact with

the SH3 domain of Src kinases such as Lck, a key tyrosine kinase in T cell activation (Nunes et al., 2008). Additionally, it recruits CD2 associated protein (CD2AP) which aids in cytoskeleton polarisation, as well as CD2 binding protein 1 (CD2BP1) which may have a role in inhibiting T cell activation (Dustin et al., 1998; H. Yang & Reinherz, 2006). There have also been reports of the CD2-CD58 interaction aiding in the reversal of T cell anergy and the Amplification of signalling pathways through the recruitment of LAT and SHP-2 (Boussiotis et al., 1994). T cells are better able to respond to IL-12, upon monocyte interaction via the CD2-CD58 axis, allowing them to better proliferate (Gollob et al., 1996). Additionally, in CD28 negative T cells, CD2 co-stimulation has been identified as the major T cell activation pathway (Leitner et al., 2015).

Recent work has focused on the location CD2 within the immune synapse and how this might affect its function (Demetriou et al., 2020; Kaizuka et al., 2009). As detailed in Figure 5.1, the arrangement of the immune synapse can be divided into different compartments, each with different distances to the central CD3-TCR complex, allowing for the physical exclusion of CD45, which can otherwise inhibit T cell activation by dephosphorylating ITAMs (Davis & van der Merwe, 2006). The placement of CD2 within this structure has been variously proposed to be within the cSMAC, in close proximity to the TCR-CD3 complex, as well as being reported to be mainly found further away, in a region between the pSMAC and dSMAC, termed the ‘corolla’. In reality it seems as though CD2 is fairly mobile as the immune synapse forms and there may be a proportion of CD2 in both locations, which varies at different stages of immune synapse formation (Demetriou et al., 2020; Siokis et al., 2018). In the later stages of T cell activation, it seems to be in the corolla on the outside of the pSMAC, however at earlier timepoints it also may be present in the cSMAC and has been detected during a co-IP of the TCR-CD3 complex (Brown et al., 1989).

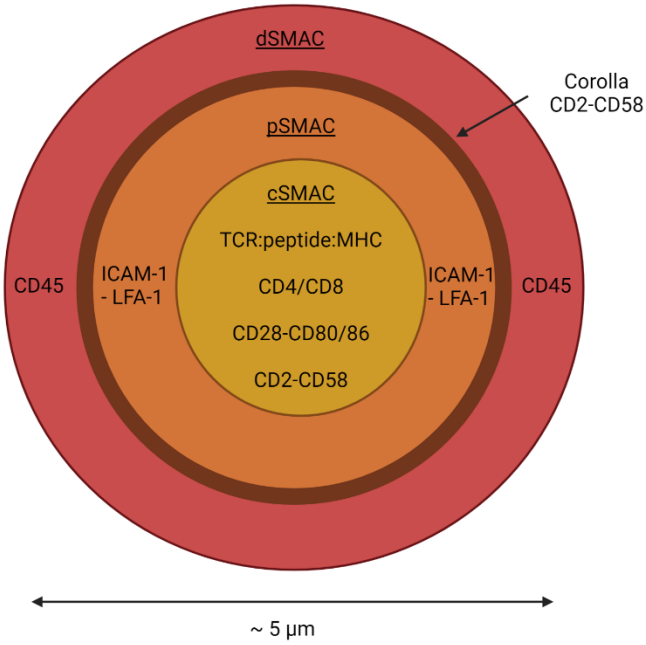

Figure 5.1: Schematic of reported CD2-CD58 spatial placement within the immune synapse.

Birds eye view of the interface between the T cell and antigen presenting cell, formed of the central supra-molecular activation complex (cSMAC, yellow) which contains the cire interacting components, surrounded by the peripheral SMAC (pSMAC, orange), which is in turn surrounded by the distal SMAC (dSMAC, red). An area in between the pSMAC and dSMAC (brown) has been termed the 'corolla' and has been reported to be where CD2-CD58 is enriched in later stages of the immune synapse formation. Diagram inspired from (Huppa & Davis, 2003).

We therefore sought to investigate the role of CD2 in the context of bispecific T cell engagers and determine if CD2 enrichment within the immune synapse, independent from CD58 binding, improves T cell activation.

5.2 Chapter Hypothesis and Aims

5.2.1 Chapter Hypothesis

We hypothesise that the CD2-CD58 is critical in the determining the sensitivity of BiTEs and TriTEs, similarly to native TCRs and CAR-Ts. We additionally hypothesise that CD2 is an important co-stimulatory protein in T cell activation and its presence within the immune synapse will increase the potency of the NKG2D BiTE.

5.2.2 Chapter Aims

1. Determine the role of the CD2-CD58 axis in BiTE-mediated T cell activation.

2. Design and production of new NKG2D TriTEs which contain a CD2 binding moiety to enrich CD2 within the immune synapse and improve the NKG2D BiTE.

5.3 Results

5.3.1 Engaging CD2, in conjunction with CD3/CD28 stimulation, increases T cell activation.

To determine the effect of CD2 on T cell activation, PBMC-derived T cells were incubated with a commercially available antibody cocktail that contained an anti-CD3 and an anti-CD28 antibody complex with or without an anti-CD2 antibody complex included. Whilst the concentration and ratio of each antibody was proprietary, the suppliers have stated that the concentrations of aCD3 and aCD28 were equal.

As shown in Figure 5.2, the addition of the aCD2 antibody to the activation cocktail increases the expression of T cell activation markers at a variety of doses until a plateau seems to be reached at 0.3 µL/well, with the aCD3/aCD28 cocktail barely reaching the same level of activation with a 10-fold increase in dose. This suggested that there could be a significant advantage to engaging CD2 during T cell activation.

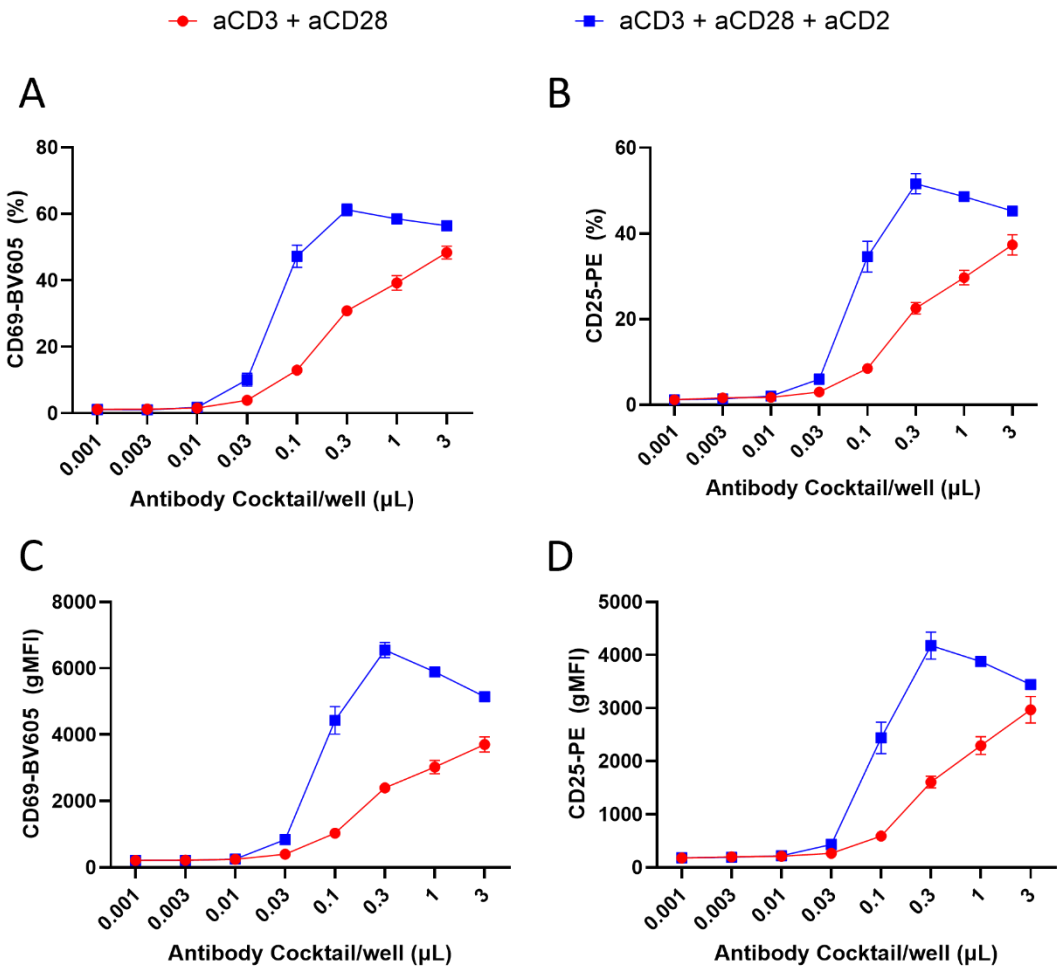

Figure 5.2: Binding of CD2 increases T cell activation.

PBMC-derived T cells were incubated with varying amounts of either an aCD3/aCD28 antibody cocktail or an aCD3/aCD28/aCD2 antibody cocktail for 72 hours. T cells were stained for expression of activation markers, CD69 (A, C) and CD25 (B, D) and analysed via flow cytometry. Average percentage positive (A + B), using unstimulated control to gate at 1% for each cell line, and gMFI (C + D) are presented. N= 3 biological replicates. Error bars indicate mean +/- SD.

5.3.2 The CD2:CD58 axis is critical in the sensitivity of the NKG2D BiTE and TriTE.

Following the recent publication that in semi solid systems that disruption of the CD2-CD58 axis leads to a decrease in sensitivity to peptides presented on MHC molecules and that some CAR-T modalities are unable to utilise the interaction reducing their sensitivity to antigen, we sought to identify

whether this was also the case for bispecific T cell engagers (Burton et al., 2023). To assess constructs targeting NKG2D, we utilised the glioblastoma cell line U87, in which CD58 has been knocked out, kindly donated by the Dushek lab (verification of successful knock out shown in Appendix C).

As previously mentioned, the efficacy of the NKG2D TriTE in the context of GBM, was explored by a previous DPhil student in which U87 cells were used extensively (Baugh et al., 2024). In this work the NKG2D BiTE showed little efficacy and so was not tested further. Consistent with this, when testing the potency of the two constructs in co-culture experiments with U87-WT cells, we observed higher cytotoxicity with the NKG2D TriTE in comparison to the NKG2D BiTE (Figure 5.3A+E). The absence of the CD2-CD58 interaction was highly disruptive in both cytotoxicity and T cell activation, with a 100-fold increase in the concentration of NKG2D TriTE required in the CD58KO cell line to achieve the equivalent reduction in viability seen in the wildtype U87 co-culture (~40 % viability, Figure 5.3E). We additionally saw a similar effect with the highest doses of NKG2D BiTE, showing a decrease in potency with the CD58 KO cell line (Figure 5.3A-D).

Here we have shown the importance of the CD2-CD58 interaction for NKG2D BiTE and TriTE-mediated T cell activation and associated cytotoxicity. We additionally can see that the decrease in potency between the NKG2D BiTE and TriTE caused by the decrease in overall avidity to the target cell. This is further magnified by the removal of the CD2-CD58 interaction, which is reducing the overall avidity between the target cell and T cell.

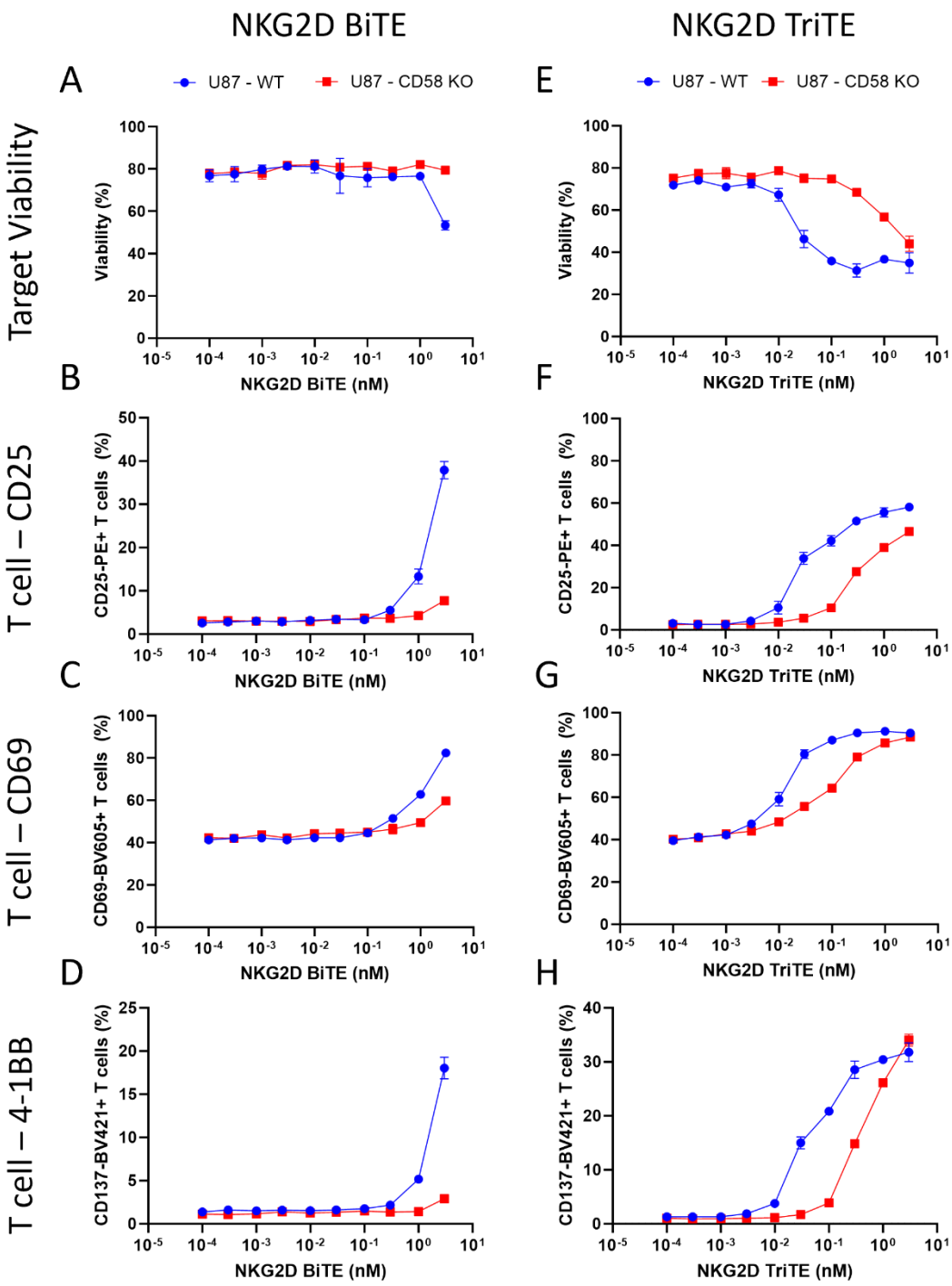

Figure 5.3: CD2-CD58 interaction increases efficacy of NKG2D BiTE and TriTE.

A co-culture of U87-WT, or U87-CD58 KO cells, and PBMC-derived T cells were treated with a range of doses of either the NKG2D BiTE or TriTE for 72 hours. Cells were then stained for T cell activation markers, CD25 (B + F), CD69 (C + G) and 4-1BB (D + H), for analysis via flow cytometry along with a viability dye to determine target cell viability (A + E). Average percentage positive, using unstimulated control to gate at 1% for each cell line are presented for T cell activation markers (B-D, F-H). N = 3, error bars indicate mean +/- SD.

5.3.3 Incorporating CD2 into the immune synapse may help to increase T cell activation.

We next wanted to assess the role of CD2 within the immune synapse and ascertain if the CD2-C58 interaction is important for the tethering of the two cell together or having CD2 within the immune synapse, independent of its interaction with CD58, leads to significant increases in T cell activation. We therefore sought to investigate the effect of bringing CD2 into the immune synapse, independent of its interaction with CD58.

To do this, we designed NKG2D ligand T cell engagers that also contained an aCD2 scFv to also incorporate CD2 into the immune synapse by bringing the protein into closer proximity to CD3 and the NKG2D ligand.

As previously discussed in the introduction of this chapter, the positioning of CD2 within the immune synapse structure may prove to be critical to its function (Demetriou et al., 2020). Therefore, we initially aimed to generate T cell engagers that included the aCD2 scFv at various positions within the constructs to vary the length between CD2 and CD3 within the synapse. We initially chose to add the CD2 scFv to the NKG2D BiTE due to the reduced number of possible orientations as well as concerns for protein production yields as we had experienced limited yields when producing the NKG2D TriTE.

We identified an aCD2 scFv sequence that had previously been used to target extracellular vesicles to T cells (Connelly et al., 1998; Stranford et al., 2024). As far as we are aware, both the binding affinity and binding site are unknown. To determine the optimal orientation of the new CD2 binding NKG2D TriTEs, the aCD2 scFv was inserted either upstream, downstream or in between the NKG2D ectodomain and aCD3 scFv of the NKG2D BiTE (Figure 5.4A). Control constructs were generated in a similar manner using the CtrlNB-aCD3 BiTE constructs utilised in previous chapters. Correct insertion was confirmed by Sanger sequencing. As previously described, the aCD2 containing TriTEs were produced in HEK293 cells, and the clarified supernatant concentrated around 20-fold. Correct protein

size was determined by SDS-PAGE and immunoblotting for His tag. We confirmed that all aCD2 containing TriTEs were detected in the supernatant at roughly the correct size (Figure 5.4B). The yield of proteins containing the NKG2D ectodomain was much lower than those containing the control nanobody, consistent with the yields of the NKG2D BiTE and TriTE.

To assess the binding ability of the constructs, PBMC-derived T cells were stained with 1nM of aCD2 containing TriTEs or controls, followed by detection using an anti-His tag antibody (Figure 5.4C). Prior to staining, T cells were treated with an anti-CD3 antibody, to block the binding of TriTEs via CD3, or isotype control. The OKT3 anti-CD3 clone was utilised to block binding to CD3 as it binds to the same epitope as the L2K scFv, utilised in the BiTEs/TriTEs here, however has 100-fold higher affinity (Segaliny et al., 2023). In general, we see a reduction in binding when the CD3 epitope is blocked.

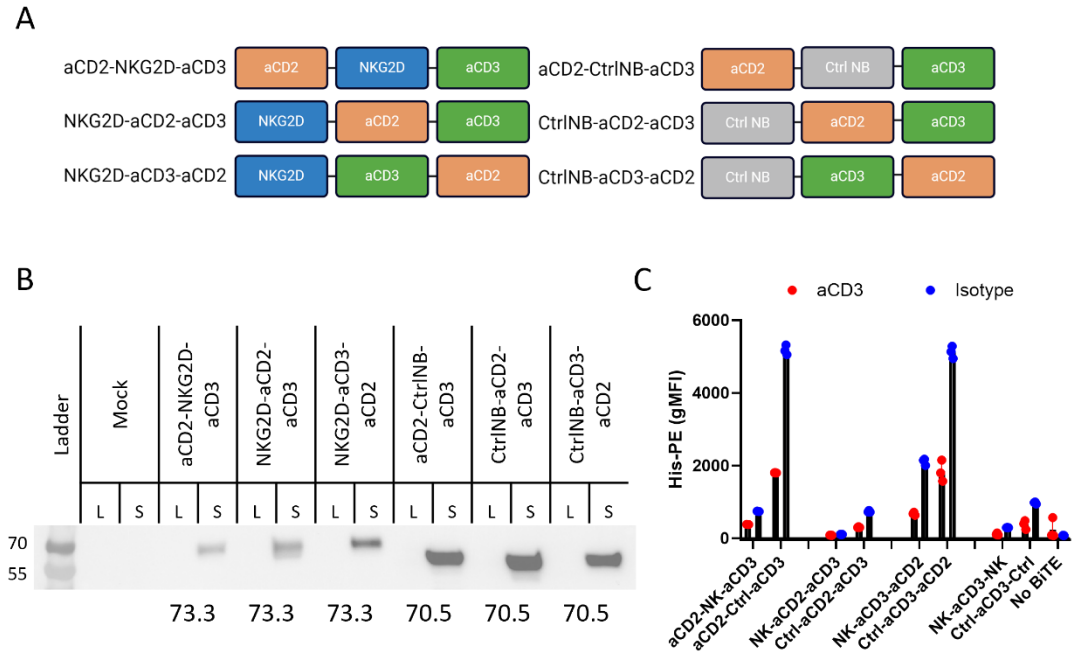

Figure 5.4: Construction of CD2 binding TriTEs.

(A) Schematic of NKG2D TriTEs containing an aCD2 scFv in various configurations. All constructs generated included an N-terminal immunoglobulin secretion signal peptide and a C-terminal decahistidine tag (His) tag. Domains were linked by GS linkers to allow flexibility (SSGGGGS). (B) HEK293 cells were transfected with plasmid DNA. Lysate (L) and supernatant (S) were harvested 72 hours post transfection and supernatant was concentrated (~ 40-fold).

Expression was assessed by His-tag immunoblot. Expected size shown below each sample. (C) Ability of constructs to bind to CD2 on T cells was assessed by staining of PBMC-derived T cells. T cells were initially stained with an anti-CD3 antibody (OKT3), to block TriTE binding via CD3, or isotype control. Cells were then stained with 1 nM of the NKG2D TriTE, aCD2 containing NKG2D TriTE or matched control. Binding was detected using an anti-his tag – PE antibody and was analysed via flow cytometry. N=3. Error bars indicate mean +/- SD.

Having the aCD2 scFv in the middle of the construct heavily inhibits the ability of the construct to bid to T cells at all, most likely to due the protein being unable to correctly fold or causing steric hindrance (Figure 5.5C). Additionally, having the NKG2D ectodomain within the protein negatively affects the binding via aCD3 in comparison to the control nanobody. Having the aCD2 binding moiety at either the N or C terminal of the proteins resulted in control constructs that were able to bind to T cells in a CD2 dependent manner. Of the NKG2D ectodomain containing aCD2 TriTEs, having the aCD2 at the C terminus of the construct (NK-aCD3-aCD2) lead to the highest amount of CD2 dependent binding. Having the aCD2 at the N terminal of the protein also showed some binding ability to both CD3 and CD2, however much lower than the C terminal version. The control NB, aCD2 TriTEs showed similar binding profiles. Therefore, the constructs with aCD2 at either the C or N terminal were taken forward for functional testing.

As shown previously, in the co-culture using U87-CD58KO cells where the CD2-CD58 interaction is absent, the NKG2D TriTE induces T cell mediated cytotoxicity, whereas the NKG2D BiTE shows no effect (Figure 5.5). However, in the U87-WT co-culture, we see a significantly greater increase in T cell activation and lower in target cell viability when treated with the NKG2D BiTE, as well as with the NKG2D TriTE. This suggests the CD2-CD58 interaction can potentiate BiTE activity. Despite significantly greater CD69 expression with the aCD2-NK-aCD3 configuration, the potency of either of the NKG2D, aCD2 TriTE configurations does not exceed that of the NKG2D BiTE which contains the same amount of NKG2D ligand binding domains (Figure 5.5C-D). T cell activation was however significantly greater for one of the control constructs, Ctrl-aCD3-aCD2, in both co-cultures as well as

in the monoculture, suggesting CD2 clustering with CD3 is inducing T cell activation. This was not seen as dramatically in the aCD2-Ctrl-aCD3 construct, which resulted in a significant but less dramatic increase in CD69 than the Ctrl-aCD3-aCD2 construct; and did not induce CD25 expression. The placement of aCD2 and aCD3 within these TriTEs is likely to be an important part of this difference. Both Ctrl, NB TriTEs showed similar CD2 binding ability to each other, and so differences seen are not due to binding ability (Figure 5.4C).

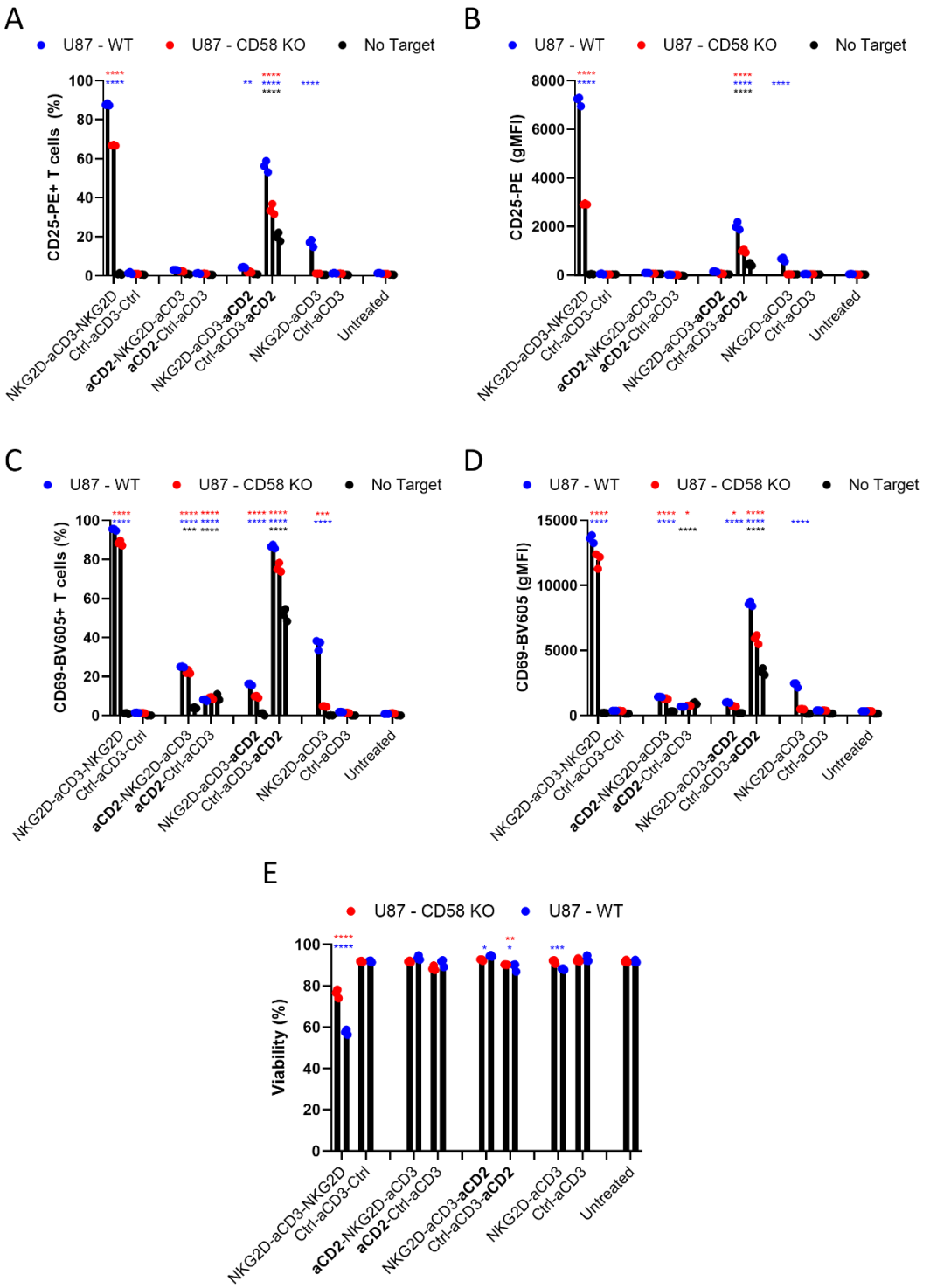

Figure 5.5: CD2 and CD3 clustering induce activation of T cells, independent from a target antigen.

A co-culture of U87-WT, or U87-CD58 KO cells, and PBMC-derived T cells were treated 1 nM NKG2D BiTE, NKG2D TriTE, aCD2 scFv containing NKG2D TriTEs, or matched controls, for 72 hours. Cells were then stained for T cell activation markers, CD25 (A-B) and CD69 (C-D) for analysis via flow cytometry along with a viability dye to determine target cell viability (E).

Average percentage positive, using unstimulated control to gate at 1% for each cell line are presented for T cell activation markers (A + C). Data shown as average mean fluorescence (B +D). N = 3, represented as mean +/- SD. Statistical significance assessed by two-way ANOVA with Dunnett's multiple comparisons test to untreated, $p<0.05$ *, $p<0.01$ **, $p<0.001$ ***, $p<0.0001$ ****.

5.4 Discussion

The results in this chapter focus on determining the effect of the CD2-CD58 interaction in the context of T cell engagers targeting NKG2D ligands, and to determine if there was a positive effect of having CD2 enriched in the immune synapse independently from its interaction with CD58.

Firstly, in order to establish the effect CD2 stimulation has on T cell activation, we stimulated PBMC-derived T cells with antibody cocktails to stimulate via CD3 and CD28 in the presence or absence of an CD2 antibody (Figure 5.2). We saw dramatically greater T cell activation when also engaging CD2, needing 10x the dose of the aCD3 + aCD28 treatment to reach the equivalent activation based on CD25 and CD69 expression.

Next, to investigate the importance of the role of the CD2-CD58 interaction in BiTE mediated T cell activation, we utilised the GBM cell line U87, along with a paired CD58 KO cell line. In Figure 5.3 we saw a decrease in T cell activation and associated cytotoxicity in the CD58 KO cells line in comparison to the WT cell line, showing an increase in sensitivity to the NKG2D ligands present on the target cells, this is consistent with other groups who have also looked into the role of CD2 and CD58 on bispecific T cell engager mediated cytotoxicity (Patel et al., 2024; Y. Shen et al., 2022). We hypothesise that the lower number of contact points between the two cells in the CD58 KO cell line can be compensated via an increase in the concentration of T cell engager which is providing alternative adherence between the two cells.

We have shown that engaging CD2 alongside CD3 and CD28, increases the level of T cell activation, highlighting an intracellular signalling role of CD2, consistent with literature (Figure 5.2, (Kaizuka et al., 2009; Leitner et al., 2015)). To determine if the presence of CD2 in the immune synapse alone would lead to an increase in T cell activation, we added an anti CD2 scFv to the NKG2D BiTE (Figure 5.4A), which shows little to no potency against either the U87 WT or CD58 KO cell lines. Unfortunately, the addition of the aCD2 scFv to the NKG2D BiTE, especially in certain configurations, abolished its ability to bind to T cells (Figure 5.4C), and potentially also NKG2DL+ tumour cells, although this was not tested. In Figure 5.5 we saw that the most potent T cell activation, other than that induced by the NKG2D TriTE, was due to the Ctrl-aCD3-aCD2 construct which was able to increase T cell activation significantly, with CD69 expression being within similar ranges of the NKG2D TriTE. We also saw higher levels of activation markers in the co-cultures, versus the monoculture, mostly likely due to the availability of ligands for other co-stimulatory proteins. The WT-U87 co-culture also showed higher levels of T cell activation than the CD58 KO, suggesting that the binding of the aCD2 scFv did not abolish the CD2:CD58 interaction. Future work should be carried out to map the binding epitope of the aCD2 scFv.

One the basis of the data available we are unable at present to conclude whether the activation seen required cross-linking of T cells via CD2 on one cell and CD3 on another, or if the clustering of CD2 and CD3 on a single T cells is sufficient to activate T cells. These of course do not have to be mutually exclusive. It would be the more likely option that once the TriTE has bound to the T cell via one of CD2 or CD3, that the closest epitope of the other to bind to would be on the same T cell. It should be noted that, despite the CD69 and CD25 expression being significantly greater in the Ctrl-aCD3-aCD2 treated conditions, there was only slightly lower target cell viability observed, similar to that of the NKG2D BiTE which showed much lower levels of activation. Therefore, CD3-CD2 clustering on T cells may be sufficient for the early stages of T cell activation, however it doesn't seem sufficient to mediate the later, cytotoxic stages. This could be further investigated by looking at later T cell activation markers such as CD107a and granzyme production which indicate degranulation.

Furthermore, this activation does not occur when the aCD2 and aCD3 scFvs are further apart as in the aCD2-CtrlNB-aCD3 configuration (Figure 5.5). This not only suggests that CD2 does in fact have a significant co-stimulatory role in T cell activation, independent of adhesion via CD58, but also that the distances between these molecules, even at the nm scale, is critical.

As briefly discussed in the introduction to this chapter, the optimal placement of CD2, at specific timings of the immune synapse formation, is not fully understood. The fully formed immune synapse has been estimated to be around 5 µm wide, whilst the variable regions of antibodies are typically 10-18 nm apart (Demetriou et al., 2020; Staufer et al., 2022). Therefore, the antibodies utilised in Figure 5.2, resulting in an increase in T cell activation, would have brought CD2 into nm range of CD3 and CD28, resulting in CD2 most likely being within the cSMAC of the synapse. Similarly, based on published crystal structures, we have estimated the length of the pseudo synapse produced by the NKG2D BiTE to be 19.5 nm. From this we can assume that, in both the aCD2-Ctrl-aCD3 and the Ctrl-aCD3-aCD2 treated cultures, the aCD2 would be within the cSMAC region of the immune synapse, and that CD2 must be within a very close range of CD3 to initiate T cell activation as seen with the Ctrl-aCD2-aCD3 configuration but not aCD2-Ctrl-aCD3.

Our lab has previously developed constructs to engage CD28 into the immune synapse during BiTE mediated T cell activation (Scott et al., 2019). In that work an anti-CD28 scFv was added at the N terminus of a CD206-BiTE designed for M2 macrophage targeting with the aCD3 scFv at the C terminus, as well as a second version which contained a second aCD3 ScFv domain. The proteins containing two CD3 scFvs had improved ability to activate T cells and retained its target antigen specificity. In contrast, the TriTE containing both an aCD3 and aCD28 scFv resulted in even greater T cell activation and was no longer target antigen dependent, indicating that T cell activation can occur due to CD3-CD28 clustering at a greater distance. This therefore suggests that proximity required of different T cell co-stimulatory receptors to the CD3-TCR complex for T cell activation, along with the proximity of other CD3-TCR complexes, varies.

To better understand the spatial arrangements that need to occur during T cell activation we would ideally produce constructs with aCD2 and CD3 with varying distances between them. We could also of course do this with other co-stimulatory molecules such as CD28, 4-1BB, and OX40, whose co-stimulatory functions have been found to be advantageous in CAR-T therapies (Smirnov et al., 2024). The combined stimulation of multiple co-stimulatory molecules has been shown to produce a wider signalling response and a more diverse cytokine profile (Andrews et al., 2020; Skånland et al., 2014; Tapia-Galisteo et al., 2023).

We could then use this information to engineer more potent antigen-specific T cell engagers by understanding the optimal distance for the different co-stimulatory molecules in relation to CD3. However non-specific, or antigen independent, T cell activation will always be a concern when developing immunotherapies due to the frequent presence of most target antigens on at least some normal cells, albeit often at low levels, potentially leading to risk of cytokine release syndrome (Shimabukuro-Vornhagen et al., 2018). Gene therapy using oncolytic viruses provide one possible solution to this, allowing the therapeutic to be produced within the tumour itself at higher concentrations that would likely be tolerated by *intra venous* delivery.

In conclusion, in this chapter we have shown that the CD2-CD58 interaction increases the sensitivity of NKG2D BiTEs and TriTEs, similar to that seen for other BiTEs as well as CAR-T cells (Burton et al., 2023; Patel et al., 2024; Y. Shen et al., 2022). We have additionally shown that the recruitment of CD2 into the immune synapse, independent from CD58 binding, induces significant T cell activation. This could be a promising approach, especially in tumours that have acquired mutations to downregulate CD58 as an immune evasion mechanism.

Chapter 6: Impact of sNKG2D ligands on T cell activation and strategies for inhibition.

6.1 Introduction

The role of the NKG2D/NKG2D ligand axis has been extensively studied for its role the in immunosurveillance step of the immunoediting model, allowing elimination of malignant cells that exhibit malignant stress through the upregulation of NKG2D ligands (NKG2DLs) on their cell surface (Schreiber et al., 2011). The importance of this interaction is further exemplified in a NKG2D KO model, in which mice show higher rates of spontaneous tumour formation compared to WT mice (Guerra et al., 2008). Lower NKG2D receptor expression on immune cells is involved in the progression to the immune evasion step of this model, aided by the release of soluble NKG2DLs ligands (sNKG2DL) which act as a decoy, as well as strategies to downregulate initial receptor expression on the cell surface (Groh et al., 2002; Raffaghello et al., 2004). sNKG2DL, with MICA being the most well characterised, can bind to the NKG2D receptor on a multitude of immune cells, most prominently on NK cells, as well as CD8+ T cells and some γδ T cells. Upon binding, the sNKG2DL lead to the internalisation and degradation of the NKG2D receptor, inevitably leading to fewer receptors present on the cell surface (Cao et al., 2007; Groh et al., 2002; Song et al., 2006).

MICA, MICB and ULBP2 have been detected in the serum of cancer patients in variety of different cancers, including various haematopoietic cancers as well as solid tumour cancers of the colon, lung, prostate and skin and have been associated with a worse prognosis (Doubrovina et al., 2003; Hilpert et al., 2012; Jinushi et al., 2008; G. Liu et al., 2013; Nückel et al., 2010; Paschen et al., 2009; Yamaguchi et al., 2012). In contrast, healthy donor serum showed minimal to no soluble MICA (sMICA) or MICB (sMICB) (Xing & Ferrari de Andrade, 2020b). sNKG2DL have also been shown to inhibit immunotherapy with high sMICA associated with poor overall survival in metastatic

melanoma patients treated with the anti-CTLA-4 immune checkpoint inhibitor, ipilimumab (Koguchi et al., 2015).

As previously discussed, shedding of NKG2DLs, via proteolytic cleavage or via packaging into extracellular vesicles, has been shown to contribute to the tumour immune evasion, especially through NK cells. In general, NKG2DLs with transmembrane domains (such as MICA, MICB and ULBP2) are shed via proteases, whereas ligands tethered via GPI-anchors are likely to be shed via extracellular vesicles (such as ULBP1, ULBP3 and MICA*008, which contains a single insertion leading to a truncated protein which associates via a GPI anchor) (Ashiru et al., 2013). The fact that tumour cells in general have been shown to release a higher level of EVs compared to normal cells hints towards an evolved strategy to possibly remove problematic proteins from their surface (L. Zhang & Yu, 2019).

Proteolytic cleavage of MICA, and presumably MICB, is a two-step process. In the first step, the disulphide bond in the ectodomain between residues 202 and 258 is removed by the disulphide isomerase, ERp5 (Kaiser et al., 2007; X. Wang et al., 2009). This leads to a conformational change, which has been hypothesised to facilitate the exposing of the cleavage site for proteases. Once the cleavage site is exposed, the ligand is cleaved from the transmembrane domain by a protease, many of which are commonly upregulated in cancer. The ADAM (a disintegrin and metalloproteases) and MMP (matrix metalloproteases) families are most commonly linked to the shedding NKG2DLs, with ADAM10 and ADAM17 being the most well documented (Waldhauer et al., 2008). Fittingly, high expression of Erp5, required for the initial step of MICA cleavage, is often seen in conjunction with an increase in ADAM10 expression in tumours (Zocchi et al., 2012), consistent with high expression of both proteins being required to escape recognition via NKG2D+ immune cells.

High expression of either ADAM10 or ADAM17 have been linked to unfavourable outcomes in a multitude of cancers including breast, brain, colorectal, lung, prostate, renal and ovarian, as well as being shown to contribute to a variety of different immunotherapy treatments via cleavage of the

target antigen (Ding et al., 2004; Hedemann et al., 2018; Lendeckel et al., 2005; P. C. C. Liu et al., 2006; Orme et al., 2020; Roemer et al., 2004; Saad et al., 2019; Sikora-Skrabaka et al., 2022; Yoneyama et al., 2018; Zheng et al., 2007). ADAM10 is an alpha secretase, most famously known for its role in preventing the formation of the amyloid β which is associated with Alzheimer's disease (Lammich et al., 1999). ADAM17, also known as tumour necrosis factor-α converting enzyme (TACE), is well-documented to be responsible for the cleavage of proTNFα to allow the release of soluble TNFα as part of the inflammatory response, as well as being responsible for the shedding of more than 80 other protein precursors, including cytokines, growth factors and adhesion molecules (Black et al., 1997; Zunke & Rose-John, 2017).

Aderbasib (INCB7839) is a structurally related molecule to INCB3619, one of the first inhibitors of both ADAM10 and ADAM17; and has been reported to have superior pharmacokinetic properties (Mullooly et al., 2016). Aderbasib was tested in a clinical trial in combination with Herceptin in HER2+ breast cancer patients, with a reported mid-trial overall response rate of 40% in the highest dosed group and an 80% reduction in soluble HER2 detected in patient serum (Friedman et al., 2009). It has also been tested in a clinical trial in conjunction with rituximab in DLBCL patients (NCT02141451) and is currently in clinical trials for treatment of recurrent high-grade gliomas in children (NCT04295759), however there has been no data published for either trial.

GI254023X, an ADAM10 selective inhibitor, has been shown to inhibit the shedding of known ADAM10 substrates such as IL-6R, CXCL1, CXCL16 and more recently, MICA and MICB (Hundhausen et al., 2003; Lammich et al., 1999; Metz et al., 2012; Y. Zhang, Hu, et al., 2022). In the human neuroblastoma cell line, IMR-32, an increase of MICA and MICB was detected on the cell surface with the combination of chemotherapy and GI254023X, which made the cells more sensitive to NK cell mediated killing, which shows the potential therapeutic benefit of inhibiting these proteins (Y. Zhang, Hu, et al., 2022).

As an alternative way to prevent the shedding of MICA/B, Ferrari de Andrade et al. developed a monoclonal antibody to inhibit the shedding of the ligands by blocking the cleavage site (De Andrade et al., 2018). Mice were immunised with the, highly conserved, α3 domain of MICA and the 7C6 antibody was identified for further studies. This was based on its ability to prevent the shedding of MICA and MICB from the cell surface as well as increasing the levels of NKG2DLs present on the cell surface. Treatment with the 7C6 antibody led to a reduced in number of lung metastasis in two mouse models, in an NK cell-mediated manner. To determine the contribution of inhibiting cleavage of MICA and B on the cytotoxicity observed, a 7C6-DANA mutant which abrogates the binding to the Fc receptor, was produced. With this version, NKG2D-dependent cytotoxicity of the target cell is observed, albeit to a lower level than the 7C6 antibody with Fc engagement capacity (De Andrade et al., 2018).

The contribution of sNKG2DL on immunosuppression in the tumour is well documented, however in general the therapeutic effect of reducing their levels has mainly focussed on NK cell mediated tumour lysis (Groh et al., 2002). The role of NKG2D as a co-stimulatory molecule for CD8+ T cells is increasingly being elucidated including it being reported that NKG2D-induced T cell activation leads to an increase amount of cytokines produced per cell as well as diversifying the cytokine profile (Kavazović et al., 2017; Kohlhapp et al., 2023; Lerner et al., 2023).

In this chapter we aim to elucidate the the effects of sNKG2DL on BiTE mediated T cell activation and further investigate the effect of ADAM10 and ADAM17 inhibitors as a method to decrease the shedding of NKG2DLs to prevent immunosuppression whilst simultaneously stabilising the levels of NKG2DLs on the cell surface. Finally, we will explore the use of the identified 7C6 binding epitope to mimic this phenotype whilst also increasing the affinity between the target cell and T cell, as an improvement to the NKG2D TriTE.

6.2 Chapter Hypothesis and Aims

6.2.1 Chapter Hypothesis

We hypothesise that by inhibiting the shedding of NKG2DLs we can increase the number of available NKG2DLs to target on the cell membrane, as well as prevent the NKG2DLs ligand-mediated immunosuppression.

6.2.2 Chapter aims

1 - Determine the effect of sNKG2DL on T cell activation.

2 - Investigate the use of an anti-MICA/B scFv to increase affinity of a BiTE to the tumour cell whilst inhibiting proteolytic cleavage of the ligands.

6.3 Results

6.3.1 Soluble NKG2D ligands selectively inhibit NKG2D ligand-targeting BiTEs.

Firstly, we set out to determine if there was a correlation between the amount of shed NKG2DLs and the ability of samples to inhibit T cell activation, both generally and also by NKG2DL-specific BiTEs. Due to the limited availability of commercial kits for soluble ULBP1-6, and the majority of the literature at present discussing MICA and MICB, this chapter will focus on sMICA and sMICB. Using patient-derived, malignant peritoneal ascites fluid, we analysed the inhibitory effects of samples on experimental activation of T cells and compared this to the levels of sMICA and sMICB.

Nine ascitic samples were analysed for the presence of sMICA and sMICB, referred to as AS1-9. As shown in Figure 6.1A+B, 7/9 samples contained detectable levels of sMICA with AS1 containing the highest concentration at 9.9 ng/mL. Samples 7 and 9 did not contain detectable levels of sMICA. All ascitic samples contained detectable levels of sMICB with AS1 again containing the highest levels at 36 ng/mL which was far higher than any of the other samples. AS3 and AS8 also contained high levels of sMICB at 8 ng/mL and 3 ng/mL respectively.

To determine whether the concentration of sMICA/B in ascitic fluid had a suppressive effect on experimental T cell activation, the inhibitory activity of each ascitic fluid was estimated using a T cell activation assay. To activate them, PBMC-derived T cells were treated with aCD3/aCD28 DynaBeads in the presence of each ascitic fluid for 72 hours. T cells were then analysed by flow cytometry to detect the upregulation of activation markers CD25 and 4-1BB (Figure 6.1 C+D). Five out of nine samples resulted in lower CD25 expression when compared to the T cells activated in 2% RPMI, with AS6 showing little effect and AS3-5 actually increasing the level of CD25 expression on T cells in comparison. In general, a similar trend between samples was seen for 4-1BB levels, although none of the ascites fluids induced 4-1BB higher than that in the 2% RPMI control treatment.

AS7 was identified as being the most inhibitory sample, assessed by induction of both CD25 and 4-1BB. When plotting the soluble ligand levels against the CD25 expression data we can see little to no correlation between the level of T cell activation and concentration of sMICA or sMICB as shown by the Pearson's correlation score of 0.03790 and -0.1608, respectively (Figure 6.1 E + F). There was also no correlation between the total concentration of sMICA and sMICB with T cell activation (r = -0.08798, data not shown). It follows that levels of NKG2DLsLs, or at least sMICA/B, do not seem to associate with the ability of ascites samples to influence non-specific activation of T cells.

Due to the lack of correlation between the suppression of T cell activation and levels of sMICA or sMICB, it is unlikely that sNKG2DLs are the key immune-inhibitory factors within ascitic fluid and that other components are causing the suppressive phenotype.

It has also been reported that sNKG2DL result in the internalisation and degradation of NKG2D on the surface of NK cells as well as CD8+ T cells (Groh et al., 2002). In humans T cells, NKG2D is a co-stimulatory receptor for cytotoxic CD8+ T cells which has been shown to be important in the co-stimulation of T cell activation. Inhibition of this interaction may be detrimental for T cell therapies, such as BiTEs (Kavazović et al., 2017; Kohlhapp et al., 2023; Lerner et al., 2023).

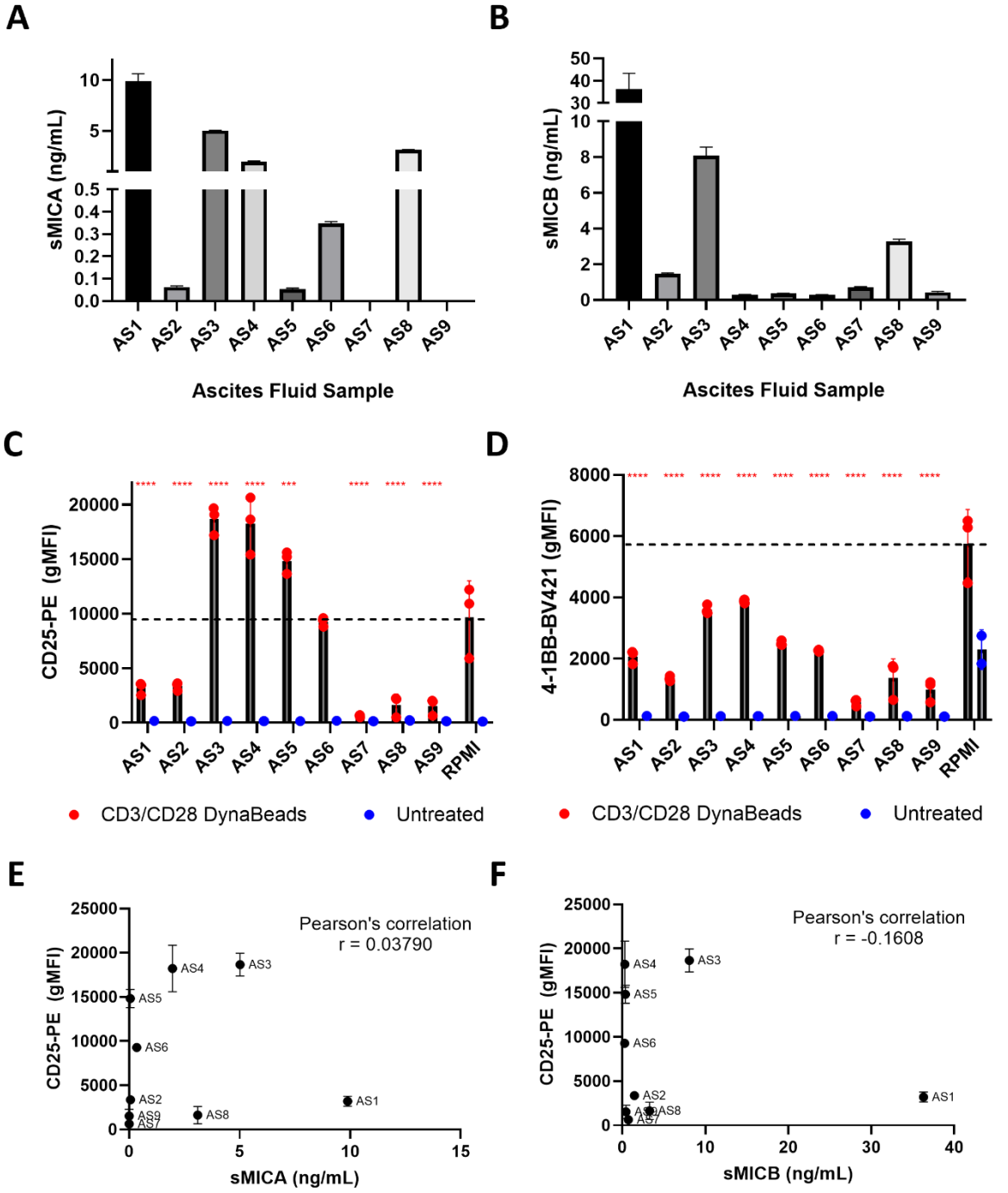

Figure 6.1: There is no correlation between sMICA and sMICB with decreasing T cell activation. Patient derived ascitic fluid (AS1-9) was analysed for (A) sMICA or (B) sMICB via sandwich ELISA and quantified against a standard curve. (C+D) PBMC-derived T cells were co-cultured with ascitic fluid in the presence or absence of aCD3/aCD28 Dynabeads for 72 hours. T cells were stained for T cell activation markers CD25 (C) and 4-1BB (D) and analysed via flow cytometry. Average gMFI shown. N = 3, error bars indicate mean +/- SD. Statistical significance assessed by two-way ANOVA with Dunnett's multiple comparisons test to 2% RPMI control, $p<0.001$ ***, $p<0.0001$ ****. (E+F) Comparison of sMICA (E) and sMICB (F) to the level of T cell activation in the presence of ascitic fluids.

To evaluate the effect of sNKG2DL on T cell activation by aCD3 stimulus alone, a sMICA inhibition assay was carried out by adding increasing concentrations of sMICA to BiTE experiments. To identify which cancer cell line to use for these assays, a panel of cell line conditioned media was analysed for the levels of sMICA/B after 72 hours. As shown in Figure 6.2, conditioned supernatant from A549 cells, a human non-small cell lung adenocarcinoma, contained the highest levels of both sMICA and sMICB and was therefore prioritised for use.

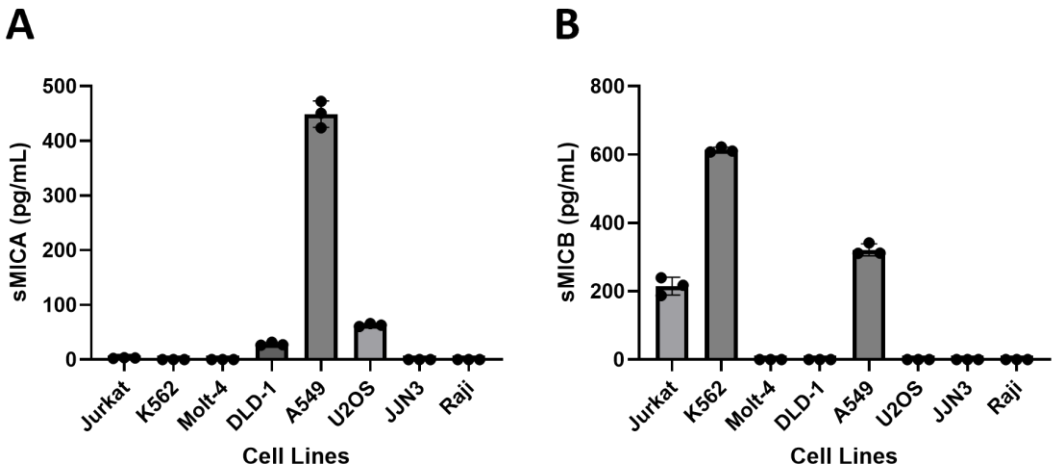

Figure 6.2: Some cancer cell lines secrete detectable levels of sMICA and sMICB, with the lung adenocarcinoma cell line, A549, expressing the most.

Conditioned supernatant was collected from cancer cell lines 72 hours after seeding. sMICA (A) and sMICB (B) were detected via sandwich ELISA and levels of protein were determined via comparison to a provided standard curve. N=3, error bars show mean +/- SD.

Varying concentrations of recombinant sMICA were added to co-cultures of A549 cells and PBMC-derived T cells that were treated with either the NKG2D TriTE or an EpCAM BiTE (kindly provided by Dr Hena Khalique) to determine if sNKG2DL had a negative effect on TriTE-mediated T cell activation. As shown in Figure 6.3, there was a sNKG2DL dose-dependent increase in target cell viability when treated with the NKG2D TriTE, however no significant increase was seen when treated with the EpCAM BiTE. This was explained by a sNKG2DL dose-dependent decrease in both T cell activation markers CD25 and CD69 seen when treated with the NKG2D TriTE, but not with the EpCAM BiTE. As the decrease in T cell activation is not occurring across both T cell engagers, we can deduce that the

reduction in T cell activation and cytotoxicity seen for the NKG2D TriTE treated co-cultures is likely due to the sMICA acting as a competitive inhibitor to the TriTE, preventing the TriTE from binding to the NKG2DLs present on the target cell membrane.

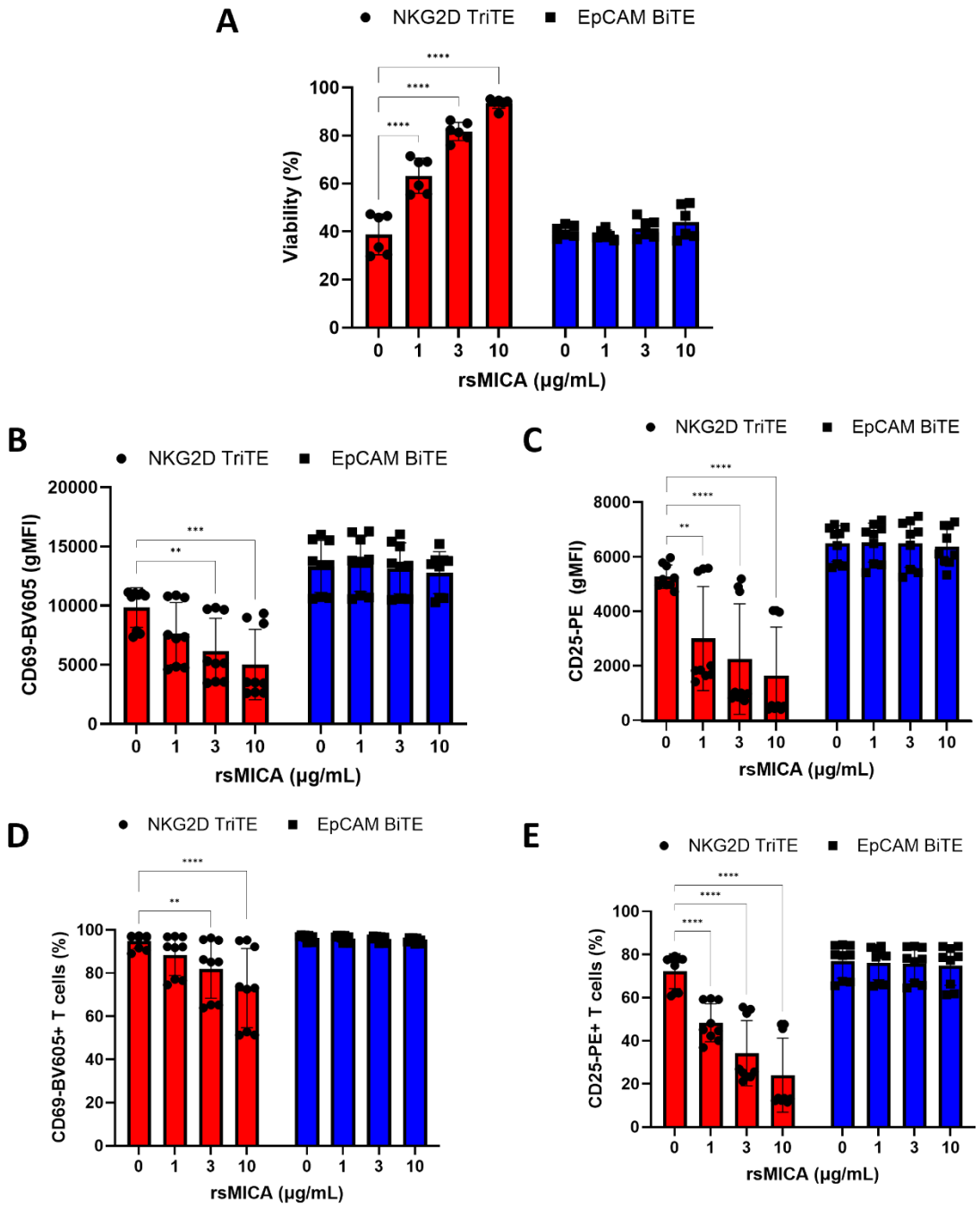

Figure 6.3: Soluble MICA inhibits NKG2D TriTE mediated T cell activation, but not all T cell activation.

Co-cultures of A549 cells and PBMC-derived T cells were treated with either 1 nM of NKG2D TriTE or EpCAM BiTE in the presence of varying amounts of recombinant sMICA (rsMICA) for 72 hours. (A) Viability was determined using an XTT assay on A549 cells once T cells were removed. (B) PBMC-derived T cells were stained for activation markers, CD69 (B+D) and CD25 (C+E) and analysed via flow cytometry. Data shown as average medium fluorescence (B+C), and percentage positive based on unstimulated T cells (D-E). N = 3, error bars shown mean +/- SD. Statistical

significance assessed by two-way ANOVA with Dunnett's multiple comparisons test to 0 µg/mL sMICA treated. p< 0.01 **, p<0.001 ***, p<0.0001 ****.

6.3.2 sMICA/B can be reduced through inhibition of ADAM proteases.

Whilst sMICA and sMICB do not seem to have an inhibitory effect on T cell activation, it may still be advantageous to decrease the shedding in the tumour microenvironment to increase the potency of the NKG2D BiTE and TriTE. By reducing the shedding of the ligands from the tumour cell, we hypothesise that there will be an increase in the number of ligands present on the target cell membrane. Additionally, although it seems at least *in vitro* there is no negative effect of inhibiting T cell co-stimulation via sMICA, this may not be the case *in vivo* where there are other immune cells involved, particularly NK cells.

As previously discussed, NKG2DLs are removed from the cell surface by two main mechanisms, cleavage of the extracellular domains via proteases such as ADAM 10 and 17, and release on the surface of extracellular vesicles (EV). NKG2D ligand shedding by EV secretion would be challenging to abrogate and likely require a more widespread strategy of inhibiting the exosome biogenesis pathway altogether. We therefore turned our focus to inhibiting the proteases which have been indicated to be involved in shedding of NKG2DLs. ADAM10 and ADAM17 have been reported to be the main contributors to NKG2D cleavage, which are reportedly blocked using GI254023X and TAPI-0, respectively, as well as the dual inhibitor, Aderbasib, and have shown efficacy in cancer cell lines previously (Seifert et al., 2021). In Figure 6.4A+D, the ADAM10 inhibitor, GI254023X showed a dose dependent decrease in both sMICA and sMICB detected in the supernatant of A549 cells. The ADAM17 inhibitor, TAPI-0, was less potent and showed a significant decrease in shed MICA ligands only at the highest dose of 10 µM decreasing the ligands from 408 pg/mL in the untreated sample to 258 pg/mL, resulting in a 37% reduction (Figure 6.4B+E). Similarly to GI254023X, supernatant from

Aderbasib treated A549 cells showed a dose dependent decrease resulting in a 76% reduction in detected soluble ligands after 72 hours (untreated – 408 pg/mL vs 100 μM Aderbasib treatment – 97 pg/mL, Figure 6.4C+F). For the sMICB assay, the amount of detected soluble ligands was below that of the standard curve and so whilst we can see that there is a decrease in shed MICB (Figure 6.4D-F), especially for the aderbasib treated cells, we were unable to determine the concentration. In Figure 6.4G-H, an increase in cell surface NKG2DLs can be seen, with the largest increase seen when treated with 10 or 100 μM aderbasib. This is consistent with the inhibition of ligand shedding having a positive effect on the abundance of NKG2DLs present on the cell surface.

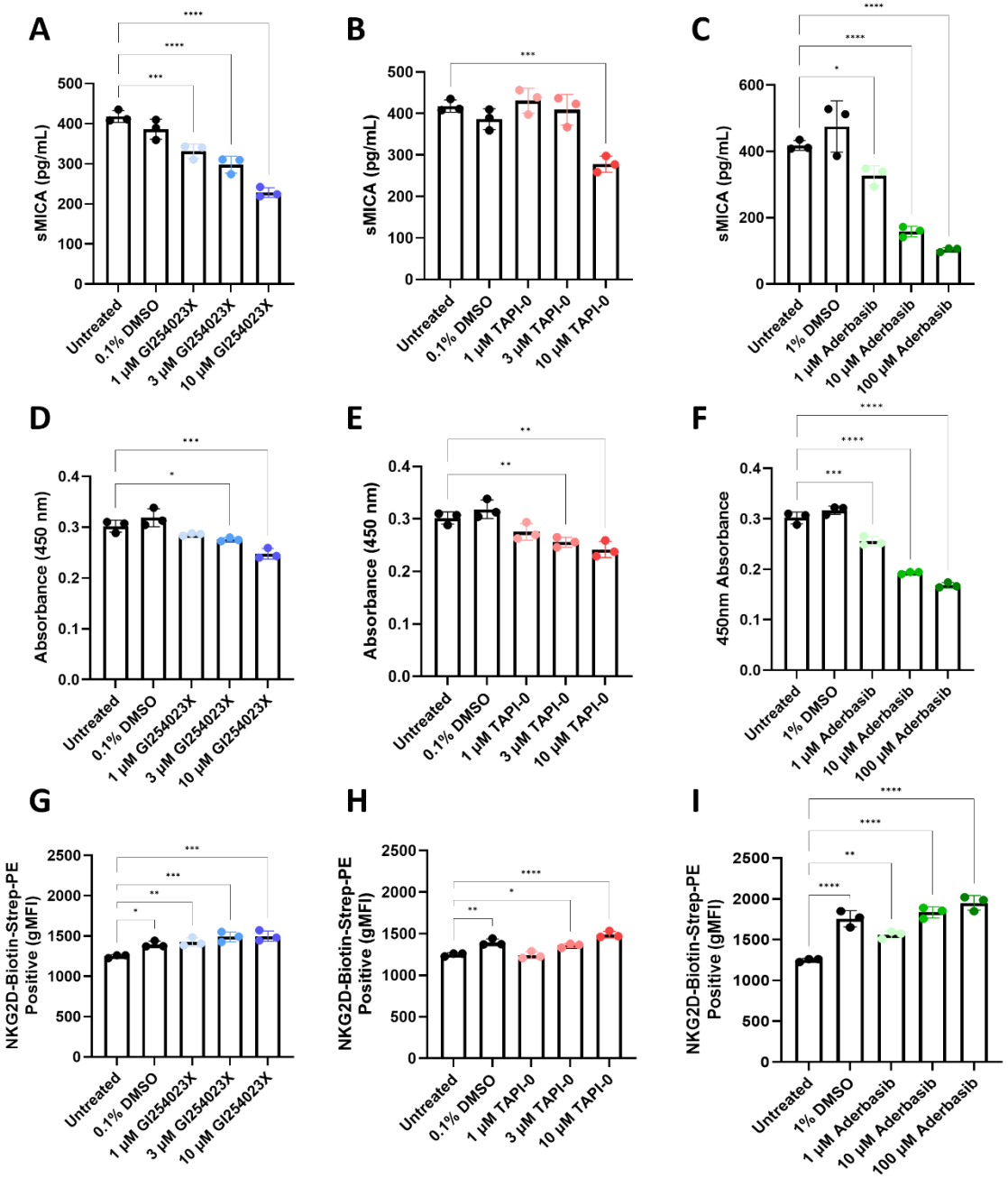

Figure 6.4: ADAM 10 and 17 inhibitor treatments reduces amount of shed MICA and MICB whilst also increasing the amount of total NKG2DLs on the cell surface.

A549 cells were treated with the indicated dose of ADAM17 inhibitor, GI254023X, ADAM10 inhibitor, TAPI-0, ADAM10/17 inhibitor, aderbasib, or vehicle control for 72 hours. Supernatant was collected and analysed via sandwich ELISA for the presence of sMICA (A-C) or sMICB (D-F). (G-I) Cells were analysed for total NKG2DLs using a biotinylated recombinant NKG2D ectodomain with a streptavidin-PE for detection via flow cytometry. N = 3, error bars shown mean +/- SD. Statistical significance assessed by one-way ANOVA with Dunnett's multiple comparisons test to untreated, $p<0.05$ *, $p<0.01$ **, $p<0.001$ ***, $p<0.0001$ ****.

6.3.3 Preventing the shedding of ligands does not improve NKG2D TriTE mediated T cell activation.

Further to the above seen increase of surface NKG2D ligand through aderbasib treatment, we hypothesised that the T cell activation through NKG2D BiTE/TriTE could be potentiated by the increase of surface ligands. Aderbasib has relatively low solubility in water and could be dissolved in DMSO at a concentration of 100 µM. Therefore, when using the highest dose of Aderbasib to inhibit ADAM proteases, the final concentration of DMSO would be 1%. We have previously noted that this concentration of DMSO inhibited the cytotoxic function of T cells (unpublished) and therefore sought to investigate the maximum dose of DMSO that we could utilise in our assay without compromising T cell function.

As shown in Figure 6.5, when using either aCD3/aCD28 beads or the NKG2D TriTE to activate T cells, a final concentration of 0.1% DMSO showed little effect in terms of CD25 expression, whereas 1% DMSO lead to a decrease for the NKG2D TriTE (Figure 6.5), consistent with the literature (Holthaus et al., 2018). There was also a similar but less dramatic difference seen in terms of target cell cytotoxicity. We therefore chose to proceed with a limit of 0.1% DMSO in further T cell assays. Due to the solubility of Aderbasib, this therefore meant the highest dose of Aderbasib used in Figure 6.4, 100 µM, could not be used as the this would require a final concentration of DMSO to be 1%. However, as the increase in total NKG2DLs on the cell surface and reduction in soluble ligands between the 10 µM and 100 µM dose were similar (141.2 pg/mL vs 96.2 pg/mL respectively), a meaningful effect on T cell activation should still be evident.

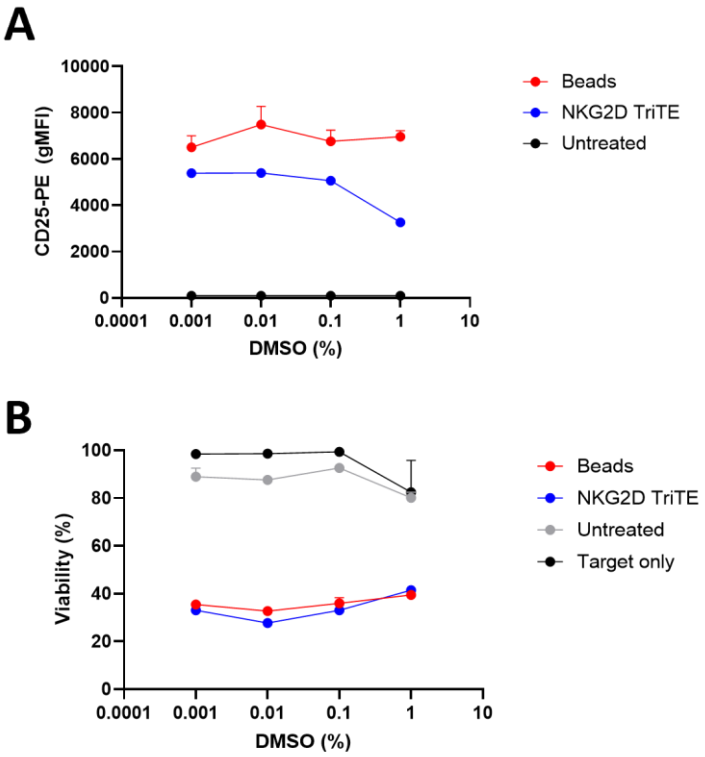

Figure 6.5: High concentrations of DMSO negatively affect T cell mediated cytotoxicity.

Co-cultures of A549 cells and PBMC-derived T cells were treated with either 1 nM NKG2D TriTE or 1 µL/well of CD3/CD28 DynaBeads in the presence of varying concentrations of DMSO for 72 hours. (A) PBMC-derived T cells were stained for CD25 to determine activation and analysed via flow cytometry. (B) Viability was determined using an XTT assay on target cells once T cells were removed. N = 1.

In Figure 6.6, A549 cells were treated with 1 or 10 µM Aderbasib, or vehicle control, whilst in a co-culture with PBMC-derived T cells. Cells were treated alongside with NKG2D T cell engagers or control constructs for 72 hours prior to analysis for T cell activation and target cell cytotoxicity. As previously seen, the NKG2D BiTE and TriTE treated co-cultures had a lower target cell viability for all treatments in comparison to the control treatments or untreated samples (Figure 6.6A). The addition of Aderbasib had no significant effect on target cell viability, indicating that the increase in NKG2DLs on the cell surface did not increase the potency of either the NKG2D BiTE or TriTE. This is supported

by the minimal increase in some T cell activation markers seen for the aderbasib treated samples (Figure 6.6B-D).

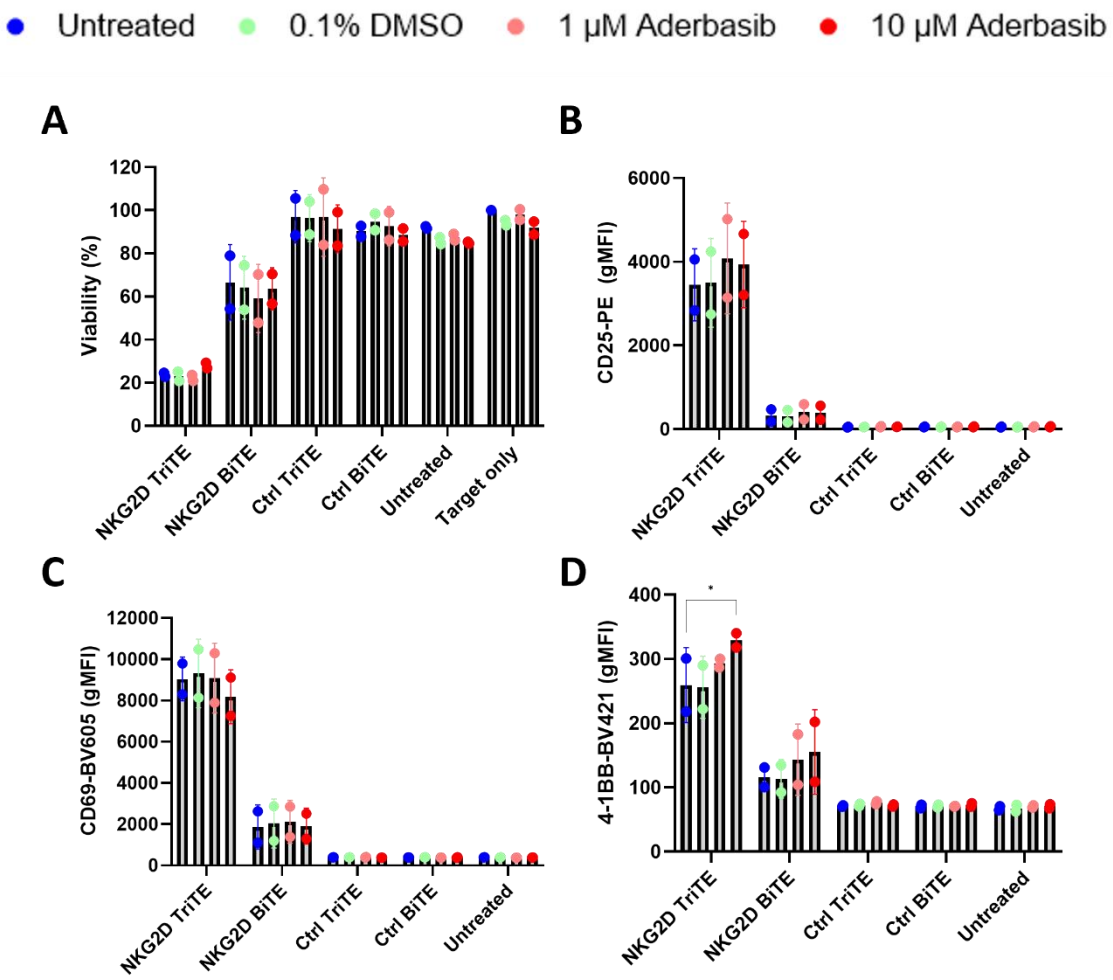

Figure 6.6: Inhibiting the cleavage of NKG2DLs with an ADAM10/17 inhibitor does not increase T cell mediated cytotoxicity.

A549 cells in a co-culture with PBMC-derived T cells were treated with 1 nM NKG2D BiTE, TriTE or associated control vectors in the presence of ADAM10/17 inhibitor aderbasib or vehicle control. (A) Viability was determined using an XTT assay on target cells once T cells were removed. PBMC-derived T cells were stained for CD25 (B), CD69 (C) and 4-1BB (D) to determine activation and analysed via flow cytometry. N = 2, error bars indicate mean +/- SD. Statistical significance assessed by two-way ANOVA with Dunnett's multiple comparisons test to untreated, $p<0.05$ *.

6.3.4 An aMICAB scFv BiTE is equally as potent as the NKG2D TriTE against cell lines expressing MICA but not when all NKG2DLs are present.

As mentioned previously (6.1), Ferrari de Andrade et al. developed an antibody targeting the α3 domain of MICA which blocks the cleavage site resulting in inhibition of MICA shedding (Ferrari De Andrade et al., 2018).

In general, we have often seen that the NKG2D BiTE and TriTE are not as potent as other BiTEs developed in our lab, as briefly shown in Figure 6.3 when comparing to the EpCAM BiTE (Freedman et al., 2017; Khalique et al., 2021). This could be due to several reasons such as the differences in affinity to the target molecule, the length of the immune synapse generated, or the abundance of the tumour antigen on the target cell surface. Traditionally, BiTEs contain two scFvs, targeting the CD3 of T cells and antigens of a target cell with high affinity. Due to the lack of availability of an scFv against NKG2DLs and the variety amongst the ligands, it was decided to use the ectodomain of the NKG2D receptor, which although this targets all ligands, it compromises on affinity. The affinity between NKG2D and MICA has been calculated to be around 1 μM (Raulet et al., 2013), and whilst the NKG2D TriTE contains two NKG2D ectodomains to increase the overall avidity, or to form the extracellular NKG2D homodimer structure, it is still likely lower than that of an scFv binding an epitope which is typically in the nM range.

We therefore sought to use higher affinity agents to target the most studied ligands, MICA and MICB, which have publicly available antibodies. We chose to base the design on the α3 domain binding, 7C6 antibody which also prevents the shedding of MICA and MICB (Ferrari De Andrade et al., 2018.). Whilst in this chapter we have shown that sMICA and sMICB seem to have minimal to no effect on NKG2D TriTE mediated cytotoxicity, however we hypothesise that the increase in affinity that comes from utilising an scFv will be more potent than using a weaker affinity against more targets.

Additionally, the aMICAB scFv binds to the base of the MICAB proteins and should lead to a shorter distance between the T cell and target cell. A tighter immune synapse of less than 20 nm has been shown to be beneficial for T cell activation (Davis & van der Merwe, 2006).

The aMICAB scFv sequences were generated using the heavy and light variable regions of the 7C6 antibody (US20200165343). To determine the best orientation, the two configurations of the heavy and light sequences were tested both in binding assays, as well as in functional assays. These constructs are referred to as aMICAB(HL) and aMICAB(LH) with H and L referring to the heavy and light sequence, respectively, and specifying the order of the sequences. The regions were linked via a GS linker and then joined to the aCD3 scFv (schematic shown in Figure 6.7A). As with previous constructs, an N-terminal immunoglobulin secretion signal and a C-terminal decahistidine tag were included to allow for secretion and detection, respectively. Constructs were cloned into the pSF backbone and sequences were verified via Sanger sequencing. As a control for non-specific activation an anti-FHA (*Filamentous hemagglutinin*) scFv fused to the aCD3 scFv was utilised, previously generated in our lab (Freedman et al., 2017).

The BiTEs were produced in HEK293 cells and supernatant was concentrated using a 10 kDa MWKO amicon filter prior to aliquoting and storing at -80^{o}C. The size of the BiTEs was determined by His tag immunoblot (Figure 6.7B). The FHA-aCD3 control BiTE was roughly the correct size, however both aMICAB BiTEs were detected at much higher molecular weights than predicted (between 80-100 kDa). Similarly to other constructs utilised in this thesis, this may be due to post-translational modifications. Additionally, the aMICAB(LH) BiTE was produced at a higher yield than the aMICAB(HL) orientation or the FHA BiTE.

To confirm the ability of the aMICAB BiTEs to bind to MICA, an ELISA was carried out. ELISA plates were coated with a commercially available MICA protein and were incubated with 1 nM of each construct for 2 hours. The binding was then detecting using an HRP-conjugated anti-His antibody. The NKG2D BiTE, TriTE as well as both conformations of the aMICAB BiTE showed a positive signal for

binding, whilst all control samples showed no binding (Figure 6.7C). The MIC(LH) BiTE showed the highest absorbance, indicating a higher proportion of the protein is functionally active.

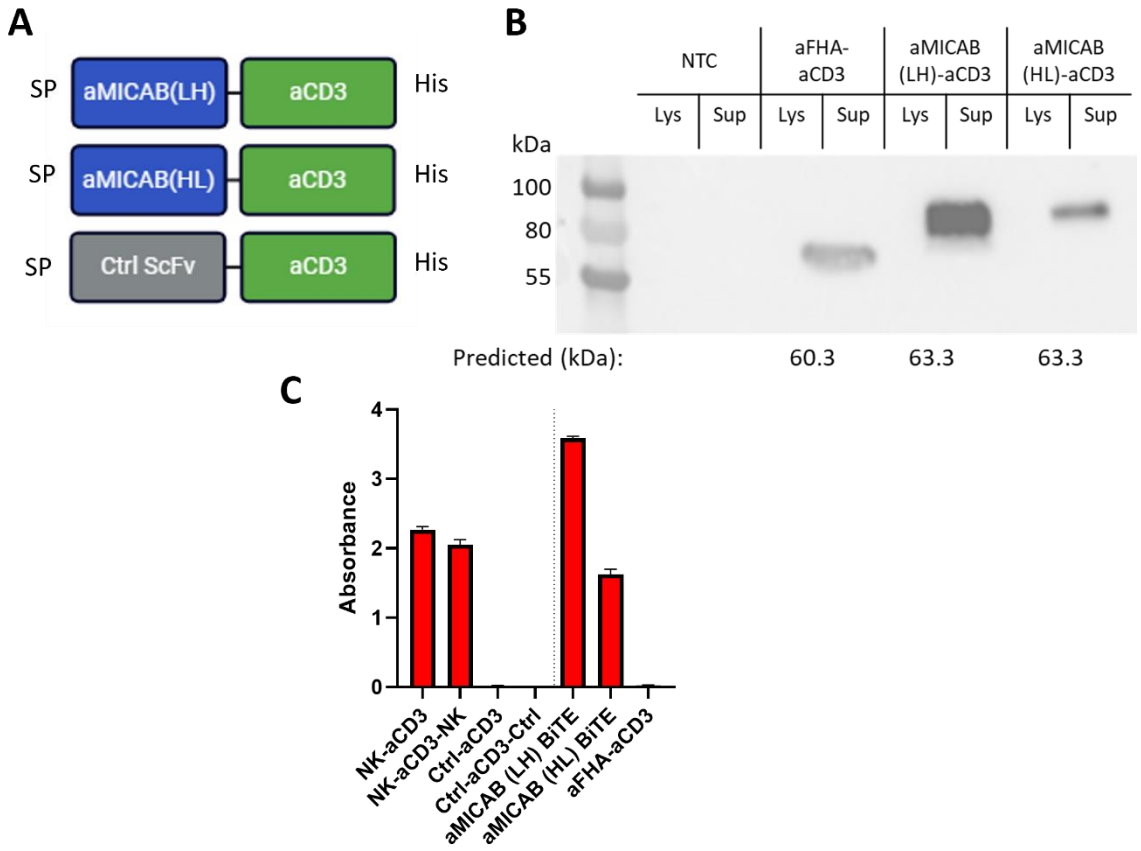

Figure 6.7: Design and expression of aMICAB BiTEs.

(A) Schematic of aMICAB BiTEs along with control constructs. All constructs generated included an N-terminal immunoglobulin secretion signal peptide (SP) and a C-terminal decahistidine tag (His) Domains were linked by GS linkers to allow flexibility (SSGGGGS). aMICAB scFvs were formed from the heavy and light variable regions of the 7C6 antibody. Both orientations were engineered into the bispecific to determine the optimal configurations. These constructs are referred to as aMICAB (HL) and aMICAB (LH) with H and L referring to the heavy and light sequence, respectively, and specifying the order of the sequences. HEK293 cells were transfected with the indicated plasmid for 72 hours. Lysate and supernatant were collected and processed as detailed in materials and methods. (B) Constructs were detected via western blot to determine they were of the correct size using an anti-His tag antibody to immunoblot. (C) Binding of the samples to recombinant MICA was carried out using an indirect ELISA using an HRP-conjugated anti-His tag antibody to detect bound constructs to the MICA coated plate.

The aMICAB BiTEs were then tested for functionality and compared to the NKG2D BiTE and TriTE to determine the most potent candidate. The colorectal cell line, DLD-1, was shown to express high levels of MICA and B as well as overall high levels of NKG2DLs (Figure 6.8A). In functional testing, the NKG2D BiTE and TriTE caused a significant decrease in cancer cell viability whilst, rather unexpectedly there was no significant difference in target cell viability from treatments with either aMICAB BiTEs (Figure 6.8B). The NKG2D BiTE and TriTE cytotoxicity was also associated with a significant increase in multiple T cell activation markers, indicating T cell dependent cytotoxicity (Figure 6.8C-H). Despite the lack of cytotoxicity, both aMICAB constructs were able to significantly activate T cells seen by an increase in CD69 and CD25 expression but not 4-1BB expression. There was minimal activation for all control constructs. As shown in Figure 6.8C-H, the aMICAB(LH) orientation was more effective than the aMICAB(HL) BiTE at inducing T cell activation as indicated by the higher expression of CD69, CD25 and 4-1BB, albeit a minimal increase in 4-1BB expression.

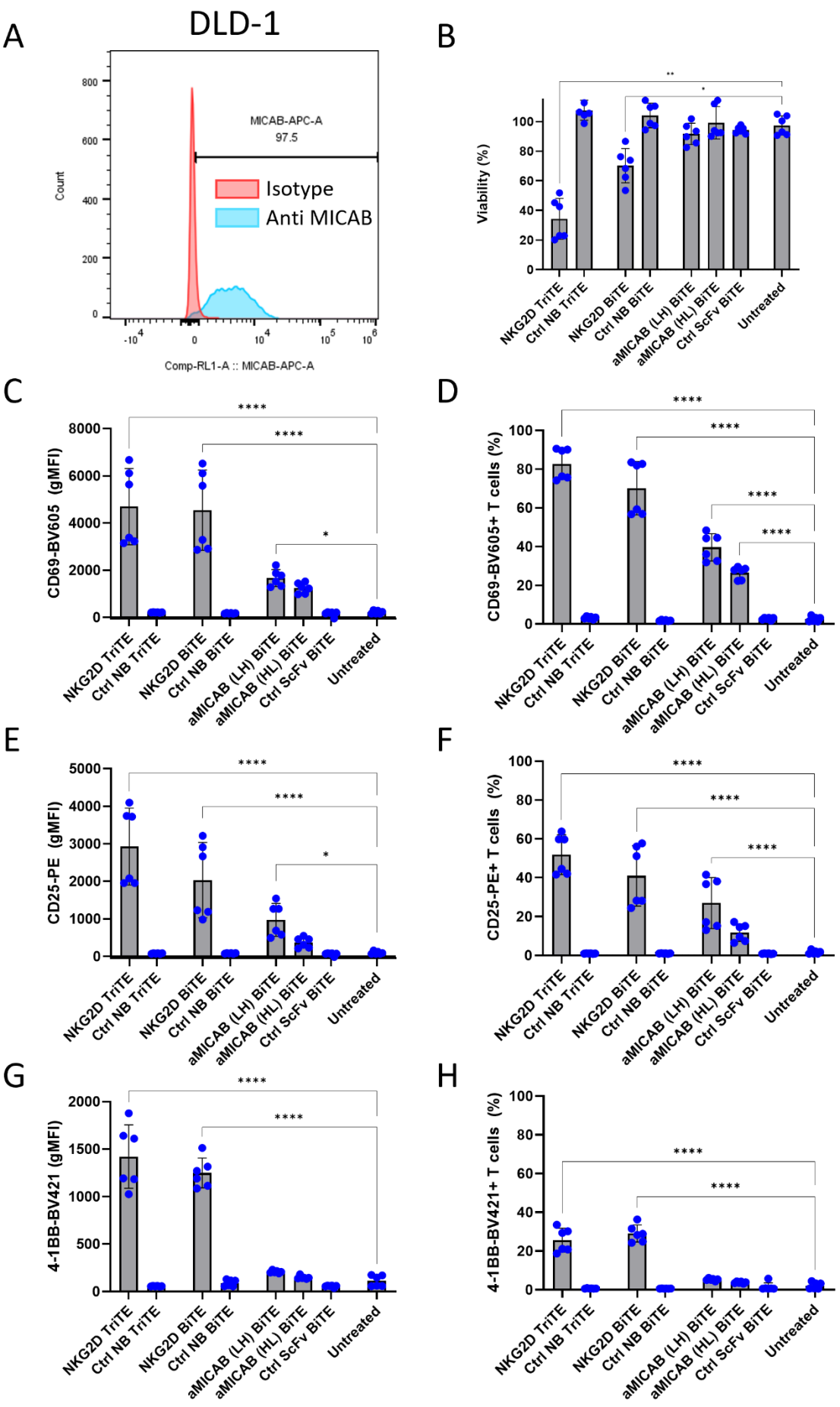
A
DLD-1
MICAB-APC-A
97.5
Isotype
Anti MICAB
Count
Comp-RL1-A :: MICAB-APC-A
B
Viability (%)
C
CD69-BV605 (gMFI)
D
CD69-BV605+ T cells (%)
E
CD25-PE (gMFI)
F
CD25-PE+ T cells (%)
G
4-1BB-BV421 (gMFI)
H
4-1BB-BV421+ T cells (%)
NKG2D TriTE
Ctrl NB TriTE
NKG2D BiTE
Ctrl NB BiTE
aMICAB (LH) BiTE
aMICAB (HL) BiTE
Ctrl ScFv BiTE
Untreated

Figure 6.8: The NKG2D TriTE outperforms the aMICAB scFv BiTEs when targeting a cancer cell line.

(A) DLD-1 cells were stained with an αMICAB-APC antibody (blue) or isotype control (red) and analysed via flow cytometry. Representative flow cytometry plot shown. (B-H) DLD-1 cells were treated with 1 nM of the indicated constructs in a co-culture with PBMC-derived T cells for 72 hours. (B) Viability was determined using an XTT assay on target cells once T cells were removed. PBMC-derived T cells were stained for CD69 (C-D), CD25 (E-F) and 4-1BB (G-H) to determine activation and analysed via flow cytometry. N = 2, error bars indicate mean +/- SD. Statistical significance assessed by one-way ANOVA with Dunnett's multiple comparisons test to untreated, $p<0.05$ *, $p<0.01$ **, $p<0.0001$ ****.

We hypothesised that as the NKG2D BiTE and TriTE performed better than the aMICAB BiTEs due to their ability to bind to all the NKG2DLs as opposed to just MICA/B. To test this theory, we utilised an engineered cell line, overexpressing MICA. We predict that as MICA is the only available ligand on the target cell, the aMICAB BiTEs would outperform the NKG2D BiTE and TriTE, due to its presumed increased affinity as well as the narrowing of the immune synapse.

To generate stable MICA expressing cell lines the MICA*004 allele was cloned in a lentiviral genome vector that contained a puromycin resistance gene. We next chose to use the hamster cell line, CHO, to transduce due to the low homology between human and hamster NKG2DLs. Lentiviral particles were generated, and CHO cells were transduced. Positive cells were selected using puromycin and stained for MICA to confirm expression (Figure 6.9A).

As shown in Figure 6.9B, the aMICAB (LH) BiTE showed equivalent potency as the NKG2D TriTE, with a significant decrease in target cell viability compared to the untreated sample. Additionally, both the aMICAB (LH) and the NKG2D TriTE outperformed the NKG2D BiTE, which mediated with no significant decrease in viability similar to the control constructs. The NKG2D TriTE and aMICAB BiTE in the LH configuration also significantly increased the expression of multiple T cell activation markers (Figure 6.9C-G). The alternative confirmation, aMICAB (HL) BiTE, also induced a significant increase in T cell activation, however we did not see a corresponding decrease in target cell cytotoxicity Figure

6.9B. The NKG2D BiTE partially induced T cell activation, with a highly significant increase in CD69 expression, as well as 4-1BB, however there was no significant increase in CD25 (Figure 6.9C-H).

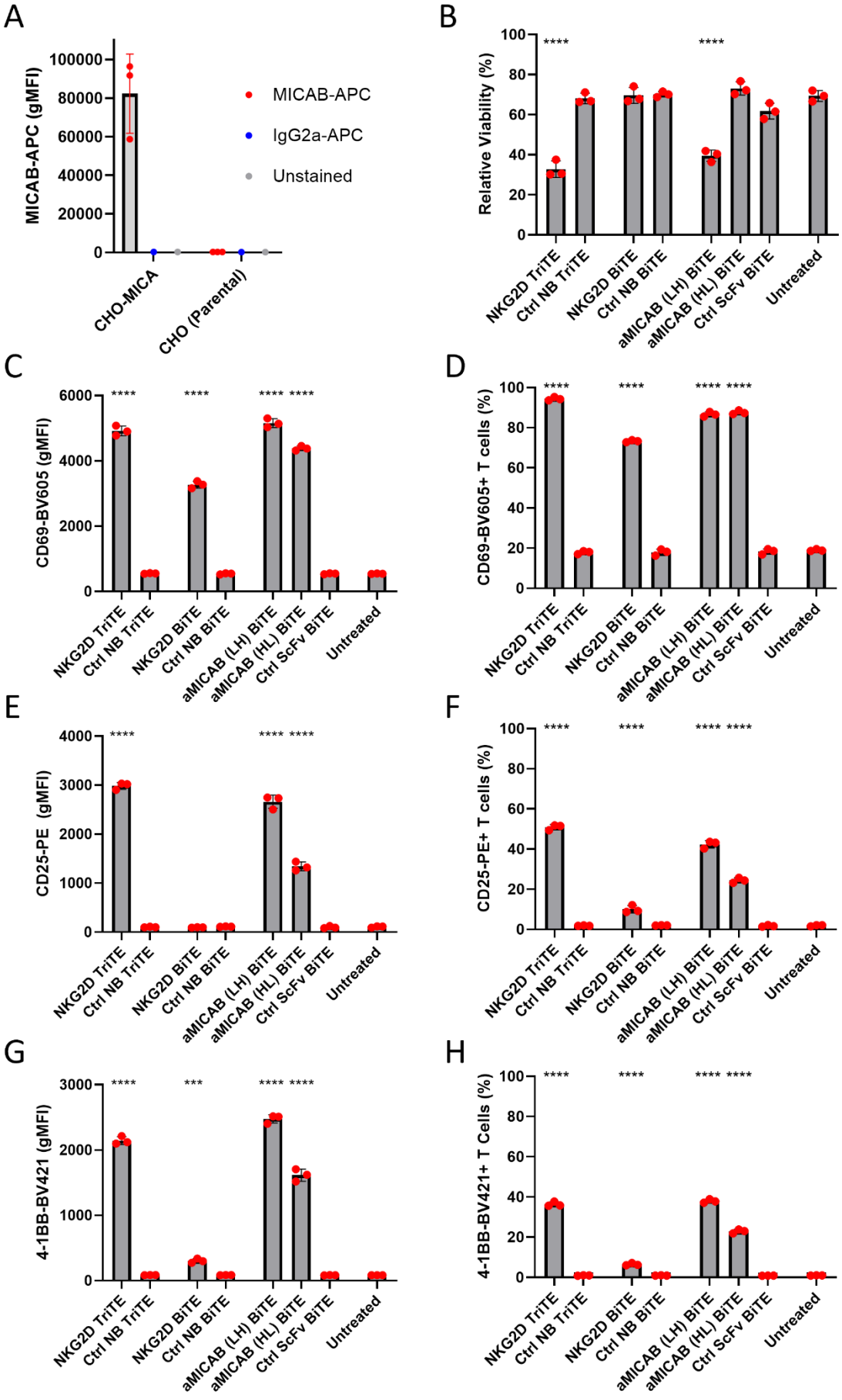
A
MICAB-APC (gMFI)
100000
80000
60000
40000
20000
0
MICAB-APC
IgG2a-APC
Unstained
CHO-MICA
CHO (Parental)
B
Relative Viability (%)
100
80
60
40
20
0
****
****
NKG2D TriTE
Ctrl NB TriTE
NKG2D BiTE
Ctrl NB BiTE
aMICAB (LH) BiTE
aMICAB (HL) BiTE
Ctrl ScFv BiTE
Untreated
C
CD69-BV605 (gMFI)
6000
4000
2000
0
****
****
****
****
D
CD69-BV605+ T cells (%)
100
80
60
40
20
0
****
****
****
****
E
CD25-PE (gMFI)
4000
3000
2000
1000
0
****
****
****
F
CD25-PE+ T cells (%)
100
80
60
40
20
0
****
****
****
****
G
4-1BB-BV421 (gMFI)
3000
2000
1000
0
****
***
****
****
H
4-1BB-BV421+ T Cells (%)
100
80
60
40
20
0
****
****
****
****

Figure 6.9: The NKG2D TriTE and the MICAB BiTE are equally as potent when targeting cell lines expressing on MICA and not other NKG2DLs.

(A) CHO cell lines stably expressing MICA were engineered using lentiviral transduction and were selected for using puromycin. Cells were stained for MICA expression using an aMICAB antibody, isotype control or were left unstained. MICA expression was determined using flow cytometry. (B-H) CHO cells overexpressing MICA*004 (CHO-MICA) were treated with 1 nM of the indicated constructs in a co-culture with PBMC-derived T cells for 72 hours. Cells were dissociated and stained for T cell activation markers CD69 (C-D), CD25 (E-F) and 4-1BB (G-H), as well as viability using a membrane permeability dye, and analysed via flow cytometry. (B) Viability of target cells (CD4-CD8-), relative to the target only control. Average percentage positive, using unstimulated control to gate at 1% for each cell line are presented for T cell activation markers (D, F, G). Data shown as average mean fluorescence (C, E, G). N = 3. Statistical significance assessed by one-way ANOVA with Dunnett's multiple comparisons test to untreated, $p<0.001$ ***, $p<0.0001$ ****.

6.4 Discussion

sNKG2DLs have been reported to impede immune mediated clearance of tumours by acting as a decoy for the NKG2D receptor found on NK and T cells (Cao et al., 2007; Groh et al., 2002; Song et al., 2006; Y. Zhang et al., 2023). This chapter focussed on determining the effect of sNKG2DLs on TriTE-mediated T cell activation and cytotoxicity.

Firstly, we investigated the abundance of sMICA and sMICB present in the acellular peritoneal ascitic fluid from patients with malignant cancer. We saw a large variation in the concentrations of both sMICA and sMICB detected, with all samples tested being positive for sMICB, whereas sMICA was detected in only 7/9 samples. (Figure 6.1A-B). It was also noted that the levels of sMICA and sMICB do not correlate with each other in individual samples. As we do not know the relative expression levels of the proteins expressed on the surface of the patients' tumour cells, we are unable to comment on whether this reflects the producer cell. Different proteases have varying specificities and so the quantity of ligands cleaved may depend both on the abundance of the ligands present on the cell surface and the specific proteases that are within the vicinity. Upon comparing the levels of sMICA/B in each ascitic fluid sample to the level of inhibition mediated on DynaBead induced T cell

activation, we saw no correlation with either sMICA or sMICB. A major limitation of these results is that we did not also detect the abundance of soluble ULBP ligands, which may alter our interpretation significantly. The immune-inhibitory component of ascitic fluid is still yet to be elucidated. Whilst there are high levels of immunosuppressive cytokines found, such as IL-6 and IL-10, found in ascitic fluid, it is often not a simple story to match this to immunosuppressive assays or patient outcomes. The answer is likely to be the combination of a variety of different factors, including immunosuppressive compounds as well the availability of metabolites such as amino acids and lipids (Gong et al., 2020; J. Shen et al., 2017).

Following from this, we sought to evaluate the effects of NKG2DLs on BiTE mediated-T cell activation, which differs from CD3/CD28 Dynabeads in that only CD3 is crosslinked during T cell activation. In Figure 6.3 we saw the dose dependent decrease in both T cell activation and target cell viability when treating co-cultures with the NKG2D TriTE but not with an EpCAM targeting BiTE. This suggests that NKG2D mediated co-stimulation is not critical for BiTE mediated activation whilst in might be for TCR-mediated activation (Groh et al., 2001; Kohlhapp et al., 2023; Lerner et al., 2023). It is most feasible that the soluble ligand is binding to the NKG2D ectodomains of the NKG2D TriTE, preventing the binding to the target cell. Whilst this is frustrating for out targeting strategy, it is possible that this mechanism could be advantageous within the tumour as the sNKG2DL would be sequestered by the NKG2D TriTE, becoming unable to cause downregulation on NK cells which seem to be more sensitive to sNKG2DL-mediated immunosuppression (Ferrari De Andrade et al., 2018). Additionally, an inhibitory role for sNKG2DL in CD8+ T cell inhibition has been described in a number of circumstances (Groh et al., 2002; Y. Zhang et al., 2023). It should also be noted that the concentrations of sMICA used in these assays are much higher than that detected in the conditioned media from cancer cell lines or in the patient ascitic fluid samples analysed (Figure 6.1A+B, Figure 6.2). Therefore, the inhibitory effect seen with the NKG2D TriTE may not be physiologically relevant, and the NKG2D TriTE is resistant to sNKG2DL-mediated suppression. We therefore concluded that sMICA does not directly inhibit T cells in BiTE-mediated cytotoxicity, however at high concentrations

can inhibit NKG2D ligand targeting TriTEs by acting as a decoy ligand. Groh et al found that soluble MICA caused the downregulation of NKG2D from the surface of CD8 T cells, resulting in lower levels of cytotoxicity compared to CD8 T cells that were not treated with soluble MICA (Groh et al., 2002). It would be interesting to look if the NKG2D receptor on CD8 T cells was downregulated in both presence of both the EpCAM BiTE and NKG2D TriTE and determine if downregulation of NKG2D effects the potency of BiTE/TriTE activated T cells. NKG2D has been identified as a co-stimulatory molecule in the activation of CD8 T cells and has also been identified as mediating the killing of MHC-I negative tumour cells, as downregulation my soluble NKG2DLs also seems to have a large inhibitory effect on CD8 T cells (Lerner et al., 2023). From our data, the EpCAM BiTE was not affected by any of the concentrations of sMICA, with the NKG2D TriTE being affected by only extremely high concentrations. This could therefore mean that BiTE-activated T cells are resistant to sNKG2DL mediated suppression.

We next turned to inhibiting the shedding of ligands as strategy to increase the cell surface expression of NKG2DLs, as well as prevent the down regulation of NKG2D on immune cells. In Figure 6.4A-F, we showed that three different small molecule inhibitors of ADAM 10 and/or ADAM17 significantly reduce the amount of sMICA and sMICB shed from a cancer cell line in a dose dependent manner. Additionally, we saw a significant increase in amount of overall NKG2DLs expression on the cell surface, however this was only slightly higher than the DMSO control (Figure 6.4G-I). After identifying the dual ADAM10/17 inhibitor, Aderbasib, as the most effective of the three treatments, we then tested if this increase in ligand expression translated to an increase in T cell activation as well as target cell cytotoxicity. In Figure 6.6, we saw no significant difference in the target cell viability, or in two out of the three T cell activation markers assessed, when treated with Aderbasib. With the highest does of Aderbasib (10 µM), we saw a slightly significant increase in 4-1BB expression (Figure 6.6D). We saw a similar pattern for the NKG2D BiTE, however it was not significantly different.

We are unsure about the kinetics of Aderbasib treatment. We measure the levels of surface NKG2DLs and sMICA/B after 72 hours. Whilst, in this assay, tumour cells were treated with Aderbasib at the same time as the addition of the T cells and NKG2D BiTE/TriTE. Pre-treatment with Aderbasib to stabilise the levels of NKG2DLs on the cell surface prior to the addition of the BiTE and T cells may have proven more effective. Furthermore, the concentrations of soluble ligands released from A549 (400 pg/mL sMICA and 600 pg/mL sMICB) may not be sufficient to inhibit the NKG2D TriTE, as seen in Figure 6.3 where much higher amounts of soluble MICA were used.

Zhang et al. found that found that chemotherapy induced senescence, in neuroblastoma cells, led to a significant increase both surface expression of MICA/B as well as an increase in sMICA/B detected in the supernatant, with the latter being attributed to an increase in ADAM10 protein levels (Y. Zhang et al., 2023). Treatment with the ADAM10 inhibitor GI254023X, utilised in this chapter, was able to provide an additive effect, by preventing the cleavage of the increasing amount of MICAB, allowing for more NK mediated tumour lysis than the chemotherapy treated condition. We were unable to determine the timings of the GI254023X treatment and NK cell addition in this study.

The final part of this chapter focussed on the development of new BiTEs that targeted only a subset of the NKG2DLs but at a higher affinity. The MICA targeting 7C6 antibody, from which aMICAB scFv was created, binds to the α3 region of MICA/B to prevent the shedding via proteolytic cleavage, promoting NKG2D- and CD16-mediated targeting by NK cells, even in HLA-negative target cells (Ferrari De Andrade et al., 2018, 2020).

As previously mentioned, the NKG2D BiTE and TriTE target NKG2DLs using the ectodomain of the NKG2D receptor, which can bind to the eight NKG2D ligands. Whilst this is one of the main advantages of these agents, owing to the improbable downregulation of all of them, this also creates a major disadvantage in that the affinity of the interaction (NKG2D-MICA affinity estimated to be ~ 1 μM) is much lower than that of an scFv binding to an epitope (Raulet et al., 2013). In comparison, the antibody from which the EpCAM scFv, used in the EpCAM BiTE, originates from has an affinity of

around 10 nM (Brischwein et al., 2006). We therefore hypothesised that a BiTE with increased affinity, against fewer targets, would be superior to the NKG2D TriTE that has lower affinity to more target proteins.

Therefore, we constructed aMICAB BiTEs containing an scFv obtained from the heavy and light sequences from the 7C6 antibody. To ensure the optimal confirmation was used, we generated two versions of the BiTE, aMICAB (LH) and aMICAB (HL), alternating the order of the sequences in the protein (Figure 6.7A). Both proteins were produced and secreted well, and were functionally able to bind to MICA, with the aMICAB (LH) configuration showing a higher level of binding than the aMICAB (HL) configuration as well as the NKG2D BiTE and TriTE (Figure 6.7B+C).

We next tested the ability of these constructs to mediate T cell activation and target cell cytotoxicity in a co-culture of DLD-1 cells and PBMC-derived T cells. As shown previously, the NKG2D BiTE and TriTE mediate significant target cell cytotoxicity; however, this was not observed with either of the aMICAB BiTEs (Figure 6.8B). NKG2D BiTE and TriTE-mediated cytotoxicity was additionally associated with high levels of multiple T cell activation markers (Figure 6.8C-H). Whilst the aMICAB (LH) BiTE was able to partially induce T cell activation, as shown by the significant change in CD69 and CD25 expression, there was no significant change in 4-1BB expression. The marginally better performance seen with the aMICAB (LH) BiTE than the aMICAB (HL) is supported by the increased binding to MICA seen in Figure 6.7C. From this data, we can conclude that, when treating DLD-1 cells, the increased affinity of the aMICAB BiTEs does not improve their potency against agents that target the full repertoire of NKG2DLs, such as the NKG2D BiTE and TriTE. This therefore suggests that the number of target ligands is a limiting factor for the aMICAB BiTEs.

Whilst we know that DLD-1 cells express high levels of MICAB as well as NKG2DLs, we do not know the proportion of total NKG2DLs that comprise MICA and MICB, and if this is consistent with other colorectal cancer cell lines or cancer types. Leivas et al. showed a large amount of variation amongst multiple myeloma patients in terms of the surface expression levels of different NKG2DLs (Leivas et

al., 2021). Whilst at least one of the NKG2DLs were detected in all patients, some of the ligands were completely absent. It would therefore be interesting to determine the expression levels of the individual NKG2DLs, instead of focussing on them as a whole.

To determine the role of affinity in BiTE-mediated cytotoxicity, we utilised an engineered CHO cell line that solely expressed MICA, and no other NKG2DLs detectable by the human NKG2D ectodomain (Figure 6.9). When MICA is the only available NKG2DL, the NKG2D TriTE and aMICAB (LH) BiTE mediate similar target cell cytotoxicity, as well as levels of T cell activation markers (Figure 6.9B-H). In comparison, co-cultures treated with the NKG2D BiTE, which also binds to the target cell via a single binding moiety like the aMICAB BiTEs, showed no significant difference in target cell viability in comparison to the untreated condition (Figure 6.9B). This suggests that whilst the increase in affinity to the ligand does result in increased potency, an increase in overall avidity has a similar effect.

We hypothesis that the levels of MICA on DLD-1 cell lines is much lower than that expressed on the engineered CHO cell lines and was therefore insufficient for the aMICAB BiTEs to mediate cytotoxicity towards the DLD-1 cells. The difference in MICA expression on the engineered CHO-MICA cell line in comparison to DLD-1 cell line would be interesting to investigate, however we would be unable to fairly compare efficacy data from the two experiments due to the targeting of cell lines originating from different species.

Similar work has been carried out by Goulding et al., in the context of CAR-T cells, whereby the 7C6 derived-scFv was presented from a CAR-T cell (α3MICAB CAR-T) and compared to a NKG2D-CAR-T cell which expressed the NKG2D ectodomain as the targeting region (Goulding et al., 2023). They showed, in both haematological and solid xenograft models, that the α3MICAB CAR-T was far superior to the NKG2D CAR-T as well as a CD19 targeting CAR-T cell treatment. This shows similar findings to those presented in Figure 6.9, in which the aMICAB (LH) BiTE outperformed the NKG2D BiTE.

In conclusion, within this chapter we have shown that whilst high concentrations of sMICA inhibited the NKG2D TriTE, they did not affect the potency of a BiTE targeting an alternative ligand, suggesting that sMICA, and potentially all sNKG2DLs, does not generally inhibit T cell activation. Additionally, the NKG2D TriTE showed only mild inhibition at the lower concentrations of sMICA, which are still above those detected in malignant ascitic fluid, indicating that NKG2D TriTE activated T cells may be resistant to sNKG2DL mediated inhibition. Furthermore, we showed that by inhibiting ADAM10 and ADAM17, we can significantly reduce the level of sMICA/B as well as increase the abundance of NKG2DLs on the cell surface. However, this does not seem to translate to an increase in BiTE-mediated cytotoxicity, most likely due to the low level of soluble ligands present in the culture media. Finally, we investigated the effect of increasing the affinity of the target cell binding moiety, utilising an scFv derived from an antibody which binds to the α3 region of MICA and MICB. When directly compared against one another in a cell line which expresses only one of the NKG2DLs, MICA, the aMICAB (LH) BiTE outperformed the NKG2D BiTE, showing that the increase in affinity, as well as potentially decreasing the distance of the immune synapse, does aid in BiTE-mediated cytotoxicity (Staufer et al., 2022). The increase in overall avidity by the addition of an extra NKG2D ectodomain however, as seen in the NKG2D TriTE, showed similar potency to the aMICAB (LH) BiTE. Therefore, in the targeting of cancer cells which express other NKG2DLs than MICA/B, such as those in cancer patients, the NKG2D TriTE would be a better candidate.

Chapter 7: Final discussion and conclusions

In the first half of this thesis, we sought to better characterise two pre-clinical therapeutic agents, the NKG2D BiTE and TriTE, which target the stress ligands known as NKG2D ligands (NKG2DLs). Both the NKG2D BiTE and TriTE contain the NKG2D receptor ectodomain, allowing them to bind to not just one, but eight therapeutic targets. Additionally, NKG2DLs are commonly upregulated in cancer due to their innate role as stress markers and are minimally expressed on normal cells.

Initially, we sought to verify for ourselves that NKG2DLs are in fact expressed on a wide range of cancer cells. Looking at a variety of cell lines from various tumour types, we were surprised to observe that not all the cell lines analysed were positive, and that there was a large range in their expression levels. We observed in cancer cell lines of B cell origin, including those derived from patients with multiple myeloma, that there was no or minimal expression of NKG2DLs, similar to the normal cell lines tested. This was at odds with multiple other reports involving these cell lines, in addition to clinical data showing the expression of multiple different NKG2DLs on plasma cell samples from a multitude of myeloma patients (Leivas et al., 2021). We concluded that this discrepancy is likely due to differences in culture conditions between different groups, a common problem in scientific research. We were surprised, however, that the cell culture medium we used (RPMI supplemented with 10% FBS) would lead to a reduction in NKG2DLs, compared to media with additional supplements such as amino acids and sodium pyruvate. Although metabolic stress was not investigated in this thesis, the availability of required metabolites has been shown to upregulate NKG2DLs in a handful of cases (Marinović et al., 2023; McCarthy et al., 2018).

Overall, we confirmed that NKG2DLs are widely expressed among cancer cell lines. We additionally observed that in the small range of non-malignant cell lines we tested, minimal NKG2DLs were expressed. These results are consistent with clinical samples obtained from patients from a variety of

different sources (Driouk et al., 2020; Ghadially et al., 2017; Sun et al., 2019; Tsukagoshi et al., 2016; Yang et al., 2019). This is promising evidence that NKG2DLs are valuable targets for immunotherapy, and that our therapeutic agents could be used in the treatment of a wide variety of cancer types.

From this work, we verified the potency of the NKG2D BiTE and TriTE agents on a variety of different cancer cell lines, as well as on one patient-derived colorectal liver metastasis sample, in which we observed a significant increase in IFN-γ release when treated with the NKG2D TriTE. This indicates that the NKG2D TriTE can effectively activate tumours *in situ*, despite the immunosuppressive conditions within. While this is promising, more patient samples are needed to further support the use of the NKG2D TriTE in this context.

We were also able to induce the expression of NKG2DLs on JJN3 cells, a multiple myeloma cell line, which were minimally susceptible to BiTE-mediated killing. However, when treated in combination with HDAC inhibitors (HDACi), which are often used as part of the treatment regimen for multiple myeloma patients, we saw that they were sensitized to NKG2D BiTE- and TriTE-mediated killing.

We additionally tested the effect of conventional cancer therapies, including radiation and chemotherapy, on NKG2DL expression in both cancer cell lines and normal cell lines. While not all treatments led to a significant increase in NKG2DL expression, all cell lines tested were susceptible to at least one. For example, DLD-1 cells exhibited the unusual behaviour of downregulating surface NKG2DLs in response to both radiation and 5-FU treatment, but a significant increase was seen upon HDACi treatment. This suggests that different cancer cells use different mechanisms to modulate immune-activating ligands, and more research is needed to determine the optimal combination of therapies when targeting NKG2DLs.

A common side effect of radiation is off-target toxicity to healthy tissues due to the path of the ionizing radiation beam. Due to the activation of the DNA damage response (DDR) pathway upon DNA damage caused by radiotherapy, we were concerned that NKG2DL surface expression could also be upregulated on normal cells, causing them to be sensitized to the NKG2D BiTE/TriTE therapy.

However, we found in the one ‘normal’ cell line tested that surface expression of NKG2DLs was not upregulated in response to a multitude of DDR-activating treatments.

From our understanding, the expression of NKG2DLs on the surface of the cell membrane is induced by the DDR pathway as an additional mechanism to ensure the damaged cell is eliminated, despite apoptosis and other ‘kill me’ mechanisms also being induced. Therefore, it makes logical sense that the increase in surface NKG2DLs would be reserved for later stages of the apoptosis pathway. Likely, in normal cells with functional DNA damage machinery, the cells will not initially upregulate their surface expression but instead halt the cell cycle and upregulate DNA repair pathways. This needs to be confirmed experimentally, as does the expansion of the ‘normal’ cell lines tested. The use of ex vivo normal tissue would improve this research further. Additionally, studies of longer duration need to be carried out since apoptosis from DNA damage typically takes much longer than the timeframes used in this thesis.

In the later part of Chapter 4, we briefly evaluated the arming of the oncolytic virus (OV), EnAd, with the NKG2D BiTE and TriTE, and observed T cell-mediated killing of target cells following viral infection when expression was under the constitutively active promoter CMV or the adenoviral major late promoter (MLP) using the splice acceptor (SA). Future work combining this virus with radiation will hopefully potentiate this activity, as seen with the oHSV-NKG2D TriTE virus in the treatment of GBM (Baugh et al., 2024; Pokrovska et al., 2020).

One major limitation of the NKG2D TriTE is its low protein yield. Whether produced via transient transfection or expressed from adenovirus, the NKG2D TriTE is produced at much lower protein yields than the control constructs and the NKG2D BiTE. While we still observed target killing from the NKG2D-armed EnAd viruses, the levels of T cell activation were quite low compared to that seen in free BiTE experiments, as well as that seen from other EnAd viruses expressing BiTEs (Freedman et al., 2017, 2018; Scott et al., 2019). This, combined with the subdued potency seen from other BiTEs

developed in our laboratory, led us to investigate and develop the strategies presented in the second half of this thesis.

In the latter part of this thesis, we focused on strategies to improve the targeting of NKG2DLs. We did this in two main ways: first, by investigating the potential benefit of incorporating the accessory protein CD2, and second, by inhibiting NKG2DL shedding to both prevent the inhibitory effects of soluble NKG2DLs (sNKG2DLs) and stabilize/increase the surface expression of the ligands on the cell surface, thereby making them available for use by the NKG2D BiTE and TriTE.

The CD2-CD58 interaction is well known for its role in aiding adhesion between T cells and antigen-presenting cells (APCs), which has been shown to increase the sensitivity of TCRs in detecting antigen (Binder et al., 2020; Burton et al., 2023). We have shown that, similarly to CAR-T cells and other BiTE molecules, the sensitivity of the NKG2D BiTE is enhanced via the CD2-CD58 interaction (Burton et al., 2023; Patel et al., 2024). Following this, we sought to investigate the role of CD2 as a co-stimulatory molecule in BiTE-mediated T cell activation. In this work, we saw that the clustering of CD2 next to CD3 in the immune synapse did indeed stimulate T cell activation. This activation was dependent on the distance between the aCD2 and aCD3 single-chain variable fragments (ScFvs). While we have demonstrated that CD2-CD3 clustering is sufficient for T cell activation, more work needs to be done to further investigate this and to compare it with the clustering of other co-stimulatory molecules.

Finally, we evaluated the potency of the NKG2D BiTE and TriTE against an aMICAB BiTE, which, while only binding 2/8 NKG2DLs, would likely bind with higher affinity. It has been shown in HER2-targeting bispecific antibodies that increased affinity improves T cell activation (Poussin et al., 2021). The aMICAB BiTE and NKG2D BiTE both bind to the target cell using a single moiety. When targeting the CHO-MICA cell line, the aMICAB BiTE was superior to the NKG2D BiTE in T cell-mediated cytotoxicity, demonstrating that increased affinity to the antigen is beneficial. However, the NKG2D TriTE, which contains an extra NKG2D ectodomain, performed similarly to the aMICAB BiTE. When the aMICAB BiTE was tested on the colorectal cell line DLD-1, we saw minimal activation of T cells and no

difference in target cell viability, while both the NKG2D BiTE and TriTE showed significant changes. Goulding et al. found that when presenting the same ScFv as the targeting domain of a CAR-T, the CAR-T was superior to an NKG2D-CAR-T at targeting multiple cancer cell lines, both of haematological and solid tumour origin (Goulding et al., 2023).

In conclusion, we have shown that the NKG2D TriTE, containing two copies of the NKG2D ectodomain, is the superior therapeutic agent evaluated in this thesis. While its efficacy needs to be further evaluated using patient-derived samples, the initial evaluation of this therapeutic is extremely promising. Additionally, we investigated the use of a higher-affinity antibody binding to a subset of NKG2DLs and found that the benefit of high-affinity binding to the target cell via fewer ligands is outweighed by the ability to bind to multiple ligands present on the target cell, at least in the case of NKG2DLs.

References

Abdul Razak, F. R., Diepstra, A., Visser, L., & Van Den Berg, A. (2016). CD58 mutations are common in Hodgkin lymphoma cell lines and loss of CD58 expression in tumor cells occurs in Hodgkin lymphoma patients who relapse. *Genes and Immunity*, *17*(6), 363–366. https://doi.org/10.1038/gene.2016.30

Anand, U., Dey, A., Chandel, A. K. S., Sanyal, R., Mishra, A., Pandey, D. K., De Falco, V., Upadhyay, A., Kandimalla, R., Chaudhary, A., Dhanjal, J. K., Dewanjee, S., Vallamkondu, J., & Pérez de la Lastra, J. M. (2023). Cancer chemotherapy and beyond: Current status, drug candidates, associated risks and progress in targeted therapeutics. *Genes & Diseases*, *10*(4), 1367–1401. https://doi.org/10.1016/J.GENDIS.2022.02.007

Andrews, K., Hamers, A. A. J., Sun, X., Neale, G., Verbist, K., Tedrick, P., Nichols, K. E., Pereira, S., Geraghty, D. E., & Pillai, A. B. (2020). Expansion and CD2/CD3/CD28 stimulation enhance Th2 cytokine secretion of human invariant NKT cells with retained anti-tumor cytotoxicity. *Cytotherapy*, *22*(5), 276–290. https://doi.org/10.1016/J.JCYT.2020.01.011

Andtbacka, R. H. I., Collichio, F., Harrington, K. J., Middleton, M. R., Downey, G., Öhrling, K., & Kaufman, H. L. (2019). Final analyses of OPTiM: a randomized phase III trial of talimogene laherparepvec versus granulocyte-macrophage colony-stimulating factor in unresectable stage III-IV melanoma. *Journal for Immunotherapy of Cancer*, *7*(1). https://doi.org/10.1186/S40425-019-0623-Z

Andtbacka, R. H. I., Kaufman, H. L., Collichio, F., Amatruda, T., Senzer, N., Chesney, J., Delman, K. A., Spitler, L. E., Puzanov, I., Agarwala, S. S., Milhem, M., Cranmer, L., Curti, B., Lewis, K., Ross, M., Guthrie, T., Linette, G. P., Daniels, G. A., Harrington, K., … Coffin, R. S. (2015). Talimogene laherparepvec improves durable response rate in patients with advanced melanoma. *Journal of Clinical Oncology*, *33*(25), 2780–2788.

https://doi.org/10.1200/JCO.2014.58.3377/ASSET/E3E1859A-1792-472F-94CB-BE02B66725F6/ASSETS/IMAGES/ZLJ9991052860005.JPEG

Asada, T. (1974). Treatment of human cancer with mumps virus. *Cancer*, 1907–1928.

Ashiru, O., López-Cobo, S., Fernández-Messina, L., Pontes-Quero, S., Pandolfi, R., Reyburn, H. T., & Valés-Gómez, M. (2013). A GPI anchor explains the unique biological features of the common NKG2D-ligand allele MICA*008. *The Biochemical Journal*, *454*(2), 295–302. https://doi.org/10.1042/BJ20130194

Asif, M., Siddiqui, A., & Perry, C. M. (2006). Human Papillomavirus Quadrivalent (types 6, 11, 16, 18) Recombinant Vaccine (Gardasil ®). In *Drugs* (Vol. 66, Issue 9).

Atkins, M. B., Lotze, M. T., Dutcher, J. P., Fisher, R. I., Weiss, G., Margolin, K., Abrams, J., Sznol, M., Parkinson, D., Hawkins, M., Paradise, C., Kunkel, L., & Rosenberg, S. A. (1999). High-Dose Recombinant Interleukin 2 Therapy for Patients With Metastatic Melanoma: Analysis of 270 Patients Treated Between 1985 and 1993. *Journal of Clinical Oncology*, *17*(7), 2105–2116. https://doi.org/10.1200/JCO.1999.17.7.2105

Atun, R., Jaffray, D. A., Barton, M. B., Bray, F., Baumann, M., Vikram, B., Hanna, T. P., Knaul, F. M., Lievens, Y., Lui, T. Y. M., Milosevic, M., O'Sullivan, B., Rodin, D. L., Rosenblatt, E., Van Dyk, J., Yap, M. L., Zubizarreta, E., & Gospodarowicz, M. (2015). Expanding global access to radiotherapy. *The Lancet Oncology*, *16*(10), 1153–1186. https://doi.org/10.1016/S1470-2045(15)00222-3

Ayantunde, A. A., & Parsons, S. L. (2007). Pattern and prognostic factors in patients with malignant ascites: A retrospective study. *Annals of Oncology*, *18*(5), 945–949. https://doi.org/10.1093/annonc/mdl499

Bachmann, M. F., Barner, M., & Kopf, M. (1999). Cd2 Sets Quantitative Thresholds in T Cell Activation. *JExpMed*, *190*(10), 1383–1392.

Barber, A., Zhang, T., Megli, C. J., Wu, J., Meehan, K. R., & Sentman, C. L. (2008). Chimeric NKG2D receptor-expressing T cells as an immunotherapy for multiple myeloma. *Exp Hematol*, *36*(10), 1318–1328. https://doi.org/10.1016/j.exphem.2008.04.010

Barnett, G. C., West, C. M. L., Dunning, A. M., Elliott, R. M., Coles, C. E., Pharoah, P. D. P., & Burnet, N. G. (2009). Normal tissue reactions to radiotherapy: towards tailoring treatment dose by genotype. *Nature Reviews Cancer 2009 9:2*, *9*(2), 134–142. https://doi.org/10.1038/nrc2587

Barton, M. B., Jacob, S., Shafiq, J., Wong, K., Thompson, S. R., Hanna, T. P., & Delaney, G. P. (2014). Estimating the demand for radiotherapy from the evidence: A review of changes from 2003 to 2012. *Radiotherapy and Oncology*, *112*(1), 140–144. https://doi.org/10.1016/j.radonc.2014.03.024

Bauer, S., Groh, V., Wu, J., Steinle, A., Phillips, J. H., Lanier, L. L., & Spies, T. (1999). Activation of NK cells and T cells by NKG2D, a receptor for stress-inducible MICA. *Science (New York, N.Y.)*, *285*(5428), 727–729. https://doi.org/10.1126/SCIENCE.285.5428.727

Baugh, R., Khalique, H., Page, E., Lei-Rossmann, J., Kok-Ting Wan, P., Johanssen, T., Ebner, D., Ansorge, O., & Seymour, L. W. (2024). Targeting NKG2D ligands in glioblastoma with a bispecific T-cell engager is augmented with conventional therapy and enhances oncolytic virotherapy of glioma stem-like cells. *J Immunother Cancer*, *12*, 8460. https://doi.org/10.1136/jitc-2023-008460

Baugh, R., Khalique, H., & Seymour, L. W. (2020). Convergent Evolution by Cancer and Viruses in Evading the NKG2D Immune Response. *Cancers 2020, Vol. 12, Page 3827*, *12*(12), 3827. https://doi.org/10.3390/CANCERS12123827

Ben-Shmuel, A., Gruper, Y., Levi-Galibov, O., Rosenberg-Fogler, H., Carradori, G., Stein, Y., Dadiani, M., Naumova, M., Nevo, R., Morzaev-Sulzbach, D., Yagel, G., Mayer, S., Nili Gal-Yam, E., & Scherz-Shouval, R. (2023). Cancer-associated fibroblasts serve as decoys to suppress NK cell anti-cancer cytotoxicity. *BioRxix*. https://doi.org/10.1101/2023.11.23.568355

Black, R. A., Rauch, C. T., Kozlosky, C. J., Peschon, J. J., Slack, J. L., Wolfson, M. F., Castner, B. J., Stocking, K. L., Reddy, P., Srinivasan, S., Nelson, N., Boiani, N., Schooley, K. A., Gerhart, M., Davis, R., Fitzner, J. N., Johnson, R. S., Paxton, R. J., March, C. J., & Cerretti, D. P. (1997). A metalloproteinase disintegrin that releases tumour-necrosis factor-α from cells. *Nature 1997 385:6618*, *385*(6618), 729–733. https://doi.org/10.1038/385729a0

Bolden, J. E., Peart, M. J., & Johnstone, R. W. (2006). Anticancer activities of histone deacetylase inhibitors. *Nature Reviews Drug Discovery 2006 5:9*, *5*(9), 769–784. https://doi.org/10.1038/nrd2133

Bose, P., Dai, Y., & Grant, S. (2014). Histone deacetylase inhibitor (HDACI) mechanisms of action: emerging insights. *Pharmacology & Therapeutics*, *143*(3), 323. https://doi.org/10.1016/J.PHARMTHERA.2014.04.004

Boussiotis, V. A., Freeman, G. J., Griffin, J. D., Gray, G. S., Gribben, J. G., & Nadler, L. M. (1994). CD2 is involved in maintenance and reversal of human alloantigen-specific clonal anergy. *Journal of Experimental Medicine*, *180*(5), 1665–1673.

Bove, C., Arcangeli, S., Falcone, L., Camisa, B., El Khoury, R., Greco, B., De Lucia, A., Bergamini, A., Bondanza, A., Ciceri, F., Bonini, C., & Casucci, M. (2023). CD4 CAR-T cells targeting CD19 play a key role in exacerbating cytokine release syndrome, while maintaining long-term responses. *Journal for ImmunoTherapy of Cancer*, *11*(1), e005878. https://doi.org/10.1136/JITC-2022-005878

Brischwein, K., Schlereth, B., Guller, B., Steiger, C., Wolf, A., Lutterbuese, R., Offner, S., Locher, M., Urbig, T., Raum, T., Kleindienst, P., Wimberger, P., Kimmig, R., Fichtner, I., Kufer, P., Hofmeister, R., Da Silva, A. J., & Baeuerle, P. A. (2006). MT110: A novel bispecific single-chain antibody construct with high efficacy in eradicating established tumors. *Molecular Immunology*, *43*(8), 1129–1143. https://doi.org/10.1016/J.MOLIMM.2005.07.034

Brocker, T., & Karjalainen, K. (1995). Signals through T cell receptor-zeta chain alone are insufficient to prime resting T lymphocytes. *Journal of Experimental Medicine*, *181*(5), 1653–1659. https://doi.org/10.1084/JEM.181.5.1653

Brown, M. H., Cantrell, D. A., Brattsand, G., Crumpton, M. J., & Gullberg, M. (1989). The CD2 antigen associates with the T-cell antigen receptor CD3 antigen complex on the surface of human T lymphocytes. *Nature*, *399*.

Brudno, J. N., & Kochenderfer, J. N. (2016). Toxicities of chimeric antigen receptor T cells: recognition and management. *Blood*, *127*(26), 3321–3330. https://doi.org/10.1182/BLOOD-2016-04-703751

Burton, J., Siller-Farfán, J. A., Pettmann, J., Salzer, B., Kutuzov, M., van der Merwe, P. A., & Dushek, O. (2023). Inefficient exploitation of accessory receptors reduces the sensitivity of chimeric antigen receptors. *Proceedings of the National Academy of Sciences of the United States of America*, *120*(2), e2216352120. https://doi.org/10.1073/PNAS.2216352120/SUPPL_FILE/PNAS.2216352120.SAPP.PDF

Cameron, B. J., Gerry, A. B., Dukes, J., Harper, J. V, Kannan, V., Bianchi, F. C., Grand, F., Brewer, J. E., Gupta, M., Plesa, G., Bossi, G., Vuidepot, A., Powlesland, A. S., Legg, A., Adams, K. J., Bennett, A. D., Pumphrey, N. J., Williams, D. D., Binder-Scholl, G., … Jakobsen, B. K. (2013). Identification of a Titin-Derived HLA-A1-Presented Peptide as a Cross-Reactive Target for Engineered MAGE A3-Directed T Cells. *Science Translational Medicine*. https://www.science.org

Cao, W., Xi, X., Hao, Z., Li, W., Kong, Y., Cui, L., Ma, C., Ba, D., & He, W. (2007). RAET1E2, a soluble isoform of the UL16-binding protein RAET1E produced by tumor cells, inhibits NKG2D-mediated NK cytotoxicity. *The Journal of Biological Chemistry*, *282*(26), 18922–18928. https://doi.org/10.1074/JBC.M702504200

Cerwenka, A., Bakker, A. B. H., McClanahan, T., Wagner, J., Wu, J., Phillips, J. H., & Lanier, L. L. (2000). Retinoic acid early inducible genes define a ligand family for the activating NKG2D receptor in mice. *Immunity*, *12*(6), 721–727. https://doi.org/10.1016/S1074-7613(00)80222-8

Cha, J. H., Chan, L. C., Li, C. W., Hsu, J. L., & Hung, M. C. (2019). Mechanisms Controlling PD-L1 Expression in Cancer. In *Molecular Cell* (Vol. 76, Issue 3, pp. 359–370). Cell Press. https://doi.org/10.1016/j.molcel.2019.09.030

Cheever, M. A., & Higano, C. S. (2011). PROVENGE (sipuleucel-T) in prostate cancer: The first FDA-approved therapeutic cancer vaccine. *Clinical Cancer Research*, *17*(11), 3520–3526. https://doi.org/10.1158/1078-0432.CCR-10-3126/84206/AM/PROVENGE-SIPULEUCEL-T-IN-PROSTATE-CANCER-THE-FIRST

Chen, D. S., & Mellman, I. (2013). Oncology meets immunology: The cancer-immunity cycle. In *Immunity* (Vol. 39, Issue 1, pp. 1–10). https://doi.org/10.1016/j.immuni.2013.07.012

Chen, L., & Flies, D. B. (2013). Molecular mechanisms of T cell co-stimulation and co-inhibition. *Nature Reviews Immunology 2013 13:4*, *13*(4), 227–242. https://doi.org/10.1038/nri3405

Chen, X., Zhang, T., Su, W., Dou, Z., Zhao, D., Jin, X., Lei, H., Wang, J., Xie, X., Cheng, B., Li, Q., Zhang, H., & Di, C. (2022). Mutant p53 in cancer: from molecular mechanism to therapeutic modulation. *Cell Death & Disease 2022 13:11*, *13*(11), 1–14. https://doi.org/10.1038/s41419-022-05408-1

Chmielewski, M., & Abken, H. (2015). TRUCKs: the fourth generation of CARs. *Expert Opinion on Biological Therapy*, *15*(8), 1145–1154. https://doi.org/10.1517/14712598.2015.1046430

Cho, H. Y., Son, W. C., Lee, Y. S., Youn, E. J., Kang, C. D., Park, Y. S., & Bae, J. H. (2021). Differential effects of histone deacetylases on the expression of nkg2d ligands and nk cell-mediated anticancer immunity in lung cancer cells. *Molecules*, *26*(13). https://doi.org/10.3390/molecules26133952

Cinier, J., Hubert, M., Besson, L., Di Roio, A., Rodriguez, C., Lombardi, V., Caux, C., & Ménétrier-Caux, C. (2021). Recruitment and expansion of tregs cells in the tumor environment—how to target them? *Cancers*, *13*(8). https://doi.org/10.3390/cancers13081850

Cohen MH, Williams G, Johnson JR, Duan J, Gobburu J, Rahman A, Benson K, Leighton J, Kim SK, Wood R, Rothmann M, Chen G, U KM, Staten AM, & Pazdur R. (2002). Approval Summary for Imatinib Mesylate Capsules in the Treatment of Chronic Myelogenous Leukemia. *Clin Cancer Res*, *8*, 935–942. https://aacrjournals.org/clincancerres/article/8/5/935/199826/Approval-Summary-for-Imatinib-Mesylate-Capsules-in

Coley, W. B. (1909). The Treatment of Inoperable Sarcoma by Bacterial Toxins (the Mixed Toxins of the Streptococcus erysipelas and the Bacillus prodigiosus). In *Mr. J. WARRINGTON HAWARD*.

Connelly, R. J., Hayden, M. S., Scholler, J. K., Tsu, T. T., Dupont, B., Ledbetter, J. A., & Kanner, S. B. (1998). Mitogenic properties of a bispecific single-chain Fv-Ig fusion generated from CD2-specific mAb to distinct epitopes. *International Immunology*, *10*(12), 1863–1872. https://doi.org/10.1093/INTIMM/10.12.1863

Correnti, C. E., Laszlo, G. S., De Van Der Schueren, W. J., Godwin, C. D., Bandaranayake, A., Busch, M. A., Gudgeon, C. J., Bates, O. M., Olson, J. M., Mehlin, C., & Walter, R. B. (2018). Simultaneous multiple interaction T-cell engaging (SMITE) bispecific antibodies overcome bispecific T-cell engager (BiTE) resistance via CD28 co-stimulation. *Leukemia*, *32*(5), 1239–1243. https://doi.org/10.1038/s41375-018-0014-3

Cosman, D., Müllberg, J., Sutherland, C. L., Chin, W., Armitage, R., Fanslow, W., Kubin, M., & Chalupny, N. J. (2001). ULBPs, novel MHC class I-related molecules, bind to CMV glycoprotein UL16 and stimulate NK cytotoxicity through the NKG2D receptor. *Immunity*, *14*(2), 123–133. https://doi.org/10.1016/S1074-7613(01)00095-4

Curio, S., Jonsson, G., & Marinović, S. (2021). A summary of current NKG2D-based CAR clinical trials. In *Immunotherapy Advances* (Vol. 1, Issue 1). Oxford University Press. https://doi.org/10.1093/immadv/ltab018

Curtsinger, J. M., & Mescher, M. F. (2010). Inflammatory Cytokines as a Third Signal for T Cell Activation. *Current Opinion in Immunology*, *22*(3), 333. https://doi.org/10.1016/J.COI.2010.02.013

D'Angelo, S. P., Araujo, D. M., Abdul Razak, A. R., Agulnik, M., Attia, S., Blay, J. Y., Carrasco Garcia, I., Charlson, J. A., Choy, E., Demetri, G. D., Druta, M., Forcade, E., Ganjoo, K. N., Glod, J., Keedy, V. L., Le Cesne, A., Liebner, D. A., Moreno, V., Pollack, S. M., … Van Tine, B. A. (2024). Afamitresgene autoleucel for advanced synovial sarcoma and myxoid round cell liposarcoma (SPEARHEAD-1): an international, open-label, phase 2 trial. *The Lancet*, *403*(10435), 1460–1471. https://doi.org/10.1016/S0140-6736(24)00319-2

Davis, S. J., & van der Merwe, P. A. (2006). The kinetic-segregation model: TCR triggering and beyond. In *Nature Immunology* (Vol. 7, Issue 8, pp. 803–809). https://doi.org/10.1038/ni1369

Deeks, E. D. (2014). Nivolumab: A review of its use in patients with malignant melanoma. *Drugs*, *74*(11), 1233–1239. https://doi.org/10.1007/S40265-014-0234-4/FIGURES/2

Deininger, M. W. N., Goldman, J. M., Lydon, N., & Melo, J. V. (1997). The Tyrosine Kinase Inhibitor CGP57148B Selectively Inhibits the Growth of BCR-ABL–Positive Cells. *Blood*, *90*(9), 3691–3698. https://doi.org/10.1182/BLOOD.V90.9.3691

Demetriou, P., Abu-Shah, E., Valvo, S., McCuaig, S., Mayya, V., Kvalvaag, A., Starkey, T., Korobchevskaya, K., Lee, L. Y. W., Friedrich, M., Mann, E., Kutuzov, M. A., Morotti, M., Wietek, N., Rada, H., Yusuf, S., Afrose, J., Siokis, A., Allan, P., … Dustin, M. L. (2020). A dynamic CD2-rich compartment at the outer edge of the immunological synapse boosts and integrates signals.

Nature Immunology 2020 21:10, *21*(10), 1232–1243. https://doi.org/10.1038/s41590-020-0770-x

Desai, R., & Neuberger, J. (2014). Donor transmitted and de novo cancer after liver transplantation. *World Journal of Gastroenterology*, *20*(20), 6170–6179. https://doi.org/10.3748/wjg.v20.i20.6170

Di, Y., Seymour, L., & Fisher, K. (2014). Activity of a group B oncolytic adenovirus (ColoAd1) in whole human blood. *Gene Therapy 2014 21:4*, *21*(4), 440–443. https://doi.org/10.1038/gt.2014.2

Diefenbach, A., Jamieson, A. M., Liu, S. D., Shastri, N., & Raulet, D. H. (2000). Ligands for the murine NKG2D receptor: expression by tumor cells and activation of NK cells and macrophages. *Nature Immunology*, *1*(2), 119–126. https://doi.org/10.1038/77793

Ding, X., Yang, L. Y., Huang, G. W., Wang, W., & Lu, W. Q. (2004). ADAM17 mRNA expression and pathological features of hepatocellular carcinoma. *World Journal of Gastroenterology*, *10*(18), 2735–2739. https://doi.org/10.3748/wjg.v10.i18.2735

Doubrovina, E. S., Doubrovin, M. M., Vider, E., Sisson, R. B., O'Reilly, R. J., Dupont, B., & Vyas, Y. M. (2003). Evasion from NK cell immunity by MHC class I chain-related molecules expressing colon adenocarcinoma. *Journal of Immunology (Baltimore, Md. : 1950)*, *171*(12), 6891–6899. https://doi.org/10.4049/JIMMUNOL.171.12.6891

Dreier, T., Lorenczewski, G., Brandl, C., Hoffmann, P., Syring, U., Hanakam, F., Kufer, P., Riethmuller, G., Bargou, R., & Baeuerle, P. A. (2002). Extremely potent, rapid and costimulation-independent cytotoxic T-cell response against lymphoma cells catalyzed by a single-chain bispecific antibody. *International Journal of Cancer*, *100*(6), 690–697. https://doi.org/10.1002/IJC.10557

Dunn, G. P., Bruce, A. T., Ikeda, H., Old, L. J., & Schreiber, R. D. (2002). *Cancer immunoediting: from immuno-surveillance to tumor escape*. http://www.nature.com/natureimmunology

Dustin, M., Olszowy, M., Holdorf, A., Li, J., Bromley, S., Desai, N., Widder, P., Rosenberger, F., van der Merwe, A., Allen, P., & Shaw, A. (1998). A Novel Adaptor Protein Orchestrates Receptor Patterning and Cytoskeletal Polarity in T-Cell Contacts. *Cell*, *94*, 667–677.

Eagle, R. A., Traherne, J. A., Ashiru, O., Wills, M. R., & Trowsdale, J. (2006). Regulation of NKG2D Ligand Gene Expression. *Human Immunology*, *67*(3), 159–169. https://doi.org/10.1016/j.humimm.2006.02.015

El-Sherbiny, Y. M., Meade, J. L., Holmes, T. D., McGonagle, D., Mackie, S. L., Morgan, A. W., Cook, G., Feyler, S., Richards, S. J., Davies, F. E., Morgan, G. J., & Cook, G. P. (2007). The requirement for DNAM-1, NKG2D, and NKp46 in the natural killer cell-mediated killing of myeloma cells. *Cancer Research*, *67*(18), 8444–8449. https://doi.org/10.1158/0008-5472.CAN-06-4230

Falcaro, M., Soldan, K., Ndlela, B., & Sasieni, P. (2024). Effect of the HPV vaccination programme on incidence of cervical cancer and grade 3 cervical intraepithelial neoplasia by socioeconomic deprivation in England: population based observational study. *BMJ*. https://doi.org/10.1136/bmj-2023-077341

Fernández-Messina, L., Ashiru, O., Agüera-González, S., Reyburn, H. T., & Valés-Gómez, M. (2011). The human NKG2D ligand ULBP2 can be expressed at the cell surface with or without a GPI anchor and both forms can activate NK cells. *Journal of Cell Science*, *124*(3), 321–327. https://doi.org/10.1242/jcs.076042

Ferrari De Andrade, L., Kumar, S., Luoma, A. M., Ito, Y., Alves Da Silva, P. H., Pan, D., Pyrdol, J. W., Yoon, C. H., & Wucherpfennig, K. W. (2020). Inhibition of MICA and MICB Shedding Elicits NK-Cell-Mediated Immunity against Tumors Resistant to Cytotoxic T Cells. *Cancer Immunol Res*. https://doi.org/10.1158/2326-6066.CIR-19-0483

Ferrari De Andrade, L., Tay, R. E., Pan, D., Luoma, A. M., Ito, Y., Badrinath, S., Tsoucas, D., Franz, B., May, K. F., Harvey, C. J., Kobold, S., Pyrdol, J. W., Yoon, C., Yuan, G.-C., Hodi, F. S., Dranoff, G., &

Wucherpfennig, K. W. (2018). Antibody-mediated inhibition of MICA and MICB shedding promotes NK cell-driven tumor immunity. *Science*.

Freedman, J. D., Duffy, M. R., Lei-Rossmann, J., Muntzer, A., Scott, E. M., Hagel, J., Campo, L., Bryant, R. J., Verrill, C., Lambert, A., Miller, P., Champion, B. R., Seymour, L. W., & Fisher, K. D. (2018). An Oncolytic Virus Expressing a T-cell Engager Simultaneously Targets Cancer and Immunosuppressive Stromal Cells. *Cancer Res*, *24*(78). https://doi.org/10.1158/0008-5472.CAN-18-1750

Freedman, J. D., Hagel, J., Scott, E. M., Psallidas, I., Gupta, A., Spiers, L., Miller, P., Kanellakis, N., Ashfield, R., Fisher, K. D., Duffy, M. R., & Seymour, L. W. (2017). Oncolytic adenovirus expressing bispecific antibody targets T-cell cytotoxicity in cancer biopsies. *EMBO Molecular Medicine*, *9*(8), 1067–1087. https://doi.org/10.15252/emmm.201707567

Friedman, S., Levy, R., Garrett, W., Doval, D., Bondarde, S., Sahoo, T., Lokanatha, D., Julka, P., Shenoy, K., Nagarkar, R., Bhattacharyya, G., Kumar, K., Nag, S., Mohan, P., Narang, N., Raghunadharao, D., Walia, M., Yao, W., Li, J., … Newton, R. (2009). Clinical Benefit of INCB7839, a Potent and Selective Inhibitor of ADAM10 and ADAM17, in Combination with Trastuzumab in Metastatic HER2 Positive Breast Cancer Patients. *Cancer Research*, *69*(24_Supplement), 5056–5056. https://doi.org/10.1158/0008-5472.SABCS-09-5056

Friese, M. A., Wischhusen, J., Wick, W., Weiler, M., Nter Eisele, G., Steinle, A., & Weller, M. (2004). RNA Interference Targeting Transforming Growth Factor-Enhances NKG2D-Mediated Antiglioma Immune Response, Inhibits Glioma Cell Migration and Invasiveness, and Abrogates Tumorigenicity In vivo. In *CANCER RESEARCH* (Vol. 64). http://aacrjournals.org/cancerres/article-pdf/64/20/7596/2520110/zch02004007596.pdf?casa_token=Xw7gYcbcURMAAAAA:gANfTmEJwLTcEw19I0Zime1h9OOlu2486i5FSuKJLWYQs7Ls0qSTetw_BNLnGi_imypn4g

Fuertes, M. B., Girart, M. V, Molinero, L. L., Domaica, Ca. I., Rossi, L. E., Barrio, M. M., Mordoh Jose, Rabinovich, G. A., & Zwirner, N. W. (2008). Epithelial-Mesenchymal Transition Induces an Antitumor Immune Response Mediated by NKG2D Receptor Induction of Innate Immune Visibility of Neuroendocrine Tumors Potentiates Immune Responses and Tumor Rejection. *The Journal of Immunology*. https://doi.org/10.4049/jimmunol.180.7.4606

Fuertes, M., Girart, M. V., Molinero, L. L., Domaica, C. I., Rossi, L. E., Barrio, M. M., Mordoh, J., Rabinovich, G. A., & Zwirner, N. W. (2008). Intracellular Retention of the NKG2D Ligand MHC Class I Chain-Related Gene A in Human Melanomas Confers Immune Privilege and Prevents NK Cell-Mediated Cytotoxicity. *The Journal of Immunology*, *180*(7), 4606–4614. https://doi.org/10.4049/jimmunol.180.7.4606

Garcia-Carbonero, R., Salazar, R., Duran, I., Osman-Garcia, I., Paz-Ares, L., Bozada, J. M., Boni, V., Blanc, C., Seymour, L., Beadle, J., Alvis, S., Champion, B., Calvo, E., & Fisher, K. (2017a). Phase 1 study of intravenous administration of the chimeric adenovirus enadenotucirev in patients undergoing primary tumor resection. *Journal for ImmunoTherapy of Cancer*, *5*(1), 71. https://doi.org/10.1186/S40425-017-0277-7

Garcia-Carbonero, R., Salazar, R., Duran, I., Osman-Garcia, I., Paz-Ares, L., Bozada, J. M., Boni, V., Blanc, C., Seymour, L., Beadle, J., Alvis, S., Champion, B., Calvo, E., & Fisher, K. (2017b). Phase 1 study of intravenous administration of the chimeric adenovirus enadenotucirev in patients undergoing primary tumor resection. *Journal for Immunotherapy of Cancer*, *5*(1). https://doi.org/10.1186/S40425-017-0277-7

Garrity, D., Call, M. E., Feng, J., & Wucherpfennig, K. W. (2005). The activating NKG2D receptor assembles in the membrane with two signaling dimers into a hexameric structure. *Proceedings of the National Academy of Sciences of the United States of America*, *102*(21), 7641. https://doi.org/10.1073/PNAS.0502439102

Gasser, S., Orsulic, S., Brown, E. J., & Raulet, D. H. (2005). The DNA damage pathway regulates innate immune system ligands for the NKG2D receptor. *Nature*, *436*(7054), 1186. https://doi.org/10.1038/NATURE03884

Ghadially, H., Brown, L., Lloyd, C., Lewis, L., Lewis, A., Dillon, J., Sainson, R., Jovanovic, J., Tigue, N. J., Bannister, D., Bamber, L., Valge-Archer, V., & Wilkinson, R. W. (2017). MHC class i chain-related protein A and B (MICA and MICB) are predominantly expressed intracellularly in tumour and normal tissue. *British Journal of Cancer*, *116*(9), 1208–1217. https://doi.org/10.1038/bjc.2017.79

Godbersen, C., Coupet, T. A., Huehls, A. M., Zhang, T., Battles, M. B., Fisher, J. L., Ernstoff, M. S., & Sentman, C. L. (2017). NKG2D ligand targeted Bispecific T Cell Engagers lead to robust antitumor activity against diverse human tumors. *Molecular Cancer Therapeutics*, *16*(7), 1335. https://doi.org/10.1158/1535-7163.MCT-16-0846

Goebeler, M. E., Knop, S., Viardot, A., Kufer, P., Topp, M. S., Einsele, H., Noppeney, R., Hess, G., Kallert, S., Mackensen, A., Rupertus, K., Kanz, L., Libicher, M., Nagorsen, D., Zugmaier, G., Klinger, M., Wolf, A., Dorsch, B., Quednau, B. D., … Bargou, R. C. (2016). Bispecific T-cell engager (BiTE) antibody construct Blinatumomab for the treatment of Patients with relapsed/refractory non-Hodgkin lymphoma: Final results from a phase I study. *Journal of Clinical Oncology*, *34*(10), 1104–1111. https://doi.org/10.1200/JCO.2014.59.1586/ASSET/41E54CFC-0A3E-4144-B056-68D75BFB28E2/ASSETS/GRAPHIC/JCO591586TA3.JPEG

Gollob, J. A., Li, ling, Kawasaki, H., Daley, J. F., Groves, C., & Ritz, J. (1996). *Molecular Interaction Between CD58 and CD2 Counter-Receptors Mediates the Ability of Monocytes to Augment T Cell Activation by IL-12'*. http://journals.aai.org/jimmunol/article-pdf/157/5/1886/1073540/1886.pdf?casa_token=N6UpQQ3QUHcAAAAA:_HDdaUhQOIyxOqJ_HVCl77didSENdbLUhZFRH2OVUxPjxblNRg3fOuMiz1CDaoCWwP1Rmw

Gong, Y., Yang, J., Wang, Y., Xue, L., & Wang, J. (2020). Metabolic factors contribute to T-cell inhibition in the ovarian cancer ascites. In *International Journal of Cancer* (Vol. 147, Issue 7, pp. 1768–1777). Wiley-Liss Inc. https://doi.org/10.1002/ijc.32990

Goulding, J., Yeh, W. I., Hancock, B., Blum, R., Xu, T., Yang, B. H., Chang, C. W., Groff, B., Avramis, E., Pribadi, M., Pan, Y., Chu, H. Y., Sikaroodi, S., Fong, L., Brookhouser, N., Dailey, T., Meza, M., Denholtz, M., Diaz, E., … Valamehr, B. (2023). A chimeric antigen receptor uniquely recognizing MICA/B stress proteins provides an effective approach to target solid tumors. *Med*, *4*(7), 457-477.e8. https://doi.org/10.1016/j.medj.2023.04.004

Gowen, B. G., Chim, B., Marceau, C. D., Greene, T. T., Burr, P., Gonzalez, J. R., Hesser, C. R., Dietzen, P. A., Russell, T., Iannello, A., Coscoy, L., Sentman, C. L., Carette, J. E., Muljo, S. A., & Raulet, D. H. (2015). A forward genetic screen reveals novel independent regulators of ULBP1, an activating ligand for natural killer cells. *ELife*. https://doi.org/10.7554/eLife.08474.001

Grimmett, E., Al-Share, B., Alkassab, M. B., Zhou, R. W., Desai, A., Rahim, M. M. A., & Woldie, I. (2022). Cancer vaccines: past, present and future; a review article. In *Discover Oncology* (Vol. 13, Issue 1). Springer Science and Business Media B.V. https://doi.org/10.1007/s12672-022-00491-4

Groh, V., Rhinehart, R., Randolph-Habecker, J., Topp, M. S., Riddell, S. R., & Spies, T. (2001). Costimulation of CD8alphabeta T cells by NKG2D via engagement by MIC induced on virus-infected cells. *Nature Immunology*, *2*(3), 255–260. https://doi.org/10.1038/85321

Groh, V., Wu, J., Yee, C., & Spies, T. (2002). Tumour-derived soluble MIC ligands impair expression of NKG2D and T-cell activation. *Nature*, *419*(6908), 734–738. https://doi.org/10.1038/NATURE01112

Groth, C., Hu, X., Weber, R., Fleming, V., Altevogt, P., Utikal, J., & Umansky, V. (2019). Immunosuppression mediated by myeloid-derived suppressor cells (MDSCs) during tumour

progression. In *British Journal of Cancer* (Vol. 120, Issue 1, pp. 16–25). Nature Publishing Group. https://doi.org/10.1038/s41416-018-0333-1

Guerra, N., Tan, Y. X., Joncker, N. T., Choy, A., Gallardo, F., Xiong, N., Knoblaugh, S., Cado, D., Greenberg, N. R., & Raulet, D. H. (2008). NKG2D-Deficient Mice Are Defective in Tumor Surveillance in Models of Spontaneous Malignancy. *Immunity*, *28*(4), 571–580. https://doi.org/10.1016/J.IMMUNI.2008.02.016/ATTACHMENT/09FB7151-E593-4CF4-9E32-C625158C57A8/MMC1.PDF

Gugler, R., & von Unruh, G. E. (1980). Clinical Pharmacokinetics of Valproic Acid. *Clinical Pharmacokinetics*, *5*(1), 67–83. https://doi.org/10.2165/00003088-198005010-00002/METRICS

Hagelstein, I., Lutz, M. S., Schmidt, M., Heitmann, J. S., Malenke, E., Zhou, Y., Clar, K. L., Kopp, H. G., Jung, G., Salih, H. R., Märklin, M., & Hinterleitner, C. (2021). Bispecific NKG2D-CD3 and NKG2D-CD16 Fusion Proteins as Novel Treatment Option in Advanced Soft Tissue Sarcomas. *Frontiers in Immunology*, *12*. https://doi.org/10.3389/fimmu.2021.653081

Han, M. Y., & Borazanci, E. H. (2023). *Malignant ascites in pancreatic cancer: Pathophysiology, diagnosis, molecular characterization, and therapeutic strategies*. https://doi.org/10.3389/fonc.2023.1138759

Hanahan, D. (2022). Hallmarks of Cancer: New Dimensions. In *Cancer Discovery* (Vol. 12, Issue 1, pp. 31–46). American Association for Cancer Research Inc. https://doi.org/10.1158/2159-8290.CD-21-1059

Hanahan, D., & Weinberg, R. A. (2000). The Hallmarks of Cancer Review. *Cell*, *100*, 57–70.

Hanahan, D., & Weinberg, R. A. (2011). Hallmarks of cancer: The next generation. In *Cell* (Vol. 144, Issue 5, pp. 646–674). https://doi.org/10.1016/j.cell.2011.02.013

Harrison, S. J., Minnema, M. C., Lee, H. C., Spencer, A., Kapoor, P., Madduri, D., Larsen, J., Ailawadhi, S., Kaufman, J. L., Raab, M. S., Hari, P., Iida, S., Vij, R., Davies, F. E., Lesley, R., Upreti, V. V., Yang,

Z., Sharma, A., Minella, A., & Lentzsch, S. (2020). A Phase 1 First in Human (FIH) Study of AMG 701, an Anti-B-Cell Maturation Antigen (BCMA) Half-Life Extended (HLE) BiTE® (bispecific T-cell engager) Molecule, in Relapsed/Refractory (RR) Multiple Myeloma (MM). *Blood*, *136*(Supplement 1), 28–29. https://doi.org/10.1182/BLOOD-2020-134063

Hashimoto, Y., Tazawa, H., Teraishi, F., Kojima, T., Watanabe, Y., Uno, F., Yano, S., Urata, Y., Kagawa, S., & Fujiwara, T. (2012). The hTERT Promoter Enhances the Antitumor Activity of an Oncolytic Adenovirus under a Hypoxic Microenvironment. *PLOS ONE*, *7*(6), e39292. https://doi.org/10.1371/JOURNAL.PONE.0039292

Hazini, A., Fisher, K., & Seymour, L. (2021). Deregulation of HLA-I in cancer and its central importance for immunotherapy. In *Journal for ImmunoTherapy of Cancer* (Vol. 9, Issue 8). BMJ Publishing Group. https://doi.org/10.1136/jitc-2021-002899

He, X., & Xu, C. (2020). Immune checkpoint signaling and cancer immunotherapy. In *Cell Research* (Vol. 30, Issue 8, pp. 660–669). Springer Nature. https://doi.org/10.1038/s41422-020-0343-4

Hedemann, N., Rogmans, C., Sebens, S., Wesch, D., Reichert, M., Schmidt-Arras, D., Oberg, H. H., Pecks, U., van Mackelenbergh, M., Weimer, J., Arnold, N., Maass, N., & Bauerschlag, D. O. (2018). ADAM17 inhibition enhances platinum efficiency in ovarian cancer. *Oncotarget*, *9*(22), 16043. https://doi.org/10.18632/ONCOTARGET.24682

Hilpert, J., Grosse-Hovest, L., Grünebach, F., Buechele, C., Nuebling, T., Raum, T., Steinle, A., & Salih, H. R. (2012). Comprehensive analysis of NKG2D ligand expression and release in leukemia: implications for NKG2D-mediated NK cell responses. *Journal of Immunology (Baltimore, Md. : 1950)*, *189*(3), 1360–1371. https://doi.org/10.4049/JIMMUNOL.1200796

Hinrichs, C. S., & Rosenberg, S. A. (2014). Exploiting the curative potential of adoptive T-cell therapy for cancer. *Immunological Reviews*, *257*(1), 56–71. https://doi.org/10.1111/IMR.12132

Ho, P., Melms, J. C., Rogava, M., Frangieh, C. J., Poźniak, J., Shah, S. B., Walsh, Z., Kyrysyuk, O., Amin, A. D., Caprio, L., Fullerton, B. T., Soni, R. K., Ager, C. R., Biermann, J., Wang, Y., Khosravi-Maharlooei, M., Zanetti, G., Mu, M., Fatima, H., … Izar, B. (2023). The CD58-CD2 axis is co-regulated with PD-L1 via CMTM6 and shapes anti-tumor immunity. *Cancer Cell*, *41*(7), 1207-1221.e12. https://doi.org/10.1016/J.CCELL.2023.05.014/ATTACHMENT/A21DB109-4E6C-4079-A6A2-F630FA15A76B/MMC6.PDF

Holthaus, L., Lamp, D., Gavrisan, A., Sharma, V., Ziegler, A. G., Jastroch, M., & Bonifacio, E. (2018). CD4+ T cell activation, function, and metabolism are inhibited by low concentrations of DMSO. *Journal of Immunological Methods*, *463*, 54–60. https://doi.org/10.1016/J.JIM.2018.09.004

Huang, A. C., & Zappasodi, R. (2022). A decade of checkpoint blockade immunotherapy in melanoma: understanding the molecular basis for immune sensitivity and resistance. In *Nature Immunology* (Vol. 23, Issue 5, pp. 660–670). Nature Research. https://doi.org/10.1038/s41590-022-01141-1

Huehls, A. M., Huntoon, C. J., Joshi, P. M., Baehr, C. A., Wagner, J. M., Wang, X., Lee, M. Y., & Karnitz, L. M. (2016). Genomically Incorporated 5-Fluorouracil that Escapes UNG-Initiated Base Excision Repair Blocks DNA Replication and Activates Homologous Recombination. *Molecular Pharmacology*, *89*(1), 53–62. https://doi.org/10.1124/MOL.115.100164

Hundhausen, C., Misztela, D., Berkhout, T. A., Broadway, N., Saftig, P., Reiss, K., Hartmann, D., Fahrenholz, F., Postina, R., Matthews, V., Kallen, K. J., Rose-John, S., & Ludwig, A. (2003). The disintegrin-like metalloproteinase ADAM10 is involved in constitutive cleavage of CX3CL1 (fractalkine) and regulates CX3CL1-mediated cell-cell adhesion. *Blood*, *102*(4), 1186–1195. https://doi.org/10.1182/BLOOD-2002-12-3775

Huppa, J. B., & Davis, M. M. (2003). T-cell-antigen recognition and the immunological synapse. *Nature Reviews Immunology 2003 3:12*, *3*(12), 973–983. https://doi.org/10.1038/nri1245

Imai, C., Mihara, K., Andreansky, M., Nicholson, I. C., Pui, C. H., Geiger, T. L., & Campana, D. (2004). Chimeric receptors with 4-1BB signaling capacity provoke potent cytotoxicity against acute lymphoblastic leukemia. *Leukemia 2004 18:4*, *18*(4), 676–684. https://doi.org/10.1038/sj.leu.2403302

Iwai, Y., Ishida, M., Tanaka, Y., Okazaki, T., Honjo, T., & Minato, N. (2002). Involvement of PD-L1 on tumor cells in the escape from host immune system and tumor immunotherapy by PD-L1 blockade. *PNAS*. www.pnas.orgcgidoi10.1073pnas.192461099

Jenkins,', M. K., Taylor, P. S., Norton, S. D., & Urdahl, K. B. (1991). CD28 delivers a costimulatory signal involved in antigen-specific IL-2 production by human T cells. *The Journal of Immunology*, *147*(8), 2461–2466. https://doi.org/10.4049/JIMMUNOL.147.8.2461

Jensen, H., Hagemann-Jensen, M., Lauridsen, F., & Skov, S. (2013). Regulation of NKG2D-ligand cell surface expression by intracellular calcium after HDAC-inhibitor treatment. *Molecular Immunology*, *53*(3), 255–264. https://doi.org/10.1016/j.molimm.2012.08.011

Jessy, T. (2011). Immunity over inability: The spontaneous regression of cancer. *Journal of Natural Science*, *1*(1). https://doi.org/10.4103/0976-9668.82318

Jinushi, M., Vanneman, M., Munshi, N. C., Tai, Y. T., Prabhala, R. H., Ritz, J., Neuberg, D., Anderson, K. C., Carrasco, D. R., & Dranoff, G. (2008). MHC class I chain-related protein A antibodies and shedding are associated with the progression of multiple myeloma. *Proceedings of the National Academy of Sciences of the United States of America*, *105*(4), 1285–1290. https://doi.org/10.1073/PNAS.0711293105/SUPPL_FILE/11293FIG8.JPG

June, C. H., Ledbetter, J. A., Linsley, P. S., & Thompson, C. B. (1990). Role of the CD28 receptor in T-cell activation. *Immunology Today*, *11*(C), 211–216. https://doi.org/10.1016/0167-5699(90)90085-N

Juneja, V. R., McGuire, K. A., Manguso, R. T., LaFleur, M. W., Collins, N., Nicholas Haining, W., Freeman, G. J., & Sharpe, A. H. (2017). PD-L1 on tumor cells is sufficient for immune evasion in

immunogenic tumors and inhibits CD8 T cell cytotoxicity. *Journal of Experimental Medicine*, *214*(4), 895–904. https://doi.org/10.1084/jem.20160801

Jung, H., Hsiung, B., Pestal, K., Procyk, E., & Raulet, D. H. (2012a). RAE-1 ligands for the NKG2D receptor are regulated by E2F transcription factors, which controlcell cycle entry. *Journal of Experimental Medicine*, *209*(13), 2409–2422. https://doi.org/10.1084/jem.20120565

Jung, H., Hsiung, B., Pestal, K., Procyk, E., & Raulet, D. H. (2012b). RAE-1 ligands for the NKG2D receptor are regulated by E2F transcription factors, which controlcell cycle entry. *Journal of Experimental Medicine*, *209*(13), 2409–2422. https://doi.org/10.1084/jem.20120565

Kagoya, Y., Tanaka, S., Guo, T., Anczurowski, M., Wang, C. H., Saso, K., Butler, M. O., Minden, M. D., & Hirano, N. (2018). A novel chimeric antigen receptor containing a JAK-STAT signaling domain mediates superior antitumor effects. *Nature Medicine*, *24*(3), 352–359. https://doi.org/10.1038/nm.4478

Kaiser, B. K., Yim, D., Chow, I. T., Gonzalez, S., Dai, Z., Mann, H. H., Strong, R. K., Groh, V., & Spies, T. (2007). Disulphide-isomerase-enabled shedding of tumour-associated NKG2D ligands. *Nature 2007 447:7143*, *447*(7143), 482–486. https://doi.org/10.1038/nature05768

Kaizuka, Y., Douglass, A. D., Vardhana, S., Dustin, M. L., & Vale, R. D. (2009). The coreceptor CD2 uses plasma membrane microdomains to transduce signals in T cells. *Journal of Cell Biology*, *185*(3), 521–534. https://doi.org/10.1083/jcb.200809136

Kantarjian, H., Stein, A., Gökbuget, N., Fielding, A. K., Schuh, A. C., Ribera, J.-M., Wei, A., Dombret, H., Foà, R., Bassan, R., Arslan, Ö., Sanz, M. A., Bergeron, J., Demirkan, F., Lech-Maranda, E., Rambaldi, A., Thomas, X., Horst, H.-A., Brüggemann, M., … Topp, M. S. (2017). Blinatumomab versus Chemotherapy for Advanced Acute Lymphoblastic Leukemia. *New England Journal of Medicine*, *376*(9), 836–847. https://doi.org/10.1056/NEJMOA1609783/SUPPL_FILE/NEJMOA1609783_DISCLOSURES.PDF

Kavazović, I., Lenartić, M., Jelenčić, V., Jurković, S., Lemmermann, N. A. W., Jonjić, S., Polić, B., & Wensveen, F. M. (2017). NKG2D stimulation of CD8+ T cells during priming promotes their capacity to produce cytokines in response to viral infection in mice. *European Journal of Immunology*, *47*(7), 1123–1135. https://doi.org/10.1002/EJI.201646805

Keir, M. E., Butte, M. J., Freeman, G. J., & Sharpe, A. H. (2008). PD-1 and Its Ligands in Tolerance and Immunity. *Annu Rev Immuno*. https://doi.org/10.1146/annurev.immunol.26.021607.090331

Kellner, C., Hallack, D., Glorius, P., Staudinger, M., Mohseni Nodehi, S., De Weers, M., Van De Winkel, J. G. J., Parren, P. W. H. I., Stauch, M., Valerius, T., Repp, R., Humpe, A., Gramatzki, M., & Peipp, M. (2012). Fusion proteins between ligands for NKG2D and CD20-directed single-chain variable fragments sensitize lymphoma cells for natural killer cell-mediated lysis and enhance antibody-dependent cellular cytotoxicity. In *Leukemia* (Vol. 26, Issue 4, pp. 830–834). Nature Publishing Group. https://doi.org/10.1038/leu.2011.288

Khalique, H., Baugh, R., Dyer, A., Scott, E. M., Frost, S., Larkin, S., Lei-Rossmann, J., & Seymour, L. W. (2021). Oncolytic herpesvirus expressing PD-L1 BiTE for cancer therapy: exploiting tumor immune suppression as an opportunity for targeted immunotherapy. *Journal for ImmunoTherapy of Cancer*, *9*(4). https://doi.org/10.1136/jitc-2020-001292

Kim, J.-Y., Son Young-Ok, Park, S.-W., Bae, J.-H., Chung, J. S., Kim, H. H., Chung, B.-S., Kim, S.-H., & Kang, C.-D. (2006). Increase of NKG2D ligands and sensitivity to NK cell-mediated cytotoxicity of tumor cells by heat shock and ionizing radiation. *EXPERIMENTAL and MOLECULAR MEDICINE*, *38*.

Klinger, M., Brandl, C., Zugmaier, G., Hijazi, Y., Bargou, R. C., Topp, M. S., Gö, N., Neumann, S., Goebeler, M., Viardot, A., Stelljes, M., Brü, M., Hoelzer, D., Degenhard, E., Nagorsen, D., Baeuerle, P. A., Wolf, A., & Kufer, P. (2012). *Immunopharmacologic response of patients with B-*

lineage acute lymphoblastic leukemia to continuous infusion of T cell-engaging CD19/CD3-bispecific BiTE antibody blinatumomab. https://doi.org/10.1182/blood-2012-01-400515

Knudson, C. J., Férez, M., Alves-Peixoto, P., Erkes, D. A., Melo-Silva, C. R., Tang, L., Snyder, C. M., & Sigal, L. J. (2021). Mechanisms of Antiviral Cytotoxic CD4 T Cell Differentiation. *Journal of Virology*, *95*(19), e00566-21. https://doi.org/10.1128/JVI.00566-21

Kochenderfer, J. N., & Rosenberg, S. A. (2013). Treating B-cell cancer with T cells expressing anti-CD19 chimeric antigen receptors. *Nature Reviews Clinical Oncology 2013 10:5*, *10*(5), 267–276. https://doi.org/10.1038/nrclinonc.2013.46

Koguchi, Y., Hoen, H. M., Bambina, S. A., Rynning, M. D., Fuerstenberg, R. K., Curti, B. D., Urba, W. J., Milburn, C., Bahjat, F. R., Korman, A. J., & Bahjat, K. S. (2015). Serum Immunoregulatory Proteins as Predictors of Overall Survival of Metastatic Melanoma Patients Treated with Ipilimumab. *Cancer Research*, *75*(23), 5084–5092. https://doi.org/10.1158/0008-5472.CAN-15-2303

Kohlhapp, F. J., O'Sullivan, J. A., Moore, T. V., Zloza, A., & Guevara-Patiño, J. A. (2023). NKG2D signaling shifts the balance of CD8 T cells from single cytokine- to polycytokine-producing effector cells. *Molecular Immunology*, *155*, 1–6. https://doi.org/10.1016/J.MOLIMM.2022.12.013

Krensky, A. M., Sanchez-Madrid, F., Robbins, E., Nagy, J. A., Springer, T. A., & Burakoff, S. J. (1983). The functional significance, distribution, and structure of LFA-1, LFA-2, and LFA-3: cell surface antigens associated with CTL-target interactions. *The Journal of Immunology*, *131*(2), 611–616. https://doi.org/10.4049/JIMMUNOL.131.2.611

Kueberuwa, G., Kalaitsidou, M., Cheadle, E., Hawkins, R. E., & Gilham, D. E. (2017). CD19 CAR T Cells Expressing IL-12 Eradicate Lymphoma in Fully Lymphoreplete Mice through Induction of Host

Immunity. *Molecular Therapy Oncolytics*, *8*, 41–51. https://doi.org/10.1016/J.OMTO.2017.12.003

Kuhn, I., Harden, P., Bauzon, M., Chartier, C., Nye, J., Thorne, S., Reid, T., Ni, S., Lieber, A., Fisher, K., Seymour, L., Rubanyi, G. M., Harkins, R. N., & Hermiston, T. W. (2008). Directed Evolution Generates a Novel Oncolytic Virus for the Treatment of Colon Cancer. *PLoS ONE*, *3*(6). https://doi.org/10.1371/JOURNAL.PONE.0002409

Lammich, S., Kojro, E., Postina, R., Gilbert, S., Pfeiffer, R., Jasionowski, M., Haass, C., & Fahrenholz, F. (1999). Constitutive and regulated alpha-secretase cleavage of Alzheimer's amyloid precursor protein by a disintegrin metalloprotease. *Proceedings of the National Academy of Sciences of the United States of America*, *96*(7), 3922–3927. https://doi.org/10.1073/PNAS.96.7.3922

Leach, D. R., Krummel, M. F., & Allison, J. P. (1996). Enhancement of Antitumor Immunity by CTLA-4 Blockade. *Science*. https://www.science.org

Lee, J. B., Kim, H. R., & Ha, S. J. (2022). Immune Checkpoint Inhibitors in 10 Years: Contribution of Basic Research and Clinical Application in Cancer Immunotherapy. In *Immune Network* (Vol. 22, Issue 1). Korean Association of Immunologists. https://doi.org/10.4110/in.2022.22.e2

Leitner, J., Grabmeier-Pfistershammer, K., & Steinberger, P. (2010). Receptors and ligands implicated in human T cell costimulatory processes. *Immunology Letters*, *128*(2), 89–97. https://doi.org/10.1016/j.imlet.2009.11.009

Leitner, J., Herndler-Brandstetter, D., Zlabinger, G. J., Grubeck-Loebenstein, B., & Steinberger, P. (2015). CD58/CD2 Is the Primary Costimulatory Pathway in Human CD28−CD8+ T Cells. *The Journal of Immunology*, *195*(2), 477–487. https://doi.org/10.4049/jimmunol.1401917

Leivas, A., Valeri, A., Córdoba, L., García-Ortiz, A., Ortiz, A., Sánchez-Vega, L., Graña-Castro, O., Fernández, L., Carreño-Tarragona, G., Pérez, M., Megías, D., Paciello, M. L., Sánchez-Pina, J., Pérez-Martínez, A., Lee, D. A., Powell, D. J., Río, P., & Martínez-López, J. (2021). NKG2D-CAR-

transduced natural killer cells efficiently target multiple myeloma. *Blood Cancer Journal*, *11*(8). https://doi.org/10.1038/s41408-021-00537-w

Lendeckel, U., Kohl, J., Arndt, M., Carl-McGrath, S., Donat, H., & Röcken, C. (2005). Increased expression of ADAM family members in human breast cancer and breast cancer cell lines. *Journal of Cancer Research and Clinical Oncology*, *131*(1), 41–48. https://doi.org/10.1007/S00432-004-0619-Y

Lerner, E. C., Woroniecka, K. I., D'Anniballe, V. M., Wilkinson, D. S., Mohan, A. A., Lorrey, S. J., Waibl-Polania, J., Wachsmuth, L. P., Miggelbrink, A. M., Jackson, J. D., Cui, X., Raj, J. A., Tomaszewski, W. H., Cook, S. L., Sampson, J. H., Patel, A. P., Khasraw, M., Gunn, M. D., & Fecci, P. E. (2023). CD8+ T cells maintain killing of MHC-I-negative tumor cells through the NKG2D–NKG2DL axis. *Nature Cancer 2023 4:9*, *4*(9), 1258–1272. https://doi.org/10.1038/s43018-023-00600-4

Li, B. H., Garstka, M. A., & Li, Z. F. (2020). Chemokines and their receptors promoting the recruitment of myeloid-derived suppressor cells into the tumor. *Molecular Immunology*, *117*, 201–215. https://doi.org/10.1016/J.MOLIMM.2019.11.014

Li, P., Morris, D. L., Willcox, B. E., Steinle, A., Spies, T., & Strong, R. K. (2001). Complex structure of the activating immunoreceptor NKG2D and its MHC class I–like ligand MICA. *Nature Immunology 2001 2:5*, *2*(5), 443–451. https://doi.org/10.1038/87757

Liang, M. (2018). Oncorine, the World First Oncolytic Virus Medicine and its Update in China. *Current Cancer Drug Targets*, *18*(2), 171–176. https://doi.org/10.2174/1568009618666171129221503

Liberti, M. V., & Locasale, J. W. (2016). The Warburg Effect: How Does it Benefit Cancer Cells? *Trends in Biochemical Sciences*, *41*(3), 211. https://doi.org/10.1016/J.TIBS.2015.12.001

Linette, G. P., Stadtmauer, E. A., Maus, M. V, Rapoport, A. P., Levine, B. L., Emery, L., Litzky, L., Bagg, A., Carreno, B. M., Cimino, P. J., Binder-Scholl, G. K., Smethurst, D. P., Gerry, A. B., Pumphrey, N. J., Bennett, A. D., Brewer, J. E., Dukes, J., Harper, J., Tayton-Martin, H. K., … June, C. H. (2013).

Cardiovascular toxicity and titin cross-reactivity of affinity-enhanced T cells in myeloma and melanoma. *Blood*. https://doi.org/10.1182/blood-2013-03

Liu, B. L., Robinson, M., Han, Z. Q., Branston, R. H., English, C., Reay, P., McGrath, Y., Thomas, S. K., Thornton, M., Bullock, P., Love, C. A., & Coffin, R. S. (2003). ICP34.5 deleted herpes simplex virus with enhanced oncolytic, immune stimulating, and anti-tumour properties. In *Gene Therapy* (Vol. 10, Issue 4, pp. 292–303). https://doi.org/10.1038/sj.gt.3301885

Liu, G., Lu, S., Wang, X., Page, S. T., Higano, C. S., Plymate, S. R., Greenberg, N. M., Sun, S., Li, Z., & Wu, J. D. (2013). Perturbation of NK cell peripheral homeostasis accelerates prostate carcinoma metastasis. *The Journal of Clinical Investigation*, *123*(10), 4410–4422. https://doi.org/10.1172/JCI69369

Liu, P. C. C., Liu, X., Li, Y., Covington, M., Wynn, R., Huber, R., Hillman, M., Yang, G., Ellis, D., Marando, C., Katiyar, K., Bradley, J., Abremski, K., Stow, M., Rupar, M., Zhuo, J., Li, Y.-L., Lin, Q., Burns, D., … Scherle, P. (2006). Identification of ADAM10 as a major source of HER2 ectodomain sheddase activity in HER2 overexpressing breast cancer cells. *Cancer Biology & Therapy*, *657*(6), 657–664. https://doi.org/10.4161/cbt.5.6.2708

Ljunggren, H. G. (2008). Cancer Immunosurveillance: NKG2D Breaks Cover. In *Immunity* (Vol. 28, Issue 4, pp. 492–494). https://doi.org/10.1016/j.immuni.2008.03.007

Lo, D. J., Weaver, T. A., Stempora, L., Mehta, A. K., Ford, M. L., Larsen, C. P., & Kirk, A. D. (2011). Selective targeting of human alloresponsive CD8+ effector memory T cells based on CD2 expression. *American Journal of Transplantation*, *11*(1), 22–33. https://doi.org/10.1111/j.1600-6143.2010.03317.x

Loeb, L. A., Loeb, K. R., & Anderson, J. P. (2003). Multiple mutations and cancer. *Proceedings of the National Academy of Sciences of the United States of America*, *100*(3), 776–781.

https://doi.org/10.1073/PNAS.0334858100/ASSET/10883BD6-72DE-4ACA-B181-A6211CE1B362/ASSETS/GRAPHIC/PQ0334858001.JPEG

Loeb, L. A., Springgate, C. F., & Battala4, N. (1974). Errors in DNA Replication as a Basis of Malignant Changes1. *CANCER RESEARCH*, *34*, 2311–2321. http://aacrjournals.org/cancerres/article-pdf/34/9/2311/2393214/cr0340092311.pdf

López-Soto, A., Huergo-Zapico, L., Acebes-Huerta, A., Villa-Alvarez, M., & Gonzalez, S. (2015). NKG2D signaling in cancer immunosurveillance. *International Journal of Cancer*, *136*(8), 1741–1750. https://doi.org/10.1002/IJC.28775

Ma, S., Li, X., Wang, X., Cheng, L., Li, Z., Zhang, C., Ye, Z., & Qian, Q. (2019). Current Progress in CAR-T Cell Therapy for Solid Tumors. *International Journal of Biological Sciences*, *15*(12), 2548–2560. https://doi.org/10.7150/IJBS.34213

Mack, M., Riethmüller, G., & Kufer, P. (1995). A small bispecific antibody construct expressed as a functional single-chain molecule with high tumor cell cytotoxicity. *Proceedings of the National Academy of Sciences*, *92*(15), 7021–7025. https://doi.org/10.1073/PNAS.92.15.7021

Maher, J., Brentjens, R. J., Gunset, G., Rivière, I., & Sadelain, M. (2002). Human T-lymphocyte cytotoxicity and proliferation directed by a single chimeric TCRζ /CD28 receptor. *Nature Biotechnology 2002 20:1*, *20*(1), 70–75. https://doi.org/10.1038/nbt0102-70

Maia, A., Schöllhorn, A., Schuhmacher, J., & Gouttefangeas, C. (2023). CAF-immune cell crosstalk and its impact in immunotherapy. In *Seminars in Immunopathology* (Vol. 45, Issue 2, pp. 203–214). Springer Science and Business Media Deutschland GmbH. https://doi.org/10.1007/s00281-022-00977-x

Majzner, R. G., & Mackall, C. L. (2018). Tumor antigen escape from car t-cell therapy. *Cancer Discovery*, *8*(10), 1219–1226. https://doi.org/10.1158/2159-8290.CD-18-0442/333744/P/TUMOR-ANTIGEN-ESCAPE-FROM-CAR-T-CELL

Mariathasan, S., Turley, S. J., Nickles, D., Castiglioni, A., Yuen, K., Wang, Y., Kadel, E. E., Koeppen, H., Astarita, J. L., Cubas, R., Jhunjhunwala, S., Banchereau, R., Yang, Y., Guan, Y., Chalouni, C., Ziai, J., Şenbabaoğlu, Y., Santoro, S., Sheinson, D., … Powles, T. (2018). TGFβ attenuates tumour response to PD-L1 blockade by contributing to exclusion of T cells. *Nature 2018 554:7693*, *554*(7693), 544–548. https://doi.org/10.1038/nature25501

Marino, N., Illingworth, S., Kodialbail, P., Patel, A., Calderon, H., Lear, R., Fisher, K. D., Champion, B. R., & Brown, A. C. N. (2017). Development of a versatile oncolytic virus platform for local intra-tumoural expression of therapeutic transgenes. *PLoS ONE*, *12*(5). https://doi.org/10.1371/journal.pone.0177810

Mariuzza, R. A., Wu, D., & Pierce, B. G. (2023). Structural basis for T cell recognition of cancer neoantigens and implications for predicting neoepitope immunogenicity. In *Frontiers in Immunology* (Vol. 14). Frontiers Media SA. https://doi.org/10.3389/fimmu.2023.1303304

Märklin, M., Hagelstein, I., Koerner, S. P., Rothfelder, K., Pfluegler, M. S., Schumacher, A., Grosse-Hovest, L., Jung, G., & Salih, H. R. (2019). Bispecific NKG2D-CD3 and NKG2D-CD16 fusion proteins for induction of NK and T cell reactivity against acute myeloid leukemia. *JITC*. https://doi.org/10.1186/s40425-019-0606-0

Matte, I., Lane, D., Laplante, C., Rancourt, C., & Piché, A. (2012). Profiling of cytokines in human epithelial ovarian cancer ascites. *American Journal of Cancer Research*, *2*(5), 566. /pmc/articles/PMC3433103/

Maude, S. L., Laetsch, T. W., Buechner, J., Rives, S., Boyer, M., Bittencourt, H., Bader, P., Verneris, M. R., Stefanski, H. E., Myers, G. D., Qayed, M., De Moerloose, B., Hiramatsu, H., Schlis, K., Davis, K. L., Martin, P. L., Nemecek, E. R., Yanik, G. A., Peters, C., … Grupp, S. A. (2018). Tisagenlecleucel in Children and Young Adults with B-Cell Lymphoblastic Leukemia. *The New England Journal of Medicine*, *378*(5), 439–448. https://doi.org/10.1056/NEJMOA1709866

Maude, S. L., Teachey, D. T., Rheingold, S. R., Shaw, P. A., Aplenc, R., Barrett, D. M., Barker, C. S., Callahan, C., Frey, N. V., Nazimuddin, F., Lacey, S. F., Zheng, Z., Levine, B., Melenhorst, J. J., Motley, L., Porter, D. L., June, C. H., & Grupp, S. A. (2016). Sustained remissions with CD19-specific chimeric antigen receptor (CAR)-modified T cells in children with relapsed/refractory ALL. *Journal of Clinical Oncology*, *34*(15_suppl), 3011–3011. https://doi.org/10.1200/JCO.2016.34.15_SUPPL.3011

Mcardel, S. L., Terhorst, C., & Sharpe, A. H. (2016). Roles of CD48 in regulating immunity and tolerance. *Clin Immunol*. https://doi.org/10.1016/j.clim.2016.01.008

McCarthy, E. F. (2006). The Toxins of William B. Coley and the Treatment of Bone and Soft-Tissue Sarcomas. *The Iowa Orthopaedic Journal*, *26*, 154. https://pmc.ncbi.nlm.nih.gov/articles/PMC1888599/

McGranahan, N., Furness, A. J. S., Rosenthal, R., Ramskov, S., Lyngaa, R., Saini, S. K., Jamal-Hanjani, M., Wilson, G. A., Birkbak, N. J., Hiley, C. T., Watkins, T. B. K., Shafi, S., Murugaesu, N., Mitter, R., Akarca, A. U., Linares, J., Marafioti, T., Henry, J. Y., Van Allen, E. M., … Swanton, C. (2016). Clonal neoantigens elicit T cell immunoreactivity and sensitivity to immune checkpoint blockade. *Science*, *351*(6280), 1463–1469. https://doi.org/10.1126/SCIENCE.AAF1490/SUPPL_FILE/MCGRANAHAN-SM.PDF

McGranahan, N., Rosenthal, R., Hiley, C. T., Rowan, A. J., Watkins, T. B. K., Wilson, G. A., Birkbak, N. J., Veeriah, S., Van Loo, P., Herrero, J., Swanton, C., Jamal-Hanjani, M., Shafi, S., Czyzewska-Khan, J., Johnson, D., Laycock, J., Bosshard-Carter, L., Gorman, P., Hynds, R. E., … Dessimoz, C. (2017). Allele-Specific HLA Loss and Immune Escape in Lung Cancer Evolution. *Cell*, *171*(6), 1259-1271.e11. https://doi.org/10.1016/j.cell.2017.10.001

Mescher, M. F., Curtsinger, J. M., Agarwal, P., Casey, K. A., Gerner, M., Hammerbeck, C. D., Popescu, F., & Xiao, Z. (2006). Signals required for programming effector and memory development by

CD8+ T cells. *Immunological Reviews*, *211*(1), 81–92. https://doi.org/10.1111/J.0105-2896.2006.00382.X

Metz, V. V, Kojro, E., Rat, D., & Postina, R. (2012). Induction of RAGE Shedding by Activation of G Protein-Coupled Receptors. *PLoS ONE*, *7*(7), 41823. https://doi.org/10.1371/journal.pone.0041823

Miki, Y., Swensen, J., Shattuck-Eidens, D., Futreal, P. A., Harshman, K., Tavtigian, S., Liu, Q., Cochran, C., Bennett, L. M., Ding, W., Bell, R., Rosenthal, J., Hussey, C., Tran, T., Mcclure, M., Frye, C., Hattier, T., Phelps, R., Haugen-Strano, A., … Rosteck, P. (1994). A Strong Candidate for the Breast and Ovarian Cancer Susceptibility Gene BRCA1. *Science*, *266*(5182), 66–71. https://doi.org/10.1126/SCIENCE.7545954

Milstein, O., Tseng, S.-Y., Starr, T., Llodra, J., Nans, A., Liu, M., Wild, M. K., Anton van der Merwe, P., Stokes, D. L., Reisner, Y., Dustin, M. L., Pathogenesis, M., Biology, S., & William Dunn, S. (2008). Nanoscale Increases in CD2-CD48-mediated Intermembrane Spacing Decrease Adhesion and Reorganize the Immunological Synapse * □ S From the Programs in and the. *Journal of Biological Chemistry*, *283*, 34414–34422. https://doi.org/10.1074/jbc.M804756200

Minton, J. P. (1973). Mumps Virus and BCG Vaccine in Metastatic Melanoma. *Archives of Surgery*, *106*(4), 503–506. https://doi.org/10.1001/ARCHSURG.1973.01350160117019

Morgan, R. A., Chinnasamy, N., Abate-Daga, D., Gros, A., Robbins, P. F., Zheng, Z., Dudley, M. E., Feldman, S. A., Yang, J. C., Sherry, R. M., Phan, G. Q., Hughes, M. S., Kammula, U. S., Miller, A. D., Hessman, C. J., Stewart, A. A., Restifo, N. P., Quezado, M. M., Alimchandani, M., … Rosenberg, S. A. (2013). Cancer regression and neurological toxicity following anti-MAGE-A3 TCR gene therapy. *Journal of Immunotherapy*, *36*(2), 133–151. https://doi.org/10.1097/CJI.0B013E3182829903

Mullooly, M., Mcgowan, P. M., Crown, J., & Duffy, M. J. (2016). The ADAMs family of proteases as targets for the treatment of cancer. *Cancer Biology & Therapy*, *17*. https://doi.org/10.1080/15384047.2016.1177684

Neelapu, S. S., Locke, F. L., Bartlett, N. L., Lekakis, L. J., Miklos, D. B., Jacobson, C. A., Braunschweig, I., Oluwole, O. O., Siddiqi, T., Lin, Y., Timmerman, J. M., Stiff, P. J., Friedberg, J. W., Flinn, I. W., Goy, A., Hill, B. T., Smith, M. R., Deol, A., Farooq, U., … Go, W. Y. (2017). Axicabtagene Ciloleucel CAR T-Cell Therapy in Refractory Large B-Cell Lymphoma. *The New England Journal of Medicine*, *377*(26), 2531–2544. https://doi.org/10.1056/NEJMOA1707447

Nikitin, P. A., & Luftig, M. A. (2012). The DNA damage response in viral-induced cellular transformation. *British Journal of Cancer*, *106*(3), 429–435. https://doi.org/10.1038/BJC.2011.612

Nisonoff, A., & Rivers, M. M. (1961). Recombination of a mixture of univalent antibody fragments of different specificity. *Archives of Biochemistry and Biophysics*, *93*(2), 460–462. https://doi.org/10.1016/0003-9861(61)90296-X

Nückel, H., Switala, M., Sellmann, L., Horn, P. A., Dürig, J., Dührsen, U., Küppers, R., Grosse-Wilde, H., & Rebmann, V. (2010). The prognostic significance of soluble NKG2D ligands in B-cell chronic lymphocytic leukemia. *Leukemia*, *24*(6), 1152–1159. https://doi.org/10.1038/LEU.2010.74

Nunes, R. J., Castro, M. A. A., Gonçalves, C. M., Bamberger, M., Pereira, C. F., Bismuth, G., & Carmo, A. M. (2008). Protein Interactions between CD2 and Lck Are Required for the Lipid Raft Distribution of CD2. *The Journal of Immunology*, *180*(2), 988–997. https://doi.org/10.4049/jimmunol.180.2.988

O'Connor, M. J. (2015). Targeting the DNA Damage Response in Cancer. *Molecular Cell*, *60*(4), 547–560. https://doi.org/10.1016/J.MOLCEL.2015.10.040

Offner, S., Hofmeister, R., Romaniuk, A., Kufer, P., & Baeuerle, P. A. (2006). Induction of regular cytolytic T cell synapses by bispecific single-chain antibody constructs on MHC class I-negative tumor cells. *Molecular Immunology*, *43*(6), 763–771. https://doi.org/10.1016/J.MOLIMM.2005.03.007

Orme, J. J., Jazieh, K. A., Xie, T., Harrington, S., Liu, X., Ball, M., Madden, B., Charlesworth, M. C., Azam, T. U., Lucien, F., Wootla, B., Li, Y., Villasboas, J. C., Mansfield, A. S., Dronca, R. S., & Dong, H. (2020). ADAM10 and ADAM17 cleave PD-L1 to mediate PD-(L)1 inhibitor resistance. *OncoImmunology*, *9*(1). https://doi.org/10.1080/2162402X.2020.1744980

Panobinostat approved for multiple myeloma. (2015). *Cancer Discovery*, *5*(5), OF4. https://doi.org/10.1158/2159-8290.CD-NB2015-040/335377/P/PANOBINOSTAT-APPROVED-FOR-MULTIPLE

Paschen, A., Sucker, A., Hill, B., Moll, I., Zapatka, M., Xuan, D. N., Geok, C. S., Gutmann, I., Hassel, J., Becker, J. C., Steinle, A., Schadendorf, D., & Ugurel, S. (2009). Differential clinical significance of individual NKG2D ligands in melanoma: Soluble ULBP2 as an indicator of poor prognosis superior to S100B. *Clinical Cancer Research*, *15*(16), 5208–5215. https://doi.org/10.1158/1078-0432.CCR-09-0886/347293/P/DIFFERENTIAL-CLINICAL-SIGNIFICANCE-OF-INDIVIDUAL

Patel, A., Andre, V., Eguiguren, S. B., Barton, M. I., Burton, J., Denham, E. M., Pettmann, J., Mørch, A. M., Kutuzov, M. A., Siller-Farfán, J. A., Dustin, M. L., van der Merwe, P. A., & Dushek, O. (2024). Using CombiCells, a platform for titration and combinatorial display of cell surface ligands, to study T-cell antigen sensitivity modulation by accessory receptors. *EMBO Journal*, *43*(1), 132–150. https://doi.org/10.1038/S44318-023-00012-1/SUPPL_FILE/44318_2023_12_MOESM9_ESM.PDF

Paz-Ares, L., Champiat, S., Lai, W. V., Izumi, H., Govindan, R., Boyer, M., Hummel, H. D., Borghaei, H., Johnson, M. L., Steeghs, N., Blackhall, F., Dowlati, A., Reguart, N., Yoshida, T., He, K., Gadgeel, S.

M., Felip, E., Zhang, Y., Pati, A., … Owonikoko, T. K. (2023). Tarlatamab, a First-in-Class DLL3-Targeted Bispecific T-Cell Engager, in Recurrent Small-Cell Lung Cancer: An Open-Label, Phase I Study. *Journal of Clinical Oncology*, *41*(16), 2893–2903. https://doi.org/10.1200/JCO.22.02823

Pelner, L., Fowler, G. A., & Nauts, H. C. (1958). Effects of concurrent infections and their toxins on the course of leukemia. *Acta Medica Scandinavica. Supplementum*, *338*, 1–47. https://pubmed.ncbi.nlm.nih.gov/13605619/

Pende, D., Rivera, P., & Marcenaro, S. (2002). *Major Histocompatibility Complex Class I-related Chain A and UL16-Binding Protein Expression on Tumor Cell Lines of Different Histotypes: Analysis of Tumor Susceptibility to NKG2D*. https://www.researchgate.net/publication/11050190

Podestà, M. A., Binder, C., Sellberg, F., DeWolf, S., Shonts, B., Ho, S. H., Obradovic, A., Waffarn, E., Danzl, N., Berglund, D., & Sykes, M. (2020). Siplizumab selectively depletes effector memory T cells and promotes a relative expansion of alloreactive regulatory T cells in vitro. *American Journal of Transplantation*, *20*(1), 88–100. https://doi.org/10.1111/ajt.15533

Pokrovska, T. D., Jacobus, E. J., Puliyadi, R., Prevo, R., Frost, S., Dyer, A., Baugh, R., Rodriguez-Berriguete, G., Fisher, K., Granata, G., Herbert, K., Taverner, W. K., Champion, B. R., Higgins, G. S., Seymour, L. W., & Lei-Rossmann, J. (2020). External Beam Radiation Therapy and Enadenotucirev: Inhibition of the DDR and Mechanisms of Radiation-Mediated Virus Increase. *Cancers 2020, Vol. 12, Page 798*, *12*(4), 798. https://doi.org/10.3390/CANCERS12040798

Proctor, R. N. (2012). The history of the discovery of the cigarette–lung cancer link: evidentiary traditions, corporate denial, global toll. *Tobacco Control*, *21*(2), 87–91. https://doi.org/10.1136/TOBACCOCONTROL-2011-050338

Purbhoo, M. A., Sutton, D. H., Brewer, J. E., Mullings, R. E., Hill, M. E., Mahon, T. M., Karbach, J., Jäger, E., Cameron, B. J., Lissin, N., Vyas, P., Chen, J.-L., Cerundolo, V., & Jakobsen, B. K. (2006). *Quantifying and Imaging NY-ESO-1/LAGE-1-Derived Epitopes on Tumor Cells Using High Affinity*

T Cell Receptors. http://journals.aai.org/jimmunol/article-pdf/176/12/7308/1215696/zim01206007308.pdf

Raffaghello, L., Prigione, I., Airoldi, I., Camoriano, M., Levreri, I., Gambini, C., Pende, D., Steinte, A., Ferrone, S., & Pistoia, V. (2004). Downregulation and/or Release of NKG2D Ligands as Immune Evasion Strategy of Human Neuroblastoma. *Neoplasia (New York, N.Y.)*, *6*(5), 558. https://doi.org/10.1593/NEO.04316

Rathe, S. K., Popescu, F. E., Johnson, J. E., Watson, A. L., Marko, T. A., Moriarity, B. S., Ohlfest, J. R., & Largaespada, D. A. (2019). Identification of candidate neoantigens produced by fusion transcripts in human osteosarcomas. *Scientific Reports 2019 9:1*, *9*(1), 1–11. https://doi.org/10.1038/s41598-018-36840-z

Raulet, D. H. (2003). Roles of the NKG2D immunoreceptor and its ligands. In *Nature Reviews Immunology* (Vol. 3, Issue 10, pp. 781–790). European Association for Cardio-Thoracic Surgery. https://doi.org/10.1038/nri1199

Raulet, D. H., Gasser, S., Gowen, B. G., Deng, W., & Jung, H. (2013). *Regulation of Ligands for the NKG2D Activating Receptor*. https://doi.org/10.1146/annurev-immunol-032712-095951

Rhim, A. D., Oberstein, P. E., Thomas, D. H., Mirek, E. T., Palermo, C. F., Sastra, S. A., Dekleva, E. N., Saunders, T., Becerra, C. P., Tattersall, I. W., Westphalen, C. B., Kitajewski, J., Fernandez-Barrena, M. G., Fernandez-Zapico, M. E., Iacobuzio-Donahue, C., Olive, K. P., & Stanger, B. Z. (2014). Stromal elements act to restrain, rather than support, pancreatic ductal adenocarcinoma. *Cancer Cell*, *25*(6), 735–747. https://doi.org/10.1016/j.ccr.2014.04.021

Rizvi, N. A., Hellmann, M. D., Snyder, A., Kvistborg, P., Makarov, V., Havel, J. J., Lee, W., Yuan, J., Wong, P., Ho, T. S., Miller, M. L., Rekhtman, N., Moreira, A. L., Ibrahim, F., Bruggeman, C., Gasmi, B., Zappasodi, R., Maeda, Y., Sander, C., … Chan, T. A. (2015). Mutational landscape determines

sensitivity to PD-1 blockade in non-small cell lung cancer. *Science*, *348*(6230), 124–128. https://doi.org/10.1126/SCIENCE.AAA1348/SUPPL_FILE/RIZVI-SM.PDF

Robert, C., & Rassool, F. V. (2012). HDAC Inhibitors: Roles of DNA Damage and Repair. *Advances in Cancer Research*, *116*, 87–129. https://doi.org/10.1016/B978-0-12-394387-3.00003-3

Roemer, A., Schwettmann, L., Jung, M., Roigas, J. A. N., Kristiansen, G., Schnorr, D., Loening, S. A., Jung, K., & Lichtinghagen, R. (2004). Increased mRNA expression of ADAMs in renal cell carcinoma and their association with clinical outcome. *Oncology Reports*, *11*(2), 529–536. https://doi.org/10.3892/OR.11.2.529

Romain, G., Strati, P., Rezvan, A., Fathi, M., Bandey, I. N., Adolacion, J. R. T., Heeke, D., Liadi, I., Marques-Piubelli, M. L., Solis, L. M., Mahendra, A., Vega, F., Cooper, L. J. N., Singh, H., Mattie, M., Bot, A., Neelapu, S. S., & Varadarajan, N. (2022). Multidimensional single-cell analysis identifies a role for CD2-CD58 interactions in clinical antitumor T cell responses. *Journal of Clinical Investigation*, *132*(17). https://doi.org/10.1172/JCI159402

Ropero, S., & Esteller, M. (2007). *The role of histone deacetylases (HDACs) in human cancer*. https://doi.org/10.1016/j.molonc.2007.01.001

Rudd, C. E., Taylor, A., & Schneider, H. (2009). CD28 and CTLA-4 coreceptor expression and signal transduction. In *Immunological Reviews* (Vol. 229, Issue 1, pp. 12–26). https://doi.org/10.1111/j.1600-065X.2009.00770.x

Russell, S. J., & Peng, K. W. (2007). Viruses as anticancer drugs. *Trends in Pharmacological Sciences*, *28*(7), 326–333. https://doi.org/10.1016/J.TIPS.2007.05.005/ASSET/69AF3B57-A4FE-457A-AFA9-48EF7A889C62/MAIN.ASSETS/GR1B1.SML

Saad, M. I., Rose-John, S., & Jenkins, B. J. (2019). ADAM17: An Emerging Therapeutic Target for Lung Cancer. *Cancers*, *11*(9). https://doi.org/10.3390/CANCERS11091218

Sallman, D. A., Kerre, T., Havelange, V., Poiré, X., Lewalle, P., Wang, E. S., Brayer, J. B., Davila, M. L., Moors, I., Machiels, J. P., Awada, A., Alcantar-Orozco, E. M., Borissova, R., Braun, N., Dheur, M. S., Gilham, D. E., Lonez, C., Lehmann, F. F., & Flament, A. (2023a). CYAD-01, an autologous NKG2D-based CAR T-cell therapy, in relapsed or refractory acute myeloid leukaemia and myelodysplastic syndromes or multiple myeloma (THINK): haematological cohorts of the dose escalation segment of a phase 1 trial. *The Lancet Haematology*, *10*(3), e191–e202. https://doi.org/10.1016/S2352-3026(22)00378-7

Sallman, D. A., Kerre, T., Havelange, V., Poiré, X., Lewalle, P., Wang, E. S., Brayer, J. B., Davila, M. L., Moors, I., Machiels, J. P., Awada, A., Alcantar-Orozco, E. M., Borissova, R., Braun, N., Dheur, M. S., Gilham, D. E., Lonez, C., Lehmann, F. F., & Flament, A. (2023b). CYAD-01, an autologous NKG2D-based CAR T-cell therapy, in relapsed or refractory acute myeloid leukaemia and myelodysplastic syndromes or multiple myeloma (THINK): haematological cohorts of the dose escalation segment of a phase 1 trial. *The Lancet Haematology*, *10*(3), e191–e202. https://doi.org/10.1016/S2352-3026(22)00378-7

Sauer, M., Schuldner, M., Hoffmann, N., Cetintas, A., Reiners, K. S., Shatnyeva, O., Hallek, M., Hansen, H. P., Gasser, S., & Von Strandmann, E. P. (2017a). CBP/p300 acetyltransferases regulate the expression of NKG2D ligands on tumor cells. *Oncogene*, *36*(7), 933–941. https://doi.org/10.1038/onc.2016.259

Sauer, M., Schuldner, M., Hoffmann, N., Cetintas, A., Reiners, K. S., Shatnyeva, O., Hallek, M., Hansen, H. P., Gasser, S., & Von Strandmann, E. P. (2017b). CBP/p300 acetyltransferases regulate the expression of NKG2D ligands on tumor cells. *Oncogene*, *36*(7), 933–941. https://doi.org/10.1038/onc.2016.259

Schreiber, R. D., Old, L. J., & Smyth, M. J. (2011). Cancer immunoediting: Integrating immunity's roles in cancer suppression and promotion. *Science*, *331*(6024), 1565–1570. https://doi.org/10.1126/SCIENCE.1203486

Schulz, U., Kreutz, M., Multhoff, G., Stoelcker, B., Köhler, M., Andreesen, R., & Holler, E. (2010). Interleukin-10 promotes NK cell killing of autologous macrophages by stimulating expression of NKG2D ligands. *Scandinavian Journal of Immunology*, *72*(4), 319–331. https://doi.org/10.1111/J.1365-3083.2010.02435.X

Schuster, S. J., Bishop, M. R., Tam, C. S., Waller, E. K., Borchmann, P., McGuirk, J. P., Jäger, U., Jaglowski, S., Andreadis, C., Westin, J. R., Fleury, I., Bachanova, V., Foley, S. R., Ho, P. J., Mielke, S., Magenau, J. M., Holte, H., Pantano, S., Pacaud, L. B., … Maziarz, R. T. (2019). Tisagenlecleucel in Adult Relapsed or Refractory Diffuse Large B-Cell Lymphoma. *The New England Journal of Medicine*, *380*(1), 45–56. https://doi.org/10.1056/NEJMOA1804980

Schuster, S. J., Svoboda, J., Chong, E. A., Nasta, S. D., Mato, A. R., Anak, Ö., Brogdon, J. L., Pruteanu-Malinici, I., Bhoj, V., Landsburg, D., Wasik, M., Levine, B. L., Lacey, S. F., Melenhorst, J. J., Porter, D. L., & June, C. H. (2017). Chimeric Antigen Receptor T Cells in Refractory B-Cell Lymphomas. *The New England Journal of Medicine*, *377*(26), 2545–2554. https://doi.org/10.1056/NEJMOA1708566

Scott, E. M., Jacobus, E. J., Lyons, B., Frost, S., Freedman, J. D., Dyer, A., Khalique, H., Taverner, W. K., Carr, A., Champion, B. R., Fisher, K. D., Seymour, L. W., & Duffy, M. R. (2019). Bi- And tri-valent T cell engagers deplete tumour-associated macrophages in cancer patient samples. *Journal for ImmunoTherapy of Cancer*, *7*(1). https://doi.org/10.1186/s40425-019-0807-6

Segaliny, A. I., Jayaraman, J., Chen, X., Chong, J., Luxon, R., Fung, A., Fu, Q., Jiang, X., Rivera, R., Ma, X., Ren, C., Zimak, J., Niklas Hedde, P., Shang, Y., Wu, G., & Zhao, W. (2023). A high throughput bispecific antibody discovery pipeline. *Commun Biol*. https://doi.org/10.1038/s42003-023-04746-w

Seifert, A., Düsterhöft, S., Wozniak, J., Koo, C. Z., Tomlinson, M. G., Nuti, E., Rossello, A., Cuffaro, D., Yildiz, D., & Ludwig, A. (2021). The metalloproteinase ADAM10 requires its activity to sustain

surface expression. *Cellular and Molecular Life Sciences*, *78*(2), 715–732. https://doi.org/10.1007/s00018-020-03507-w

Serrano, A. E., Menares-Castillo, E., Garrido-Tapia, M., Ribeiro, C. H., Hernández, C. J., Mendoza-Naranjo, A., Gatica-Andrades, M., Valenzuela-Diaz, R., Žiga, R., López, M. N., Salazar-Onfray, F., Aguillón, J. C., & Molina, M. C. (2011). Interleukin 10 decreases MICA expression on melanoma cell surface. *Immunology and Cell Biology*, *89*(3), 447–457. https://doi.org/10.1038/ICB.2010.100

Serritella, A. V., Saenz-Lopez Larrocha, P., Dhar, P., Liu, S., Medd, M. M., Jia, S., Cao, Q., & Wu, J. D. (2024). The Human Soluble NKG2D Ligand Differentially Impacts Tumorigenicity and Progression in Temporal and Model-Dependent Modes. *Biomedicines*, *12*(1), 196. https://doi.org/10.3390/BIOMEDICINES12010196/S1

Sewell, A. K. (2012). Why must T cells be cross-reactive? In *Nature Reviews Immunology* (Vol. 12, Issue 9, pp. 669–677). https://doi.org/10.1038/nri3279

Seymour, L. W., & Fisher, K. D. (2016). Oncolytic viruses: Finally delivering. In *British Journal of Cancer* (Vol. 114, Issue 4, pp. 357–361). Nature Publishing Group. https://doi.org/10.1038/bjc.2015.481

Shahinian, A., Pfefer, K., Lee, K. P., Kündig, T. M., Kishihara, K., Wakeham, A., Kawai, K., Ohashi, P. S., Thompson, C. B., & Mak, T. W. (1993). Differential T Cell Costimulatory Requirements in CD28-Deficient Mice. *Science*, *261*(5121), 609–612. https://doi.org/10.1126/SCIENCE.7688139

Shen, J., Pan, J., Du, C., Si, W., Yao, M., Xu, L., Zheng, H., Xu, M., Chen, D., Wang, S., Fu, P., & Fan, W. (2017). Silencing NKG2D ligand-Targeting miRNAs enhances natural killer cell-mediated cytotoxicity in breast cancer. *Cell Death and Disease*, *8*(4). https://doi.org/10.1038/cddis.2017.158

Shen, M. J., Xu, L. J., Yang, L., Tsai, Y., Keng, P. C., Chen, Y., Lee, S. O., & Chen, Y. (2017). *Radiation alters PD-L1/NKG2D ligand levels in lung cancer cells and leads to immune escape from NK cell cytotoxicity via IL-6-MEK/Erk signaling pathway*. *8*(46), 80506–80520. www.impactjournals.com/oncotarget

Shen, Y., Eng, J. S., Fajardo, F., Liang, L., Li, C., Collins, P., Tedesco, D., & Nolan-Stevaux, O. (2022). Cancer cell-intrinsic resistance to BiTE therapy is mediated by loss of CD58 costimulation and modulation of the extrinsic apoptotic pathway. *J Immunother Cancer*, *10*, 4348. https://doi.org/10.1136/jitc-2021-004348

Shi, H., & Shao, B. (2023). *LFA-1 Activation in T-Cell Migration and Immunological Synapse Formation*. https://doi.org/10.3390/cells12081136

Shimabukuro-Vornhagen, A., Gödel, P., Subklewe, M., Stemmler, H. J., Schlößer, H. A., Schlaak, M., Kochanek, M., Böll, B., & Von Bergwelt-Baildon, M. S. (2018). Cytokine release syndrome. *Journal for ImmunoTherapy of Cancer*. https://doi.org/10.1186/s40425-018-0343-9

Shin Lee, Y., Choi, H., Cho, H.-R., Son, W.-C., Park, Y.-S., Kang, C.-D., & Bae, J. (2021). Downregulation of NKG2DLs by TGF-β in human lung cancer cells. *BMC Immunology*, *22*. https://doi.org/10.1186/s12865-021-00434-8

Sikora-Skrabaka, M., Walkiewicz, K. W., Nowakowska-Zajdel, E., Waniczek, D., & Strzelczyk, J. K. (2022). ADAM10 and ADAM17 as Biomarkers Linked to Inflammation, Metabolic Disorders and Colorectal Cancer. *Current Issues in Molecular Biology*, *44*(10), 4517–4527. https://doi.org/10.3390/CIMB44100309

Silberman, A. W. (1982). Surgical debulking of tumors. *Surg Gynecol Obstet*, *155*(4), 577–585.

Siokis, A., Robert, P. A., Demetriou, P., Dustin, M. L., & Meyer-Hermann, M. (2018). F-Actin-Driven CD28-CD80 Localization in the Immune Synapse. *Cell Reports*, *24*(5), 1151–1162. https://doi.org/10.1016/j.celrep.2018.06.114

Skånland, S. S., Moltu, K., Berge, T., Aandahl, E. M., & Taskén, K. (2014). T-cell co-stimulation through the CD2 and CD28 co-receptors induces distinct signalling responses. *Journal of Biochem*.

Smirnov, S., Mateikovich, P., Samochernykh, K., & Shlyakhto, E. (2024). Recent advances on CAR-T signaling pave the way for prolonged persistence and new modalities in clinic. *Frontiers in Immunology*, *15*, 1335424. https://doi.org/10.3389/FIMMU.2024.1335424/BIBTEX

Smith-Garvin, J. E., Koretzky, G. A., & Jordan, M. S. (2009). T cell activation. *Annual Review of Immunology*, *27*(Volume 27, 2009), 591–619. https://doi.org/10.1146/ANNUREV.IMMUNOL.021908.132706/CITE/REFWORKS

Song, H., Kim, J. K., Cosman, D., & Choi, I. (2006). Soluble ULBP suppresses natural killer cell activity via down-regulating NKG2D expression. *Cellular Immunology*, *239*(1), 22–30. https://doi.org/10.1016/J.CELLIMM.2006.03.002

Spiegel, J. Y., Patel, S., Muffly, L., Hossain, N. M., Oak, J., Baird, J. H., Frank, M. J., Shiraz, P., Sahaf, B., Craig, J., Iglesias, M., Younes, S., Natkunam, Y., Ozawa, M. G., Yang, E., Tamaresis, J., Chinnasamy, H., Ehlinger, Z., Reynolds, W., … Miklos, D. B. (2021). CAR T cells with dual targeting of CD19 and CD22 in adult patients with recurrent or refractory B cell malignancies: a phase 1 trial. *Nature Medicine 2021 27:8*, *27*(8), 1419–1431. https://doi.org/10.1038/s41591-021-01436-0

Staufer, O., Leithner, A., Zhou, S., Crames, M., Comeau, S., Young, D., Low, S., Jenkins, E., Davis, S. J., Nixon, A., Pefaur, N., Kasturirangan, S., & Dustin, M. L. (2022). Segmental flexibility of bispecific T-cell engagers regulates the dynamics of immune synapse formation. *BioRxiv*. https://doi.org/10.1101/2022.06.15.496334

Stephen Hodi, F., O, S. J., McDermott, D. F., Weber, R. W., Sosman, J. A., Haanen, J. B., Gonzalez, R., Robert, C., Schadendorf, D., Hassel, J. C., Akerley, W., van den Eertwegh, A. J., Lutzky, J., Lorigan, P., Vaubel, J. M., Linette, G. P., Hogg, D., Ottensmeier, C. H., Lebbé, C., … Urba, W. J. (2010).

Improved Survival with Ipilimumab in Patients with Metastatic Melanoma A bs tr ac t. *N Engl j Med*, *8*, 711–734. https://doi.org/10.1056/NEJMoa1003466

Stern-Ginossar, N., Gur, C., Biton, M., Horwitz, E., Elboim, M., Stanietsky, N., Mandelboim, M., & Mandelboim, O. (2008). Human microRNAs regulate stress-induced immune responses mediated by the receptor NKG2D. *Nature Immunology*, *9*(9), 1065–1073. https://doi.org/10.1038/NI.1642

Stone, J. D., Aggen, D. H., Schietinger, A., Schreiber, H., & Kranz, D. M. (2012). A sensitivity scale for targeting T cells with chimeric antigen receptors (CARs) and bispecific T-cell Engagers (BiTEs). *Oncoimmunology*, *1*(6), 863. https://doi.org/10.4161/ONCI.20592

Stork, R., Campigna, E., Robert, B., Müller, D., & Kontermann, R. E. (2009). Biodistribution of a bispecific single-chain diabody and its half-life extended derivatives. *Journal of Biological Chemistry*, *284*(38), 25612–25619. https://doi.org/10.1074/JBC.M109.027078

Stranford, D. M., Simons, L. M., Berman, K. E., Cheng, L., DiBiase, B. N., Hung, M. E., Lucks, J. B., Hultquist, J. F., & Leonard, J. N. (2024). Genetically encoding multiple functionalities into extracellular vesicles for the targeted delivery of biologics to T cells. *Nature Biomedical Engineering*, *8*(4), 397–414. https://doi.org/10.1038/s41551-023-01142-x

Sun, Q., Hong, Z., Zhang, C., Wang, L., Han, Z., & Ma, D. (2023). Immune checkpoint therapy for solid tumours: clinical dilemmas and future trends. In *Signal Transduction and Targeted Therapy* (Vol. 8, Issue 1). Springer Nature. https://doi.org/10.1038/s41392-023-01522-4

Tafani, M., Sansone, L., Limana, F., Arcangeli, T., De Santis, E., Polese, M., Fini, M., & Russo, M. A. (2016). The Interplay of Reactive Oxygen Species, Hypoxia, Inflammation, and Sirtuins in Cancer Initiation and Progression. In *Oxidative Medicine and Cellular Longevity* (Vol. 2016). Hindawi Limited. https://doi.org/10.1155/2016/3907147

Tapia-Galisteo, A., Compte, M., Álvarez-Vallina, L., & Sanz, L. (2023). When three is not a crowd: trispecific antibodies for enhanced cancer immunotherapy. *Theranostics*, *13*(3), 1028–1041. https://doi.org/10.7150/thno.81494

Tekguc, M., Wing, J. B., Osaki, M., & Sakaguchi, S. (2021). Treg-expressed CTLA-4 depletes CD80/CD86 by trogocytosis, releasing free PD-L1 on antigen-presenting cells. *PNAS*.

Textor, S., Fiegler, N., Arnold, A., Porgador, A., Hofmann, T. G., & Cerwenka, A. (2011). Human NK Cells Are Alerted to Induction of p53 in Cancer Cells by Upregulation of the NKG2D Ligands ULBP1 and ULBP2. *Cancer Reserach*. https://doi.org/10.1158/0008-5472.CAN-10-3211

Tian, Y., Xie, D., & Yang, L. (2022). Engineering strategies to enhance oncolytic viruses in cancer immunotherapy. *Signal Transduction and Targeted Therapy 2022 7:1*, *7*(1), 1–21. https://doi.org/10.1038/s41392-022-00951-x

Upshaw, J. L., Arneson, L. N., Schoon, R. A., Dick, C. J., Billadeau, D. D., & Leibson, P. J. (2006). *NKG2D-mediated signaling requires a DAP10-bound Grb2-Vav1 intermediate and phosphatidylinositol-3-kinase in human natural killer cells*. https://doi.org/10.1038/ni1325

Valero, C., Lee, M., Hoen, D., Zehir, A., Berger, M. F., Seshan, V. E., Chan, T. A., & Morris, L. G. T. (2021). Response Rates to Anti–PD-1 Immunotherapy in Microsatellite-Stable Solid Tumors With 10 or More Mutations per Megabase. *JAMA Oncology*, *7*(5), 739–743. https://doi.org/10.1001/JAMAONCOL.2020.7684

van der Merwe, P. A., Barclay, A. N., Mason, D. W., Davies, E. A., Davis, S. J., Morgan, B. P., Tone, M., Krishnam, A. K. C., & Ianelli, C. (1994). Human Cell-Adhesion Molecule CD2 Binds CD58 (LFA-3) with a Very Low Affinity and an Extremely Fast Dissociation Rate but Does Not Bind CD48 or CD59. *Biochemistry*, *33*(33), 10149–10160. https://doi.org/10.1021/BI00199A043/ASSET/BI00199A043.FP.PNG_V03

Van Rooij, N., Van Buuren, M. M., Philips, D., Velds, A., Toebes, M., Heemskerk, B., Van Dijk, L. J. A., Behjati, S., Hilkmann, H., El Atmioui, D., Nieuwland, M., Stratton, M. R., Kerkhoven, R. M., Keşmir, C., Haanen, J. B., Kvistborg, P., & Schumacher, T. N. (2013). Tumor exome analysis reveals neoantigen-specific T-cell reactivity in an ipilimumab-responsive melanoma. *Journal of Clinical Oncology*, *31*(32). https://doi.org/10.1200/JCO.2012.47.7521/ASSET/4092B8D6-6491-43CD-BEC8-343360DBB1A8/ASSETS/IMAGES/ZLJ9991036630003.JPEG

Venitt, S. (1996). Mechanisms of spontaneous human cancers. *Environmental Health Perspectives*, *104*(Suppl 3), 633. https://doi.org/10.1289/EHP.96104S3633

Venkataraman, G. M., Suciu, D., Groh, V., Boss, J. M., & Spies, T. (2007). Promoter Region Architecture and Transcriptional Regulation of the Genes for the MHC Class I-Related Chain A and B Ligands of NKG2D. *The Journal of Immunology*, *178*(2), 961–969. https://doi.org/10.4049/JIMMUNOL.178.2.961

Ville, S., Poirier, N., Blancho, G., & Vanhove, B. (2015). Costimulatory blockade of the CD28 / CD80-86 / CTLA-4 balance in transplantation: Impact on memory T cells? *Frontiers in Immunology*, *6*(JUL), 153996. https://doi.org/10.3389/FIMMU.2015.00411/BIBTEX

Vogels, R., Zuijdgeest, D., van Rijnsoever, R., Hartkoorn, E., Damen, I., de Béthune, M.-P., Kostense, S., Penders, G., Helmus, N., Koudstaal, W., Cecchini, M., Wetterwald, A., Sprangers, M., Lemckert, A., Ophorst, O., Koel, B., van Meerendonk, M., Quax, P., Panitti, L., … Havenga, M. (2003). Replication-Deficient Human Adenovirus Type 35 Vectors for Gene Transfer and Vaccination: Efficient Human Cell Infection and Bypass of Preexisting Adenovirus Immunity. *Journal of Virology*, *77*(15), 8263–8271. https://doi.org/10.1128/JVI.77.15.8263-8271.2003/ASSET/30BE2451-DE46-411B-9945-BE5233E5FC4A/ASSETS/GRAPHIC/JV1530106006.JPEG

Vyas, M., Reinartz, S., Hoffmann, N., Reiners, K. S., Lieber, S., Jansen, J. M., Wagner, U., Müller, R., & von Strandmann, E. P. (2017). Soluble NKG2D ligands in the ovarian cancer microenvironment are associated with an adverse clinical outcome and decreased memory effector T cells independent of NKG2D downregulation. *Oncoimmunology*, *6*(9). https://doi.org/10.1080/2162402X.2017.1339854

Wagner, J. lC., Sleggs, C. A., & Marchand, P. (1960). Diffuse Pleural Mesothelioma and Asbestos Exposure in the North Western Cape Province. *British Journal of Industrial Medicine*, *17*(4), 260. https://doi.org/10.1136/OEM.17.4.260

Waldhauer, I., Goehlsdorf, D., Gieseke, F., Weinschenk, T., Wittenbrink, M., Ludwig, A., Stevanovic, S., Rammensee, H.-G., & Steinle, A. (n.d.). *Tumor-Associated MICA Is Shed by ADAM Proteases*. https://doi.org/10.1158/0008-5472.CAN-07-6768

Wang, L., Guo, W., Guo, Z., Yu, J., Tan, J., Simons, D. L., Hu, K., Liu, X., Zhou, Q., Zheng, Y., Colt, E. A., Yim, J., Waisman, J., & Lee, P. P. (2024). PD-L1-expressing tumor-associated macrophages are immunostimulatory and associate with good clinical outcome in human breast cancer. *Cell Reports Medicine*, *5*(2). https://doi.org/10.1016/j.xcrm.2024.101420

Wang, X., Lundgren, A. D., Singh, P., Goodlett, D. R., Plymate, S. R., & Wu, J. D. (2009). *An Six-Amino Acid Motif in the α3 domain of MICA Is the Cancer Therapeutic Target to Inhibit Shedding*. https://doi.org/10.1016/j.bbrc.2009.07.062

Ward, J., Davis, Z., DeHart, J., Zimmerman, E., Bosque, A., Brunetta, E., Mavilio, D., Planelles, V., & Barker, E. (2009). HIV-1 Vpr triggers natural killer cell-mediated lysis of infected cells through activation of the ATR-mediated DNA damage response. *PLoS Pathogens*, *5*(10). https://doi.org/10.1371/JOURNAL.PPAT.1000613

Weiss, T., Schneider, H., Silginer, M., Steinle, A., Pruschy, M., Polic, B., Weller, M., & Roth, P. (2018). NKG2D-Dependent antitumor effects of chemotherapy and radiotherapy against glioblastoma. *Clinical Cancer Research*, *24*(4), 882–895. https://doi.org/10.1158/1078-0432.CCR-17-1766

Weitzman, M. D., Carson, C. T., Schwartz, R. A., & Lilley, C. E. (2004). Interactions of viruses with the cellular DNA repair machinery. *DNA Repair*, *3*(8–9), 1165–1173. https://doi.org/10.1016/j.dnarep.2004.03.018

Wensveen, F. M., Jelenčić, V., & Polić, B. (2018). NKG2D: A master regulator of immune cell responsiveness. In *Frontiers in Immunology* (Vol. 9, Issue MAR). Frontiers Media S.A. https://doi.org/10.3389/fimmu.2018.00441

Wolf, E., Hofmeister, R., Kufer, P., Schlereth, B., & Baeuerle, P. A. (2005). BiTEs: Bispecific antibody constructs with unique anti-tumor activity. In *Drug Discovery Today* (Vol. 10, Issue 18, pp. 1237–1244). https://doi.org/10.1016/S1359-6446(05)03554-3

Woods, D., & Turchi, J. J. (2013). Chemotherapy induced DNA damage response: Convergence of drugs and pathways. *Cancer Biology & Therapy*, *14*(5), 379. https://doi.org/10.4161/CBT.23761

Xing, S., & Ferrari de Andrade, L. (2020a). NKG2D and MICA/B shedding: a “tag game” between NK cells and malignant cells. *Clinical & Translational Immunology*, *9*(12). https://doi.org/10.1002/CTI2.1230

Xing, S., & Ferrari de Andrade, L. (2020b). NKG2D and MICA/B shedding: a ‘tag game’ between NK cells and malignant cells. *Clinical & Translational Immunology*, *9*(12). https://doi.org/10.1002/CTI2.1230

Xu, F., Sternberg, M. R., Kottiri, B. J., McQuillan, G. M., Lee, F. K., Nahmias, A. J., Berman, S. M., & Markowitz, L. E. (2006). Trends in Herpes Simplex Virus Type 1 and Type 2 Seroprevalence in the United States. *JAMA*, *296*(8), 964–973. https://doi.org/10.1001/JAMA.296.8.964

Xu, X., Zhang, Y., Lu, Y., Zhang, X., Zhao, C., Wang, J., Guan, Q., Feng, Y., Gao, M., Yu, J., Song, Z., Liu, X., Golchehre, Z., Li, L., Ren, W., Pan-Hammarström, Q., Zhang, H., & Wang, X. (2024). CD58 Alterations Govern Antitumor Immune Responses by Inducing PDL1 and IDO in Diffuse Large B-Cell Lymphoma. *Cancer Research*, *84*(13), 2123–2140. https://doi.org/10.1158/0008-5472.CAN-23-2874/3443198/CAN-23-2874.PDF

Yamaguchi, K., Chikumi, H., Shimizu, A., Takata, M., Kinoshita, N., Hashimoto, K., Nakamoto, M., Matsunaga, S., Kurai, J., Miyake, N., Matsumoto, S., Watanabe, M., Yamasaki, A., Igishi, T., Burioka, N., & Shimizu, E. (2012). Diagnostic and prognostic impact of serum-soluble UL16-binding protein 2 in lung cancer patients. *Cancer Science*, *103*(8), 1405. https://doi.org/10.1111/J.1349-7006.2012.02330.X

Yang, D., Sun, B., Dai, H., Li, W., Shi, L., Zhang, P., Li, S., & Zhao, X. (2019). T cells expressing NKG2D chimeric antigen receptors efficiently eliminate glioblastoma and cancer stem cells. *Journal for ImmunoTherapy of Cancer*, *7*(1). https://doi.org/10.1186/s40425-019-0642-9

Yang, H., & Reinherz, E. (2006). Related Content PSTPIP2, a Protein Associated with Autoinnammatory Disease, Interacts with Inhibitory Enzymes SHIP1 and Csk Crucial Role of the Amino-Terminal Tyrosine Residue 42 and the Carboxyl-Terminal PEST Domain of IκBα in NF-κB Activation by an Oxidative Stress. *The Journal of Immunology*, *10*(176). https://doi.org/10.4049/jimmunol.176.10.5898

Yang, J., Zhou, W., Li, D., Niu, T., & Wang, W. (2023). BCMA-targeting chimeric antigen receptor T-cell therapy for multiple myeloma. *Cancer Letters*, *553*. https://doi.org/10.1016/J.CANLET.2022.215949

Yang, M., Yang, C. S., Guo, W. W., Tang, J. Q., Huang, Q., Feng, S. X., Jiang, A. J., Xu, X. F., Jiang, G., & Liu, Y. Q. (2017). A novel fiber chimeric conditionally replicative adenovirus-Ad5/F35 for tumor

therapy. *Cancer Biology & Therapy*, *18*(11), 833. https://doi.org/10.1080/15384047.2017.1395115

Yokokawa, J., Cereda, V., Remondo, C., Gulley, J. L., Arlen, P. M., Schlom, J., & Tsang, K. Y. (2008). Enhanced functionality of CD4+CD25highFoxP3 + regulatory T cells in the peripheral blood of patients with prostate cancer. *Clinical Cancer Research*, *14*(4), 1032–1040. https://doi.org/10.1158/1078-0432.CCR-07-2056

Yoneyama, T., Gorry, M., Sobo-Vujanovic, A., Lin, Y., Vujanovic, L., Gaither-Davis, A., Moss, M. L., Miller, M. A., Griffith, L. G., Lauffenburger, D. A., Stabile, L. P., Herman, J., & Vujanovic, N. L. (2018). ADAM10 Sheddase Activity is a Potential Lung-Cancer Biomarker. *Journal of Cancer*, *9*(14), 2559. https://doi.org/10.7150/JCA.24601

Zelefsky, M. J., Fuks, Z., Happersett, L., Lee, H. J., Ling, C. C., Burman, C. M., Hunt, M., Wolfe, T., Venkatraman, E. S., Jackson, A., Skwarchuk, M., & Leibel, S. A. (2000). Clinical experience with intensity modulated radiation therapy (IMRT) in prostate cancer. *Radiotherapy and Oncology*, *55*(3), 241–249. https://doi.org/10.1016/S0167-8140(99)00100-0

Zhang, C., Wang, Y., Zhou, Z., Zhang, J., & Tian, Z. (2009). Sodium butyrate upregulates expression of NKG2D ligand MICA/B in HeLa and HepG2 cell lines and increases their susceptibility to NK lysis. *Cancer Immunology, Immunotherapy*, *58*(8), 1275–1285. https://doi.org/10.1007/s00262-008-0645-8

Zhang, L., & Yu, D. (2019). Exosomes in cancer development, metastasis, and immunity. *Biochimica et Biophysica Acta. Reviews on Cancer*, *1871*(2), 455. https://doi.org/10.1016/J.BBCAN.2019.04.004

Zhang, T., Barber, A., & Sentman, C. L. (2006). Generation of Antitumor Responses by Genetic Modification of Primary Human T Cells with a Chimeric NKG2D Receptor. *Cancer Res*, *66*(11), 5927–5960. https://doi.org/10.1158/0008-5472.CAN-06-0130

Zhang, T., Hong-Ting Jou, T., Hsin, J., Wang, Z., Huang, K., Ye, J., Yin, H., & Xing, Y. (2023). Talimogene Laherparepvec (T-VEC): A Review of the Recent Advances in Cancer Therapy. *J. Clin. Med.*, *12*, 1098. https://doi.org/10.3390/jcm12031098

Zhang, Y., Fu, Q., Huang, T., Liu, Y., Chen, G., & Lin, S. (2022). Ionizing radiation-induced DNA damage responses affect cell compressibility. *Biochemical and Biophysical Research Communications*, *603*, 116–122. https://doi.org/10.1016/J.BBRC.2022.03.032

Zhang, Y., Hu, R., Xi, B., Nie, D., Xu, H., & Liu, A. (2022). Mechanisms of Senescence-Related NKG2D Ligands Release and Immune Escape Induced by Chemotherapy in Neuroblastoma Cells. *Frontiers in Cell and Developmental Biology*, *10*, 829404. https://doi.org/10.3389/FCELL.2022.829404/BIBTEX

Zhang, Y., Luo, F., & Dong, K. (2023). Soluble NKG2D ligands impair CD8+ T cell antitumor function dependent of NKG2D downregulation in neuroblastoma. *Oncology Letters*, *26*(1). https://doi.org/10.3892/ol.2023.13883

Zhang, Y., Qian, J., Gu, C., & Yang, Y. (2021). Alternative splicing and cancer: a systematic review. *Signal Transduction and Targeted Therapy 2021 6:1*, *6*(1), 1–14. https://doi.org/10.1038/s41392-021-00486-7

Zhao, H., Zhuang, Y., Li, R., Liu, Y., Mei, Z., He, Z., Zhou, F., & Zhou, Y. (2019). Effects of different doses of X-ray irradiation on cell apoptosis, cell cycle, DNA damage repair and glycolysis in HeLa cells. *Oncology Letters*, *17*(1), 42–54. https://doi.org/10.3892/ol.2018.9566

Zhao, L., Wang, W. J., Zhang, J. N., & Zhang, X. Y. (2014). 5-Fluorouracil and interleukin-2 immunochemotherapy enhances immunogenicity of non-small cell lung cancer A549 cells through upregulation of NKG2D ligands. *Asian Pacific Journal of Cancer Prevention*, *15*(9), 4039–4044. https://doi.org/10.7314/APJCP.2014.15.9.4039

Zhao, Y., Cao, Y., Chen, Y., Wu, L., Hang, H., Jiang, C., & Zhou, X. (2021). B2M gene expression shapes the immune landscape of lung adenocarcinoma and determines the response to immunotherapy. *Immunology*, *164*(3), 507–523. https://doi.org/10.1111/imm.13384

Zheng, X., Jiang, F., Katakowski, M., Kalkanis, S. N., Hong, X., Zhang, X., Zhang, Z. G., Yang, H., & Chopp, M. (2007). Inhibition of ADAM17 reduces hypoxia-induced brain tumor cell invasiveness. *Cancer Science*, *98*(5), 674–684. https://doi.org/10.1111/J.1349-7006.2007.00440.X

Zingoni, A., Vulpis, E., Loconte, L., & Santoni, A. (2020). NKG2D Ligand Shedding in Response to Stress: Role of ADAM10. *Frontiers in Immunology*, *11*, 530304. https://doi.org/10.3389/FIMMU.2020.00447/BIBTEX

Zocchi, M. R., Catellani, S., Canevali, P., Tavella, S., Garuti, A., Villaggio, B., Zunino, A., Gobbi, M., Fraternali-Orcioni, G., Kunkl, A., Ravetti, J. L., Boero, S., Musso, A., & Poggi, A. (2012). High ERp5/ADAM10 expression in lymph node microenvironment and impaired NKG2D ligands recognition in Hodgkin lymphomas. *Blood*, *119*(6), 1479–1489. https://doi.org/10.1182/BLOOD-2011-07-370841

Zunke, F., & Rose-John, S. (2017). The shedding protease ADAM17: Physiology and pathophysiology. *Biochimica et Biophysica Acta (BBA) - Molecular Cell Research*, *1864*(11), 2059–2070. https://doi.org/10.1016/J.BBAMCR.2017.07.001

Chapter 7: Appendix

7.1 Appendix A- Buffer Recipes

	Recipe
TAE buffer (50x)	242 g Tris, 100 mL 0.5 M EDTA and 57.1 mL Glacial Acetic Acid in 1 L DI water
SDS Running buffer (10x)	19.8 g Tris, 86.4 g glycine, 6 g SDS in 1L DI water
Native Running buffer (10x)	19.8 g Tris, 86.4 g glycine in 1L DI water
MACS buffer	0.5% BSA, 2 mM EDTA in PBS

7.2 Appendix B – DNA and protein sequences

Secretion signal peptide

DNA sequence

ATGGGATGGAGCTGCATCATCCTATTCCTCGTGGCGACGGCCACTGGAGTGCATAGCGAACTGGTG

Amino acid sequence

MGWSCIILFLVATATGVHSELV

GS linker sequence

DNA sequence

TCCTCCGGCGGCGGTGGAAGC or TCCAGCGGCGGAGGCGGTTCC

Amino acid sequence

SSGGGGS

Decahistidine tag

DNA sequence

CATCACCATCACCATCACCACCATCACCAT

Amino acid sequence

HHHHHHHHHH

NKG2D ectodomain

DNA sequence

TTCCTAAACTCATTATTCAACCAAGAAGTTCAAATTCCCTTGACCGAAAGTTACTGTGGCCCATGTCCTAAAAACT

GGATATGTTACAAAAATAACTGCTACCAATTTTTTGATGAGAGTAAAAACTGGTATGAGAGCCAGGCTTCTTGTAT

GTCTCAAAATGCCAGCCTTCTGAAAGTATACAGCAAAGAGGACCAGGATTTACTTAAACTGGTGAAGTCATATCA

TTGGATGGGACTAGTACACATTCCAACAAATGGATCTTGGCAGTGGGAAGATGGCTCCATTCTCTCACCCAACCT

ACTAACAATAATTGAAATGCAGAAGGGAGACTGTGCACTCTATGCCTCGAGCTTTAAAGGCTATATAGAAAACTG

TTCAACTCCAAATACATACATCTGCATGCAAAGGACTGTG

Amino acid sequence

FLNSLFNQEVQIPLTESYCGPCPKNWICYKNNCYQFFDESKNWYESQASCMSQNASLLKVYSKEDQDLLKLVKSYH

WMGLVHIPTNGSWQWEDGSILSPNLLTIIEMQKGDCALYASSFKGYIENCSTPNTYICMQRTV

CD3 scFv

DNA sequence

GATGTGCAACTCGTGCAGTCCGGTGCGGAAGTGAAAAAGCCGGGCGCGAGCGTCAAAGTGTCATGCAAGGCG

TCAGGATATACGTTTACTAGATACACTATGCACTGGGTGCGCCAGGCACCTGGTCAGGGCCTTGAATGGATCGGC

TACATCAATCCGTCGAGAGGCTACACTAATTACGCGGACTCAGTCAAAGGGCGCTTCACGATTACGACCGACAA

GTCCACCTCGACTGCATACATGGAACTGTCCTCGCTGAGAAGCGAGGACACCGCTACTTACTACTGCGCTAGATA

CTACGATGATCACTACTGCCTCGATTACTGGGGCCAGGGAACCACTGTCACGGTGTCATCGGGAGAGGGCACCT

CAACCGGATCAGGGGGATCGGGAGGCTCGGGCGGCGCAGACGACATCGTCCTGACCCAGTCGCCCGCCACCT

TGTCGCTGTCCCCAGGAGAAAGAGCGACCCTGTCATGCCGGGCGTCGCAAAGCGTGAGCTATATGAATTGGTAT

CAGCAGAAGCCAGGAAAGGCGCCGAAGAGATGGATCTACGACACCTCCAAGGTCGCTTCAGGTGTCCCGGCTA

GATTCTCAGGATCGGGATCAGGAACGGACTACTCCCTGACCATCAATTCACTGGAAGCAGAAGATGCGGCCACC

TACTACTGTCAGCAGTGGTCCTCCAACCCGCTGACTTTCGGAGGCGGAACTAAGGTCGAGATCAAG

Amino acid sequence

DVQLVQSGAEVKKPGASVKVSCKASGYTFTRYTMHWVRQAPGQGLEWIGYINPSRGYTNYADSVKGRFTITTDKS

TSTAYMELSSLRSEDTATYYCARYYDDHYCLDYWGQGTTVTVSSGEGTSTGSGGSGGSGGADDIVLTQSPATLSLSPG

ERATLSCRASQSVSYMNWYQQKPGKAPKRWIYDTSKVASGVPARFSGSGSGTDYSLTINSLEAEDAATYYCQQWSS

NPLTFGGGTKVEIK

Rabies S protein nanobody

DNA sequence

GAGGTCCAGTTGGTTGAGTCAGGGGGTGGCCTTGTTCAGGCTGGCGGGAGCCTCCGACTGAGTTGCGCGGCC
AGTGGTAGAACTCTGTCTAGTTATCGAATGGGGTGGTTTCGGCAAGCGCCAGGGAAGGAACGAGAGTTTATCTC
CACGATTAGTTGGAACGGGCGCTCTACCTATTATGCTGACTCCGTCAAGGGCCGCTTCATATTCAGTGAAGACAA
TGCAAAGAATACGGTCTATCTGCAAATGAACAGTCTGAAACCAGAGGACACCGCTGTATACTATTGCGCTGCGGC
ACTTATTGGCGGGTATTATAGCGATGTCGATGCTTGGTCATATTGGGGTCCTGGTACCCAAGTCACTGTGTCCTCA

Amino acid sequence

EVQLVESGGGLVQAGGSLRLSCAASGRTLSSYRMGWFRQAPGKEREFISTISWNGRSTYYADSVKGRFIFSEDNAKN
TVYLQMNSLKPEDTAVYYCAAALIGGYYSDVDAWSYWGPGTQVTVSS

CD2 ScFv

DNA sequence

AATATCATGATGACCCAGTCTCCAAGCTCCCTGGCTGTTTCTGCCGGCGAGAAGGTGACCATGACATGCAAGAG
CAGCCAAAGCGTGCTGTACAGCAGCAACCAGAAGAACTACCTGGCTTGGTACCAGCAAAAACCTGGACAGAGC
CCTAAGCTGCTGATCTACTGGGCTAGCACCAGAGAGAGCGGAGTGCCTGATAGATTCACAGGCAGCGGCAGCG
GCACAGATTTCACCCTGACAATCAGCTCCGTGCAGCCCGAGGACCTGGCCGTGTACTACTGCCATCAGTACCTGA
GCAGCCACACATTCGGCGGAGGCACCAAGCTGGAAATCAAGCGGGGCGGAGGTGGCTCTGGAGGCGGTGGA
TCTGGTGGTGGCGGATCACAACTGCAGCAGCCTGGCGCCGAGCTGGTGCGGCCTGGCAGCAGCGTGAAGCTG
AGCTGTAAAGCCTCTGGCTACACCTTTACCAGATACTGGATTCACTGGGTCAAGCAGAGACCCATCCAGGGCCT
GGAATGGATCGGCAACATCGACCCCAGCGACAGTGAAACCCACTACAACCAGAAATTCAAGGACAAGGCCACA
CTGACCGTGGACAAGTCCTCTGGAACAGCCTACATGCAGCTGTCTAGCCTGACCAGCGAGGACAGCGCCGTGTA
TTATTGCGCCACCGAGGATCTCTACTACGCCATGGAATACTGGGGCCAGGGCACCAGCGTGACCGTGTCCTCC

Amino acid sequence

NIMMTQSPSSLAVSAGEKVTMTCKSSQSVLYSSNQKNYLAWYQQKPGQSPKLLIYWASTRESGVPDRFTGSGSGT

DFTLTISSVQPEDLAVYYCHQYLSSHTFGGGTKLEIKRGGGGSGGGGSGGGGSQLQQPGAELVRPGSSVKLSCKASG

YTFTRYWIHWVKQRPIQGLEWIGNIDPSDSETHYNQKFKDKATLTVDKSSGTAYMQLSSLTSEDSAVYYCATEDLYYA

MEYWGQGTSVTVSS

EpCAM ScFv

DNA sequence

ATGGGATGGAGCTGCATCATCCTATTCCTCGTGGCGACGGCCACTGGAGTGCATAGCGAACTGGTGATGACTCA

GTCCCCGTCATCCCTGACGGTGACCGCCGGCGAGAAGGTCACCATGTCGTGCAAGTCCTCGCAAAGCCTGCTTA

ACAGCGGCAACCAGAAAAACTACCTCACGTGGTATCAGCAAAAGCCAGGTCAACCCCCAAAACTGCTCATCTAC

TGGGCGAGCACCCGCGAGTCGGGGGTGCCAGACCGGTTCACCGGCTCCGGGTCAGGAACTGATTTCACCCTAA

CCATCAGCTCGGTGCAAGCGGAGGACCTGGCCGTGTACTACTGCCAAAATGATTACTCGTACCCTCTGACCTTTG

GAGCGGGCACCAAGCTCGAAATCAAGGGCGGTGGAGGAAGCGGCGGGGGAGGCTCAGGTGGGGGAGGATC

AGAAGTCCAACTGCTGGAGCAGTCAGGAGCCGAACTGGTCCGCCCGGGAACCTCCGTCAAGATTTCCTGTAAG

GCTTCCGGCTACGCTTTTACCAATTACTGGCTGGGCTGGGTCAAGCAAAGACCGGGGCATGGCCTGGAGTGGA

TCGGCGACATCTTCCCAGGGAGCGGCAACATCCACTACAACGAGAAGTTCAAGGGGAAAGCGACTCTGACTGC

CGACAAATCATCCAGCACCGCCTACATGCAGCTGTCGTCGCTCACTTTCGAAGACAGCGCGGTGTACTTTTGTGC

TCGGCTCCGGAACTGGGATGAACCAATGGACTACTGGGGACAAGGAACTACCGTGACCGTCTCCTCCCTCGAG

Amino acid sequence

MGWSCIILFLVATATGVHSELVMTQSPSSLTVTAGEKVTMSCKSSQSLLNSGNQKNYLTWYQQKPGQPPKLLIYWAS

TRESGVPDRFTGSGSGTDFTLTISSVQAEDLAVYYCQNDYSYPLTFGAGTKLEIKGGGGSGGGGSGGGGSEVQLLEQ

SGAELVRPGTSVKISCKASGYAFTNYWLGWVKQRPGHGLEWIGDIFPGSGNIHYNEKFKGKATLTADKSSSTAYMQL

SSLTFEDSAVYFCARLRNWDEPMDYWGQGTTVTVSSLE

MICAB ScFv (LH)

DNA sequence

GATATCCAGATGACCCAGACCACATCTTCCCTGAGCGCTTCTCTGGGCGATAGAGTGACAATCAGCTGCAGCGCC

AGCCAGGACATTTCTAATTACCTGAACTGGTACCAGCAGAAGCCCGACGGCACCGTGAAGCTGCTGATCTACGA

CACCAGTATCCTGCACCTGGGCGTGCCCAGCAGATTCAGCGGCAGCGGCTCCGGCACAGATTACAGCCTGACCA

TCAGCAATCTGGAACCTGAAGATATCGCCACCTACTACTGCCAGCAATACAGCAAGTTCCCACGGACCTTCGGCG

GCGGAACCACCCTGGAGATCAAGGGAGGAGGAGGCAGCGGCGGAGGCGGCAGCGGAGGCGGCGGCTCTCA

GATCCAGCTGGTGCAGTCTGGTCCTGAGCTGAAAAAGCCTGGAGAAACCGTGAAAGTGTCTTGTAAAGCCAGC

GGCTATATGTTCACCAACTATGCCATGAACTGGGTCAAGCAGGCCCCTGAGAAGGGCCTGAAGTGGATGGGCTG

GATCAACACCCACACCGGCGACCCCACCTACGCCGACGACTTCAAGGGCAGAATCGCCTTCAGCCTCGAGACA

AGCGCTAGCACCGCCTACCTGCAAATCAACAACCTGAAGAACGAGGATACAGCCACATACTTTTGCGTGCGGAC

ATACGGCAACTACGCCATGGACTACTGGGGCCAGGGCACCTCCGTTACCGTGTCCTCCGCCAAGACCACGGCTC

CTTCCGTGTACCCCCTGGCCCCTGTGTGCGGCGACACAACTGGCAGCAGCGTGACCCTGGGATGTCTGGTGAAG

GGCTACTTCCCTGAGCCTGTGACCCTTACATGGAACAGCGGCAGCCTGAGCAGCGGCGTGCACACATTTCCAGC

CGTGCTGCAGAGCGACCTGTACACCCTGTCTAGCTCTGTGACCGTCACAAGCAGC

Amino acid sequence

DIQMTQTTSSLSASLGDRVTISCSASQDISNYLNWYQQKPDGTVKLLIYDTSILHLGVPSRFSGSGSGTDYSLTISNLEP

EDIATYYCQQYSKFPRTFGGGTTLEIKGGGGSGGGGSGGGGSQIQLVQSGPELKKPGETVKVSCKASGYMFTNYAM

NWVKQAPEKGLKWMGWINTHTGDPTYADDFKGRIAFSLETSASTAYLQINNLKNEDTATYFCVRTYGNYAMDYW

GQGTSVTVSSAKTTAPSVYPLAPVCGDTTGSSVTLGCLVKGYFPEPVTLTWNSGSLSSGVHTFPAVLQSDLYTLSSSVT

VTSS

MICAB ScFv (HL)

DNA sequence

CAGATCCAGCTGGTCCAGAGCGGACCTGAGCTGAAAAAGCCTGGCGAGACAGTGAAAGTGTCCTGCAAGGCC

TCCGGCTACATGTTCACCAACTACGCCATGAACTGGGTGAAGCAGGCCCCTGAGAAGGGCCTGAAGTGGATGG

GCTGGATCAATACCCACACCGGCGACCCCACCTACGCAGATGACTTCAAGGGCAGAATCGCCTTCTCTCTGGAA

ACCAGCGCCAGCACCGCCTACCTGCAGATCAACAACCTGAAGAACGAGGATACAGCCACCTACTTCTGCGTGCG

GACCTACGGCAACTACGCCATGGACTACTGGGGCCAGGGCACAAGCGTGACCGTGTCTTCTGCCAAGACCACA

GCTCCATCTGTGTACCCCCTGGCCCCAGTGTGCGGCGACACCACAGGCAGCTCTGTCACCCTGGGCTGTCTGGT

GAAAGGATATTTTCCCGAGCCTGTGACACTGACCTGGAACAGCGGCAGCCTGAGCAGCGGCGTGCACACGTTT

CCTGCCGTGCTGCAAAGCGACCTGTACACCCTGAGCAGCTCCGTGACCGTTACAAGCAGCGGCGGCGGCGGAT

CTGGCGGCGGCGGATCCGGAGGCGGAGGCAGCGACATTCAGATGACCCAGACCACCTCCTCCCTCTCTGCTAG

CCTGGGAGATAGAGTGACAATCAGCTGTAGCGCTTCTCAGGACATCAGCAACTACCTGAACTGGTACCAGCAAA

AGCCTGATGGCACCGTGAAGCTGCTGATCTACGACACCAGCATCCTGCACCTGGGCGTGCCTAGCCGGTTCAGC

GGCTCTGGAAGCGGCACTGATTACAGCCTCACAATCAGCAATCTGGAACCTGAGGACATCGCCACATATTACTGC

CAGCAGTACAGCAAGTTCCCCAGAACCTTCGGCGGCGGAACAACACTGGAAATCAAG

Amino acid sequence

QIQLVQSGPELKKPGETVKVSCKASGYMFTNYAMNWVKQAPEKGLKWMGWINTHTGDPTYADDFKGRIAFSLET

SASTAYLQINNLKNEDTATYFCVRTYGNYAMDYWGQGTSVTVSSAKTTAPSVYPLAPVCGDTTGSSVTLGCLVKGYF

PEPVTLTWNSGSLSSGVHTFPAVLQSDLYTLSSSVTVTSSGGGGSGGGGSGGGGSDIQMTQTTSSLSASLGDRVTIS

CSASQDISNYLNWYQQKPDGTVKLLIYDTSILHLGVPSRFSGSGSGTDYSLTISNLEPEDIATYYCQQYSKFPRTFGGG

TTLEIK

MICA*004

DNA sequence

ATGGGTCTAGGTCCAGTGTTTCTACTACTAGCTGGCATCTTTCCTTTTGCCCCTCCAGGCGCCGCCGCCGAGCCTC

ACTCCCTGCGGTACAACCTGACAGTCCTGTCCTGGGATGGATCCGTGCAGTCTGGCTTTCTGGCTGAAGTGCAC

CTGGACGGCCAGCCCTTCCTCCGCTACGATCGGCAGAAGTGCAGAGCCAAGCCTCAGGGCCAATGGGCCGAG

GATGTCCTGGGAAACAAGACCTGGGACAGAGAGACACGGGACCTGACCGGCAATGGCAAGGACCTGCGGATG

ACCCTGGCCCACATTAAGGACCAGAAAGAGGGTCTGCACTCTTTGCAAGAAATCAGAGTGTGCGAGATCCACG

AGGACAACTCCACCAGATCCAGCCAGCACTTCTACTACGACGGCGAGCTGTTCCTCTCCCAGAACGTGGAAACC

GAGGAATGGACCGTGCCTCAAAGCTCTAGAGCCCAGACACTGGCTATGAACGTGCGGAACTTCCTGAAGGAGG

ACGCCATGAAAACCAAGACCCACTACCACGCTATGCACGCCGACTGCCTGCAGGAACTGAGGAGATACCTGGA

ATCCTCTGTGGTGCTGAGACGGAGAGTGCCCCCTATGGTGAACGTGACCAGATCTGAGGCTTCCGAGGGAAATA

TCACCGTGACCTGCCGGGCCTCCAGCTTCTATCCCAGAAACATCACCCTGACCTGGCGGCAGGACGGCGTGTCC

CTGTCTCACGACACCCAGCAGTGGGGCGACGTGCTGCCTGATGGCAACGGCACCTACCAGACCTGGGTGGCCA

CCCGGATCTGCCAGGGCGAAGAGCAGAGATTCACCTGTTACATGGAACATTCGGGCAACCATTCTACACACCCC

GTGCCATCTGGCAAGGTGCTGGTGCTCCAGTCCCACTGGCAGACCTTCCACGTCTCTGCTGTGGCTGCTGCCGC

TGCTGCCATCTTCGTAATCATCATCTTCTACGTGAGATGTTGCAAGAAGAAGACATCCGCCGCCGAGGGCCCTGA

GCTGGTGAGCCTGCAAGTTCTGGATCAGCATCCTGTGGGCACCAGCGACCACAGAGACGCTACCCAGCTGGGC

TTCCAGCCTCTGATGTCCGCTCTGGGCTCCACCGGCTCTACTGAGGGAGCCTGA

Amino acid sequence

MGLGPVFLLLAGIFPFAPPGAAAEPHSLRYNLTVLSWDGSVQSGFLAEVHLDGQPFLRYDRQKCRAKPQGQWAED

VLGNKTWDRETRDLTGNGKDLRMTLAHIKDQKEGLHSLQEIRVCEIHEDNSTRSSQHFYYDGELFLSQNVETEEWT

VPQSSRAQTLAMNVRNFLKEDAMKTKTHYHAMHADCLQELRRYLESSVVLRRRVPPMVNVTRSEASEGNITVTCR

ASSFYPRNITLTWRQDGVSLSHDTQQWGDVLPDGNGTYQTWVATRICQGEEQRFTCYMEHSGNHSTHPVPSGKV

LVLQSHWQTFHVSAVAAAAAAIFVIIIFYVRCCKKKTSAAEGPELVSLQVLDQHPVGTSDHRDATQLGFQPLMSALG

STGSTEGA*

Primers for cloning into virus

SA - CAAATAAAGTTTGCGATCGCTACCCTGCATTTCTCTCTTCAGGGccgccgccATGGGATGGAGCTGCATCAT

CMV - CAAATAAAGTTTGCGATCGCTACCCTGCACGTCAGCTTACCTTTTTGGCAGG

Reverse - GAATTGATTTTCAAATAAACAAGTTCCTGCAGGATAGCTGACG

7.3 Appendix C – Verification of KO in U87 cell line

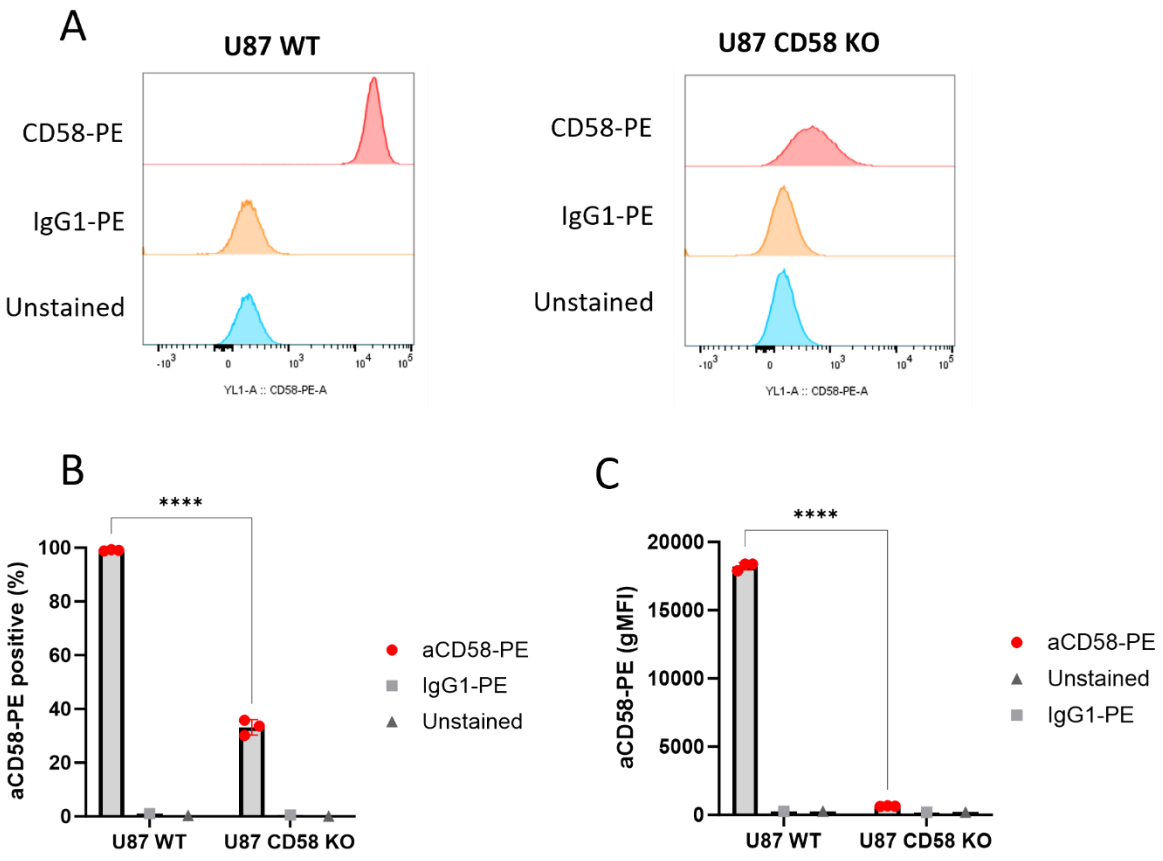

Verification of U87 CD58 KO.

U87-WT and U87-CD58 KO cells were stained with a PE-conjugated aCD58 antibody or appropriate isotype for analysis via flow cytometry. A) Individual flow cytometry plots showing PE expression for unstained, isotype or aCD58-PE. Average percentage positive (B), using unstained control to gate at 1% for each cell line, and gMFI (C) are presented.